UNIVERSIDADE DE LISBOA

FACULDADE DE FARMÁCIA

Development of three-dimensional umbilical cord-derived mesenchymal stem cell cultures for differentiation into hepatocyte-like cells: a potential breakthrough in toxicological drug screening

Madalena Zincke dos Reis Fernandes Cipriano

Orientadora: Doutora Joana Paiva Gomes Miranda

Co-orientadores: Doutor Jorge Miguel Silva Santos
Doutora Katrin Zeilinger

Tese especialmente elaborada para a obtenção do grau de Doutor em Farmácia, especialidade de Toxicologia

2017

UNIVERSIDADE DE LISBOA

FACULDADE DE FARMÁCIA

Development of three-dimensional umbilical cord-derived mesenchymal stem cell cultures for differentiation into hepatocyte-like cells: a potential breakthrough in toxicological drug screening

Madalena Zincke dos Reis Fernandes Cipriano

Orientadora: Doutora Joana Paiva Gomes Miranda

Co-orientadores: Doutor Jorge Miguel Silva Santos
Doutora Katrin Zeilinger

Tese especialmente elaborada para a obtenção do grau de Doutor em Farmácia, especialidade de Toxicologia

Júri:

Presidente: Doutora Matilde da Luz dos Santos Duque da Fonseca e Castro, Professora Catedrática e Directora da Faculdade de Farmácia da Universidade de Lisboa

Vogais: Doutor Jorge Manuel Lira Gonçalves Ruas, Associate Professor, Karolinska Institutet, Sweden
Doutor Félix Dias Carvalho, Professor Catedrático, Faculdade de Farmácia da Universidade do Porto
Doutora Diana Esperança dos Santos Nascimento, Investigadora Auxiliar, Instituto de Engenharia Biomédica da Universidade do Porto
Doutora Sofia de Azeredo Pereira Costa, Professora Auxiliar, Faculdade de Ciências Médicas da Universidade Nova de Lisboa
Doutora Cecília Maria Pereira Rodrigues, Professora Catedrática, Faculdade de Farmácia da Universidade de Lisboa
Doutor Nuno Filipe da Rocha Guerreiro de Oliveira, Professor Auxiliar com Agregação, Faculdade de Farmácia da Universidade de Lisboa
Doutora Joana Paiva Gomes Miranda, Investigadora Auxiliar, Faculdade de Farmácia da Universidade de Lisboa

iMed.ULisboa / Fundação para a Ciência e Tecnologia, Portugal

2017

This work has been performed at:

Chemical Biology and Toxicology Group, Research Institute for Medicines (CBT, iMed.ULisboa) in the Faculty of Pharmacy of University of Lisbon, Portugal; ECBio, S.A., Portugal; and Berlin-Brandenburg Center for Regenerative Therapies (BCRT) in the Charité Universitätsmedizin in Berlin, Germany; under the scientific supervision of Joana Paiva Gomes Miranda, PhD, and co-supervision of Miguel Silva Santos, PhD, and Dr. med. vet. Katrin Zeilinger.

Madalena Cipriano is a recipient of a PhD fellowship (SFRH/BD/87508/2012) from the Fundação para a Ciência e Tecnologia (FCT), Lisboa, Portugal and this work was developed within the framework of the FCT funded project “Development of 3D culture models for human UCX® cell-derived hepatocytes for predictive toxicology and cell therapy”, reference PTDC/SAU-TOX/110457/2009.

ACKNOWLEDGEMENTS

First and foremost I would like to express my special appreciation to my advisors.

To Joana Miranda, my main advisor, special thanks for believing in me. While I was still an undergraduate student, you gave me the opportunity to start a small research project and patiently teach me all about the basic laboratory and cell culture rules, techniques and tricks. You also lighted up the science bug on me and tought me to run for what I wanted. You always pushed me to grow as a researcher. I always felt constant support and friendship, especially in the most difficult times. Thank you for the opportunity to be part of our team, for creating the conditions of a complete education at several levels, scientifically, socially and humanly. With you I learned how important it is to be part of a team, support other team members and to live in different environments to strength your capacities.

A special acknowledgement is also due to Miguel Santos. Thank you for the relentless support and availability, as well as critical thinking and scientific discussions, crucial for the great course of this work.

To Katrin Zeillinger my co-advisor, for all the support and trust, as well as for welcoming me into her research group, in the Charité – Universitätsmedizin Berlin (Germany). Without your cooperation and support a significant part of this work would not have been possible.

An acknowledgement is also due to the Faculdade de Farmácia, Universidade de Lisboa, in particular to the Departamento de Ciências Toxicológicas e Bromatológicas, and the Research Institute for Medicines (iMed.ULisboa) for the facilities and conditions that allowed me to develop my PhD work, as well as to the Charité – Universitätsmedizin and ECBio, SA,.

To the Portuguese government (Fundação para a Ciência e a Tecnologia) and FEDER for the funding, namely my PhD grant (SFRH/BD/87508/2012) and to the project funding (PTDC/SAU-TOX/110457/2009), as well as the strategic projects PEst-OE/SAU/ UI4013/2011 and UID/DTP/04138/2013.

To all my colleagues from the Chemical Biology and Toxicology Group, special thanks for all the help and constant support. I would like to thank Professor Matilde Castro, the CBT coordinator at the time I joined CBT, for all support during this thesis.

To my first lab colleagues Ana Sofia Coelho and Joana Marques. Joana, you are much more than a CBT colleague but a friend for life in and outside of science. I would also acknowledge Elysse Filipe, Patrícia Guerreiro, Pedro Pinheiro, Ana and João. To Inês Ferreira for receiving me in her home in Berlin, and for being always there for scientific and political discussions. I

am also especially thankful to Sérgio, Inês, Bernardo and Joana Rodrigues, present in this last period of this thesis, for growing together as a team.

To Professor Nuno Oliveira for his support, scientific discussions and for being always present.

To ECBio, SA, in particular to Miguel and also to Rita Barcia, Pedro Cruz and Hélder Cruz, for supporting my work, for providing the stem cells, for the scientific discussions and contribution for paper manuscripts. I am also grateful for being always welcome to run experiments there.

To AG Zeillinger, Bioreactor Group, the Berlin-Brandenburg Center for Regenerative Therapies (BCRT) in the Charité Universitätsmedizin in Berlin, Germany. Words cannot express how thankful I am for the warm welcome and the way you took me into your group and made me feel at home (even when home was quite far away). To Fanny, for being always there to solve bioreactor problems and to arrange social activities. A special acknowledgement to Nora Freyer, for being always there for scientific, political and cultural discussions. You were my support during a new chapter of my life that made me grow so much in those short 6 months. I would also acknowledge the support of Christine, Marco, Thomas and Jasmina that were also part of these great times.

To Ruas Jorge Group, Molecular and Cellular Exercise Physiology, Department of Physiology and Pharmacology, Karolinska Institutet in Stockholm, Sweden. In particular to Jorge Ruas and Jorge Correia for welcoming me in their lab and for the scientific input on a crucial moment of the work here presented.

To Sofia Pereira and her CEDOC team, namely Catarina, Nádia and Nuno for the precious collaboration and support in the last year of this project in the HPLC methods and data analysis as well as for being so kind and helpful to me.

Finally, I need to acknowledge my always supporting family, my friends and my team for being there and believing in me.

ABSTRACT

A standard truly predictive in vitro hepatic model has been sought for reducing animal testing, increasing drug development efficiency and improving prediction of adverse drug reactions. The liver is the main organ responsible for xenobiotic metabolism, being particularly exposed to chemicals and its metabolites. The currently available hepatic in vitro models are insufficient. Those present low biotransformation activity, quickly lose its differentiated phenotype in vitro and/or have relevant interspecies differences. Therefore, the differentiation of stem cells (SC) into hepatocyte-like cells (HLC) has been suggested as an alternative approach to provide a representative human hepatic model. However, a functional hepatocyte-like phenotype has not yet been achieved.

In this thesis, we intended to demonstrate that by (i) using a human neonatal mesenchymal stem cell (hnMSC) source, UCX®, (ii) designing a protocol to differentiate this hnMSC into HLC using the cytokines and growth factors present during liver embryogenesis and (iii) resorting to 3D culture conditions would provide an environment closer to the in vivo, and allow a more representative cellular morphology, gene expression and biological behaviour of the hepatocyte.

Umbilical cord matrix hnMSC were selected for the hepatic differentiation due to its high availability, expansion capacity and genomic stability upon expansion, and, due to its more primordial origin, its higher differentiation capacity relative to other MSC sources. The hepatic differentiation protocol was step-wise developed under 2D cell culture conditions. FGF-2 at 4 ng/mL and the absence of FGF-4 resulted in an improved endoderm commitment and foregut induction during the first step of the differentiation protocol. The epigenetic modifiers trichostatin A (TSA), 5-azacytidine (5-AZA) and dimethyl sulfoxide (DMSO) were tested for an improved hepatoblast formation and maturation to HLC. The 21 day-long protocol was extended up to day 34, when a global gene expression analysis was performed. Transcriptomic analyses placed HLC between the HepG2 cell line and hpHep and distant from hnMSC and allowed us to understand how close we were from the hepatocyte transcriptome. HLC were also characterized up to day 34 at protein and functional level. DMSO at the concentration of 1 % and the cell passage day 17 of the differentiation with 24h of 5-AZA treatment, resulted in the best tested protocol. HLC were able to store glycogen, produce albumin and urea and express genes encoding for key hepatic enzymes. Most importantly, HLCs displayed stable UGTs, EROD (CY1A1/2), ECOD (CYP2B6, 1A2 and 2E1), CYP1A1, CYP2C9 and CYP3A4-dependent activities for 13 days at levels comparable to those observed in cultured primary rat hepatocytes. The presence of the hepatic drug transporters

OATP-C and MRP-2 and evaluation of CYP450 activity and induction of a wide range of enzymes was observed for the first time on hnMSC derived HLCs.

To further mimic the in vivo developing liver and thus achieve a more mature hepatic phenotype we established the 3D cultures. hnMSC 3D cultures aimed at evaluating hnMSC self-assembling capacity as well as the effect of this cell culture condition on its proliferation and/or differentiation potential. Viable and low proliferative hnMSC spheroids were obtained by resorting to (i) dynamic cultures using spinner flask suspension cultures (SFSC); and (ii) static cultures using ultra-low attachment (ULA) plates. In addition, 3D culture primed the hnMSC to produce a rich ECM and was successfully adapted to serum free conditions, which is particularly relevant for the hepatic differentiation.

3D culture of HLCs was established as spheroids, formed in ULA plates, and into a hollow-fiber perfused bioreactor designed for high density hepatocyte culture. 3D-HLC showed a partial hepatic zonation, observed by immunofluorescence and glycogen storage staining, and an improved hepatic functionality relative to 2D-HLC, namely by converting drugs into its specific metabolites and by producing higher amounts of glutathione. A thorough evaluation of 3D-HLCs biotransformation competency was confirmed using the model drug nevirapine (NVP). 3D HLCs distinguished from 2D-HLC by producing all phase I and II metabolites and by showing the modulation of phase I, II and III enzymes expression upon 10 days of NVP treatment. HLC thilomic profile was also presented for the first time. NVP resulted in an increased glutathione synthesis and oxidation in 3D HLC indicating a higher susceptibility to NVP toxic metabolites relative to 2D-HLC.

The thesis that hnMSC were capable of differentiation into HLC was here proved. By resorting to 3D culture conditions a more representative hMSC-based in vitro model of the liver physiological conditions was developed, extensively characterized and reinforced by the NVP study. This work highlights the relevance of stem cell derived HLC as an alternative model to study drug metabolism and unveil toxicity alerts associated with drug metabolism and bioactivation. The cellular system here developed is a step towards the 3 R´s implementation in terms of mechanistic studies as well as high-throughput drug screening.

Keywords:

Umbilical-cord matrix mesenchymal stem cells; Hepatic differentiation; Three-dimensional cell cultures; In vitro alternative models; In vitro toxicology

RESUMO

O processo de desenvolvimento de um novo fármaco é dispendioso, longo e tem uma taxa de sucesso de apenas 11 %. A falta de eficácia ou segurança das moléculas em desenvolvimento correspondem a cerca de 30 % da taxa de insucesso, que ocorre maioritariamente nas fases IIb e III. Pelo que, é essencial compreender melhor e o mais precocemente possível os mecanismos de ação e toxicidade das moléculas em desenvolvimento. Para isso, são necessários modelos celulares mais relevantes. que utilizem células humanas para evitar as diferenças entre espécies, e que sejam fisiologicamente mais representativos, permitindo assim reduzir os custos e a experimentação animal.

O fígado é um órgão essencial para o processo de avaliação da segurança e eficácia de novas moléculas devido ao seu papel na biotransformação. O processo de biotransformação regula, de certa forma, a disponibilidade de um fármaco e seus metabolitos em circulação, em particular no que respeita aos fármacos de administração oral. Quer a molécula mãe quer os seus produtos de biotransformação podem ser responsáveis pelos efeitos tóxicos dos xenóbioticos diretamente no fígado ou em outros órgãos. Assim, o estudo da biotransformação e da hepatotoxicidade é particularmente importante no desenvolvimento não clínico. As linhas celulares atualmente utilizadas em estudos in vitro, como as células HepG2 (de origem tumoral), apresentam uma capacidade de biotransformação baixa e pouco representativa, enquanto os hepatócitos primários (isolados de tecidos animais ou de biopsias humanas), perdem a sua capacidade de biotransformação com o tempo em cultura. Os hepatócitos primários humanos apresentam ainda uma disponibilidade muito limitada. Para tentar colmatar as falhas dos atuais modelos in vitro, a diferenciação de células estaminais (CE) em células tipo-hepatócito (CTH) tem sido sugerida como uma fonte alternativa de células humanas. No entanto, ainda não foi possível originar com sucesso uma população de CTH madura derivada de CE.

Neste sentido, a tese aqui apresentada pretendeu demonstrar que (i) utilizando células estaminais mesenquimais humanas isoladas da matriz do cordão umbilical (UCX®), (ii) desenvolvendo um protocolo de diferenciação baseado no conhecimento das citoquinas e fatores de crescimento envolvidos no desenvolvimento embrionário do fígado e (iii) recorrendo a sistemas de cultura tridimensionais (3D) resultaria num ambiente in vitro mais semelhante ao dos tecidos in vivo, proporcionando uma morfologia celular, expressão génica e comportamento biológico mais representativo do hepatócito. Como tal, permitindo a obtenção de CTH funcionais e competentes.

A escolha da população específica de células estaminais mesenquimais neonatais humanas (CEMnh) neste trabalho prende-se com a sua elevada capacidade de proliferação e estabilidade cromossómica, elevada disponibilidade e reduzidas questões éticas. A origem neonatal desta população de CEMnh surge também como uma vantagem destas por apresentarem uma menor marca epigenética do estilo de vida e idade do dador, uma capacidade de diferenciação superior em comparação com outras células estaminais mesenquimais, e numa reduzida imunogenicidade, que permite uma potencial aplicação clínica das células diferenciadas.

O protocolo de diferenciação hepática foi primeiramente desenvolvido em culturas em monocamada (2D). Os três passos do protocolo de diferenciação hepática in vitro compreendem o comprometimento com a linhagem endodérmica, a diferenciação hepática em hepatoblastos e a sua maturação em CTH. Neste processo, o comprometimento com a linhagem endodérmica e a indução da parte anterior do trato gastrointestinal foram melhorados pela presença de FGF-2 a 4 ng/mL e pela ausência de FGF-4. Os modificadores epigenéticos tricostatina A (TSA), 5-azacitidina (5-AZA) e dimetil sulfóxido (DMSO) foram também testados nas etapas de formação de hepatoblastos e de maturação em CTH. O protocolo de diferenciação tem a duração de 21 dias sendo que a cultura de CTH foi mantida e monitorizada até ao dia 34. O protocolo com DMSO à concentração de 1 %, uma passagem celular ao dia 17 e a adição de 5-AZA a este dia resultou no melhor protocolo testado. As CTH demonstraram capacidade de armazenar glicogénio, produzir albumina e ureia e expressar genes essenciais para as funções dos hepatócitos. As CTH mostram também atividade de UGT, EROD (CY1A1/2), ECOD (CYP2B6, 1A2 e 2E1), CYP1A1, CYP2C9 e CYP3A4 que se manteve ao longo de 13 dias em cultura, com níveis comparáveis aos observados em culturas de hepatócitos primários isolados de rato. A avaliação da atividade e indução de uma vasta gama de enzimas do CYP450 assim como atividade de enzimas de fase II e a presença dos transportadores hepáticos OATP-C e MRP-2 foi observada pela primeira vez em CTH derivadas CEMhn. Finalmente, a análise global de expressão génica (transcriptómica) ao dia 34 da diferenciação mostrou que as CTH se posicionam entre a linha celular HepG2 e os hepatócitos primários humanos e distantes das células indiferenciadas. Esta análise permitiu-nos avaliar a proximidade entre o transcriptoma das CTH e o do hepatócito humano.

No sentido de obter um fenótipo de CTH mais relevante as CEMnh foram cultivadas sob a forma de esferoides com o objetivo de avaliar a sua viabilidade em 3D e qual o efeito deste tipo de cultura no seu potencial de diferenciação e proliferação. Os esferoides foram obtidos através de (i) culturas dinâmicas em suspensão em sistemas de vasos agitados (SSVA) e de

(ii) culturas estáticas usando placas de cultura de baixa aderência (PCBA). As culturas 3D de CEMnh foram caracterizadas de acordo a dimensão dos esferoides, a viabilidade celular e a capacidade de produzir matriz extracelular. Nestas condições de cultura, os esferoides mostraram uma reduzida capacidade de proliferação, como observado pela marcação com Ki-67 e pela quantificação da biomassa, e conduziram à secreção de uma matriz extracelular rica, constituída por colagénio tipo I e IV, fibronectina e laminina. As CEMnh, mantidas sob a forma de esferoides, também mantiveram as suas características de células estaminais mesenquimais durante pelo menos 3 dias em cultura, nomeadamente a capacidade de diferenciação em adipócitos, osteoblastos e condroblastos. Desta forma, assegurando que a diferenciação seria iniciada em CEMnh indiferenciadas. Estas culturas foram ainda adaptadas a condições de cultura sem soro, essencial para as suas futuras aplicações clínicas e na diferenciação hepática.

A diferenciação em CTH foi então implementada em 3D (i) sob a forma de esferoides (PCBA) e (ii) num bioreactor de perfusão de fibra oca, desenvolvido para a cultura de hepatócitos. As culturas 3D mostraram uma zonação hepática parcial, observada pela coloração de glicogénio e pela deteção dos transportadores hepáticos OATP-C e MRP-2 por imunofluorescência. O fenótipo das CTH nas culturas tridimensionais também se distinguiu das culturas em monocamada pela maior capacidade de converter fármacos como o bupropion e o diclofenac nos seus metabolitos de fase I e de sintetizar glutationa. Uma avaliação mais profunda da capacidade de biotransformação das CTH foi avaliada utilizando o fármaco nevirapina (NVP) como modelo. O tratamento com NVP, pelo período de 10 dias, resultou na produção de todos os metabolitos de fase I e II de NVP nas culturas 3D por oposição às culturas 2D onde os metabolitos de fase II foram detetados em muito baixas quantidades. As CTH em 3D também mostraram modulação da expressão génica de enzimas de fase I, II e III enquanto as culturas 2D apenas mostraram modulação de enzimas de fase I. O perfil *tiolómico* foi determinado pela primeira vez em CTH. O tratamento com NVP alterou particularmente o perfil *tiolómico* da cultura 3D, tendo as CTH mostrado um aumento da síntese de glutationa assim como um aumento do seu estado de oxidação, indicando que as CTH em 3D apresentam uma maior suscetibilidade à NVP e aos seus metabolitos tóxicos.

Em suma, a utilização destas CEMnh e o protocolo de diferenciação desenvolvido nesta tese permitiram obter células do tipo hepatócito. A tese de que as condições de cultura tridimensionais, na presença de citocinas e factores de crescimento envolvidos no desenvolvimento embrionário do fígado resultaria num modelo hepático in vitro mais representativo foi aqui comprovada, e reforçada pelo estudo da biotransformação da nevirapina. Assim, o sistema celular aqui desenvolvido destaca a importância da

diferenciação de células estaminais em CTH como um modelo alternativo para o estudo do metabolismo e toxicidade de fármacos, particularmente dos que dependem de bioactivação. Desta forma, este trabalho apresenta-se como mais um passo no sentido da implementação da política dos 3 Rs indo também ao encontro das necessidades da indústria farmacêutica em termos da sua aplicação para estudos de mecanismos farmacológicos e toxicológicos bem como o estudo inicial de um elevado número de moléculas (*high-throughput screening*).

Palavras-chave:

Células estaminais da matriz do cordão umbilical; Diferenciação hepática; Culturas celulares tridimensionais; Modelos alternativos; Toxicologia in vitro

LIST OF PUBLICATIONS AND COMUNICATIONS

The scientific content of the present thesis has been included in the following publications:

Cipriano M, Pinheiro PFP, Sequeira C, Santos JM, Oliveira NG, Marques MM, Castro M, Pereira AS, Miranda JP. *The integrated assessment of nevirapine biotransformation unveils the biocompetence of a 3D in vitro model of human hepatocyte-like cells for liver function studies* (submitted for publication)

Cipriano M, Oliveira NG, Miranda JP. *Revisiting 3D liver models for drug metabolism and toxicology studies: A critical perspective*. (submitted for publication)

Cipriano M, Miranda JP. *Strategies for deriving stem cells into hepatocyte-like cells and its drug screening potential applications.* (in preparation)

Cipriano M, Correia JC, Camões SP, Oliveira NG, Cruz P, Cruz H, Castro M, Ruas JL, Santos JM, Miranda JP. *The role of epigenetic modifiers on extended cultures of functional hepatocyte-like cells derived from human neonatal mesenchymal stem cells*. Arch Toxicol. 2017; 91:2469-89. DOI 10.1007/s00204-016-1838-0.

Cipriano M, Freyer N, Knöspel F, Oliveira NG, Barcia R, Cruz P, Cruz H, Santos JM, Zeilinger K, Miranda JP. 2016. *Self-Assembled 3D Spheroids and Hollow-fibre Bioreactors improve MSC-Derived Hepatocyte-Like Cell Maturation In Vitro*. Arch Toxicol. 2017; 91:1815-32. DOI 10.1007/s00204-016-1838-0

Santos JM, Camões SP, Filipe E, **Cipriano M**, Barcia R, Filipe M, Teixeira M, Mosqueira D, Nascimento DS, Simões S, Gaspar M, Pinto-do-Ó P, Cruz P, Cruz H, Castro M, Miranda JP. *3D spheroid cell culture of umbilical cord tissue-derived MSCs (UCX®) leads to enhanced paracrine induction of wound healing*. Stem Cell Res Ther. 2015; 6(1): 90-109. DOI: 10.1186/s13287-015-0082-5

Other publications containing methods described in this thesis:

Grilo NM, Correia MJ, Miranda JP, **Cipriano M,** Serpa J, Marques MM, Monteiro EC, Antunes AM, Diogo LL, Pereira SA. *Unmasking efavirenz neurotoxicity: Time matters to the underlying mechanisms*. Eur J Pharm Sci. 2017; 105:47-54

Pinheiro PF, Harjivan SG, Martins IL, Marinho AT, **Cipriano M**, Camões S, Antunes AMM, Pereira SA, Oliveira, C, Castro M, Marques MM, Miranda JP. *Stirred cultures of hepatocyte spheroids as an alternative in vitro system for drug biotransformation studies: Nevirapine bioactivation*. Arch Toxicol. 2017; 91: 1199. DOI 10.1007/s00204-016-1792-x.

The scientific content of the present thesis has been presented in the following oral communications:

Cipriano M, Pinheiro PFP, Santos JM, Oliveira NG, Marques MM, Antunes AM, Castro M, Pereira AS, Miranda JP JP. *3D in vitro cultures of human Hepatocyte-Like Cells as an alternative model for drug biotransformation studies: nevirapine case study*. Abstract in Abstract book. SPF 2017 (XLVII Reunião Anual da Sociedade Portuguesa de Farmacologia/XXXVI Reunião de Farmacologia Clínica/XVII Reunião de Toxicologia), Coimbra, Portugal. February 2-4, 2017.

Cipriano M, Correia JC, Camões SP, Oliveira NG, Castro M, Ruas JL, Santos JM, Miranda JP. *Global gene expression analysis of extended cultures of functional hepatocyte-like cells derived from human neonatal mesenchymal stem cells*. Abstract in Abstract book. SPF 2017 (XLVII Reunião Anual da Sociedade Portuguesa de Farmacologia/XXXVI Reunião de Farmacologia Clínica/XVII Reunião de Toxicologia), Coimbra, Portugal. February 2-4, 2017.

Cipriano M, Freyer N, Knöspel F, Camões SP, Santos JM, Cruz H, Oliveira NG, Castro M, Zeilinger K, Miranda JP. *3D culture models for the maturation of stem cell derived hepatocyte-like cells applied to drug metabolism studies*. Abstract in Abstract book. SPF 2016 (XLVI Reunião Anual da Sociedade Portuguesa de Farmacologia/XXXV Reunião de Farmacologia Clínica/XVI Reunião de Toxicologia), Oporto, Portugal. February 4-6, 2016.

Cipriano M, Freyer N, Knöspel F, Camões SP, Santos JM, Cruz H, Oliveira NG, Castro M, Zeilinger K, Miranda JP. *3D culture models for the maturation of stem cell derived hepatocyte-like cells: spheroid culture and hollow-fiber bioreactor as potential in vitro alternatives for drug metabolism studies*. Abstract in Abstract book. HeMiBio International Symposium: Biology meets technology for liver toxicity testing, Leuven, Belgium. December 2-3, 2015. (Award for best Abstract, Selection for Oral Presentation)

Cipriano M, Camões S, Barcia RN, Cruz P, Cruz H, Santos JM, Oliveira NG, M Castro, Miranda JP. *The effect of epigenetic modifiers on the phenotype of hepatocyte-like cells derived from human neonatal mesenchymal stem cells*. Abstract in Abstract book. 7th iMed.ULisboa Postgraduate Students Meeting, Lisbon, Portugal. July 15-16, 2015. (Award for Best Oral Presentation)

Cipriano M, Santos JM, Cruz P, Cruz H, Barcia RN, Oliveira NG, Miranda JP. *Human neonatal mesenchymal stem cells undergo hepatic differentiation and present metabolic activity over time*. Abstract in Abstract book. SPF 2015 (XLV Reunião Anual da Sociedade

Portuguesa de Farmacologia/XXXIV Reunião de Farmacologia Clínica/XV Reunião de Toxicologia), NOVA Medical School, Lisbon, Portugal. February 5-6, 2015

The scientific content of the present thesis has been presented in the following poster communications:

Cipriano M, Oliveira NG, Cruz P, Cruz H, Castro M, Santos JM, Miranda JP. *3D culture models improve MSC-derived hepatocyte-like cell maturation in vitro: Usefulness for drug metabolism studies*. XIV International Congress of Toxicology and the X Mexican Congress of Toxicology (ICT2016) Merida, Yucatan, Mexico, 2-6 October, 2016

Cipriano M, Belém B, Rodrigues JS, Cruz P, Cruz H, Oliveira NG, Castro M, Santos JM, Miranda JP, *Off-the-shelf hepatocyte-like cells (HLCs): Characterization of cryopreserved human mesenchymal stem cell-derived HLCs*. 52nd Congress of the European Societies of Toxicology, Eurotox 2016 "Protecting Public and Environmental Health by understanding and communicating toxicology" Seville, Spain, 4-7 September, 2016

Cipriano M, Oliveira NG, Cruz P, Cruz H, Castro M, Santos JM, Miranda JP, *Self-Assembled 3D Spheroids of MSC-Derived Hepatocyte-Like Cells for in vitro Toxicity Studies*. 17th EUSAAT 2016 3 Rs Congress, Linz, Austria. August 24-27, 2016.

Cipriano M, Freyer N, Knöspel F, Santos JM, Cruz H, Oliveira NG, Castro M, Zeilinger K, Miranda JP. *3D culture models for the maturation of stem cell derived hepatocyte-like cells: spheroid culture and hollow-fiber bioreactor as potential in vitro alternatives for drug metabolism studies*. 8th Post-Graduate iMed.UL Students Meeting; Lisbon, Portugal, Jul 15-16, 2016.

Cipriano M, Freyer N, Knöspel F, Camões SP, Santos JM, Cruz H, Oliveira NG, Castro M, Zeilinger K, Miranda JP. *3D culture models for the maturation of stem cell derived hepatocyte-like cells: spheroid culture and hollow-fiber bioreactor as potential in vitro alternatives for drug metabolism studies*. HeMiBio International Symposium: Biology meets technology for liver toxicity testing, Leuven, Belgium. December 2-3, 2015.

Cipriano M, Freyer N, Knöspel F, Barcia R, Cruz P, Cruz H, Oliveira NG, Santos JM, Zeilinger K, Miranda JP. 2015. *3D culture strategies for improved MSCs-derived hepatocyte-like cells: potential toxicological and clinical applications*. The Liver Meeting® 2015, San Francisco, United States of America. November 13-17, 2015.

Cipriano M, Camões SP, Barcia RN, Cruz P, Oliveira NG, Castro M, Miranda JP. *Role of epigenetic modifiers on human neonatal mesenchymal stem cells differentiation into hepatocyte-like cells*. 51st Congress of the European Societies of Toxicology, Eurotox 2015 "Bridging Sciences for Safety", Oporto, Portugal. September 13-16, 2015.

Cipriano M, Freyer N, Knöspel F, Camões SP, Santos JM, Cruz H, Oliveira NG, Castro M, Zeilinger K, Miranda JP. *Improvement of mesenchymal stromal cell differentiation into hepatocyte-like cells using 3D culture models: Potential in vitro alternatives for drug metabolism studies*. 51st Congress of the European Societies of Toxicology, Eurotox 2015 "Bridging Sciences for Safety", Oporto, Portugal. September 13-16, 2015.

Cipriano M, Medeiros A, Santos JM, Cruz H, Cruz P, Barcia R, Oliveira NG, Miranda JP. *Improvement of hepatocyte-like characteristics of differentiated UCX® using 3D cultures*. 50th Congress of the European Societies of Toxicology, Eurotox 2014 "Advancing Science for Human and Environmental Health", Edinburgh, UK. September 7-10, 2014.

Cipriano M, Medeiros A, Filipe E, Santos JM, Cruz H, Cruz P, Barcia R, Oliveira NG, Miranda JP. *UCX® cells: A primordial stem cell source for in vitro differentiation into hepatocyte-like cells (HLCs).* 50th Congress of the European Societies of Toxicology, Eurotox 2014 "Advancing Science for Human and Environmental Health", Edinburgh, UK. September 7-10, 2014.

Cipriano M, Medeiros A, Filipe E, Cruz H, Cruz P, Santos JM, Barcia R, Miranda JP. *In vitro differentiation of UCX® cells into hepatocyte-like cells*. 5th Postgraduate iMed.UL Students Meeting, Lisbon, Portugal. July 2013.

Cipriano M, Medeiros A, Filipe E, Cruz H, Cruz P, Santos JM, Barcia R, Miranda JP. *In vitro differentiation of UCX® cells into hepatocyte-like cells*. EMBO Workshop on Liver and Pancreas Development, Function and Disease. Cape Sounio, Athens, Greece. May 26-30, 2013.

Patent:

Miranda JP, Santos JM, Filipe E, Filipe M, Teixeira M, **Cipriano M,** Barcia R, Cruz P, Cruz H, Castro M, 2014. *Method for deriving hepatocyte-like cell from neonatal mesenchymal stromal cells in 3D culture conditions*. Portugal: ECBio; [INPI, Provisional Patent:49857/14]

TABLE OF CONTENTS

LIST OF FIGURES

LIST OF TABLES

ABREVIATIONS

2D	Two dimensional
3-MC	3-methylcholantherene
3D	Three dimensional
3 Rs	Reduced, Replace and Refine
4-MU	4-methylumbelliferone
5-AZA	5-azacytidine
ABC	ATP-binding cassette family
Ac-LDL	Acetylated low-density lipoprotein
ADMET	Absorption, Distribution, Metabolism, Excretion and Toxicity
AFP	Alpha fetoprotein
AhR	Aryl hydrocarbon receptor
ALB	Albumin
AR	Androgen receptor
ASC	Adult stem cells
AT	Alpha 1-Antitripsin
AT-MSC	Adipose tissue MSC
BCA	Bicinchoninic acid
BCRP	Breast cancer resistance protein
BM-MSC	Bone marrow mesenchymal stem cells
BMP	Bone morphogenic proteins
BSA	Bovine serum albumin
BSEP	Bile salt export pump
c/EBPα	CCAAT/enhancer binding protein
CAR	Constitutive androstane receptor
cDNA	Complementary deoxyribonucleic acid
CHMP	Committee for Medicinal Products for Human Use
CK-18	Cytokeratin 18
CK-19	Cytokeratin 19
CYP450	Cytochrome P-450 superfamily
CYS	Cysteine
CYS-GLY	Cysteinylglycine
DAPI	4',6-diamidino-2-phenylindole
DILI	Drug-induced liver injury
DMSO	Dimethyl sulfoxide
DNMTi	DNA methyltransferase inhibitors
ECM	Extracellular matrix
ECOD	7-Ethoxycoumarin-O-deethylase
ECVAM	European Centre for the Validation of Alternative Methods
EGF	Epidermal growth factor

EM	Epigenetic modifiers
EMA	European Medicines Agency
EPA	Environmental Protection Agency
ER	Estrogen receptor
EROD	7-Ethoxyresorufin-O-deethylase
ESC	Embryonic stem cells
FBS	Foetal bovine serum
FDA	Food and Drug Administration
FDA/PI	Flurescein diacetate/Propidium iodide
FGF-2	Fibroblast growth factor-2
FGF-4	Fibroblast growth factor-4
FMO	flavin-containing monooxygenases
Foxa1-3	Forkhead box a1 to 3
FP7	*7th Framework Programme for Research and Technological Development* (2007-
G6P	Glucose-6-phosphate
GAPDH	glyceraldehyde-3-phosphate dehydrogenase
GATA 4-6	GATA binding factor 4 to 6
GCL	Glutamate cysteine ligase
γGT	Gama glutamyltranspeptidase
GLU-CYS	Glutamil-cysteine
Gp130	Glycoprotein 130
GR	Glucocorticoid receptor
GSH	Reduced glutatione
GSSG	Oxidized glutatione
GST	Glutathione transferases
H&E	Hematoxylin-Eosin staining
H2020	Eurpean Uninion Framework Programme for Research and Innovation (2014-2020)
HbLC	Hepatoblast-like cells
HDACi	Histone deacetylase inhibitors
HepaRG	Human hepatoma cell line
HepG2	Human hepatoma cell line
HepPar1	positive marker for hepatocellular differentiation
hERG	Human Eher-a-go-go Related Gene
hESCs	Human embryonic stem cells
HGF	Hepatocyte growth factor
HHEX	Hematopoietically-expressed homeobox protein
hiPSC	Human induced Pluripotent Stem Cells
HL-60	Human promyelocytic leukemia cells
HLA-DR	Human Leukocyte Antigen - antigen D Related
HLC	Hepatocyte-like cells
HNF-4α	Hepatocyte nuclear factor 4α

hnMSC	Human neonatal mesenchymal stromal cell
hpHep	Human primary hepatocytes
HTS	High Throughput Screening
hUCM-MSC	Human umbilical cord matrix mesenchymal stromal cells
Huh7	Human hepatoma cell line
ICCVAM	Interagency Coordinating Committee on the Validation of Alternative Methods
ICH	International Conference on Harmonisation of Technical Requirements for
IPA	Ingenuity Pathway Analysis
ISCT	International Society for Cellular Therapy
ISSCR	International Society for Stem Cell Research
ITS	Insulin–transferrin–sodium selenite
JAK/Stat3	Janus Kinase/Signal Transducer and Activator of Transcription 3
KLF4	Kruppel-like factor 4
LA	Linoleic Acid
LDH	Lactate dehydrogenase
LDL	Low-density lipoprotein cholesterol
LMWT	Low molecular weight thiol
MAO	monoamine oxidases
MAPK	Mitogen-activated protein kinases
MDR	Multidrug resistance protein
MR	Mineralocorticoid receptor
MRP	Multidrug resistance-associated protein
MRP-2	Multidrug resistance protein 2
MSC	Mesenchymal Stem Cells
MT	Methytransferases
MTS	3-(4,5-dimethylthiazol-2-yl)-5-(3-carboxymethoxyphenyl)-2-(4-sulfophenyl)-2H-
NADPH	Nicotinamide adenine dinucleotide phosphate
NAT	N-Acetytransferase
NPC	non-parenchymal cells
NTCP	Na+/bile acid cotransport protein
NVP	Nevirapine
OAT	Organic anion transporter family
OATP	Organic anion transporter protein family
OATP-C	Organic anion-transporting polypeptide C
OCT-4	Octomer-binding transcription factor-4
OCT	Organic cation transporter family
OECD	Organisation for Economic Cooperation and Development
OSM	Oncostatin M
OST	Organic solute transporter
P/S/A	Peninsilin/streptomicin/ amphotericin B
PAS	Periodic acid Schiff's staining

PBPK	Physiologically-Based Pharmacokinetic
PBS	Phosphate Buffered Saline (pH=7,4)
PCA	Principal Component Analysis
PDSC	placenta derived stem cells
Pdx 1	Pancreatic and duodenal homeobox 1
PFA	Paraformaldehyde
PPAR	Peroxisome proliferator activated receptor
PR	Progesterone receptor
Prox1	Prospero homeobox protein 1
PXR	Pregnane X receptor
qPCR	Quantitative real-time Polymerase Chain Reaction
REACH	Registration, Evaluation, Authorization and Restriction of Chemicals
RNS/ROS	Reactive nitrogen species / Reactive oxigen species
rpHep	Rat primary hepatocytes
RXR	Retinoid X receptor
SB	Sodium butyrate
SC	Stem cell
SCID	Severe Combined Immunodeficiency
SD	Standard deviation
SEM	Standard error of the mean
SFSC	Spinner flask suspension culture
Sox17	Sry-related HMG box 17
STM	Septum transverse mesenchyme
SULT	Sulfotransferases
TAT	Tyrosine aminotransferase
TDO	Tryptophan-2,3-dioxygenase
TGF-β	Transforming growth factor β
TGZ	Troglitazone
Tm	Melting temperature
TSA	Trichostatin A
UCX®	ECBio's proprietary Umbilical Cord eXpanded hnMSCs isolated from the Wharton's
UGT	uridine 5'-diphosphate glucuronosyltransferase
ULA	Ultra-low attachment
US Tox21	Toxicity Testing in the 21st century: A vision and a strategy
VPA	Valproic acid
WJ-MSC	Wharton's Jelly mesenchymal stem cells

Chapter 1. General Introduction

Part of the scientific content of the present chapter has been included in the following publications:

Cipriano M, Oliveira NG, Miranda JP. *Revisiting 3D liver models for drug metabolism and toxicology studies: A critical perspective*. (submitted for publication)

Cipriano M, Miranda JP. *Strategies for deriving stem cells into hepatocyte-like cells and its drug screening potential applications.* (in preparation)

Earlier and better understanding of drug mechanisms of action and toxicity is essential to improve the R&D process of a new drug [1, 2]. In fact, there is a relevant number of drug withdrawals for toxicological reasons, of which 21 % is due to hepatotoxicity [3]. The liver is the main organ responsible for xenobiotic metabolism, being particularly exposed to chemicals and its metabolites. Moreover, the hepatocyte is a particularly complex cell type that presents more individual functions than other ~200 terminally differentiated cell types in the human body [4].

1.1 Liver physiology and function

The liver is composed of 4 lobes, contains 5 cell types and distinct extracellular matrix (ECM) compositions. The liver parenchymal cells are the hepatocytes and the non-parenchymal cells are Kupffer cells, sinusoidal endothelial cells, bile duct epithelial cells and Ito cells (stellate cells). Hepatocytes represent 60 % of the liver's cells, about 80 % of liver total cell mass and are responsible for the liver's synthetic and metabolic functions. Hepatocytes are arranged in single-cell thick plates as represented in **Figure 1.1.**

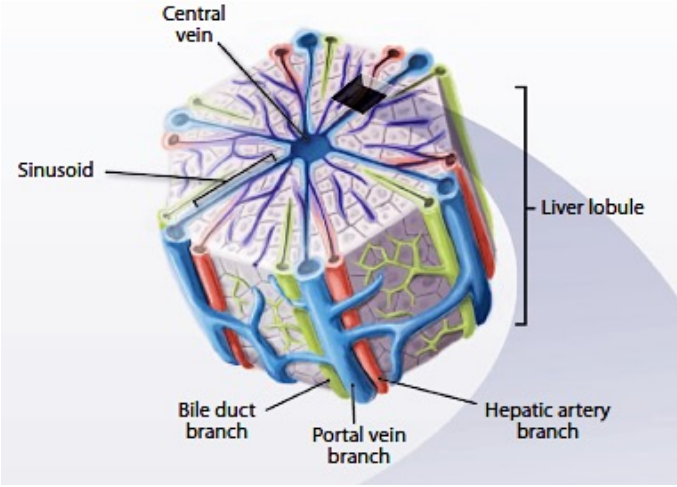

Figure 1.1 Multiscale liver tissue structures contribute to the diverse functional roles of the liver. Hierarchical structure of the liver consisting of repeated functional tissue units, the liver lobules [5].

Regardless of hepatocytes' morphological similarity, its functions vary per its location within the hepatic lobule, namely when located either closer to the periportal vein or to the central vein (**Figure 1.2**). This phenomenon is named hepatic zonation. Periportal hepatocytes are characterized by higher oxygen presence, glycogen synthesis from lactate and urea production since the blood that irrigates these hepatocytes flows from the whole circulation. On the other hand, the perivenus phenotype is exposed to lower oxygen pressure, and presents higher xenobiotic metabolism and glycogen synthesis from glucose given that these

cells are partially irrigated by blood flowing from the enterohepatic circulation [6, 7]. In the hepatic lobule, the blood flows toward the hepatic vein within the space of Disse contacting with the exposed surface areas of the hepatocyte plates, where toxins and nutrients within the blood stream are extracted by the hepatocytes. Kupffer cells are liver macrophages residing in the sinusoids. Their functions include phagocytosis of old red blood cells and bacteria as well as heme conversion into bilirubin. Sinusoidal endothelial cells are fenestrated allowing proteins to pass freely through the sinusoidal endothelium into the space of Disse, where they directly contact with hepatocytes, in a bi-directional fashion, meaning that proteins and other substances produced, stored or processed by the liver can also be transferred back into the blood. Bile duct epithelial cells line the interlobular bile ducts within the portal triads. Finally, Ito or stellate cells are found in the space of Disse and play an important role in liver fibrosis once these cells are responsible for collagen production [7, 8].

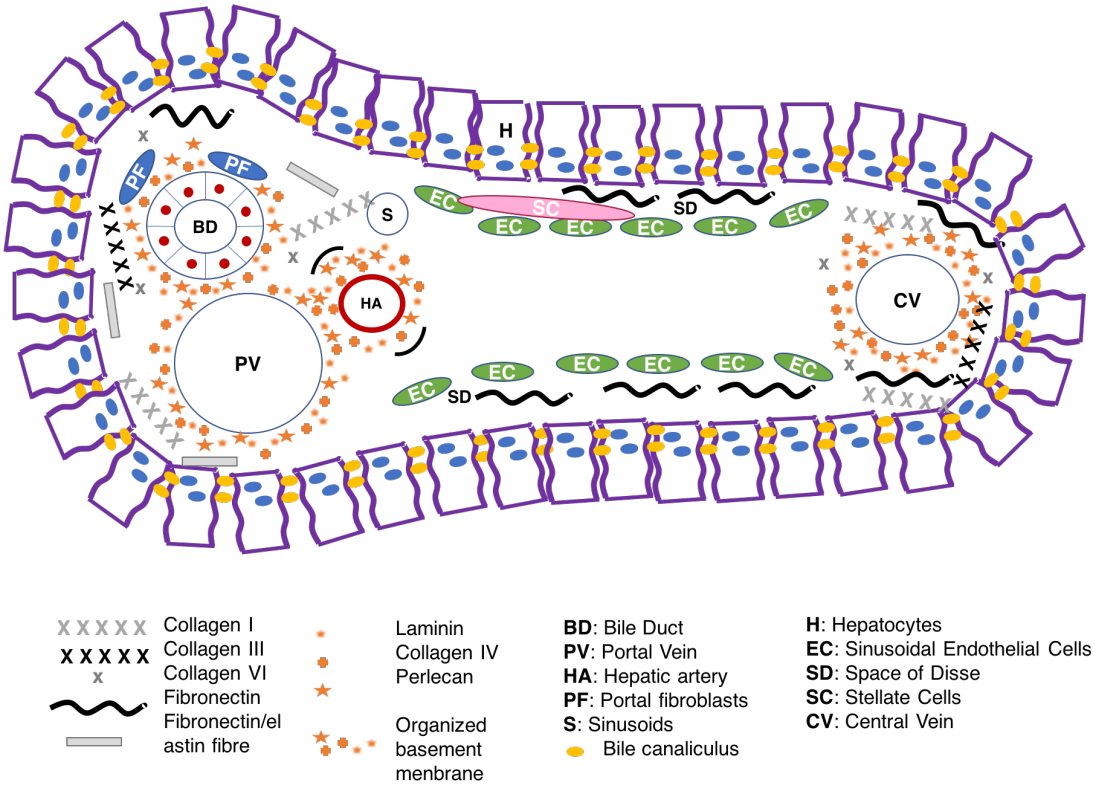

Figure 1.2 Distribution of extracellular matrix (ECM) in the liver acinus. A basement membrane is localized in the periportal and perivenous regions. Adapted from [7].

Besides the cellular component, the liver ECM composition and stiffness is of major importance for the maintenance of the parenchymal and non-parenchymal cell function. As represented in **Figure 1.2**, the hepatic parenchyma ECM is constituted by fibronectin and type I and III collagen, whereas the basal membrane, surrounding the blood vessels, is composed

by laminin, type IV collagen and perlecan. The endothelial sinusoids lack a basal lamina since the liver has no continuous barrier between epithelial cell surface and the plasma [7].

1.2 Role of liver in absorption, distribution, metabolism, excretion and toxicity (ADMET)

The liver is a unique organ regarding the large number of vital functions. Its main functions are nutrient homeostasis, by storing glycogen through glucose metabolism; ammonia detoxification, by synthetizing urea; filtration of particulates; protein synthesis, such as albumin; biotransformation of endo and xenobiotics; cholesterol synthesis and homeostasis; formation of bilirrubin and billiary secretion [9]. It is, thus, strategically located to maintain the body's metabolic homeostasis and it plays an essential role in ADMET (absorption, distribution, metabolism, excretion and toxicity) process for most drugs. In fact, the liver is one of the first organs contacting with oral xenobiotics after the process of absorption, through the portal vein. Within the liver, the distribution of molecules is facilitated by: (i) the capillary endothelium porosity, since the hepatic sinusoids present fenestrae that have 50 to 150 nm in diameter; (ii) the presence of specialized membrane transporters; (iii) accumulation in cell organelles and reversible intracellular binding. The hepatocytes' high exposure to xenobiotics and its metabolic defence mechanisms contribute to molecules biotransformation and subsequent excretion. About 73 % of the 200 most prescribed drugs suffer biotransformation as primary elimination pathway, whereas, 22 % and 5 % suffer renal and biliary elimination, respectively (**Figure 1.3**.) [10]. The biotransformation mechanisms are classified as phase I, II and III reactions as schematically represented in **Figures 1.3** and **1.4**.

1.2.1 Phase I metabolism

Phase I reactions are responsible for the increase in compounds' polarity by introducing or unmasking a functional group (*e.g.,* -OH, -COOH, -NH_2, or -SH) within a molecule to enhance its hydrophilicity. It can occur through direct introduction of the functional group or by modifying existing functionalities. This might result in the reduction of ketones or aldehydes to alcohols, the oxidation of alcohols to acids, hydrolysis of ester and amides, the reduction of azo and nitro compounds or also the oxidative N-, O-, and S-dealkylation. Several enzymes are responsible for phase I reactions; those include the cytochrome P450 (CYP450) enzymes, flavin-containing monooxygenases (FMOs), monoamine oxidases (MAOs) and xanthine oxidase/aldehyde oxidase (XO/AO) [10, 11]. As represented in **Figure 1.3**, CYP450 enzymes are responsible for 75 % of the drug metabolism of the 200 most prescribed drugs. There is a

total of 18 human CYP450 gene families among which only three have a role in xenobiotic metabolism, whereas the remaining families are involved in cholesterol biosynthesis, vitamin D metabolism, bile acid metabolism and biosynthesis catabolism of steroids [7, 12]. CYP3A, CYP2C and CYP1A are the most important enzyme families involved in drug metabolism, being responsible for 70 % of drug biotransformation, representing 50 % of CYP450 enzymes in the liver. The overall CYP450 metabolism shows a different distribution of metabolized drugs by each CYP450 enzyme (**Table 1.1**) when compared to the data presented in **Figure 1.3**, that refers to the 200 most prescribed drugs. In fact, the relative amount of CYP450 enzymes in the liver is not directly correlated with the extension of drugs biotransformation and its activity is susceptible of specific induction, which results in an altered capacity to biotransform its substrates (**Table 1.1**).

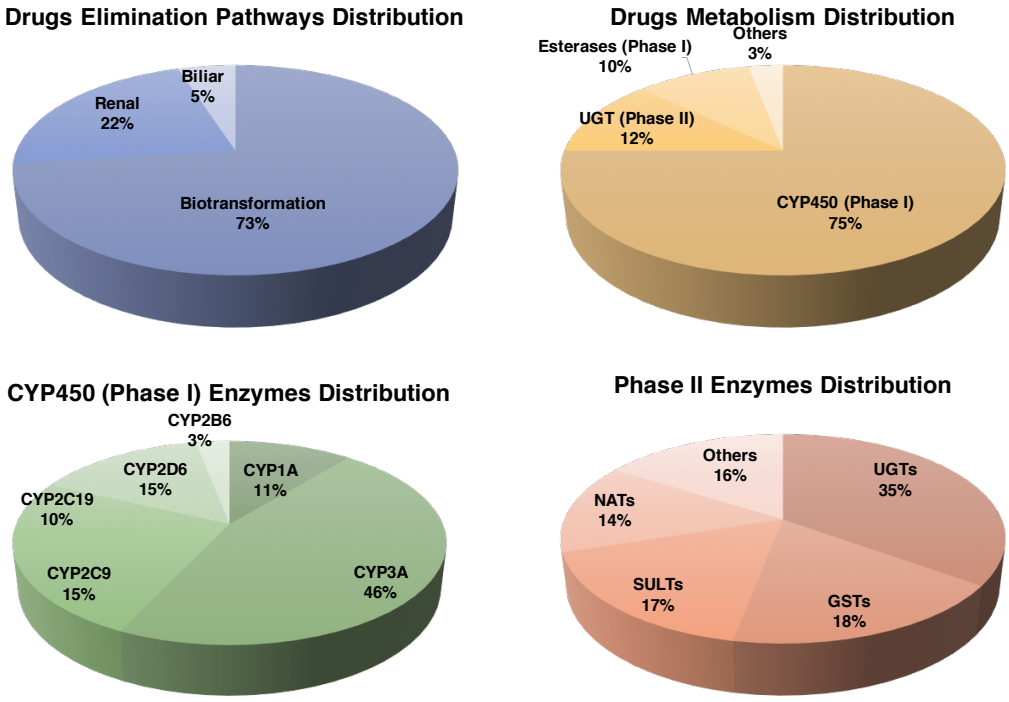

Figure 1.3 Elimination and Metabolism of the top 200 most prescribed drugs in 2002. [10, 11]

1.2.2 Phase II metabolism

Phase II reactions are characterized by the addition of a functional group through conjugation reactions performed by UDP-Glucuronosyltransferases (UGT), Sulfotransferases (SULT), Glutathione transferases (GST), aminoacid transferases, N-Acetytransferase (NAT) or Methytransferases (MT).

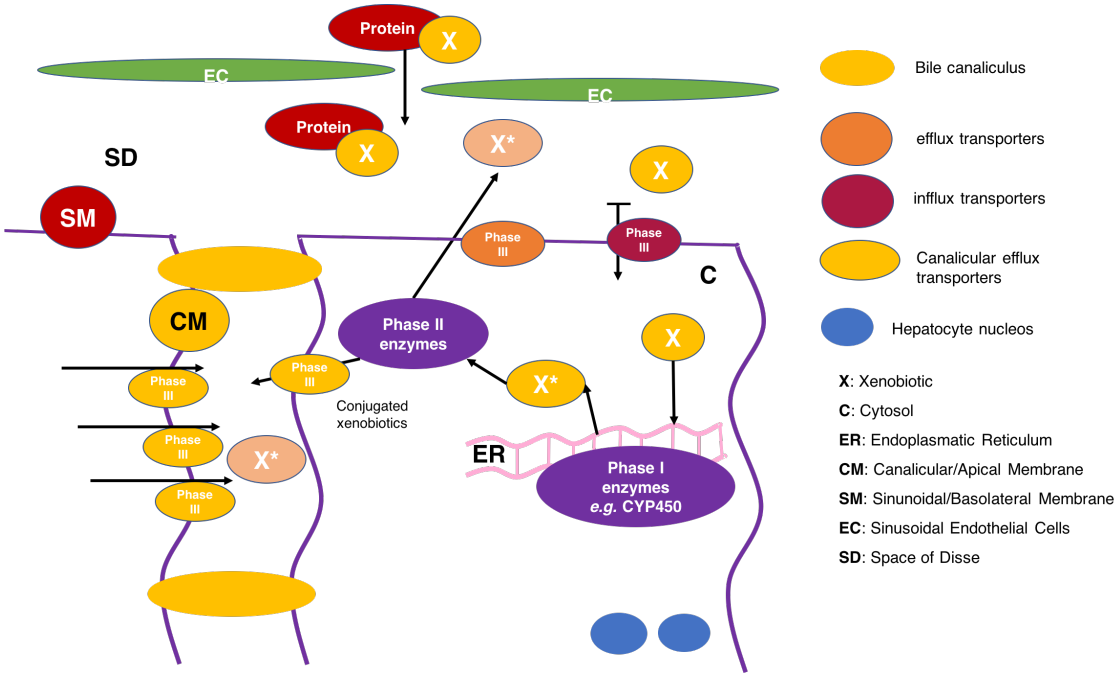

Figure 1.4 Elimination and Metabolism of drugs by the hepatocyte. Lipophilic xenobiotics (X) flow in sinusoidal blood and diffuse through the endothelial cell fenestrations into the space of Disse while still protein bound. Drugs may enter the hepatocyte by active transport or passive diffusion. Inside the cell, a drug will typically encounter a specific phase I enzyme, *e.g.* a CYP450 enzyme, capable of binding to the drug, and converting it to more water soluble and chemically reactive metabolites (X*). Typically, the resultant metabolite undergoes conjugation to a polar ligand in a reaction catalyzed by phase II enzymes. The resultant conjugated metabolite is then secreted by efflux transporters into the biliary canaliculus for excretion in bile, or secreted back into sinusoidal blood for ultimate excretion in urine, referred to as phase III metabolites. [7, 9, 13].

UGTs are responsible for 35 % of phase II drug metabolism being also important in bilirubin, steroid hormone, thyroid hormone, bile acid, and fat-soluble vitamin metabolism [14]. There are two broad families named UGT1 and UGT2, also known as the phenol/bilirubin family and the steroid/bile salt family, respectively. The liver is the major organ for glucuronidation, being UGT1A1 and UGT2B7 the most relevant enzymes for drug metabolism in the human liver [15].

SULTs are divided into four families, with the cytosolic SULTs being the most relevant enzymes for xenobiotic metabolism. In humans three SULT families, SULT1, SULT2, and SULT4, have been identified, containing at least 13 distinct members [16]. Within SULT1 family the isoform SULT1A1 was identified in a variety of species whereas SULT1A2, SULT1A3 and SULT1A4 were only identified in humans. In fact, SULT1A1 is the most expressed SULT in human liver [16]. SULT1A1 and SULT1A3 are abundantly expressed in the fetal liver whereas in adult liver SULT1A3 expression is much lower [16].

Table 1.1 Relative abundance of human CYP450 enzymes and their contribution to drug metabolism.

	Enzyme content in liver (% total CYP450)	Metabolized drugs by enzyme (%)	Examples of common substrates	Examples of common inducers
CYP3A4/5	29-30 %	30.2 %	Testosterone	Rifampicin Phenobarbital Carbamazepine
CYP2D6	1.5-4 %	20 %	Codeine Timolol Flecainide Dextromethorphan	Piperidines Dexamethasone Rifampicin
CYP2C9	12 %	12.8 %	(S) - Warfarin Phenytoin Rosiglitazone Tolbutamide	Rifampicin Carbamazepine
CYP2C8	7%	4.7 %	Ibuprofen Paclitaxel Cerivastatin	Rifampicin Carbamazepine
CYP2C19	0.2 %	6.8 %	Amitriptyline Diazepam Phenobarbital Lansoprazole (R/S) - Warfarin	Rifampicin Prednisone
CYP1A2	12-13 %	8.9 %	Caffeine Melatonin (R) - Warfarin	Rifampicin Phenobarbital
CYP2E1	7 %	3 %	Ethanol Paracetamol	Acetone Ethanol
CYP2B6	0.2-5 %	7.2 %	Nictoine Bupropion Cyclophosphamide Efavirenz	Clotrimazole Rifampicin Phenobarbital

Adapted from [17, 18]

GSTs are divided into two super-families comprising cytoplasmic and membrane bound enzymes. The cytoplasmic GSTs might also be present in nucleolus, mitochondria and peroxisomes and are responsible for 18 % of drug metabolism (**Figure 1.3**). This superfamily comprises five classes: α (A1-A4), μ (M1-M5), π (P1), κ (K1) and θ (T1, T2) [19]. In the liver,

GSTα is the most predominant class followed by GSTμ [20]. GSTs reduce the formation of hydroperoxides of fatty acids, phospholipids, cholesterol, and act against the redox-cycling of some quinone containing compounds, through glutathione conjugation. Thus, GST is part of the defence mechanisms against reactive oxygen species. GSTs have also an important role on the transport of a wide variety of both endogenous and exogenous compounds [21]. Glutathione (GSH) conjugation is not always enzymatic since hydrophobic molecules containing an electrophilic atom might react non-enzymatically with glutathione. This includes a variety of electrophilic xenobiotics resulting in glutathione conjugates that are thioethers, formed by nucleophilic attack of glutathione thiolate anion (GS–) with an electrophilic carbon atom in the xenobiotic containing electrophilic heteroatoms (O, N, or S) [9].

1.2.3 Phase III metabolism

Phase III reactions comprise the role of the transport of endo and xenobiotics and its metabolites. The hepatic transporters can be classified as (i) influx transporters, located in the sinusoidal/basolateral membrane, responsible for the uptake of molecules into the hepatocytes; and (ii) efflux transporters, that are mostly located in the canalicular/apical membranes, but may also be located in the sinusoidal/basolateral membrane as represented in **Figure 1.5**. The influx transporters include the Na^+/bile acid cotransport protein (NTCP) and three families of organic ion exchanger transporters: OATP, the organic anion transporter protein family; OCT, the organic cation transporter family; and OAT, the organic anion transporter family [7]. The OATP family is also named as glycoprotein transporters, particularly important for drug transport and bilirubin uptake. OATP1B1 and OATP1B3 are liver specific, being OATPC1A2 and OATP2B1 also present in liver [22]. The efflux transporters include the ATP-binding cassette (ABC) family and the organic solute transporter α/β (OSTα / OSTβ), responsible for bile acid transport. The canalicular/apical ABC family transporters comprise two functional classes: (i) the solute transporters such as the cation transporter multidrug resistance protein 1 (MDR1) also known as P-glycoprotein 1, the bile salt export pump (BSEP), the xenobiotic transporter breast cancer resistance protein (BCRP), and the multidrug resistance-associated protein 2 (MRP-2) also known as multi-specific organic anion transporter 2; and (ii) the translocators such as the phospholipid flippase MDR3, and the ABC half transporters involved in cholesterol transport ABCG5/8. On the sinusoidal/basolateral membrane there is the OSTα/OSTβ transporter and the ABC transporters: MRP1 that transports various organic anions including GSH, glucuronide and sulfate conjugates of several drugs; MRP3 that is an organic anion transporter that primarily transports bile salts and drugs into the blood; MRP4 and MRP5 that can transport cyclic nucleotides and

nucleoside analogues; and MRP6, which substrate specificity is still unclear. The more relevant hepatic transporters involved in drug transport are OATP1B1, MRP-2, BCRP and MDR1 [7]; whereas MRP1 and MRP3 expression is more relevant in cholestatic conditions, when both are substantially induced. Thus, the existence of this transporters allow large (>400 Da) amphiphilic molecules, xenobiotics or its metabolites to be eliminated by the hepatocytes [9].

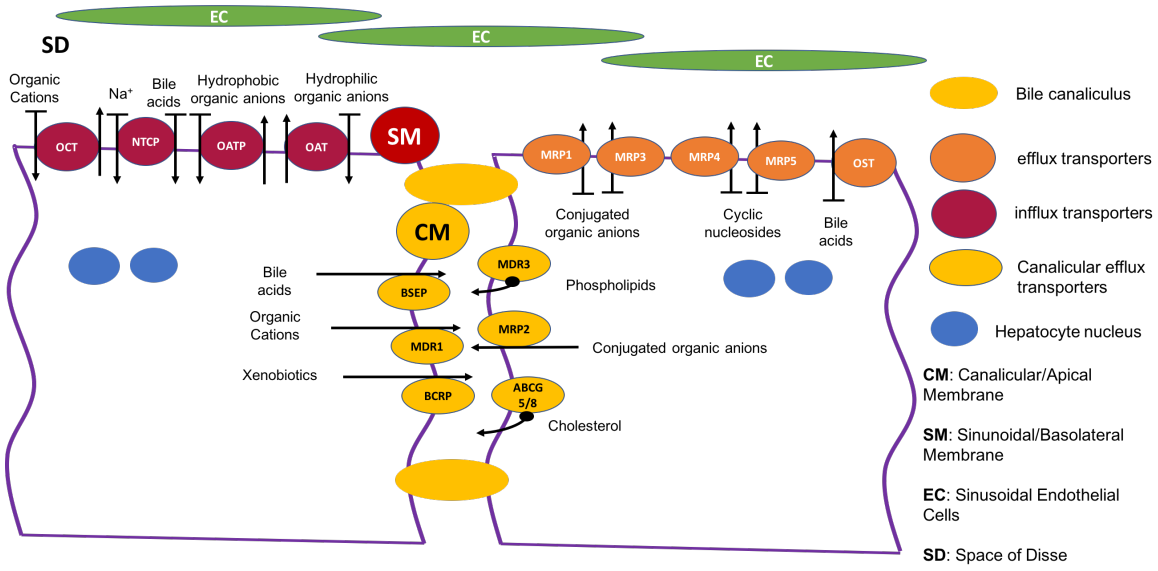

Figure 1.5 Schematic representation of the hepatic transporters in the sinusoidal/basolateral and in the canalicular/apical membrane of hepatocytes. [7, 9, 13].

1.2.4 Regulation of the metabolism of xenobiotics: the role of nuclear receptors

Detoxifying enzymatic and transport systems, comprising phase I, II and III enzymes, are regulated at the gene expression level by nuclear receptors. Nuclear receptors are activated by both xenobiotics and endogenous lipophilic substances, being also named as xenosensors or lipid sensors, respectively. The nuclear receptor gene superfamily is divided into: (i) nuclear steroid hormone receptors and (ii) the orphan nuclear receptors. The nuclear steroid hormone receptors are activated by endogenous steroid hormones binding to the DNA as homodimers. Examples of nuclear steroid hormone receptors include the glucocorticoid receptor (GR), mineralocorticoid receptor (MR), estrogen receptor (ER), androgen receptor (AR) and progesterone receptor (PR). The orphan nuclear receptors bind to the DNA as heterodimers with the retinoid X receptor (RXR). The orphan nuclear receptors include the constitutive androstane receptor (CAR), the pregnane X receptor (PXR), and the peroxisome proliferator activated receptor-alpha (PPARα) being frequently activated by xenobiotics [23]. The aryl hydrocarbon receptor (AhR) also plays an important role as xenosensor although not falling

into the nuclear receptor family [24]. PXR and CAR expression is also mediated by the GR. Examples of prototypical chemical inducers of these receptor systems include phenobarbital, a CAR activator; rifampicin, a human PXR activator; and the fibrate drug, clofibrate, a PPARα activator [24, 25].

The mechanism of xenosensor activation is similar for the different receptors. Briefly, it consists in the ligand binding to the receptor in the cytoplasm, the interaction with co-activators, dimerization with a partner protein forming a DNA-binding heterodimer, translocation to the nucleus, binding to DNA through response elements, recruitment of transcription factors and gene transcription, resulting in increased mRNA levels of xenobiotic-biotransforming enzymes and transporters [9, 26].

In drug metabolism, PXR and CAR are the most relevant nuclear receptors, regulating a number of genes involved in drug metabolism and transport such as *CYP3A*, *CYP1A*, *CYP2C9*, members of the UGT, SULT and carboxylesterase families and the hepatic transporters *OATP1*, *MDR1* and *MRP2* [27], as represented in **Table 1.2**. CAR alone is also known to upregulate the genes *CYP2B*, *CYP2C*, *CYP3A*, NADPH-CYP reductase, SULTs, UGTs, and GSTs, as well as the hepatic transporters *MRP3* and *MRP4* [24]. AhR regulates *CYP1A* induction [24, 28].

The molecular regulation of phase II enzymes is still not fully understood and the available studies are more scarce than for phase I and III enzymes [15]. UGTs and SULTs induction, inhibition and regulation mechanisms are the ones with higher impact on xenobiotic metabolism, followed by GSTs. In fact, the difficulty of studying phase II enzymes relies on its broad substrate and unclear regulation mechanisms, since phase II metabolism commonly depends on the exposure to phase I metabolites and on the rate of drug and metabolites transport into and out of the hepatocytes. UGT regulation may be mediated through AhR (*UGT1A6* and *UGT1A9* induction), CAR and PXR (*UGT1A1*). SULTs regulation is still controversial. Although it is agreed that both GR and PXR upregulate *SULT1A* and *SULT2A* in rat, human *SULT1A* expression is not altered by glucocorticoids [29].

Table 1.2 Xenosensors target genes associated with xenobiotic metabolism and transport in humans and rodent animal models.

	Human		Animal Models		
	Gene	**Receptor**	**Gene**	**Origin**	**Receptor**
Phase I enzymes	*CYP2A6*	PXR	*CYP1a1*	Mouse	CAR
	CYP2B6	CAR/PXR	*CYP1a2*	Mouse	CAR
	CYP2C8	CAR/PXR	*CYP2a4*	Mouse	CAR
	CYP2C9	CAR/PXR	*CYP2b10*	Mouse	CAR/PXR
	CYP2C19	CAR/PXR	*CYP2B1/2*	Rat	CAR/PXR
	CYP3A4	CAR/PXR	*CYP2c29*	Mouse	CAR
	CYP3A7	PXR	*CYP3a11*	Mouse	CAR/PXR
	CYP4F12	PXR	*CYP3A2*	Rat	PXR
	CYP7A1	PXR	*CYP3A23*	Rat	PXR
	FMO5	CAR			
Phase II enzymes	*UGT1A1*	CAR/PXR/AhR	*Ugt1a1*	Mouse	CAR/PXR
	UGT1A3	PXR	*Ugt1a6*	Mouse	CAR
	UGT1A6	PXR	*Ugt1a9*	Mouse	CAR/PXR
	GSTA1	PXR	*Ugt2b1*	Mouse	CAR
			Ugt2b5	Mouse	PXR
			Gsta1/2	Mouse	CAR/PXR
			Gst (α,π,μ)	Mouse	PXR
			Sult2a1	Mouse	CAR/PXR
			Sult1e1	Mouse	CAR/PXR
			Sult2a2	Mouse	CAR/PXR
	SULT1A1	CAR	*SULT1A1*	Rat	PXR
			SULT1B1	Rat	PXR
			SULT2A3/4	Rat	PXR
Phase III enzymes	*MDR1*	CAR/PXR	*Mdr1a*	Mouse	CAR/PXR
	MRP2	CAR/PXR	*Mdr1b*	Mouse	PXR
	MRP3	CAR	*Mrp1*	Mouse	CAR
	MRP4	CAR	*Mrp2*	Mouse	CAR/PXR
	OATP2	PXR			

Adapted from [24, 28]

1.3 Mechanisms of drug induced hepatotoxicity

The liver has a unique differentiation and regeneration capacity, quickly reacting to injury and cell loss through biochemical reactions and cellular processes, based on complex gene regulation activities. The highly active biotransformation activity of the liver contributes to the first-passage effect that avoids the exposure of the organism to high concentrations of oral xenobiotics. As such, the metabolism and elimination processes are essential for the liver's protective role but also makes it more exposed to molecule's toxic effects displayed by a plethora of chemicals. Thus, the liver is also a key target organ of xenobiotic toxicity. One of the major safety regards on new drug development is drug induced liver injury (DILI). DILI has an incidence of 1-2 cases per 100,000 people. However, it should be noted that DILI accounts for more than 50 % of acute liver failure occurrences and represents one of the major causes of withdrawal of drugs from the market [30]. Some examples are bromofenac, ebrotinin and troglitazone, or even nevirapine (NVP), risperidone, trovafloxacin and nefazone that were labeled with hepatic *black box warnings* [31, 32].

DILI can be classified as intrinsic or idiosyncratic hepatotoxicity, and the latter can be an allergic immune-mediated hypersensitivity, or non-allergic metabolic injury [33]. Intrinsic hepatotoxicity is direct, dose-dependent and predictable whereas idiosyncratic hepatotoxicity occurs without obvious dose-dependency, in an unpredictable fashion and with a short latency time particularly after re-exposure [34, 35]. Idiosyncratic hepatotoxicity is particularly difficult to mimic in in vitro models. As such, in vitro hepatotoxicity models are mainly focused on accessing metabolism related toxicity, namely on identifying potential metabolites of the parent drug and its mechanisms of toxicity. Moreover, this is essential in the early stages of drug development and thus, only intrinsic hepatotoxicity will be further mentioned. Intrinsic toxicity can occur through direct damage, through failure of repairing mechanisms and through immune mediated responses, attributed directly to the interaction of the ultimate toxic molecule, the parent drug or the product if its biotransformation, with an endogenous target through non-covalent or covalent binding, hydrogen abstraction, electron transfer or enzymatic reactions resulting in dysfunction or destruction of target molecules. Specifically, toxicity may occur through the interaction of toxicants with proteins, impairing its function or by alteration of its conformation or structure. Toxicants may also interact with protein critical moieties, such as thiol groups, that are commonly related to enzymes catalytic activity. Thereby, molecular toxicity may lead to impairment of internal and external cellular maintenance.

Impairment of internal maintenance can be due to ATP depletion, Ca^{2+} accumulation and ROS/RNS (reactive oxygen species/reactive nitrogen species) generation which may result in

cell apoptosis [9, 36]. Nimesulide, a non-steroidal anti-inflammatory drug (NSAID), is reported to cause severe hepatotoxicity through molecular mechanisms involved in deranged oxidant-antioxidant homeostasis and mitochondrial dysfunction. In fact, nimesulide toxicity is related to redox imbalance along with oxidative stress, reduction of NADPH and GSH pools and, consequently, increased superoxide and secondary ROS/RNS generation. This alteration on redox equilibrium leads to oxidative damage of cellular macromolecules [37]. Additionally, nimesulide causes mitochondrial activity reduction, mitochondria depolarization and membrane permeability loss followed by release of apoptotic proteins [37]. Another common direct hepatotoxic drug is paracetamol that can lead to fatal liver damage and is an example of the importance of the balance of metabolic pathways on xenobiotics toxicity. This drug is metabolized mainly by conjugation with sulfate and glucuronic acid and, to a lesser extent, by oxidation through microsomal mono-oxygenases. Paracetamol oxidation generates N-acetyl-p-benzoquinone imine (NAPQI) a toxic metabolite that is detoxified by glutathione conjugation. Overdose of paracetamol originates an increased concentration of NAPQI that results from the saturation of the conjugation pathways and depletion of cofactors, namely of sulfate pools and favours the oxidative metabolism of paracetamol, depleting all the glutathione pool. Consequently, not only the glutathione pool is depleted, but also, the NAPQI (toxic metabolite) accumulates in the organism exerting its toxicity which leads to hepatic necrosis [38]. Paracetamol toxicity is also related to Ca^{2+} accumulation and activation of endonucleases, DNA damage and necrotic and apoptotic cell death through its protein-arylating intermediate metabolite [39].

Impairment of the external maintenance of the tissue can have a major impact when a tissue is unable to perform its main functions. The deregulation of the biotransformation processes may result in altered transporter and enzyme functions that may originate intrahepatic cholestasis leading to toxic accumulation of metabolism products in hepatocytes [39, 40]. The inhibition of hepatic synthesis of coagulation factors by exposure to coumarins, is also an example of this mechanism of toxicity: coumarins do not directly harm the liver. However, the synthesis of coagulation factors in the liver is impaired by overexposure to coumarins, resulting in whole body damage since this inhibition may cause death by hemorrhagic shock [9].

Hepatotoxicity may also be a consequence of impaired molecular repair mechanisms of (i) proteins, as occurs by thioredoxin reduction of oxidized thiol catalytic moieties, with methionine sulfoxide reductases catalyzing the latter process; of (ii) lipids, as occurs when lipoperoxidation is counteracted by the presence of reductants and glutathione peroxidase and reductase; and of (iii) DNA. DNA has high reactivity with electrophiles and free radicals

but nuclear DNA is remarkably stable due to the availability of repair mechanisms such as direct repair, excision repair and recombinant repair. The mitochondrial DNA, however, lacks histones and efficient repair mechanisms and therefore is more prone to damage [9]. Cellular and tissue repair is well present in response to toxic stimuli reverting damage through elimination of injured cells by apoptosis or necrosis and regeneration of the tissue by proliferation and production of new extracellular matrix. In fact, inappropriate repair and adaptation to a repeated exposure to a xenobiotic can result in tissue necrosis, fibrosis or carcinogenesis. Tissue necrosis occurs when molecular repair mechanisms are inefficient, are depleted or the molecular damage is not readily reversible [9]. Hepatic fibrosis, cirrhosis, results from chronic exposure to chemicals such as methotrexate, high doses of retinol (vitamin A) and iron intoxication. Those chemicals trigger stellate cells to respond to cytokines and growth factors secreted by non-parenchymal cells (NPC), including themselves. This results in an induction of extracellular matrix production during tissue repair that does not cease properly. Thus, there is an excessive deposition of extracellular matrix of abnormal composition [9]. Carcinogenesis can result from failure of DNA repair that leads to mutation of critical genes, inappropriate control of regulatory gene regions over expression of critical genes, failure to induce apoptosis, and failure to terminate cell proliferation [9], being inorganic arsenic an example of an hepatic carcinogenic [41].

Furthermore, adaptation to toxicity may result from biological changes causing: (i) diminished delivery of toxicant to the target, (ii) decreased susceptibility of the target, (iii) increased capacity of the repairing mechanisms or (iv) strengthening of the mechanisms that compensate for toxicant-inflicted dysfunctions. Induction or inhibition of several enzymes, such as detoxifying enzymes, *e.g.* from the CYP450 family, repair enzymes as thioredoxins, as well as induction of tolerance of cellular receptors [9], are examples of adaptation mechanisms presenting an indirect toxicity problem of many drugs, which is especially relevant in multiple drug prescription. Widely prescribed drugs are potent CYP450 enzyme inducers, *e.g.* phenobarbital, omeprazole and rifampicin (**Table 1.1**), or inhibitors, *e.g.* as fluoxetine, proton pump inhibitors and ciprofloxacin. Consequently, the biotransformation of other drugs that are substrates of CYP450 enzymes, or of other phase II enzymes and hepatic transporters, can be severely altered when taken simultaneously. Some xenobiotics, such as efavirenz or nevirapine, might also be simultaneously the substrate and the inducer of an enzyme or transporter and can regulate its own biotransformation (auto-inducer). Enzyme induction is included within the pharmacokinetic tolerance concept, which is defined by an alteration of drug disposition or metabolism as a function of time upon exposure to a compound resulting in a time-dependent change in the presentation of the active moiety to the

target receptor. Consequently, this can lead to overdose reactions or to sub-therapeutic exposures to drugs when normal doses are taken [9, 24, 42].

Overall, drug induced hepatotoxicity may involve metabolism of toxic reactive intermediates and covalent interactions with cell constituents. It may also interfere with membrane transport, biosynthesis processes or immunological mechanisms. The occurrence of hepatic damage may vary, depending on the nature of immune responsiveness as well as factors related to genetics, dietary habits and other behaviour and environment-related factors. Hence, risk factors are important parameters to consider when predicting potential hepatotoxicity risks. Risk factors are genetic polymorphisms, environmental influences on metabolizing enzymes, hormonal factors once women are statistically more sensitive, and immunological and pre-existing liver diseases, which is especially important in HIV patients with B or C hepatitis and fatty liver [36]. Genetic polymorphisms are particularly relevant risk factors regarding drug-metabolizing enzymes. Genetic polymorphisms are reported to affect drugs biotransformed by CYP2C9, CYP2C19 and CYP2B6 subfamilies, the hepatic transporters MDR1, BCRP, MRPs and OATP1B1, among others [10, 43, 44]. Some genetic polymorphisms have a confirmed impact in therapy and are commonly considered in drug development and in drug treatment (biomarkers of susceptibility). Some examples are: CYP2D6 that has a clinical impact on the bioactivation of drugs such as codeine, tramadol or tamoxifen within low or extensive metabolizers; UGT1A1, that results in benign hyperbilirubinemia, known as Gilbert–Meulengracht disease, and its genotype identification is recommended in the drug label of the topoisomerase inhibitor irinotecan; and NAT2 polymorphisms. NAT2 polymorphism is reflected in slow and rapid acetylators, that represent 50 % of Caucasian populations. Izoniazid is a substrate of NAT2 and slow acetylators have higher blood concentrations and adverse effects than the rapid acetylators [44].

1.4 Liver cell models in in vitro toxicology

Drugs are deeply involved in liver damage, but establishing causality has been a major hurdle in understanding most of the toxicity mechanisms [40]. The effect that xenobiotics can exert on induction or inhibition of detoxifying enzymes, namely from CYP450 family, hepatic transporters, repair enzymes and induction of tolerance of cellular receptors is especially difficult to predict with the currently existing in vitro and in vivo drug testing models, mainly due to interspecies and inter-individual differences. 40-50 % of drug candidates showing hepatotoxicity in humans did not present the same in animal models, which shows the importance of an improvement of in vitro models using human cells [45]. On the other hand,

relevant drugs might be excluded from development when toxicity is observed in animal models while those molecules might present no relevant human toxicity. Pantoprazol (5-(difluormethoxy)-2-[3,4-demethoxy-2-pyridyl)methylsulfinyl]-benzimidazole) is an example of a drug with relevant toxicity in rodent and canine models due to the hepatic formation of benzimidazo-2-thiol. However, this metabolite is not detected in humans and pantoprazol is today widely-used in human pharmacology as a proton pump inhibitor [46].

According to the United States National Research Council (NRC) report on "Toxicity Testing in the 21st century: A vision and a strategy" (US Tox21), the existing concepts and testing procedures are not sufficiently adequate for extrapolation to human beings, lacking physiological as well as representative assay conditions [47]. The improvement of in vitro testing using more relevant models for accurate assessment and prediction of adverse drug reactions will eventually reduce animal experimentation, following the 3R principles, it is a key to increase success in drug development and would avoid non-reasonable costs during clinical introduction of a new drug candidate [48].

The 3R principles comprise Reduction, by decreasing animal number required for a test method using integrated approaches consistent with scientific practices necessary to obtain valid results; Refinement, by improving animal well-being and reducing or eliminating pain or distress; and Replacing, by using systems alternative to animals, or using a phylogenetically lower species than the current test [49]. The development and implementation of alternative in vitro models is thus in line with the current 3R view, namely the replacement principle.

Currently, in vitro hepatotoxicity models are based on the use of liver slices, genetically engineered cells, monolayer (2D) or suspension cultures of human hepatoma cell lines or primary hepatocytes. The advantages and limitations of each tissue/cell source for in vitro testing are described in **Table 1.3**.

Table 1.3 Advantages and limitations of in vitro liver preparations.

Model	Advantages	Limitations
Isolated perfused liver	Maintenance of functions close to the in vivo organ Lobular structure preserved Functional bile canaliculi and possibility of bile collection Short-term kinetic studies	Viability: 2-3 h Study of one or a few compounds only Suitable only for liver of small animals No reduction in the number of animals used
Liver slices	Lobular structure preserved Detection of selective intra-lobular effects	Viability: 6 h to 2 days No possibility of bile collection

	Possibility to use human tissue Studies on several compounds at different concentrations	Inter-assay variability Human tissue availability / Interspecies differences
Isolated hepatocytes	Obtained from whole livers or wedge biopsies Functions close to those of in vivo hepatocytes Studies on several compounds at different concentrations Interspecies and Pharmacogenomics studies Representative of different lobular subpopulations Cryopreservation	Viability: 2-4 h No bile canaliculus Human tissue availability / Interspecies differences
Primary hepatocyte cultures (pHep)	Longer viability than isolated tissue Induction/inhibition of drug metabolizing enzymes Interspecies and Pharmacogenomic studies	Viability: 2-4 days Early phenotypic changes Altered bile canaliculi Difficult recovery of cells and maintenance of function upon cryopreservation Human tissue availability / Interspecies differences
Hepatoma cell lines (HepG2, Huh7)	High proliferation activity and good availability Stable metabolic performance Well characterized and abundant data available	Decreased drug enzyme activities Genotype instability
HepaRG	Retains many liver-specific functions (CYP450) Stable karyotype Differentiation into both hepatocyte or biliary lineages	Derived from one donor Distinct profile of phase II and III enzymes expression relative to hpHep Less available than other cell lines
Stem cell derived hepatocyte-like cells (HLC)	Good availability Analysis of genetic polymorphisms Drug testing with patient-specific cell lines for personalized medicine Characterization of differentiation/maturation processes for potential in vitro or clinical use Establishment of disease models	Costly differentiation protocols Incomplete hepatic differentiation with current protocols Lack of standardized methods for cell differentiation and characterization
Subcellular fractions	Drug enzyme activities preserved Production of metabolites for structural analysis	Short-term studies No cytosolic phase II enzyme reactions Cofactors required for activity
Genetically engineered cells	One or more human enzymes expressed Available mainly for CYPs Unlimited cell number	Use for specific purposes only No physiologic levels of enzymes

The cell culture models are advantageous relative to the use of perfused livers or liver slices since they allow longer cell culture time; and relative to subcellular fractions due to the possibility of a more complete biotransformation phenotype, including phase I, II and III. Distinct cellular models present also major drawbacks [48, 50]. Primary cultures of hepatocytes present important interspecies differences when isolated from rat. Human primary hepatocytes are scarce and present high donor variability. Furthermore, liver-isolated hepatocytes although originating representative phenotypic and functional profiles, soon lose those properties in vitro [7], thus compromising long-term metabolic studies. Human hepatoma cell lines, such as HepG2, Huh7 and HepaRG have low metabolizing activity and poor phenotype and functional match to the hepatocytes in vivo [51]. HepG2, have low levels of CYP450 enzymes but normal levels of phase II enzymes except for UGTs [52, 53], which make them appropriate for testing the toxicity of the parent compound but less suited for metabolite toxicity testing. More recently, HepaRG cells, a human hepatocellular carcinoma cell line composed of a mixture of both hepatocyte-like and biliary-like cells, has been reported to maintain hepatic functions and expression of liver-specific genes comparable to that of human primary hepatocytes (hpHep) without inter-donor variability and functional instability [54]. Nevertheless, Gerets *et al.* [55] have characterized primary human hepatocytes, HepG2 cells, and HepaRG cells at the level of mRNA/gene expression and CYP activity in response to inducers and their prediction capacity for the detection of human hepatotoxins and hepatotoxic drugs and observed that although HepaRG cells seem to be a suitable model for the induction studies, these cells were not as predictive as hpHep and were quite comparable to HepG2 cells for the prediction of human hepatotoxic drugs [55]. Lübberstedt *et al.* [56] also showed that HepaRG present comparable or even higher CYP2C9, CYP2D6 and CYP3A4 enzyme activity than that of hpHep [56] and present relevant UGT1A1 and GST activity levels [57]. However, when cultured using a three-dimensional (3D) bioreactor, HepaRG cells were not able to retain OATP1B1 activity and its detection at protein level was also significantly decreased when compared to 3D hpHep over 9 days in culture [58], being the function of hepatic transporters the NTCP and BSEP also reported to be less functional in HepaRG cells [59]. Therefore, due to the unsatisfactory phenotype of the currently available cell sources, the use of stem cell-derived hepatocyte-like cells has been proposed as an alternative cell source for in vitro hepatotoxicity studies and will be further explored in the **Section 1.6** of this Chapter.

1.4.1 3D culture systems in in vitro toxicology

The major drawback of the currently available in vitro liver preparations lays on insufficient hepatocyte-like functions and metabolic competence. A valid alternative for in vitro toxicology

testing comprise more predictive cell cultures closer to the in vivo environment. 3D cell culture systems apply tissue bioengineering approaches to obtain physiologically relevant in vitro liver cellular models. Those cell culture systems have been shown to improve the biotransformation capacities in both primary hepatocytes [48, 60-65] and hepatoma cell lines [66-68] over time in culture. In fact, by mimicking cell-to-cell and cell-to-matrix interactions such models can be of enormous impact for testing drug susceptibility effects in vitro. These systems have the potential of enabling the validation of molecules as therapeutic targets, to assess their safety, with higher accuracy and decreasing the number of sacrificed animals [66, 69].

3D cell cultures can be achieved using either dynamic or static systems. Dynamic systems might be stirred or perfused, depending on the cell culture system complexity; whereas a stirred system might be perfused [70] or not [71]. Stirred system allow for a better medium oxygenation, since the mechanic stirring facilitates oxygen diffusion as well as medium homogenization, further resembling the physiological blood flow. Mechanic stirring also creates a hydrodynamic shear stress that shall be balanced between causing cellular stress and death and improving cell performance [72]. It has been reported that some CYP450 genes are induced through blood flow-mediated shear stress [72, 73]. An in vitro study performed by Vinci *et al.* [74] showed that flow positively affects the expression and activity of detoxification genes of phase I, II and III, in primary human hepatocytes [74]. Stirred and/or perfused systems also promote a liver-like mass transfer which might induce the liver zonation phenomenon in vitro. A continuously perfused system further creates a more physiological culture condition since it has the advantages of a stirred system but further avoids fluctuations of basic cell culture parameters such as pH, oxygen, glucose and lactate concentration and accumulation of other cell culture products that are present in discontinuous renewal of fresh culture media [62-64, 70]. Mimicking the blood flow is particularly interesting in hepatocyte cell culture and in xenobiotic metabolism studies, by avoiding the accumulation of metabolites that influence the pharmacokinetics of a specific compound [75] .

3D culture systems are ease of high throughput adaptation and of up scaling, but vary in complexity and on remote monitoring of cell culture parameters. Three-dimensional systems can comprise spheroids formation (**Table 1.4**), cells adherent to a scaffold [76, 77], or more complex cellular systems such as HμREL® biochip [78], hollow-fiber bioeactor [64], multi-well perfused bioreactor [79], bioartificial livers [80] and more recently the microfluidic devices [75, 78, 81, 82] and the bioprinted systems [75] (**Table 1.5**).

Table 1.4 Advantages and limitations of spheroid cell cultures for in vitro toxicity testing applications.

Spheroid forming techniques	Advantages	Limitations
Non-adhesive surface **Ultra-low attachment plate**	Low cost Easy to perform Co-culture of different cell types	Variation in size/cell number/shape
Stirred Bioreactors	Low complexity Massive production Long-term culture Dynamic control of culture conditions Co-culture of different cell types Adaptable to perfusion Adaptable to online monitoring Easy to scale up	Require specialized equipment
NASA rotary system	Low complexity Massive production Long-term culture Dynamic control of culture conditions Better cell differentiation Co-culture of different cell types	Require specialized equipment Variation in size/cell number Cell sampling not possible
Hanging drop	Inexpensive Easy to perform Well-controlled spheroid size Fast spheroid formation Co-culture of different cell types Easy to trace spheroid assembly	Labor intensive Massive production difficult
Micro-molding	Well-controlled spheroid size Co-culture of different cell types Designed aggregate geometry	High complexity Requires specialized facilities

Adapted from [83, 84]

The multicellular spheroid is a 3D system that takes advantage of the self-assembling capacity of cells to form aggregates and maintain cell viability, over an extended time in culture while keeping a better hepatocyte-like functional phenotype when compared with 2D cultures [61, 68, 70, 85-87]. Non-adhesive surfaces allow the formation of multicellular spheroids usually under a static system. Herein, spheroid size is controlled by the cell density at inoculation and fetal bovine serum (FBS) concentration. This approach is less complex and easier to perform than other spheroid systems that require specialized training (*e.g.*, hanging drop technique),

or the use of a scaffold or matrix, or bioreaction systems. Thus, non-adhesive surfaces are especially advantageous to optimize culture medium supplementation and to test a diversity of toxic compounds using fewer cells (this system is available from a 384-well plate format to large cell culture flasks up to 636 cm^2). Non-adhesive surfaces have been previously used in small-scale 3D cell culture systems, applied either to stem cell [88, 89] or hepatic cell lines in culture [90].

The spinner flask suspension culture (SFSC) is a simple and effective stirred system that has been previously described for culturing primary hepatocytes where cells maintained their functions up to 3 weeks, namely albumin and urea secretion and biotransformation activity of phase I and phase II enzymes [61, 70, 71, 85]. Herein, the spheroid dimensions can be controlled by the agitation rate that further promotes a high homogeneity of the medium and quick dilution of toxic metabolites, while allowing a greater distribution of nutrients and oxygen, therefore reducing cell death [71]. This system has the possibility for up-scaling (125 mL to 36 L of working volume) and can be adapted to a perfusion system. It is also possible to monitor the culture online [70] or to sample and collect cells or cell culture medium for several analyses [91], which is particularly interesting for drug pharmacokinetic studies.

Another example of a perfused system is the hollow-fiber bioreactor [92-95]. This system was originally developed to function as extracorporeal liver support system. It was firstly designed to accommodate a 3D perfusion, high-density culture of human liver cells with a cell compartment volume of 800 mL [96]. This system consists on a complex capillary network, based on three independent interwoven capillary systems for arterio-venous medium perfusion, oxygen supply, and carbon dioxide removal, with an electronically controlled perfusion device with pumps for medium feed and recirculation, temperature control and a valve regulated by a gas mixing unit. There are several capillary layers, their number depending on the bioreactor size, that serve for counter-current medium perfusion through two independent capillary systems and direct membrane oxygenation of the cells located between the capillaries [62-64]. Later, the hollow-fiber bioreactor was also miniaturized to cell compartment volumes of 8, 2 and 0.5 mL for drug testing applications [63, 64, 95] and presented impressive results at a physiological [62] and biotransformation level using human primary hepatocytes in culture up to 2 weeks [64, 95]. The large number of cells that is needed and the challenging setup make this system applicable for medium throughput. In addition, cell sampling during culture time is also not feasible. Nevertheless, as with the spinner vessels this system enables online measurements and medium sample collection making it still particularly interesting for long-term studies, namely pharmacokinetic/toxicokinetic and mechanistic studies [92-95].

Table 1.5 Advantages and limitations of complex in vitro hepatotoxicity cell model systems.

Cell models	Advantages	Disadvantages
H μ REL® biochip	Moderate throughput Allows for multiple cell types and interaction between cell types Preservation of cell viability and metabolic competency Microscopic imaging and oxygen sensing Physiologically relevant ratios of liquid : cells and shear stress Requires less media and cells than traditional culture Good correlation with in vivo clearance rates	A complex system to establish and maintain Sample removal difficult No 3D tissue constructs
Hollow-fibre Reactor	Moderate throughput Counter-directional flow Scalable Long-term culture Possibility of PBPK studies Real-time monitoring of metabolic function	A complex system Microscopic evaluation is only possible in the end of the experiment High number of cells Cell sampling not possible
Multi-well perfused bioreactor	High throughput Cells form 3D tissue constructs Sustained liver-like cell functionality Physiological shear stress Good correlation with in vivo clearance rates Ability for microscopic examination	Uses greater cell numbers and larger media volumes
Bioartificial livers	Low throughput Microenvironment most similar to in vivo tissue Allows for studies of functional heterogeneity Ability to evaluate hepatotoxicity using human blood	Does not maintain viability or functionality of hepatocytes longer Requires large number of cells Currently not in use with other cell types Complex membranes needed for proper use Cell sampling not possible
Microfluidic devices	Long-term culture Laminar flow of cell culture media mimics the blood flow hemodynamics Stable low shear pressure Possibility to study multiple organs interaction Possibility of PBPK studies Real-time monitoring of metabolic function	A complex system to develop and establish Very low-sample and cell amounts

Liver bioprinting	Allows to build specific structures including endothelial and other cell types	A complex system to establish The printing process induces stress on cells

Adapted from [75, 81, 82, 97].

There is a wide variety of studies using 3D culture systems, comprising distinct cell sources such as primary rat and human hepatocytes, HepG2 cell line and HepaRG showing encouraging results as in vitro hepatotoxicity models.

Miranda *et al.* [71] showed that freshly isolated rat hepatocyte spheroid cultures could be maintained up to 21 days in culture using a stirred culture vessel (3D) bioreactor system. During this time, liver-specific functions, such as albumin and urea secretion, phase I (ECOD and testosterone hydroxylation) and phase II (UGTs) enzyme activities, and the capacity to metabolize diphenhydramine and troglitazone, were observed [71]. Using a similar cell culture system, Pinheiro *et al*. [91] also demonstrated the maintenance of the hepatic phenotype in culture by the detection of the specific hepatocyte markers ALB, CK-18, HNF-4α, MRP-2, and OATP-C, by the stable activity levels of phase I (ECOD and EROD) and phase II (SULT1A1) activities, which were modulated by nevirapine and its metabolites. Remarkably, a complete in vitro study of biotransformation mechanisms of NVP and its metabolites, including induction of enzymatic activity of phase I and II metabolites was only possible in vitro when resorting to in vitro 3D cultures [91, 98]. Resorting to co-culture systems using fibroblasts [99] or NPC [85] further improved hepatocyte functions in vitro.

Due to its lower availability studies with human hepatocytes are scarcer, though impressive results have also been reported. Tostões *et al.* [100] evaluated the feasibility of using human primary hepatocyte spheroids for repeated drug dose testing. The 3D spheroids were cultured in an automated perfusion bioreactor for 3-4 weeks in serum-free conditions [100]. These cell culture conditions allowed the maintenance of phase I enzyme expression and activity, as well as responding to induction as well of phase II enzyme expression and activity, of hepatic markers (HNF-4a, CK-18, CYP3A and ALB) presence, and of albumin and urea synthesis rates. In this study, polarity markers and bile canaliculi function were observed in human hepatocyte spheroids after two weeks of bioreactor culture [100]. Human primary hepatocytes cultured in a small-scale hollow-fiber bioreactor, with a cell compartment volume of 0.5 mL showed the preservation of CYP1A2, CYP2D6, and CYP3A4/5 activities between 40 % and 100 %, whereas CYP2B6 and CYP2C9 activities were preserved to a lesser extent up to 10 days in culture [94]. Moreover, immunofluorescence characterization also showed the presence of CYP2C9 and CYP3A4 and the drug transporters BCRP, MDR1 and MRP-2 in the

bioreactor up to 2 weeks in culture [63, 94]. These systems also displayed relevant biotransformation and toxicity profiles for several drugs including paracetamol and diclofenac [94, 95]. The use of human cryopreserved hepatocytes is also reported for 3D cultures. Bell and co-workers [87] provided a proof-of-principle that cryopreserved human primary hepatocytes spheroids could reflect liver pathologies such as cholestasis, steatosis and viral hepatitis. In this study, bile acid accumulation was mimicked upon chlorpromazine exposure, since MRP-2 and BSEP presented relevant activity and BSEP gene expression was decreased by drug exposure [87]. Moreover, these primary hepatocyte spheroids closely resembled intact liver tissues at the proteome level, whereas 2D monolayer cultures originated from the same liver tissues presented a multitude of deregulated important metabolic pathways [87]. Tsamandouras *et al.* [82] also used human cryopreserved hepatocytes to study the population variability in hepatic drug metabolism using hepatocytes from five different donors cultured in a perfused 3D human liver microphysiological system. Within this system, the metabolic depletion profile and metabolite formation of six compounds (phenacetin, diclofenac, lidocaine, ibuprofen, propranolol and prednisolone) were measured [82]. mRNA levels of 90 metabolism-related genes, and markers of functional viability (LDH release, albumin and urea production), for each donor, were identified as significant predictors of in vitro metabolic clearance. This data allowed to develop a population physiologically-based pharmacokinetic (PBPK) model for lidocaine to illustrate the translation of the in vitro output to the observed pharmacokinetic variability in vivo, being this the first study of population variability in drug metabolism in the context of an in vitro microphysiological system [82].

The study from Leite *et al*. [86] presents impressive results on a 3D-bioreactor with self-assembled spheroids of HepaRG, showing the induction of CYP1A2, 2B6, 2C9, and 3A4 and UGT enzymes [86]. Long-term functionality was shown by 7-week stable profiles of albumin secretion and the formation of tissue-like arrangements including bile canaliculi-like structures and polar distribution of transporters [86]. Herein, the system biocompetency was evaluated by the study of paracetamol cytotoxicity as evaluated by LDH activity quantification, showing the same profile over 1 month in culture [86].

Despite several interesting in vitro liver models are reported in the literature [5, 7, 17, 46, 61, 63-65, 70, 71, 74, 82, 83, 85, 90, 95, 99, 101], a comprehensive and systematic comparison between distinct cell culture systems that would allow its wide adoption for pharmacological and toxicological applications is still scarce. It should also be noted that the added value of a specific cell culture system for the prediction of drug action and toxicity in human liver, depends on the specific study goals.

In fact, the comparison of cell culture systems and cell sources is a challenging task. Cell viability and stability, morphological and architectural features, phase I and phase II metabolic capacity, response to a large panel of well-accepted reference drugs, as well as the physiological preservation of key metabolic and signalling pathways under long-term cultures shall be taken into consideration. Thus, several hepatotoxicity studies that evaluated diclofenac (**Table 1.6**) and troglitazone (**Table 1.7**) considering distinct cell sources and culture conditions were collected from the literature for a comprehensive review of the differences on the obtained IC_{50} values in different models.

Table 1.6 Diclofenac cytotoxicity endpoints observed in different cell types and cell culture systems.

Cell Type	Cell Culture System	Exposure Time	IC_{50} [μM] or [μM] with Observed Toxicity*	Endpoints	References
HepG2	2D	24 h	392	MTT	[104]
rpHep			331		
hpHep			763		
FaO			682		
rpHep	2D	24 h	222	ATP quantification	[105]
hpHep			138		
hHep	2D	24 h	1413	Almar Blue	[106]
Huh7			686		
HCCT-T			104		
rpHep	2D	24 h	393	LDH and MTT	[107]
FaO			700		
HepG2			750		
rpHep	2D	24 h	263	tetrazolium salt WST-1	[108]
HepG2			399		
HepG2	2D	24 h	1700	ATP quantification	[90]
cryo hpHep	2D	24 h	375	live cell protease caspase-3/7	[109]
HepG2	3D Spheroids with matrigel	24 h after 21 days in culture	1000	ATP quantification	[90]
HepG2	3D	7 days after 21	400	ATP quantification	[90]

	Spheroids with matrigel	days in culture			
rpHep HepH2	3D Spheroids in dynamic culture	24 h	*100 *500	LDH, Glucose secretion, γGT leakage	[103]
cryo hpHep	3D Spheroids	48 h 7days 28 days	190 57 46	ATP quantification	[87]
hpHep	Hollow-fibre bioreactor	10 days	*300 *1000	Decrease of Lactate secretion, increase in ammonia secretion and Lower cell density and organization in 1000 μM vs 300 μM	[95]

Diclofenac and troglitazone were selected in this *General Introduction* due to the importance of the drug metabolism for its hepatotoxicity, and thus it is expected to observe a higher toxicity in more competent systems. Diclofenac is one of the most prescribed NSAID worldwide [102]. Diclofenac causes rare albeit significant cases of serious hepatotoxicity with a fatality rate of 10 % [102]. As such, diclofenac was herein selected as a hepatotoxicant dependent on bioactivation. Diclofenac toxicity may be attributed to its reactive metabolites 4-OH-diclofenac, diclofenac-acyl-glucuronide and 4-OH-diclofenac-acyl-glucuronide [102]. 4-OH-diclofenac is its main metabolite, metabolized by CYP2C9; whereas 5-OH-diclofenac is formed in a lower extent, by CYP3A4. Diclofenac and both OH-diclofenac can suffer glucuronic acid conjugation, by UGT2B7, and be eliminated across the canalicular plasma membrane into the bile by MRP-2 [102]. Therefore, diclofenac metabolism comprises phase I, II and III enzyme activities. Diclofenac toxicity studies are scarce in comparing monolayer and 3D cell cultures. In a recent study diclofenac metabolism and toxicity was investigated in perfused 3D bioreactors using primary human hepatocytes [95]. However, no data for its comparison with monolayer cell culture is reported. Although no IC_{50} value was calculated, Xu *et al.* [103] observed toxicity for concentrations higher than 0.5 μM [103]. Moreover, it was observed that diclofenac significantly increased LDH release in liver spheroids but not in HepG2 spheroids [103], suggesting that a higher bioconversion of diclofenac and its metabolites in 3D may be occurring, resulting in its more toxic sub-products and consequently in higher cytotoxicity.

Table 1.7 Troglitazone cytotoxicity endpoints observed in different cell types and cell culture systems.

Cell Type	Cell Culture System	Exposure Time	IC_{50} [μM] or [μM] with Observed Toxicity*	Endpoints	References
co-culture of rpHep and NPC	2D	48 h	*from 10 μM in LDH *from 50 μM in ATP	LDH release and ATP quantification	[99]
co-culture of hpHep and NPC	2D	48 h	*from 100 μM in LDH *from 100 μM in ATP	LDH release and ATP quantification	[99]
cryo hpHep	2D	24 h	100 μM	live cell protease and caspase-3/7	[109]
HepG2	2D	24 h	200 μM	ATP quantification	[90]
HepaRG	2D	24 h after 5 days in culture	40 μM	ATP quantification	[101]
HepaRG	2D	24 h after 22 days in culture	300 μM	ATP quantification	[101]
rpHep and NPC co-culture	3D Scaffold	1 to 8 days	*from 50 μM in LDH *from 50 μM in ATP	LDH release and ATP quantification	[99]
co-culture of hpHep and NPC	3D Scaffold	1 to 8 days	*from 10 μM in LDH *from 1 μM in ATP	LDH release and ATP quantification	[99]
hpHep	3D Spheroids	8 days 14 days	9 μM 7 μM	ATP quantification	[116]
HepaRG	3D Spheroids	8 days 14 days	10 μM 1 μM	ATP quantification	[116]
HepaRG	3D Spheroids	24 h after 5 days in culture	400 μM	ATP quantification	[101]
HepaRG	3D Spheroids	24 h after 22 days in culture	>500 μM	ATP quantification	[101]
HepG2	3D Spheroids with matrigel	24 h after 21 days in culture	200 μM	ATP quantification	[90]
HepG2	3D Spheroids with matrigel	7 days after 21 days in culture	55 μM	ATP quantification	[90]

HepG2/ C3A	3D spheroids in a micro-physiological chip	24 h	*285 μM	oxygen uptake mitocondrial demage	[81]

Troglitazone (TGZ) is a thiazolidinedione derivative developed for the treatment of type II diabetes that was withdrawn due to non-immune idiosyncratic toxicity, with 100 liver failure cases in 1.9 million patients [110]. TGZ is extensively metabolized by CYP3A4 and GST, it is a CYP3A and 2B6 inducer and is able, as well as its sulfate conjugate, to inhibit BSEP [111, 112]. This leads to an increased formation of troglitazone metabolites as well as to its intracellular accumulation, resulting in intrahepatic cholestasis, mitochondria dysfunction, covalent binding to proteins, macromolecular damage ultimately leading to apoptosis [113]. TGZ is more toxic in humans than in rodent models [99, 114]. In 3D human liver models increased sensitivity to TGZ toxicity was observed (**Table 1.7**), which may be related to higher formation of metabolites due to higher induction. Nonetheless, Gunness *et al.* [101] obtained discrepant results, with a 3D model of HepaRG cells being 10 times less sensitive to troglitazone than the monolayer model after 24h of exposure and 5 days in culture [101]. This decreased sensitivity might reflect a higher clearance, commonly increased in 3D cultures due to the cellular architecture. In fact, HepaRG cells present an unproportioned [101] activity of phase I, II and III that might interfere with drug and metabolite clearances. These latter observations may possibly explain the differences between rats and humans, since rats have a higher TGZ clearance comparing with humans [115].

In sum, **Tables 1.6** and **1.7** show that hepatic cell lines still present relevant differences showing in general a lower sensitivity to drugs whose toxicity depends on drug biotransformation, even when more physiologically relevant cell culture systems are adopted. Thus, besides their disadvantages, primary hepatocytes are still the gold standard for in vitro studies since these are currently the cells presenting the more representative phenotype of the liver in vivo, particularly when cultured using 3D cell culture approaches.

1.5 Development, validation and regulatory acceptance of alternative in vitro toxicology approaches for hepatic systems

The main aim of all hazard and risk assessment strategies is to assess human health effects. According to OECD (Organisation for Economic Cooperation and Development) TG 417 [117], toxicokinetics should be evaluated in vivo using the rat as test system [117]. Ideally, in silico

and in vitro methods should model human toxicokinetic processes and use human cells and/or tissues. However, as already mentioned, there is a limited availability of human hepatic cells and tissues, and several ethical concerns are often raised in obtaining/using them. Moreover, given the well described species differences hepatic phase I and phase II biotransformation pathways studies are difficult to extrapolate from other species to humans [118]. Thus, other approaches are being developed since a stronger scientific foundation offers the prospect of improved risk-based regulatory decisions [119, 120].

Regulatory authorities and related agencies namely, ICH (International Conference on Harmonisation of Technical Requirements for Registration of Pharmaceuticals for Human Use), European Commission, OECD, EURL-ECVAM (European Union Reference Laboratory - European Centre For Validation of Alternative Methods), ICCVAM (Interagency Coordinating Committee on the Validation of Alternative Methods), REACH (Registration, Evaluation, Authorization and Restriction of Chemicals) and US Tox21 collaborative program, expect to generate more robust data on the potential risks of environmental agents and pharmaceuticals to humans and to expand capabilities to test target molecules more efficiently [120]. They are also prepared to face alternative testing approaches that reduce animal testing and increase drug development efficiency and prediction level of adverse drug reactions and the path for this includes improving *in vitro* testing and using new in vitro technologies [48, 121-128]. EU-ToxRisk is an example of an integrated project, funded by Horizon 2020 (€ 30 million) involving 38 European partners and one from the USA. This project will integrate advances in in vitro and in silico toxicology, read-across methods, and adverse outcome pathways, continuing the strategy of SEURAT-1, a projected integrated in the FP7 initiative that was the first EU-funded project addressing the issue of alternatives to animal testing for prediction of repeated dose systemic toxicity [120].

The specific objectives of EU-ToxRisk are the “development of a new way of risk assessment” comprising the development of new non-animal methods with special emphasis on their acceptance and implementation in regulatory contexts [120]. Several alternative methods, in other fields of toxicology than toxicokinetics and hepatotoxicity, are already scientifically validated, accepted by competent regulatory bodies including OECD, FDA (Food and Drug Administration) and EPA (Environmental Protection Agency), and are in use for regulatory toxicology purposes, thus reducing or fully replacing living animals in toxicology experimentation [129]. However, no hepatic metabolism studies are yet validated and accepted by the regulatory authorities as alternative methods [130]. The ECVAM Status Report on the Development, Validation and Regulatory Acceptance of Alternative Methods and Approaches from 2016 reports only two alternative in vitro toxicokinetic models under

evaluation: (i) *In vitro hepatic biotransformation – CYP induction: HepaRG and cryopreserved human hepatocytes* and (ii) *In vitro Fish Hepatic Metabolism,* to avoid the use of fish bio-concentration tests [130]. Currently, EURL ECVAM coordinates the "Multi-study Validation Trial for cytochrome P450 (CYP) induction providing a reliable human-metabolic competent standard model or method using the human cryopreserved HepaRG cell line and cryopreserved human hepatocytes".

Overall, this fully supports the European policy and world-wide interest in developing and implementing alternative in vitro toxicology methods for the risk assessment in hepatic systems. As reviewed in **Section 1.4**, the use of 3D systems improved the quality of data and allowed to produce more relevant results. However, the data present high variability that might result from distinct cell sources, experimental endpoints and inter-laboratory differences. This highlights the need of alternative robust cell sources, able to recreate physiologically relevant phenotypes and to represent specific genotypes of interest, which are pertinent such as genetic variations in metabolizing enzymes with importance in drug response. Stem cell derived hepatocyte-like cells and their adaptation to more physiologically relevant cell culture systems have been recently proposed for filling this gap [131].

1.6 Stem cell application on in vitro toxicology

Stem cells (SC) are an ubiquitous presence in the living organisms being essential in every moment of development and maintenance of life. Since the development of the first stem cell line, in 1981 [132], the scientific interest in SCs has been growing exponentially [51]. SCs are considered a very valuable and promising cell source for their potential application in cell therapy, and more recently in drug discovery. SCs enable more robust human hazard identification and optimized drug development strategies [125].

SCs are designated as embryonic, extra-embryonic, neonatal or adult SCs according to their role in development and origin. More recently, other cells designated as induced pluripotent stem cells (hiPSC) that re-programed to a pluripotent state from mature cell populations, presenting embryonic stem cell-like characteristics, have been identified [133]. Stem cells are considered as such by presenting indefinite self-renewal, plasticity and the ability of multi-lineage differentiation. Different SC sources present different potentialities and drawbacks for each particular application. Human embryonic stem cells (hESC) and hiPSC are pluripotent cells, presenting a higher differentiation potential than adult stem cells. hESC offer considerable advantages for clinical applications when compared to immortalized cells or primary cell cultures, as they are genetically normal (diploid) and do not exhibit the extend of

donor-dependent variability, characteristic of primary cells [134]. However, their utilization drives many ethical, technical, and legal concerns [135-137]. Alternative sources of SC, such as hiPSCs and adult stem cells do not present such ethical concerns. Several laboratories established protocols for differentiation of hiPSCs into hepatocytes [138], which can restore liver function in animal models of liver failure [139]. However, hiPSCs are not yet ready for transplanting into patients. Most iPSCs have been generated with integrating vectors, which may not get silenced efficiently or could disrupt endogenous genes [140]. Furthermore, there is evidence that iPSC therapy can lead to tumor formation and before clinical use, researchers need to focus on safety of hiPSC therapy in light of the potential for tumor formation [137]. Both hiPSC and hESC, present a high teratoma forming potential in vivo [141] as well as high genomic instability, namely by accumulating of mutations [142], which is not observed in adult stem cells such as mesenchymal stromal cells (MSC). Adult stem cells are part of tissue homeostasis and responsible for regenerating damaged tissues. These cells can be distinguished per origin of tissue, stage of development, genes expressed and differentiation ability [143, 144].

1.6.1 Mesenchymal stromal cells (MSC)

MSC classification is still controversial, being commonly defined as adult SC, fetal or neonatal SCs depending on its origin. Independently of their origin, MSC are characterized in vitro according to international standards, namely the ones defined by the International Society for Cell Therapy (ISCT) [145]. The three ISCT criteria are plastic adherence, the tri-lineage differentiation capacity (adipocyte, chondrocyte and osteoblast) and a specific surface marker profile, as evaluated by flow cytometry, consisting on a population where at least 95 % cells express CD105, CD73 and CD90; and less than 2 % cells express CD45, CD34, CD14 or CD11b, CD79α or CD19 and HLA-DR. MSCs can be isolated from a number of neonatal tissues, such as: fetal blood, liver and bone marrow [146], amniotic sac and fluid, placenta [146-148], umbilical cord blood [149], umbilical cord matrix [150-154]; and from adult tissues, such as adipose tissue, brain, spleen, liver, kidney, lung, bone marrow, muscle, thymus and pancreas [155].

For toxicological and regenerative medicine applications, MSC present many advantages as the ease of isolation from non-controversial sources at a relatively low-cost, in contrast with hESC. Additionally, MSC do not require feeder layers or high serum conditions comparing to ESC [156] and, although they are not an infinite cell source, these cells do show a satisfactory proliferative capacity in vitro [157]. The most studied MSC are derived from bone marrow (BM-

MSC), the tissue from which MSC were firstly identified and harvested, and from the adipose tissue (AT-MSC). More recently, cells derived from extra-embryonic tissues such as placenta and umbilical cord matrix (UCM-MSC) or blood became a more interesting cell source due to the non-invasive access and to its more primitive origin. These neonatal MSC sources show less of the donor variability seen with other sources of MSC due to donor age, health conditions, clinical history or lifestyle. Moreover, MSC derived from the umbilical cord tissue, in particular, maintain high chromosomal stability upon expansion in vitro in opposition to ESC [151] and iPSC [144, 149, 156-158], which is of special interest for clinical applications and to produce homogeneous populations of differentiated cells. Furthermore, MSC from the umbilical cord tissue are obtained in reproducible conditions and have been demonstrated to have a quite high differentiation capacity into cells of mesodermal origin such as myoblasts and cardiomyocytes [159], ectodermal as neurons, and endodermal origin as insulin-producing cells and hepatocyte-like cells (HLC). Human neonatal MSC (hnMSC) have demonstrated, along with the potential of differentiation into the hepatic lineage [160], other advantages relative to other MSC sources. Namely, hnMSC are isolated from a highly available source, do not suffer transformation and present lower epigenetic marks related with the donor life style [161, 162]. Nevertheless, hnMSC might be obtained from donors with distinct pharmacogenetic profiles and, thus, being particularly interesting for inter-individual pharmacogenomic studies. Thus, hnMSC present a very promising, and still scarcely explored cell source for in vitro toxicology studies.

1.6.2 Deriving human hepatocyte-like cells (HLC) from stem cells by mimicking liver embryogenesis

An efficient production of differentiated hepatocytes from SC has been sought by researchers and pharmaceutical industry. The aim is to improve reliability and accuracy of drug screening [163] by the possibility of using human cells and of building physiologically representative cell culture models. The differentiation of stem cells into HLCs have been attempted from hiPSC, hESC [138, 164-167] and also from adult stem cells, mainly from MSC such as human BM-MSC [168, 169], human AT-MSC [170, 171] or human UCM-MSC [172-179]. However, it is agreed that a completely mature HLC population has not yet been achieved.

Differentiation strategies to derive HLC from SC can include: (i) the addition of soluble medium factors, including growth factors, cytokines and hormones; (ii) rebuilding the in vivo cell-to-matrix and cell-to-cell interactions; and (iii) determining cell fate via genetic or epigenetic modification [180]. All these strategies aim at mimicking the development of hepatocytes in

vivo. Liver development is described in models of mouse, chicken and zebra fish and scarcely in human embryos. The major events in early mammalian endoderm development are described in **Figure 1.6**.

To clarify the gene regulation and the signalling events of liver development four main steps are considered: (i) Endoderm induction; (ii) Foregut and hepatic competence induction; (iii) Hepatoblast and liver bud formation; and (iv) Differentiation of hepatoblast into hepatocyte.

(i) Endoderm induction, in vivo, occurs during gastrulation. The endodermal germ layer is established and emerges as a sheet of cells from the anterior end of the primitive streak [181]. Signalling by the growth factor Nodal initiates endoderm and mesoderm formation in a concentration-dependent manner. Low concentrations of Nodal originate mesoderm formation while high concentrations originate endoderm formation. The transcription factors induced by Nodal are Sox17 and Foxa1-3, which regulate a cascade of genes responsible for the endoderm specification [114]. The endoderm induction step in vitro has been tested on embryonic stem cells and iPSCs through cell exposure to Activin A, a growth factor from the same family as Nodal, TGF-β family [114, 182-184].

(ii) The next step on development is foregut and hepatic competence induction that occurs when the endoderm forms a primitive gut tube that is subdivided into foregut, midgut and hindgut. Each domain expresses a specific transcription factor: Hhex in foregut, Pdx1 in the midgut and Cdx in the hindgut (**Figure 1.6 c**). The embryonic liver originates from the ventral foregut endoderm. Herein, gradients of fibroblast growth factor (FGF), Wnt, bone morphogenetic protein (BMP) and retinoic acid secreted from the adjacent mesoderm are responsible for this patterning of endoderm [185-187]. FGF and Wnts/β-catenin are secreted from the posterior mesoderm, repress foregut fate and promote hindgut development by inhibiting the expression of the *Hhex* gene, which is essential for liver development. The absence of Wnt/β-catenin by its inhibition initiates liver development [186]. Only the foregut endoderm is competent to develop into the liver possibly due to the expression of transcription factors like Foxa2, Gata-4, Gata-6 and Hhex [188]. In vitro, this step is mimicked by exposing cells to growth factors such as FGFs and EGF once they activate the *Hhex* gene expression [114, 185].

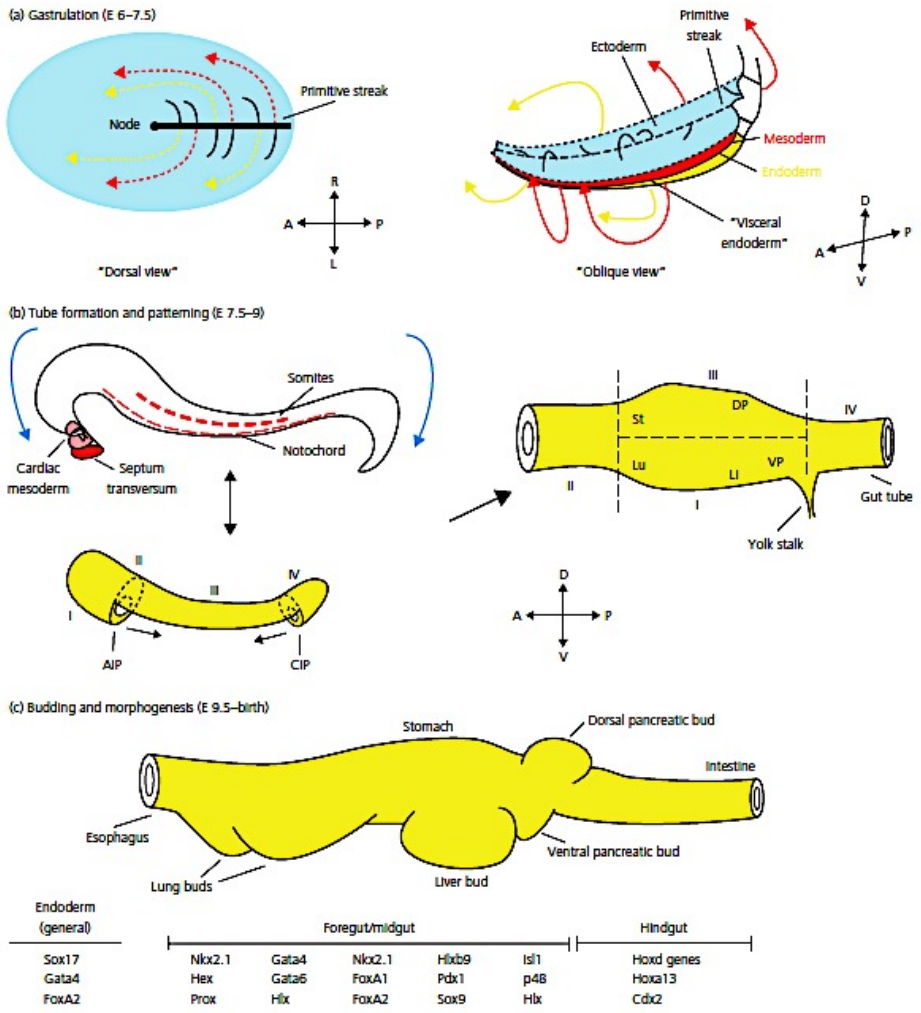

Figure 1.6 Major events in early mammalian endoderm development. (a) Gastrulation. (left) The embryonic epiblast (blue) viewed from above. Epiblast cells (solid black) migrate down through the primitive streak, becoming mesoderm (dashed red) or endoderm (dashed yellow) cells. (right) Oblique view of migrating epiblast cells, in which formation of the new mesoderm and endoderm is visible. (b) Tube formation and patterning. (left) The mesoderm and ectoderm have been pulled back to reveal the endoderm below. At this stage, the anterior endoderm is adjacent to the cardiac mesoderm and septum transversum (which mediate liver induction) whereas more dorsal portions of the endoderm are in contact with the notochord (which mediates pancreas induction). The folds of the anterior intestinal portal (AIP) and caudal intestinal portal (CIP) form the gut tube as they migrate towards each other at the midline. Blue arrows indicate the process of turning, by which the embryo switches from a convex to a concave shape, with the endoderm on the "inside". The roman numeral designations are derived from fate-mapping studies and indicate the prospective regions of endoderm that will give rise to later endoderm derivatives. (right) The relative position of endoderm domains changes with the completion of gut tube folding; the region that previously constituted the most anterior portion of endoderm (I) shifts to the ventral midline and gives rise to lung (Lu), liver (Li), and ventral pancreas (VP). (c) Budding and morphogenesis. Budding of endoderm derivatives begins shortly after the gut tube is formed and involves many transcription factors. DP, dorsal pancreas; E, embryonic day; St, stomach. From [189].

(iii) Afterwards, hepatoblast and liver bud formation takes place once the foregut receives signals from the developing heart and septum transversum mesenchyme (STM), which releases FGF and BMP respectively. These signals induce hepatic fate in the ventral foregut endoderm [190, 191]. After hepatic specification, cells start to express hepatic markers such as Albumin (ALB), α-fetoprotein (AFP), transcription factors as c/EBPα and HNF-4α and change their morphology from cuboidal to pseudostratified columnar epithelium, forming the liver bud. Then, the layer involving hepatic endoderm breaks down and the hepatoblasts migrate into STM. Hhex, Gata-4, Gata-6, Prox1, Onecut-1 and Onecut-2 are crucial for the delamination process [55]. At this stage the liver bud undergoes exponential growth and becomes the major site of fetal haematopoiesis. STM and hepatic mesenchyme secrete FGF, BMP, Wnt, Retinoic Acid and HGF, which promote hepatoblast proliferation and survival [181, 185, 191, 192]. This step is generally mimicked in vitro using FGF and BMP to mimic signals sent by the developing heart and STM, which induce a transformation in cell disposal and morphology [190, 191]. Herein, hepatocyte growth factor (HGF) is also commonly used to promote hepatoblast formation as well as cell culture supplements like insulin–transferrin–sodium selenite (ITS) and nicotinamide, that synergistically affect the hepatic driving pathway [181].

(iv) Finally, hepatoblasts, that are bipotent cells, can differentiate into hepatocytes or biliary epithelial cells. Initially, hepatoblasts express genes associated with both adult hepatocytes (*HNF4A*, *ALB*, *CK18*) and biliary epithelial cells (*CK19*), as well as fetal liver genes such as AFP. Hepatoblasts in contact with the portal vein form a monolayer followed by a bilayer of cuboidal biliary precursors, increasing the expression of biliary genes and the down-regulation of hepatic genes. One factor responsible for the induction of hepatoblast differentiation into hepatocytes is oncostatin M (OSM) secreted by haematopoietic cells in the liver [193]. It induces metabolic maturation through gp130 and JAK/Stat3 signaling pathways [194]. These secreted factors regulate several liver-enriched transcription factors including C/EBPα, HNF-1α, Foxa1-3, nuclear hormone receptors and HNF-4α which control hepatocyte gene expression [181, 195]. In addition to conventional protocols using growth factors Takayama *et al*. [166] sequential transduced of Sox17, Hhex, and HNF-4α on hESC and hiPSC, which induced further HLC maturation [166]. In fact, the transcription factor HNF-4α, plays a critical role in liver development and function as lipid and glucose metabolism. The maturation of hepatocytes and formation of extrahepatic bile ducts are gradual. This process continues even after birth [181] and is mimicked in vitro by the use factors such as OSM, and dexamethasone [193, 196].

Stem cell-derived HLCs may be characterized in vitro at four levels such as morphological, RNA, protein and enzymatic activity levels [180]. Since MSC and hepatocytes derive from different germ layers, the process of differentiation of MSC into HLC must involve a successful *transdifferentiation*, which is a still poorly understood process [180]. This issue and the lack of homogeneity between MSC populations, due to cell origin, isolation, purifying and expanding methods render HLCs differentiation a more challenging task. In fact, Takayama *et al.* [166] identified that differentiation efficacies differed between human iPSC lines, possibly due to the difference of epigenetic memory of original cells or to the difference of the inserted position of the foreign genes for the reprogramming [166]. This observation is reinforced also by several authors [140, 197] and highlights the advantages of a neonatal MSC source.

1.6.3 hMSC differentiation into HLC

MSCs have been reported as presenting important differences in their transcriptomes with respect to their source. De Kock *et al.* [160] suggested that the neonatal, the umbilical cord tissue cells WJ-MSCs presented a favourable transcriptome regarding hepatocyte differentiation in comparison with the gold standards of mesoderm-derived stem cells: hAT-MSC, BM-MSC and human skin derived precursors (hSKP) [160]. Interestingly, hUCM derived MSCs have been reported to express early endoderm markers, such as *GATA-4* [151], *GATA-5*, *GATA-6*, *SOX9* and *SOX17* and liver progenitor markers such as *DKK1, DPP4, DSG2, CX43* and *CK19* [150, 160]. Lee *et al.* [198] study highlighted the importance of MSC cell source accordingly to its potential applications [160, 161]. This study evaluated neonatal MSCs such as chorionic-villi MSC, amnion MSC, chorionic plate MSC and WJ-MSC and adult MSC (BM- and AT-MSCs) and showed that the more primordial MSC sources, neonatal MSCs, presented a better hepatocyte differentiation phenotype [198].

Despite the advantages of hnMSC, few differentiation studies are available regarding these cells [172, 174, 176, 179, 199]. Anzalone *et al.* [161] extensively characterized hnMSCs and its differentiation potential into HLCs in comparison with other MSCs sources, highlighting their advantages relative to BM-MSC and AT-MSC. A comparison of placenta derived stem cells (PDSC) and BM-MSC also showed the superiority of the neonatal stem cells for in vitro hepatotoxicity studies, since PDSCs-derived HLCs showed higher sensitivity to toxicants exposure [200]. One example is the report by Campard *et al.* [172], where the potential of hUCM-MSC to differentiate into HLCs using a three-step protocol that mimic the in vivo liver embryogenesis was evaluated, comprising a more complete analysis of cell phenotype, including biotransformation activity. Using this protocol, a population of differentiated cells with

hepatocyte-like characteristics was obtained. Differentiated HLCs expressed the hepatic markers ALB, Glucose-6-phosphatase (G6P), Tryptophan-2,3-dioxygenase (TDO), α1-Antitrypsin (AT), Tyrosine aminotransferase (TAT) and exhibited CYP3A4 activity as well as glycogen accumulation, and urea production. However, other crucial hepatic markers were still not present such as HepPar1, HNF-4α and CYP2B6, neither CYP3A4 induction after exposure to phenobarbital, and AFP, which implies that a mature phenotype was not achieved [172]. More recently, Zhang *et al.* [174] and Zhou *et al*. [177], differentiated hUCM-MSC into HLC using two-step protocols, achieving positive staining for CK-18, ALB and AFP; whereas HLCs were negative for CK-19, LDL uptake capacity and glycogen storage and presented a fibroblastic morphology [174, 177]. Therefore, presenting less mature phenotype than the one reported by Campard *et al.* [172].

Considering that the transcription of genes governing cell-fate during development critically depends on the chromatin accessibility, epigenetic modifiers (EM) have also been suggested for improving HLC phenotype. Those have been considered to modulate the intricate interplay between chromatin modulation, including histone (de)acetylation and DNA (de)methylation, and liver-enriched transcription factors that occur during embryonic development [201]. Their use was extensively reviewed by Snykers *et al.* [201] for the differentiation of stem cells into HLCs as well as for the maintenance of a hepatic phenotype in cultures of primary hepatocytes [201]. The more commonly used EM are histone deacetylase inhibitors (HDACi) namely trichostatin A (TSA), sodium butyrate and valproic acid, and DNA methyltransferase inhibitors (DNMTi), namely 5-azacytidine (5-AZA). The general mechanism of action of these agents is represented in **Figure 1.7**.

An *et al.* [202] tested the effect of valproic acid prior to subjecting cells to the differentiation protocol and observed albumin presence (though not its production in cell culture supernatant), improved LDL uptake, urea production and glycogen storage [202]. More recently, Mortezaee *et al.* [203] observed an improved HLC phenotype by differentiating hnMSC isolated from the umbilical cord matrix and introducing 1 mM sodium butyrate and 1 μM retinoic acid in a two-step differentiation of a 28 days protocol. Cells characterization consisted only on *AFP* and *HNF1A* gene expression, PAS staining and albumin production [203]. Raout *et al.* [204] evaluated the effect of valproic acid and miR-122-5p on the hepatic differentiation of hnMSC isolated from the umbilical cord matrix and observed gene expression of some hepatic markers, glycogen storage, albumin and urea production, presence of albumin and CYP3A4 [204].

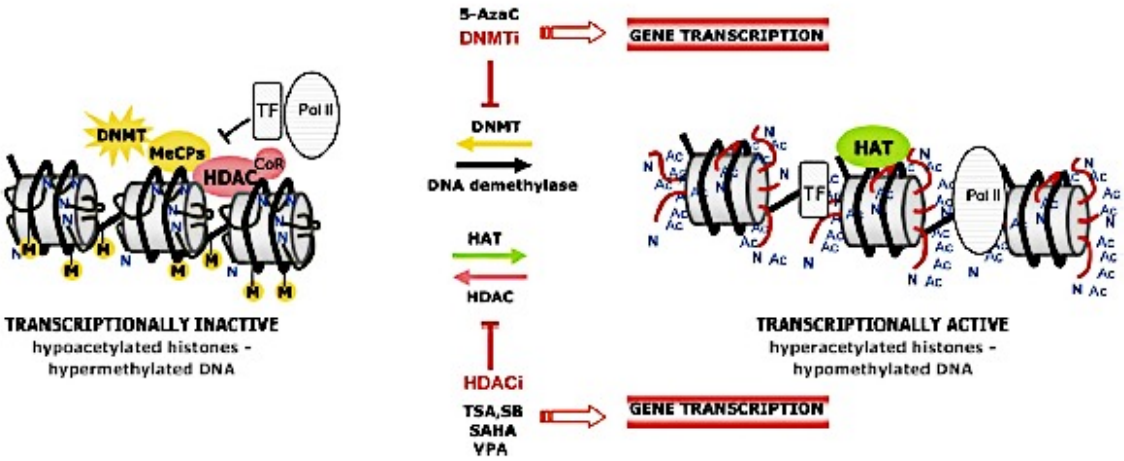

Figure 1.7. Epigenetic control of gene transcription. Inhibition of gene transcription typically corresponds to hypermethylated CpG islands in gene promoter regions and deacetylated histone tails at local chromatin domains. The indirect mechanism of gene silencing may involve binding of methyl-binding proteins (MeCp) to methylated cytosine and subsequent recruitment of HDAC-corepressor (CoR) complexes, resulting in a non-permissive heterochromatin status that blocks binding of transcription factors (TF) and polymerase II RNA complexes (PolII) to target promoter sequences. The direct mechanism may involve the direct interference of TF with HDAC or methylated CpG sites within the promoter. HDAC inhibitors (HDACi) and DNMT inhibitors (DNMTi) modulate the chromatin structure, creating an open, transcriptionally active euchromatin configuration at gene coding and regulatory regions, accessible for TF, thereby facilitating gene transcription. Abbreviations: 5-AzaC, decitabine; M, 5-methyl cytosine at CpGs; SB, sodium butyrate; TSA, trichostatin A; VPA, valproic acid. From [201].

5-AZA has been applied for promoting the differentiation of stem cells into various cell types [205-207]. 5-AZA is a competitive inhibitor of DNA cytosine methyltransferases [208]. However, it can also exert its epigenetic modifying activity directly or indirectly through different mechanisms [209] including interference with RNA methylation and modulation of nonsense-mediated mRNA decay efficiency in a MYC-dependent manner [210, 211]. Regarding hepatocyte differentiation, 5-AZA was administered in vivo to 20 days gestational age rat foetuses resulting in a quick maturation of hepatocyte morphology 18h after treatment as well as higher expression of genes such as *TAT* and *ALB*, reflecting a temporal advance of changes that would occur later in liver development [212]. On hepatocyte differentiation protocols in vitro, 5-AZA has only been attempted on hAT-MSCs by Seeliger *et al*. [213], and on umbilical blood derived MSCs by Yoshida *et al*. [214] being applied 24h prior the differentiation induction since proliferation is needed for the incorporation of 5-AZA into cellular DNA. 5-AZA at 20 μM [213] improved glucose secretion, and CYP1A1/2 and CYP2B6 activity. Urea production was similar in both freshly isolated hepatocytes and cells not exposed to 5-AZA [213]. On the other hand, Yoshida *et al*. [214] achieved a significantly higher ALB, c/EBP-α, CYP1A1/2 and PAS positive cells, as well as higher urea production and ALB gene

expression after 21 days of differentiation than in non-treated cells [214]. However, a less mature phenotype than the one observed by Seeliger *et al*. [213] was obtained.

DMSO has also been proposed as an epigenetic modifier that induces hepatic differentiation though its mechanisms are still poorly understood. In fact, DMSO has been extensively reported a as differentiation inducer for several cell lines such as HepaRG [54] and HL-60 [215] and more recently for progenitor cells [216-219] and stem cells differentiation [183, 217, 220-224]. The effect of DMSO on stem cell differentiation was thoroughly studied by Cheety *et al.* [225] that observed an activation of the retinoblastoma protein in DMSO treated cells. DMSO is further responsible for a higher proportion of cells in early G1 phase [225]. This cell cycle phase is of high importance for cell differentiation and a prolonged G1 phase has been reported as an indication of a differentiated status by reflecting loss of pluripotency and gain of lineage specific markers [226]. Thus, the DMSO treatment may increase the responsiveness of the stem cells differentiation signals, enhancing differentiation across all germ layers, and improving terminal differentiation into functional derivatives [225]. During spontaneous differentiation of hESCs, DMSO treatment resulted in a selective downregulation of key markers associated with stemness (Oct-4, Sox-2, Nanog and Rex-1); ectoderm (Nestin, TuJ1, NEFH and Keratin-15); mesoderm (HAND-1, MEF-2C, GATA-4 and cardiac-actin); and endoderm (SOX-17, GATA-6) [222]. DMSO has been also reported to promote hypo- and hypper phosphorylation of several cellular proteins [227, 228], on phosphatidiylinositol signaling [229] as well as to increase membranes permeability and floppiness [230], namely by transiently opening water pores and facilitating Ca^{2+} entrance into the cells [231]. Su *et al*. [232] reported that in cultures of primary rat hepatocytes, DMSO at a concentration of 2 % was able to maintain normal transcription factors pattern on cultured cells, thus reflecting more relevant CYP450 enzyme activities, namely by restoring HNF-4α and c/EBP-α levels that rapidly decreased in cultures without DMSO [232].

1.6.4 Stem cell derived HLC resorting to 3D culture strategies

3D culture systems have been shown to increase the functions of hepatocytes in vitro. Therefore, some authors have attempted to mimic the ontogenic environment of liver by using 3D cell cultures, to promote the hepatogenic differentiation and hepatocyte maturation [97, 122, 180]. 3D cell cultures have also been applied to SCs, although scarce in number, with great success to study the maintenance of their undifferentiated phenotype for long culturing periods [233, 234] and to promote cellular differentiation and maturation [235-237].

The use of 3D cell culture systems on HLCs derived from hnMSCs has to our best knowledge only been reported by our group [173]. It had been described for other sources of MSCs [238-242], and in a higher number using hiPSCs and hESCs [122, 184, 236, 243, 244]. The 3D strategies used for the purpose of hepatic differentiation include the use of scaffolds [122, 238, 240-242, 245], clustering into natural or synthetic matrix [244], self-assembled spheroids [122, 173, 236, 239] or hollow-fiber bioreactors [173, 184, 243].

Gieseck *et al*. [244] showed the ability of hiPSCs to differentiate into HLCs detecting the presence of ALB, AFP, AT, as well as CYP3A4 activity under 2D and 3D cell cultures, the last consisting of cell clustering onto collagen matrix. However, the presence of the hepatic transporter MRP-2 was only detected under the 3D cell culture system [244]. Moreover, 2D culture maintained CYP3A4 activity for 20 days after the achievement of a differentiated phenotype, whereas the 3D culture could maintain not only a stable CYP3A4 activity but also albumin production, with a simultaneous decrease of AFP production, until day 50 after differentiation [244].

Nano-scaffold structures were used to culture human BM-MSC-derived HLCs. Herein, the expression of *ALB*, *AFP*, *CK18*, *CK19* and *CYP3A4* was observed as well as an increased ability to produce urea and transferrin relative to 2D and to undifferentiated cells [245]. Baharvand *et al*. [122] also observed higher albumin, AFP and urea production in a 28-day long protocol, when comparing 2D and 3D cultures of human embryonic stem cell derived-HLCs, using embryoid bodies cultured in 24-well tissue culture dishes containing a 3D scaffold as 3D strategy [122].

By resorting to self-assembled spheroid strategies, Subramanian *et al*. [236] showed an improved hepatic phenotype of hESC derived HLC when cultured on spheroid static cultures, namely regarding albumin secretion and decrease of AFP expression that was maintained for 2 weeks in culture [236]. Considering HLC derived from MSCs, Okura *et al*. [239] observed hepatocyte characteristics on HLC clusters derived from adipose tissue hMSC as ALB and AT presence, urea production and glycogen storage capacity but the comparison with 2D cell cultures is scarce [239]. Stem cell differentiation using the hollow-fiber bioreactor was attempted using hESC and resulted in an upregulation of pathways related to steroid hormone biosynthesis, ABC transporters and CYP-dependent metabolism of xenobiotics in comparison to 2D cultures, also revealing maturation of the HLCs in this environment [243]. Freyer *et al*. [184] also showed that this 3D bioreactor improved hiPSC-derived HLCs differentiation with increased albumin secretion, CYP2B6 activity, and allowing the formation of tissue-like structures with cell-to-cell contacts, in comparison with 2D cultures. However, some aspects

of hepatic functionality such as AFP expression, and the absence of CYP2C9 activity and expression of the biliary transporter MRP-2 protein presence could not be detected [184]. This cell culture system was also studied for the maturation of hnMSC-derived HLCs and compared with a self-assembled spheroid under a static culture and a respective monolayer control. HLCs displayed a more mature hepatocyte-like phenotype under both 3D cultures than in the 2D culture, namely at biotransformation level and the differences between both systems were subtle. The spheroids revealed higher bupropion conversion whereas bioreactor showed increased albumin production and capacity to biotransform diclofenac [173]. This highlights the potential of 3D systems for cell maturation and maintenance of specific cell functions. In fact, as showed in **Section 1.4**. toxicological studies using a human hepatocyte cell line in 3D conditions have shown different sensitivity to molecules when compared to 2D cultures [66], probably due to a more complete biotransformation phenotype.

1.6.5 Stem cell based in vitro hepatotoxicity models

The reports of hepatotoxicity studies using HLCs are still scarce and despite the demonstrated advantage of 3D culture for cell differentiation and maturation, the latter are even scarcer.

Some studies describe and compare the potential of HLCs for toxicological applications with each other and with the industry gold standard cellular models: HepG2 and cryopreserved human primary hepatocytes. The toxicological advantage of hiPSC-derived HLCs was observed by Sjogren *et al*. [246] study, where HLCs better predicted drug induced apoptosis than Huh7 and HepaRG [246]. Another study, from Holmgren *et al*. [247], evaluated the response of hiPSC derived HLCs to specific hepatotoxic drugs over 14-days exposure [247]. The hiPSC-derived hepatocytes revealed to be more sensitive to the toxic compounds after extended exposures. In addition to conventional cytotoxicity, evidence of steatosis was also observed in the cells exposed to troglitazone [247]. Moreover, the IC_{50} value is of 20 μM, 60 μM and 100 μM after 14, 7 or 2 days of exposure [247], falling into the range of human primary hepatocytes (**Table 1.7**). The use of hESC and hiPSC-derived HLCs was also compared in a study by Medine and co-workers [248]. Both HLCs showed a hepatocyte-like phenotype with positive staining of albumin and HNF-4α, E-CAD, AT and CYP3A4 as well as displaying CYP3A4, 2C9 and 1A2 activity. However, only hESC-derived HLCs displayed CYP2C9-dependent cytotoxicity similarly to human cryopreserved primary hepatocytes [248]. Recently, it was also demonstrated that hiPSC and hESC-derived HLCs presented cytotoxicity, cellular multi-functional parameters, CYP450 enzyme activity profiles closer to hpHeps than HepG2 [249]. Once again, hESC-derived HLCs revealed improved hepatic function with higher

correlation with hpHep than hiPSC derived-HLCs. Remarkably, in this study it was possible to demonstrate that the hepatotoxic mechanism of aflatoxin B1, a well-known mycotoxine, was mediated by CYP3A4 using a stem cell-derived hepatocyte model [249].

Tasnim *et al.* [197] also performed a complete comparative study of 2D and 3D cultures of HLCs, resorting to spheroid formation into a matrix of galactosylated cellulosic sponges, focusing on its in vitro hepatotoxicity potential applications. Two hiPSC lines and one hESC line were used to derive HLC [197]. The better performance of hESC-derived HLCs as well as a high variability of different hiPSC lines were reinforced, which is in accordance with other studies [140, 250]. In this study, the cells were differentiated under 2D cultures for 20 days and seeded into 3D culture or 2D control cultures for an extended period of 12 days. 3D culture did not change albumin production. However, hepatic markers expression, urea secretion, and CYP3A4, 1A2 and 2B6 activities and induction were significantly higher in 3D comparing with 2D. The HLC CYP450 activity reached 30-150 % higher than human cryopreserved hepatocytes activity in one hiPSC cell line and in hESC-derived HLC [197]. Upon paracetamol, troglitazone, and methotrexate exposure, hESC-HLCs predicted better paracetamol cytotoxicity regardless of the cell culture systems, and 3D hESC-HLCs predicted better methotrexate cytotoxicity than 3D hiPSC-HLC. Both stem cell-derived HLC 3D cultures were more sensitive than primary hepatocytes to troglitazone exposure, conversely to 2D HLCs [197].

The exploitation of MSC-derived HLCs as an in vitro cell model for hepatotoxicity studies is less reported than of hiPSC or hESC. Rodrigues and co-workers [251] derived HLC from human neonatal skin precursors (hSKP) expressing *ALB*, as well as biotransformation enzymes such as *CYP1B1*, *FMO1*, *GSTA4*, *GSTM3*, and the drug transporters *ABCC4*, *ABCA1* and *SLC2A5* [251]. This hSKP-HLC responded to paracetamol exposure as primary human hepatocytes concerning the toxicogenomic evaluation of "liver damage", "liver proliferation", "liver necrosis" and "liver steatosis" [251]. More recently, Rodrigues *et al.* [162] showed that, similarly to in vitro primary hepatocytes, hSKP-HLC were also able to display a steatosis phenotype upon VPA induction with some features in common with in vivo observations of mild steatosis, whereas advanced steatosis was not possible to mimic [162]. Both studies are, to our knowledge, the first report in which human postnatal stem cells are described as a potentially relevant cell source for in vitro hepatotoxicity drug testing, namely steatogenic compounds and compounds interfering with lipid metabolism.

In summary, major challenges to be overcome for the relevant application of SC-derived hepatocytes in toxicology still exist: (i) the immature phenotype since only hepatocyte-like cells

expressing low levels of liver-specific markers, especially drug metabolizing and detoxifying enzymes, are usually obtained [166, 252, 253]; (ii) the lack of defined and validated endpoints of hepatic differentiation and maturation; (iii) the lack of standardization and data using relevant positive controls; and (iv) the generation and maintenance of functional hepatocytes in high numbers [253]. Once these questions are solved, in vitro toxicogenomics, transcriptomics, proteomics and metabolomics technologies as well as progress in high throughput screening can be applied to hepatocytes of human origin derived from stem cells [163]. In fact, the emergence of mechanistic models for toxicity testing, including in vitro disease models, and its introduction at the timeframe of lead selection and optimization, in parallel with in vitro pharmacokinetic studies, will significantly reduce compound attrition rate by selection of safer and more efficacious lead molecules. The upcoming stem cell-based toxicity testing models might have an important future role on addressing safety gaps of present drug discovery and development.

Chapter 2. Aim

UCX® is a highly homogeneous, extensively characterized and therapy-driven population of human neonatal mesenchymal stromal/stem cells (hnMSC), registered as a trademark and resulting from a patented generation method [154]. UCX® are obtained in high numbers and are already in pre-clinical trials for several cardio-vascular and auto-immune disorders. The consistent and controlled fabrication process of UCX® [154, 254] and its neonatal source that proved to be relevant for MSCs hepatic differentiation [160, 200] makes this cell population a privileged candidate to use for hepatic differentiation procedures to obtain models for in vitro toxicology. The aim of this work was to derive hepatocyte-like cells (HLC) from UCX® to address and solve the following problems:

(i) The difficult task of obtaining and maintaining functional hepatocytes in vitro, in quality and numbers that would be compatible to high throughput drug screening (important for the pharmaceutical industry);

(ii) The development of a 3D culture system for UCX® cell expansion and/or maintenance and improvement of the hepatic differentiation or the differentiated phenotype.

The main goal of this thesis was to obtain differentiated HLC of human origin with a mature phenotype, showing high and persistent levels of biotransformation activity in a scalable 3D culture condition that could be routinely used by pharmaceutical industry in drug screening. To achieve this general aim the following specific objectives were proposed:

- Use the 3D culture strategies for maintaining and expanding UCX® cells focusing on the development of 3D cultures to support, maintain and expand UCX® cells for further HLC differentiation. For this, the 3D UCX® cells structures will be cultured in suspension using stirred tank vessels (spinner vessels) and static cultures using ultra-low attachment plates;

- Develop a differentiation protocol to derive HLC from UCX®, taking into consideration the cytokines and growth factors present during liver embryogenesis;

- Improve UCX®-derived hepatocyte phenotype by resorting to 3D culture technology, applying the previously optimized differentiation protocol to the 3D culture conditions: self-assembled spheroids and a multi-compartment 3D perfusion bioreactor. Such environment provides more physiologic conditions essential to the developmental process, such as cell-to--cell interactions allowing a higher biological activity to be achieved in terms of liver-specific markers levels and drug detoxifying enzymes and further fulfilling the toxicological/cell therapy applications herein proposed;

- Evaluate UCX®-derived hepatocytes, namely their hepatocyte-like character in both 2D and 3D cell culture by their morphological and phenotypic characteristics, including

metabolic/biotransformation ability, when exposed to drugs as a proof-of-concept of HLCs culture in terms of their potential interest for in vitro toxicology applications.

My thesis is that 3D culture conditions in the presence of cytokines and growth factors involved in liver embryogenesis would result in a hMSC-based in vitro model more representative of the liver physiological conditions, which could be standardized and therefore routinely used for toxicology screening. This could meet the most pressing pharmaceutical industry needs and give a step forward in predictive toxicology, with possible applications in cell therapy.

Chapter 3 describes the development of a differentiation strategy to derive hepatocyte-like cells from UCX® cells. Previous stem cell hepatocyte differentiation studies were considered, namely, the one by Campard *et al.* [172] to our knowledge, the only work reporting hepatocyte differentiation from hUCM-MSC. Campard *et al.* [172] describes a differentiation protocol, however a more complicated MSC isolation method was employed and some inconsistency in hepatic markers expression was revealed, which perhaps demonstrates a less than mature HLC output. Nevertheless, such protocol was the starting point for the differentiation protocol herein developed through an intensive characterization of HLC under 8 distinct differentiation protocols, using 2D cultures for practical reasons. The generated HLC were evaluated for the chemical optimization of the differentiation protocol, were tested under extended cell culture times, up to day 34, and characterized for its transcriptome in comparison with human primary hepatocytes.

Besides, the obtained HLC presented relevant hepatocyte-like characteristics, the hypothesis of further improving its phenotype in 3D culture was evaluated. Therefore, Chapter 4 describes the optimization and characterization of UCX® under 3D cultures for maintaining and expanding UCX® cells.

In Chapter 5, HLC culture was adapted to two distinct 3D cultures: self-assembled spheroids and the hollow-fiber bioreactor to optimize the cell culture environment for HLC maturation. The obtained functional HLC were once again deeply characterized at gene expression, protein, enzymatic activity and capacity to biotransform reference drugs under these cell culture systems.

Finally, Chapter 6 describes the proof-of-concept study of the 3D spheroids as model for in vitro study of drugs that undergo hepatic biotransformation, by mimicking the human nevirapine biotransformation and induction profile.

Chapter 3. The role of epigenetic modifiers on extended cultures of functional hepatocyte-like cells derived from human neonatal mesenchymal stem cells

The scientific content of the present chapter has been included in the following publication:

Cipriano M, Correia JC, Camões SP, Oliveira NG, Cruz P, Cruz H, Castro M, Ruas JL, Santos JM, Miranda JP. *The role of epigenetic modifiers on extended cultures of functional hepatocyte-like cells derived from human neonatal mesenchymal stem cells*. Arch Toxicol. 2017;91:2469-89. DOI 10.1007/s00204-016-1838-0

3.1 Abstract

The development of predictive in vitro stem cell-derived hepatic models for toxicological drug screening is an increasingly important topic. Herein, umbilical cord tissue-derived mesenchymal stromal cells (hnMSCs) underwent hepatic differentiation using an optimized three-step core protocol of 24 days that mimicked liver embryogenesis with further exposure to epigenetic markers, namely the histone deacetylase inhibitor trichostatin A (TSA), the cytidine analogue 5-azacytidine (5-AZA) and dimethyl sulfoxide (DMSO). FGF-2 and FGF-4 were also tested to improve endoderm commitment and foregut induction during *Step 1* of the differentiation protocol, being *HHEX* expression increased with FGF-2 (4 ng/mL). DMSO (1 %, v/v) when added at day 10 enhanced cell morphology, glycogen storage ability, enzymatic activity and induction capacity. Moreover, the stability of the hepatic phenotype under the optimized differentiation conditions was examined up to day 34. Our findings showed that hepatocyte-like cells (HLCs) acquired the ability to metabolise glucose, produce albumin and detoxify ammonia. Global transcriptional analyses of the HLCs showed a partial hepatic differentiation degree. Global analysis of gene expression in the different cells revealed shared expression of gene groups between HLCs and hpHeps (human primary hepatocytes) that were not observed between HepG2 and hpHeps. In addition, bioinformatics analysis of gene expression data placed HLCs between the HepG2 cell line and hpHeps and distant from hnMSCs. The enhanced hepatic differentiation observed was supported by the presence of the hepatic drug transporters OATP-C and MRP-2 and gene expression of the hepatic markers *CK18, TAT, AFP, ALB, HNF4A* and *CEBPA*; and by their ability to display stable UGTs, EROD, ECOD, CYP1A1, CYP2C9 and CYP3A4-dependent activities at levels either comparable with or even higher than those observed in primary hepatocytes and HepG2 cells. Overall, an improvement of the hepatocyte-like phenotype was achieved for an extended culture time suggesting a role of the epigenetic modifiers in hepatic differentiation and maturation and presenting hnMSC-HLCs as an advantageous alternative for drug discovery and in vitro toxicology testing.

Keywords:

hnMSC; Hepatocyte-like cells; CYP metabolism; Drug transporters; Epigenetic modifiers.

3.2 Introduction

The pharmaceutical industry faces considerable challenges regarding political and social pressure to reduce the cost of medicines. The drug development process is expensive, lasts on average 10-15 years and shows a success rate of only 11 % for all therapeutic areas. The majority of drug attrition is due to lack of efficacy or safety that occurs essentially in the clinical phases IIb and III of drug development [2]. Liver damage is also an important cause of new drug failures, post-marketing withdrawals or relabeling with black box warnings, of which 21 % accounts for hepatotoxicity [3]. This is mostly due to the fact that hepatotoxicity is difficult to predict in early stages of drug development, making the improvement of pre-clinical models, namely human cellular models, particularly relevant concerning human safety. The need of an available source of human hepatocytes is therefore of major importance for in vitro toxicology applications [255].

Human primary hepatocytes (hpHeps) are not easily available and they are not much proliferative in healthy conditions or in vitro given their highly-differentiated cell type [7]. Additionally, these cells quickly lose their normal functions, namely metabolism of xenobiotics, when isolated and maintained in culture. Human cell lines as HepG2, Huh7, and more recently HepaRG, have also been used to study hepatic metabolism of new molecules and toxicants. However, these immortalized cell models still present crucial drawbacks for predictive hepatotoxicity such as an incomplete metabolic profile regarding phase I, phase II and hepatic transporters [7], resulting in distinct toxicity profiles for the same compounds, when compared to primary hepatocytes [50, 246].

Differentiation of stem cells (SC) has been suggested as an alternative approach for obtaining functional hepatocyte-like cells (HLC). Sjogren *et al.* [246] showed that induced pluripotent stem cell (iPSC)-derived hepatocytes are better toxicity predictors than Huh7 and HepaRG for drugs that cause apoptosis via mitochondrial-driven mechanisms. However, although the scientific community has already achieved impressive results, a completely mature HLC population derived from SCs has not yet been achieved [255, 256]. MSC, in particular, are a promising SC type, regarding availability, expandability, ethical and safety concerns [154, 257-259], when compared to iPSC or ESC. Despite its mesenchymal nature, MSCs derived from human bone marrow [168], human adipose tissue [171] or human umbilical cord tissue [172, 174, 179] have been described as able to undergo hepatocyte differentiation. In a comparative study, Lee *et al*. [198] showed that neonatal MSC, namely placenta-derived MSCs (including chorionic-villi MSCs, amnion MSCs, chorionic plate MSCs and WJ-MSCs) presented a better hepatocyte-like phenotype after differentiation than adult MSCs, such as human AT-MSC and

BM-MSC, reinforcing that each MSC type has a different differentiation potential and the importance of the choice of the primary MSC source [160].

The few papers reporting hepatic differentiation of human neonatal umbilical cord tissue-derived MSCs (hnMSC-UCM) [172, 179] characterize the obtained HLCs in terms of urea and albumin production, positive glycogen storage, acetylated low-density lipoprotein (Ac-LDL) uptake and the presence of hepatic markers as CK-18, albumin (ALB) and α-fetoprotein (AFP) through immunohistological or gene expression analyses. These studies did not contemplate a deeper evaluation of the metabolic potential of these cells regarding phase I, II and III metabolic activities. Most importantly, the maintenance of cell functionality in culture was not evaluated. Some publications do evaluate CYP and hepatic transporter presence in iPSC or human ESC-derived HLCs [260, 261], but this analysis using MSCs has still not been thoroughly explored. Considering hnMSC-UCM, Campard *et al.* [172] investigated the activity of CYP3A4 only and tested if hnMSC-UCM-derived HLCs would respond to the phenobarbital induction stimuli, which was not observed. Additionally, essential hepatic markers such as HNF-4α and CYP2B6 were not detected, as well as HepPar1, a highly sensitive marker of hepatocyte's mitochondria. More recently, Zhang *et al.* [174] and Zhou *et al*. [177] published on differentiation of hnMSC-UCM into HLCs, using a two-step protocol but the achieved phenotype is less mature than the reported by Campard *et al.* [172], presenting positive staining for CK-18, ALB and AFP. Nevertheless, the cells presented a fibroblast-like morphology and did not present glycogen storage and Ac-LDL uptake capacities [174, 177].

Considering that the transcription of genes governing cell-fate during development critically depends on the chromatin accessibility, epigenetic modifiers (EM) have also been suggested for improving HLC phenotype. In this study, a total of eight protocols were used to test the differentiation capacity of a specific population of hnMSC-UCM, UCX® [257-259], isolated using a method which was fully adapted in compliance with advanced therapy medicinal product (ATMP) regulatory requirements [254]. This differentiation procedure was performed using a combination of different cytokines in order to mimic liver embryogenesis and the addition of EM. The EM tested in this work are small molecules that have been previously described and applied in vitro as promoters of hepatic differentiation, namely trichostatin A (TSA), dimethyl sulfoxide (DMSO), and 5-azacytidine (5-AZA). TSA is a histone deacetylase inhibitor (HDAC-I) [168], DMSO exerts an epigenetic modulation through less described mechanisms [222] and the cytidine analogue 5-AZA is a small molecule that inhibits DNA methylation [213, 214]. hnMSCs showed the ability to commit with the endoderm lineage and to differentiate into mature HLCs. Moreover, the addition of EM and the optimized differentiation protocol resulted in an improved cell phenotype and a remarkable maintenance

of HLC hepatic functions in culture was achieved, locating HLCs closer to hpHeps as shown by global gene expression.

3.3 Material and Methods

3.3.1 Reagents

Cell culture supplements were purchased from Lonza (Basel, Switzerland), unless otherwise stated. Trypsin-EDTA, fetal bovine serum (FBS), insulin-transferrin-selenium solution (ITS) and non-essential amino acids supplement (NEAA) were purchased from Gibco®/Life Technologies (Madrid, Spain). 7-ethoxyresorufin and 7-ethoxycoumarin were purchase from Alfa Aesar (Karlsruhe, Germany). Hepatocyte growth factor (HGF), fibroblast growth factors (FGF-2 and FGF-4) and oncostatin-M (OSM) were purchased from Peprotech (Rocky Hill, NJ, USA). Finally, Iscove's modified Dulbecco's medium (IMDM), alpha modified Eagle's medium (α-MEM), epidermal growth factor (EGF), dexamethasone, DMSO, nicotinamide, 5-AZA, trypan blue, periodic acid, Schiff's reagent Mayer's hematoxylin, amylase, Hank's balanced salt solution (HBSS), 4-methylumbelliferone (4-MU), β-glucuronidase/arylsulfatase, resorufin, 3-methylcholantherene (3-MC), omeprazole and rifampicin were acquired from Sigma-Aldrich (Madrid, Spain).

3.3.2 Rat-tail collagen extraction and plate coating

Rat-tail collagen extraction was performed based on Rajan *et al.* [262]. Briefly, rat-tails were washed twice in 70 % ethanol prior to skin removal using sirurgical material. Tendon fibres were pulled out, separated from bone and cartilaginous tissue and suspended in PBS. Fibres were then washed three times and immersed for 1 hour in 70 % EtOH before being transferred into 0.1 % acetic acid and stirred during 48 hours at 4°C, for fibre acid digestion. The solution was centrifuged at 16000 x *g* for 90 minutes at 4 ºC. The supernatant was collected, lyophilized and the resultant solid stored at -80 °C until further use.

For collagen plate coating, lyophilized collagen was dissolved in a final concentration of 1 mg/mL in 0.1 % acetic acid and diluted to 0.2 mg/mL in PBS. A volume of this solution covering with excess the whole area of cell culture was added to cell culture surfaces and kept for 30 minutes at 37 ºC. After incubation cell culture surfaces were left to dry under UV light for 30 minutes and washed in PBS prior to use.

3.3.3 Cell cultures

hnMSCs were isolated as described in [257-259] and expanded as undifferentiated cells in α-MEM supplemented with 10 % of FBS (v/v) (growing medium)**.** HepG2 cells were cultured in α-MEM supplemented with 10 % FBS (v/v), 1 mM of sodium pyruvate and 1 % NEAA (v/v). Cryopreserved human primary hepatocytes (hpHep; pool of 10 donors) were purchased from Invitrogen™ (Carlsbad, CA, USA; HEP10, A12176), thawed on cryopreserved hepatocyte recovery medium (CHRM; CM7000, Invitrogen™) and manipulated according to manufacturer instructions. Rat primary hepatocytes (rpHep) were isolated from Wistar rats 3- to 6-month old, weighting 200 to 400 g, obtained from Charles River Laboratories (Barcelona, Spain) and cultured according to our previous reports [61, 71, 85]. Prior to each experiment, the animals were kept in a separate cage for at least 24 hours, with *ad libitum* access to food and water. All applicable institutional and governmental regulations concerning the ethical use of animals were followed, according to the European guidelines for the protection of animals used for scientific purposes (European Union Directive 2010/63/EU) and the Portuguese Law nº 113/2013. Briefly, the animals were anesthetized with an intraperitoneal injection of ketamine (90 mg/kg body weight) and xylazine (10 mg/kg body weight) solution, for surgery. The liver was perfused *in situ*, via portal vein, for 7 minutes with a Perfusion Buffer I (0.14 M NaCl, 6.7 mM KCl, and 10 mM HEPES with pH 7.5 adjusted with 2.4 M EGTA) at 39 ºC. Subsequently, perfusion was continued with a collagenase (10 mg/100 g body weight) containing buffer (67 mM NaCl, 6.7 mM KCl, 100 mM HEPES, albumin (0.5 % m/v), and 4.8 mM $CaCl_2$, adjusted to pH 7.6) at 39 ºC for 4 min. The flow rate for the perfusion buffers was 10 mL/min. After perfusion the liver was removed from the animal and dissociated in cold Perfusion Buffer I with 10 g/L of albumin. The resultant cell suspension was filtered through gauze, centrifuged for 10 min at 50 x *g,* washed once with the medium, centrifuged again, and resuspended in the cold medium for a final concentration less than 3.5 x 10^6 cell/mL. For the enrichment of the final hepatocyte population, an additional Percoll-step was included. Five milliliters of cell suspension was layered over a 25 % Percoll solution and centrifuged at 1300 x *g* at 4 ºC for 20 min, and the hepatocytes were obtained as a pellet. The cell pellet was diluted in phosphate-buffered saline (PBS), centrifuged for 10 min at 50 x *g*, and washed twice with PBS for removing the Percoll solution. Finally, the cells were harvested in supplemented Williams'E medium for culturing. Cell viability was assessed by the trypan blue exclusion test and was, routinely, within an 85–95 %. Cells were seeded at a density of 1.6 x 10^5 cells/cm^2 on collagen pre-coated 24-well plates. The cells were cultured on Williams' E cell culture media supplemented with 10 % FBS (v/v), 1 mM sodium pyruvate (v/v), 1 % NEAA (v/v), 40 *μ*g/mL gentamicin, 100 U/mL penicillin, 100 *μ*g/mL streptomycin, 100 *μ*g/mL amphotericin B, 1.4 *μ*M

hydrocortisone and 32 U/mL human insulin. 6h after cell inoculation, medium and non-adherent cells were removed.

All cell cultures were maintained at 37 °C in a humidified atmosphere with 5 % CO_2 in air. Cell viability was assessed through trypan blue exclusion. Cell passage (hnMSC and HepG2) was performed every 72h or when cells reached 70-80 % confluence.

3.3.4 Hepatocyte differentiation of hnMSC

hnMSCs were seeded in 24-well plates (Nunc™, Wiesbaden, Germany) at a density of 1.5 x 10^5 cells/cm^2 in rat-tail collagen coated surface. Cells were allowed to proliferate for 24 hours in hnMSC growing medium. A three-step differentiation protocol was applied using as basal medium (BM) IMDM with 1 % penicillin-streptomycin-fungizone (P/S/A). Briefly, in the first step (*Step 1*), consisting of 48 hours, 4 different combination of growth factors were tested: BM supplemented with 2 % FBS, 10 ng/mL of EGF and (i) 10 ng/mL of FGF-2; (ii) 4 ng/mL of FGF-2; (iii) 4 ng/mL of FGF-2 and 10 ng/mL of FGF-4 or (iv) 10 ng/mL of FGF-2 and 10 ng/mL of FGF-4. In the second step (*Step 2*), cells were maintained for 10 days with BM supplemented with 20 ng/mL of HGF, 4 ng/mL of FGF-2, 10 ng/mL of FGF-4, 0.61 g/L of nicotinamide and 1 % ITS. In the third step (*Step 3*), at day 13 of differentiation, cells were supplemented with BM containing 8 ng/mL of OSM, 1 μM of dexamethasone and 1 % ITS. This culture medium was maintained up to day 34 of culture. The medium was renewed every 3-4 days in all protocols. DMSO (1 %, v/v), 5-AZA (20 μM) and TSA (500 nM) supplementation was performed and a total of 8 protocols evaluated, as summarized in **Table 3.1.**

Table 3.1. Summary of the DMSO, TSA and 5-AZA supplementation times in the hepatic differentiation protocols.

Protocol	1	2	3	4	5	6	7	8
DMSO	-	D13	D13		D13	D10	D10	D10
TSA	-	-	D13	D6	D6	-	D10	-
5-AZA§	-	-	-	-	-	-	-	D0

§ 24 hours of exposure time.

3.3.5 Gene expression

3.3.5.1 RNA isolation

Total RNA was isolated from samples with 0.5-1.0 million of cells using Trizol® (Life Technologies) and extraction was performed according to manufacturer instructions.

For microarray analysis of gene expression, RNA was further purified using a NZY Total RNA Isolation kit (NZYTech, Lisbon, Portugal), and quantified by measuring absorbance at 260 nm using LVis Plate mode (SPECTROstar Omega, BMG Labtech, Ortengerg, Germany). RNA integrity and sample purity were also measured using a 2100 Bioanalyzer (Agilent Technologies; Palo Alto, CA), assuring a RIN score higher than 8. Microarray analysis of hpHeps and HLC gene expression was performed using Affymetrix Human Genome U133 Plus 2.0 Gene Arrays at the Bioinformatics and Expression Analysis core facility at Karolinska Institutet (Sweden). For quantitative real time-PCR (qRT-PCR), RNA concentration was determined as above, prior to cDNA synthesis.

3.3.5.2 Microarray

Microarray data from undifferentiated hnMSCs (UCX®) and HepG2 cells, performed using the same array platform, were obtained from Gene Expression Omnibus (GSE51869 and GSE40117) (PMID: 24438697; PMID: 23393228). Subsequent analysis of differential gene expression and Principal Component Analysis (PCA) were performed using AltAnalyze (PMID: 20513647). Gene expression levels in HLCs, hnMSCs, and HepG2 cells were compared to the gene expression levels in hpHeps. Gplots heatmap.2 R package [263] was used to generate a gene expression heatmap of the 2000 genes with highest variance across the samples. Bioinformatic pathway analysis was conducted using the Ingenuity Pathways Analysis (IPA) software for genes with a fold change greater than 2 compared to the expression levels in hpHeps (Benjamini-Hochberg-corrected $p < 0.05$). The network biology-based computational platform CellNet (PMID: 25126793) was used to assess cell identity based on gene expression profiles. Venn diagrams were generated using Venny [264].

3.3.5.3 qRT-PCR

cDNA was synthesized from 1 μg RNA using NZY First-Strand cDNA Synthesis kit (NZYTech) according to the manufacturer instructions. Quantitative real time PCR was performed using SensiFAST™ SYBR® Hi-ROX kit (Bioline®, Luckenwalde, Germany). Master mix was prepared for a final reaction volume of 25 μL, using 1 μL of template cDNA and 0.1 μM of

forward and reverse primers. **Table 3.2** presents the specific human primers used for endoderm markers, progenitor hepatocytes and hepatocytes. The reaction was performed on StepOne™ Real-Time PCR System (Applied Biosystems®/ Life Technologies) consisting of a denaturation step at 95 °C for 10 minutes, 40 cycles of denaturation at 95 °C for 15 seconds, annealing at 60 °C for 1 minute and extension at 72 °C for 30 seconds. A dissociation stage was added to determine the melting temperature (Tm) of a single nucleic acid target sequence as a quality and specificity measure. The comparative Ct method ($2^{-\Delta\Delta Ct}$) was used to quantify the amount of target genes which were normalized to a reference gene *GADPH* and relative to undifferentiated cells, hnMSCs. The efficiency of each reaction was estimated from a serially diluted cDNA from a cell type expressing the target gene in order to construct a standard curve (1, 10^{-1} and 10^{-2}) for each gene.

Table 3.2 Primers used for qRT-PCR characterization of differentiated and undifferentiated hnMSCs, HepG2 and hpHeps.

	Primers	Melting temperature (Tm)	Reference
***HHEX*_F**	GCTTCAGAACCCATCCATGT	80.10	[190]
***HHEX*_R**	TTCCCCTCACGAAGAAGTTG		
***CK18*_F**	TGGTACTCTCCTCAATCTGCTG	83.61	[265]
***CK18*_R**	CTCTGGATTGACTGTGGAAGT		
***CK19*_F**	ATGGCCGAGCAGAACCGGAA	88.58	
***CK19*_R**	CCATGAGCCGCTGGTACTCC		
***HNF4A*_F**	ATTGACAACCTGTTGCAGGA	71.83	
***HNF4A*_R**	CGTTGGTTCCCATATGTTCC		
***AFP*_F**	TGCAGCCAAAGTGAAGAGGGAAGA	80.46	
***AFP*_R**	CATAGCGAGCAGCCCAAAGAAGAA		
***ALB*_F**	TGCTTGAATGTGCTGATGACAGGG	81.90	
***ALB*_R**	AAGGCAAGTCAGCAGGCATCTCATC		[266]
***TAT*_F**	TGCTGAGCAGTCTATCCACT	84.31	
***TAT*_R**	CTGCTCACAGAACTCCTGGAT		
***CEBPA*_F**	CAACACTTGTATCTGGCCTCTG	82.17	
***CEBPA*_R**	CGAGCAAAACCAAAACAAAAC		
***CYP1A1*_F**	TGGATGAGAACGCCAATGTC	86.42	

***CYP1A1*_R**	TGGGTTGACCCATAGCTTCT		
***CYP3A4*_F**	ATTCAGCAAGAAGAACAAGGACA	81.84	[267]
***CYP3A4*_R**	TGGTGTTCTCAGGCACAGAT		
***GAPDH*_F**	GAAGGTGAAGGTCGGAG	83.63	[170]
***GAPDH*_R**	GAAGATGGTGATGGGATTTC		

3.3.6 Histology

3.3.6.1 Immunocytochemistry

Cells cultured on collagen coated glass slides (Nunc™, Lab-Tek™ II Chamber Slide™) were fixed with 4 % paraformaldehyde (PFA; Sigma-Aldrich) in PBS with 4 % sucrose for 15 minutes and permeabilized with 0.3 % Triton™ X-100 (Sigma-Aldrich) in phosphate buffer saline (PBS) for 15 minutes at room temperature (RT). Blocking and incubation with antibodies was performed using a solution of 0.2 % fish skin gelatin/ 2 % bovine serum albumin (BSA) in PBS for 30 minutes at RT. Incubation with primary antibodies was performed overnight at 4 ºC: mouse anti-human CK-18 (Santa Cruz Biotechnology®, Inc, Heidelberg, Germany) diluted at 1:200; rabbit anti-human CK-19 diluted at 1:50, rabbit anti-human albumin diluted at 1:500; rabbit anti-human multidrug resistance protein-2 (MRP-2) diluted at 1:50; mouse anti-human organic anion-transporting polypeptide C (OATP-C); mouse anti-human CYP1A2 diluted at 1:100 (Santa Cruz Biotechnology®, Inc); mouse anti-human HNF-4α (R&D Systems, Minneapolis, MI, USA) diluted at 1:500; and rabbit anti-human CYP3A4 (Nosan Corporation, Yokohama, Japan) diluted at 1:500. Secondary antibody incubation with donkey anti-mouse Alexa Fluor 488 and/or goat anti-rabbit Alexa Fluor 594 (Molecular Probes®/ Life Technologies) diluted in 1:500 was performed for 1 hour at RT. ProLong® Gold Antifade Mountant with DAPI (Molecular Probes®/ Life Technologies) was used as mounting medium. Sample fluorescence was examined in fluorescence Microscope Axio Scope.A1 coupled with AxioCam HR (Carl Zeiss, Oberkochen, Germany) and images collected using AxioVision Rel. 4.7 software. Cryopreserved hpHeps, freshly isolated rpHeps cultured for one day and HepG2 were used as positive controls while undifferentiated hnMSCs were used as negative control.

3.3.6.2 Periodic acid Schiff's (PAS) staining

Cells cultured in 24-well plates were fixed with 4 % PFA in PBS. The staining was performed by incubation with 1 % periodic acid in PBS for 10 minutes, Schiff's reagent for 15 minutes and Mayer's hematoxylin counterstaining for 30 seconds. The preparations were washed with

H_2O between each step. Inner control consisted of differentiated HLCs and primary hepatocytes treated with 1 g/L of amylase in $CaCl_2$ at 30 mM, for 15 minutes at 37 °C after fixation, in order to digest the existent glycogen and assure that the pink stain corresponds to glycogen. Positive and negative controls consisted of cryopreserved hpHeps, freshly isolated rpHeps, cultured for 2 days, and HepG2 cells, and undifferentiated hnMSCs when at 70 % confluence, respectively. Staining was visualized in an inverted microscope (Olympus, Tokyo, Japan) and data images were recorded using Moticam 2500 and collected using Motic Images Plus V2.0 software (Motic, Xiamen, China).

3.3.7 Albumin and urea production

Albumin and urea quantification were determined on cell culture supernatant using an albumin ELISA kit (Bethyl Laboratories, Montgomery, TX, USA) and a quantitative colorimetric urea kit (QuantiChrom™ Urea Assay Kit, BioAssay Systems, Hayward, CA, USA), respectively. Both procedures were performed according to the manufacturer instructions. Data acquisition was done using a microplate reader (SPECTROstar Omega, BMG Labtech). The data refers to the production rate and is expressed as pg/10^6 cells.h and μg/10^6 cells.h, respectively.

3.3.8 Biotransformation activity

3.3.8.1 Phase I enzyme metabolism

CYP enzyme activity was measured by means of 7-ethoxyresorufin-O-deethylase (EROD) activity, 7-ethoxycoumarin-O-deethylase (ECOD) activity and P450-Glo™ assays (Promega, Madison, WI, USA). EROD assay mainly reflects the activity of the human isozymes CYP1A2 and CYP1A1 [268]. The procedure consisted of cell incubation with 8 mM of 7-ethoxyresorufin in non-supplemented BM for 90 minutes. The product concentration, 7-hydroxyresorufin, was measured in supernatants after 2 hours of enzymatic digestion with β-glucuronidase/arylsulfatase. The quantification was calculated using a calibration curve of resorufin in culture medium. Fluorescence was measured (Ex: 530 nm/ Em: 590 nm). ECOD assay measures human CYP2B6, CYP1A2 and CYP2E1 activities [61, 268]. The procedure consists of 90 minutes incubation with 7-ethoxycoumarin at 0.8 mM in non supplemented BM. 7-hydroxycoumarin concentration was determined after the same digestion procedure as used for EROD assay, followed by a liquid-liquid extraction step with chloroform and back-extraction of the organic phase with a solution of 5.84 % of NaCl in 0.1 M of NaOH. Fluorescence was measured (Ex: 340 nm/ Em: 460 nm). Induction of ECOD and EROD activities was performed

by 48 hour incubation with 2.5 µM of 3-MC or 100 µM of omeprazole. CYP3A4, CYP2C9 and CYP1A1 activities were assessed using the luminescent P450-Glo™ assay with the respective substrates Luciferin-PPXE, Luciferin-H and Luciferin-CEE. Each assay was performed with a final volume of 60 µL and luminescent intensity measured according to manufacturer instructions. Induction was performed by 48 hour incubation with 2.5 µM of 3-MC for CYP1A1 or 25 µM of rifampicin for CYP2C9 and CYP3A4. Luminescence and fluorescence measurements were done using a microplate reader (SPECTROstar Omega, BMG Labtech). The data is expressed as pmol/10^6 cells.h, except for CYP3A4 activity that is expressed as nmol/10^6 cells.h.

3.3.8.2 Phase II metabolism

Uridine 5'-diphosphate glucuronosyltransferases' (UGTs) activity was determined by quantification of the substrate 4-MU before and after cell incubation. The procedure was performed according to Miranda *et al.* [61] with slight modifications. Briefly, a 100 µM of 4-MU in HBSS was incubated with cells for 1 hour. The supernatants were freshly transferred into a black 96-well plate, 4 µL of NaOH at 0.1 M added per well in order to achieve pH = 11 and fluorescence was measured (Ex: 340 nm/ Em: 460 nm). UGTs activity was measured at day 1 on the cells used as negative (hnMSCs) and positive (HepG2, hpHeps and rpHeps) controls. The data is expressed as nmol/10^6 cells.h.

3.3.9 Protein quantification

For protein quantification, cells were lysed with 0.1 M of NaOH and incubated overnight at 37 ºC. Protein concentration was determined using the bicinchoninic acid (BCA) protein assay kit (Novagen, Madison, WI, USA) according to manufacturer instructions and also measured by absorbance at 280 nm using LVis Plate mode (SPECTROstar Omega, BMG Labtech). A linear calibration curve to relate total protein with cell number was generated to estimate cell number, from each cell type and for both methods of quantification.

3.3.10 Statistical analysis

The results are given as the mean ± SEM. Statistical data analysis was performed using GraphPad Prism version 6.0 (GraphPad Software, La Jolla, CA, USA). The effects on metabolic activity were evaluated by two-way ANOVA with Holm-Sidak method in order to determine whether the metabolic activity of each compound was significantly altered by the protocol, the induction of specific CYP450 enzyme inducers, over the time of culture, and to

evaluate differences between groups and controls. In all cases, $p < 0.05$ was considered statistically significant.

3.4 Results

3.4.1 The endoderm marker *HHEX* is expressed in hnMSC and induced by FGF-2

The three-step protocol developed for hepatocyte differentiation was optimized based on previously described methodologies [168, 172, 269] and considering the liver development stages: commitment, differentiation and maturation. Since hnMSCs are of mesodermal origin, particular attention was given to the endoderm commitment by testing the effect of FGF-2 at 4 ng/mL and 10 ng/mL, in the presence or absence of FGF-4 on *HHEX* gene expression (**Figure 3.1).**

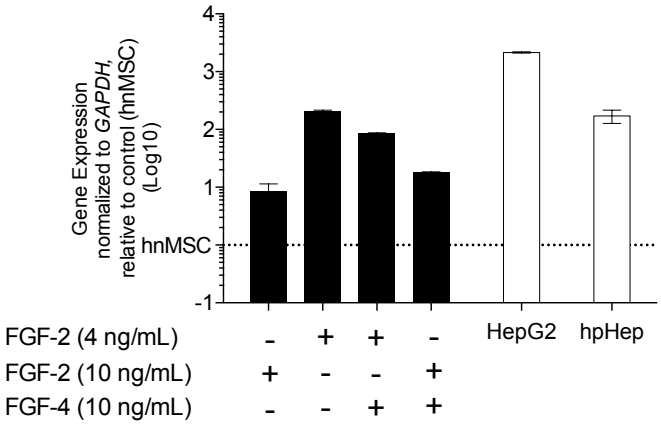

Figure 3.1 Gene expression of *HHEX* on hnMSCs after exposure to different FGF cocktails in the differentiation Step 1 (D3). qRT-PCR shows *HHEX* higher expression with 4 ng/mL of FGF-2 when compared to 10 ng/mL of FGF-2, or 4 ng/mL of FGF-2 and 10 ng/mL of FGF-4, or 10 ng/mL of FGF-2 and 10 ng/mL of FGF-4 (black bars). Positive controls (white bars) are cryopreserved hpHeps and HepG2 cell line. Data is normalized to the reference gene *GAPDH* and expressed in Log10 relative to hnMSCs (n = 3).

HHEX is an endoderm marker essential in liver development [270]. A basal expression of the *HHEX* gene was detected on hnMSCs. The addition of FGF-2 at 4 ng/mL produced a 200-fold increase in *HHEX* expression, whereas it only produced an 85-fold increase when cells were exposed to a combination of FGF-2 at 4 ng/mL and FGF-4 (10 ng/mL). Moreover, *HHEX* gene expression in the presence of FGF-2 (10 ng/mL) resulted in an 8- and 17-fold increase in the absence or presence of FGF-4, respectively. Thus, FGF-2 only was added to Step 1 of all differentiation protocols to a final concentration of 4 ng/mL.

3.4.2 Epigenetic modifiers improve hepatocyte phenotype on HLC

The epigenetic modifiers (EM) tested in this work consist of small molecules that have been previously described and applied as promoters of hepatic differentiation, namely TSA, DMSO and 5-AZA. Previously, we have evaluated TSA at concentrations ranging from 100 nM to 1000 nM being 500 nM the best tested condition (data not shown), and therefore the concentration used in this work. As for DMSO and 5-AZA, 1 % and 20 µM, respectively, were adopted according to literature [54, 213]. Furthermore, DMSO was tested alone, from days 10 and 13 onwards, or in combination with TSA or 5-AZA in a total of 8 different differentiation protocols (**Table 3.1**). During the differentiation protocol, cells in culture were maintained confluent and in serum-free conditions in order to prompt differentiation rather than proliferation. The fibroblastic morphology of hnMSC was kept during the first two steps of the differentiation protocol except for protocols 4 and 5, where TSA was added at day 6. This resulted in cell detachment (**Figure 3.2**) and therefore protocols 4 and 5 were not further pursued. From day 13 onwards, after the addition of OSM and dexamethasone, cell morphology started to change to a more epithelial-like shape with granular cytoplasm in all other protocols, *i.e.*, protocols 1-3 and 6-8 (**Figure 3.2**). At day 24, an epithelial polygonal hepatocyte-like morphology, with some binucleated cells, and glycogen storage ability were observed in HLCs obtained with protocols 1, 2, 6 and 8, where TSA was absent and DMSO was present (**Figure 3.2**). Accordingly, ALB and CK-18 were detected by immunocytochemistry. Overexpression of *HHEX* (data not shown), *CK18*, *TAT*, *CEBPA*, *HNF4A* and *CYP3A4* was observed at day 24 in all protocols (**Figure 3.3**). *CK19*, a biliary cell marker, showed low expression in all protocols. *ALB* and *AFP* overexpression was observed on protocols 1, 6 and 8 (**Figure 3.3**). In parallel, the HLC enzymatic competence, namely phase I and II activities were analysed (**Figure 3.4a**). Similar EROD activity was obtained with all protocols. However, the protocols including DMSO at day 10 (protocols 6-8) presented significant induction of EROD activity ($p < 0.01$) whereas protocols with TSA only revealed induction when concomitantly added with DMSO (protocols 3 and 7; $p < 0.05$). In particular, protocol 6 resulted in higher CYP3A4 activity when compared to the positive controls ($p < 0.05$). CYP3A4 induction was also observed with this protocol ($p < 0.05$). Regarding phase II enzymatic activity, an increased UGTs activity was observed in differentiation protocols where DMSO was added at day 10 (protocols 6, 7 and 8) when compared to its supplementation at day 13 (protocols 2 and 3), independently of TSA presence ($p < 0.001$; **Figure 3.4a**). A positive effect of 5-AZA (protocol 8) was also observed with improved UGTs activity ($p < 0.01$) when compared to the protocol where it was absent (protocol 6), as previously observed by Seeliger *et al*. [213]. Finally, the protocols without TSA, but supplemented with DMSO at day 10

(protocols 6 and 8) presented higher urea production (**Figure 3.4b**), especially protocol 6 ($p < 0.05$) where the achieved urea production was comparable to HepG2. All protocols also presented a significant increase in albumin production ability when compared to the negative control (**Figure 3.4c**).

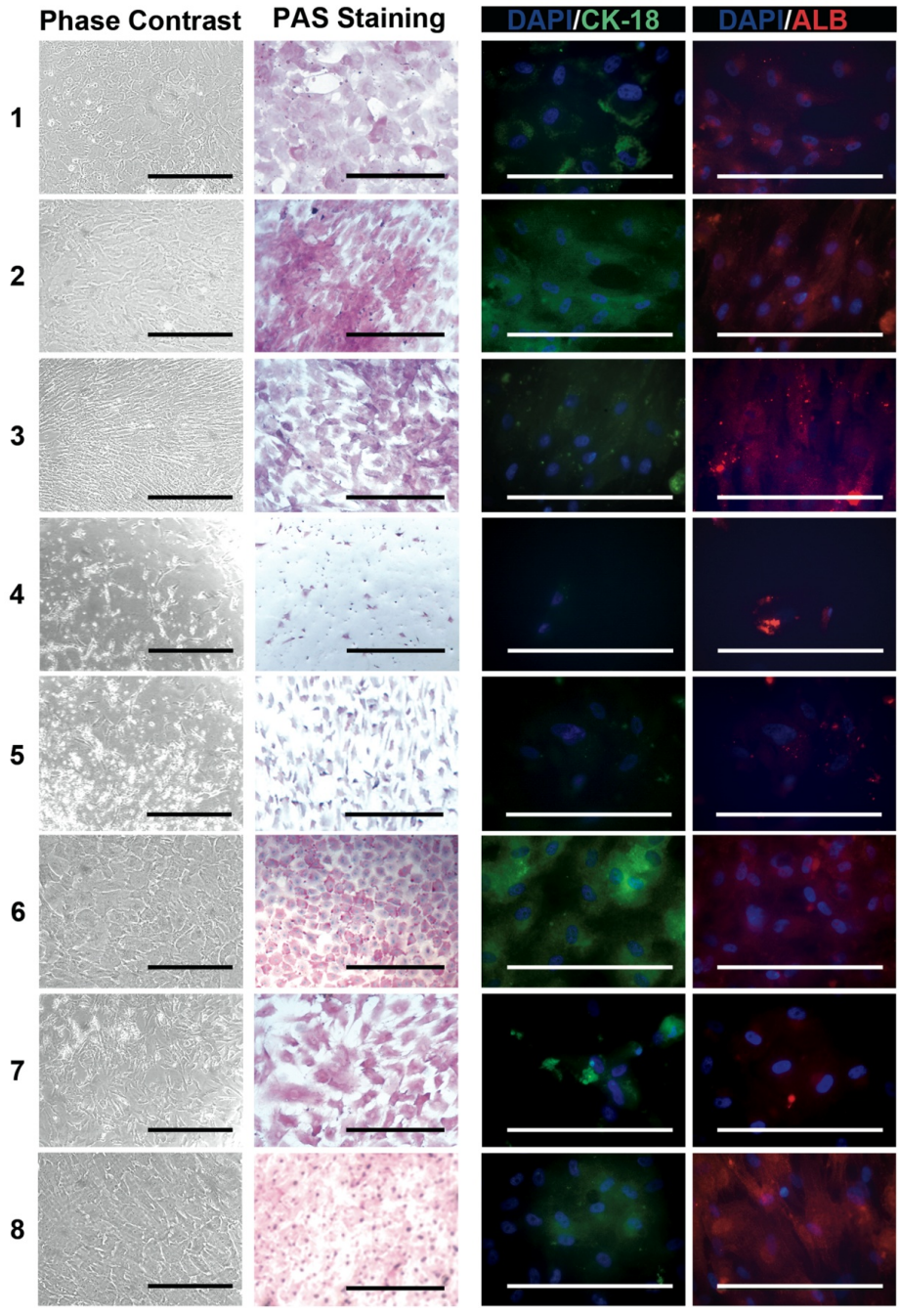

Figure 3.2 Comparative characterization of hnMSC-derived HLC obtained with the differentiation protocols 1-8 (D24). Phase contrast, PAS staining and immunocytochemical representative images reveal an epithelial morphology, glycogen storage ability and the presence of CK-18 and ALB, respectively, in HLCs from protocols 1-3, 6 and 8. In immunocytochemical analysis, cell nuclei were counterstained with DAPI. Scale bar = 50 µm.

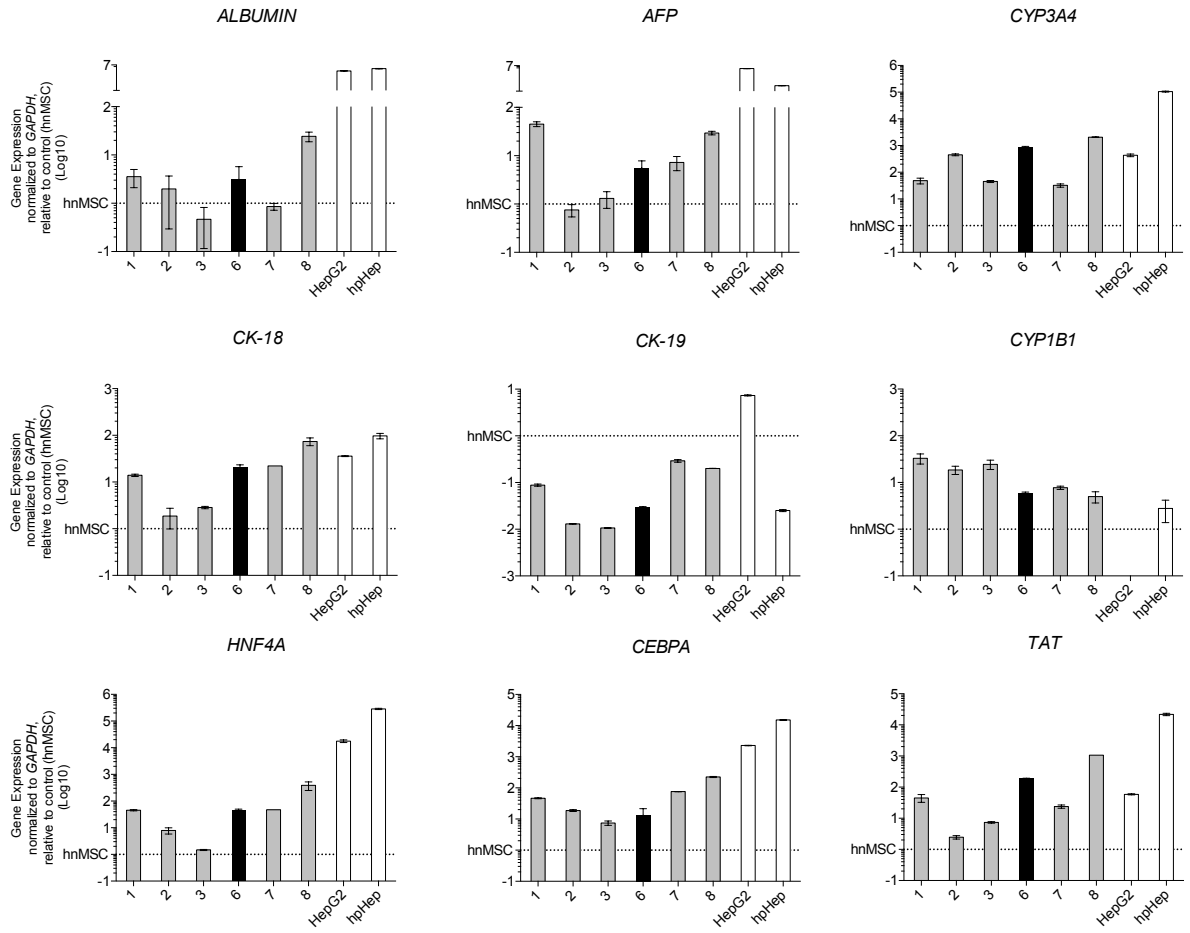

Figure 3.3 Gene expression analyses of HLC-derived from hnMSCs upon exposure to protocols 1-3 and 6-8 (D24). qRT-PCR shows over expression of the hepatic markers *ALB, AFP, CK18, HNF4A, CYP3A4, TAT* and *CEBPA* and underexpression of the biliary marker *CK19* (grey bars and black bar for protocol 6). Positive controls (white bars) are HepG2 cell line and cryopreserved hpHeps. Data is normalized to the reference gene *GAPDH* and expressed in Log10 relative to hnMSCs (n= 3).

Overall, TSA supplementation resulted in a more heterogeneous cell phenotype considering morphology and expression of hepatocyte-specific proteins (protocols 3 and 7); whereas DMSO supplementation resulted in HLCs expressing hepatocyte markers, epithelial cell morphology, homogeneous glycogen storage and improved HLC biotransformation activity (protocols 2, 6 and 8). The later was more evident when DMSO was added at day 10 (protocol 6) rather than at day 13 (protocol 2).

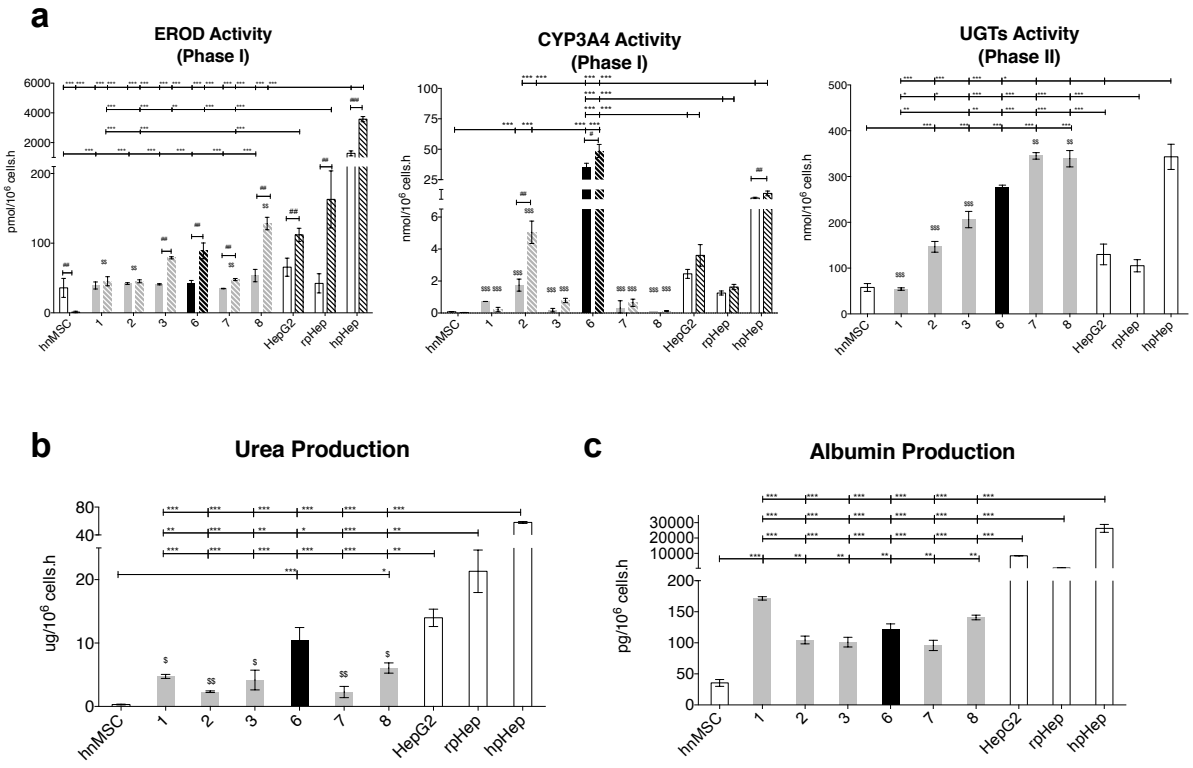

Figure 3.4 Functional capacity of HLC-derived from hnMSCs upon exposure to protocols 1-3 and 6-8 (D24). (a) Phase I (EROD and CYP3A4 activities) and phase II (UGTs activity) enzymatic activities. Induction studies (striped bars) were performed for 48 hours with 25μM of rifampicin (CYP3A4) or 2.5 μM of 3-MC (EROD). rpHeps and hpHeps were cultured for 72 hours and 24 hours for phase I and phase II assays, respectively; (b) Urea secretion; and (c) Albumin production. Grey bars correspond to HLCs differentiated using protocols 1-3 and 7-8 and black bars to protocol 6. Controls (white bars) are hnMSCs (negative control) and HepG2 cell line, rpHeps and hpHeps (positive controls). Data is represented as mean ± SEM (n = 4-6). *, **, *** Significantly differs among the controls with $p < 0.05$, $p < 0.01$ and $p < 0.001$, respectively. $^{\$}$, $^{\$\$}$, $^{\$\$\$}$ Significantly differs from protocol 6 with $p < 0.05$, $p < 0.01$ and $p < 0.001$, respectively. $^{\#}$, $^{\#\#}$ Significantly induced activity with $p < 0.05$ and $p < 0.01$, respectively.

3.4.3 hnMSC-derived HLC present a partial hepatic differentiation at the transcriptional and functional levels at day 34

The need for a competent alternative model for drug metabolism studies encouraged us to examine the stability of hepatic phenotype in culture. Overall, protocol 6 provided the best condition where HLCs showed results that are comparable to the positive controls. Thus, hnMSC-derived HLCs were kept in culture until day 34, revealing an epithelial morphology and the presence of binucleated cells and maintaining confluence throughout the cell culture period (**Figure 3.5**). Differentiation efficiency and phenotype maintenance was further evaluated at the transcriptional and functional levels. PAS straining demonstrated glycogen storage ability of HLCs up to day 34 in culture (**Figure 3.5**). Albumin and urea secretion was

also stable during the full culture period, showing levels higher than hnMSCs ($p < 0.05$; **Figure 3.6).**

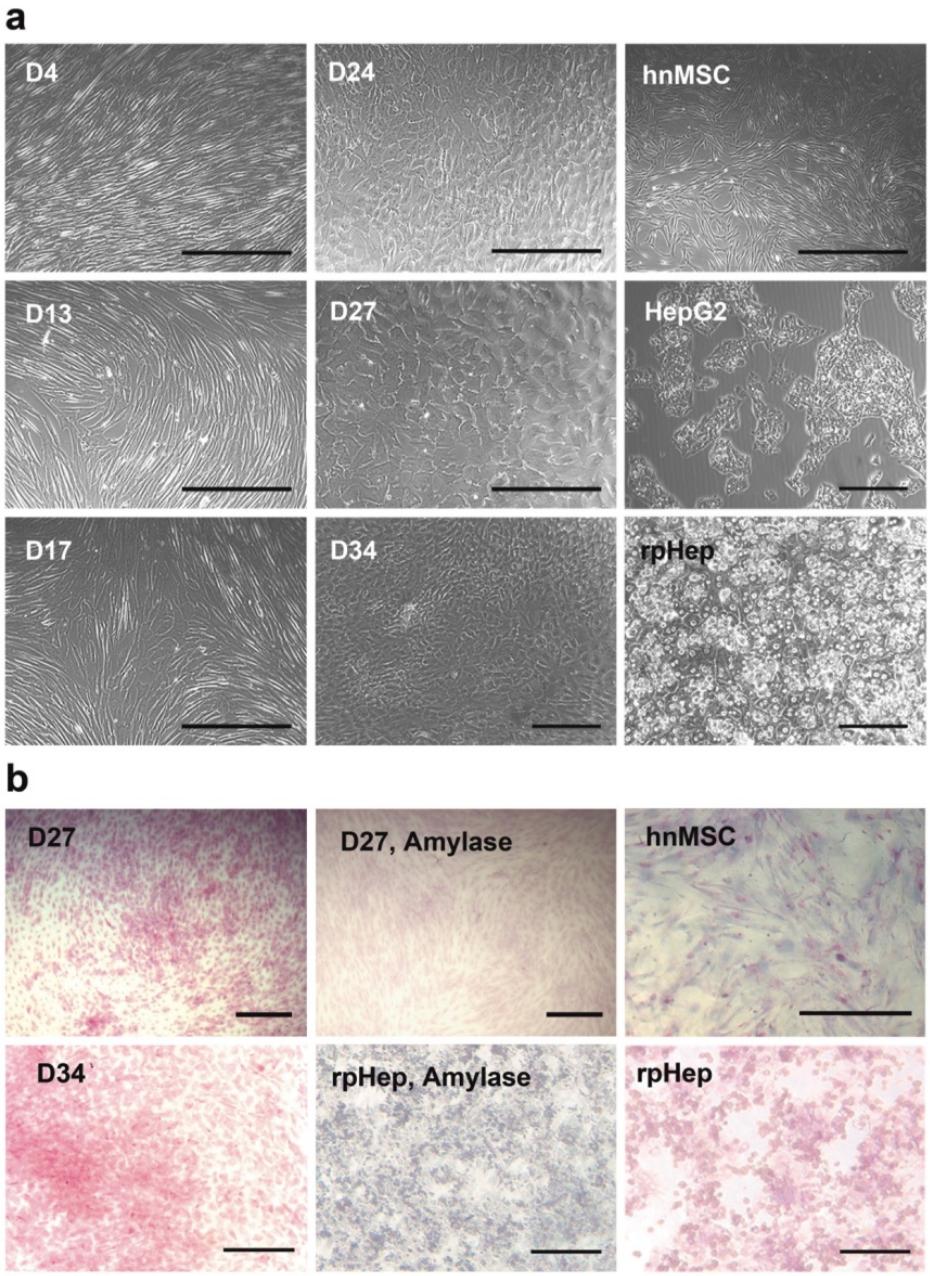

Figure 3.5 hnMSCs-HLC morphology and glycogen storage ability upon sequential exposure to liver-specific factors and DMSO supplementation from day 10 onwards. (a) Cell morphology of hnMSCs during the differentiation process at days 4, 13, 17, 24, 27 and 34 and of undifferentiated hnMSCs (negative control), HepG2 cell line and rpHeps (positive controls); (b) PAS staining of HLCs at days 27 and 34 of undifferentiated hnMSCs (negative control) and rpHeps (positive controls). HLCs and rpHeps stained after digestion with amylase in order to access the specificity of the observed staining are also presented. Controls are hnMSCs (negative control) and rpHeps (positive controls). Representative images were acquired with phase-contrast microscopy. Scale bar = 50 µm.

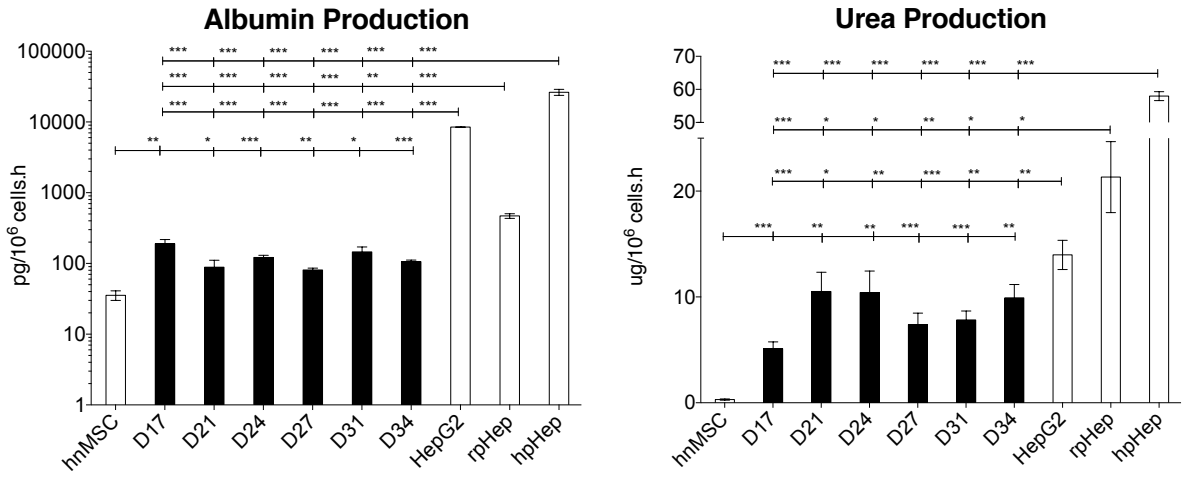

Figure 3.6 Effect of culture time on albumin and urea production in HLC-derived from hnMSCs up to day 34 in culture upon sequential exposure to liver-specific factors and DMSO supplementation from day 10 onwards (black bars). Undifferentiated hnMSCs and HepG2 cell line, rpHeps and hpHeps are negative and positive controls, respectively (white bars). Data is represented as mean ± SEM (n = 4-6). *, **, *** Significantly differs among the controls with $p < 0.05$, $p < 0.01$ and $p < 0.001$, respectively.

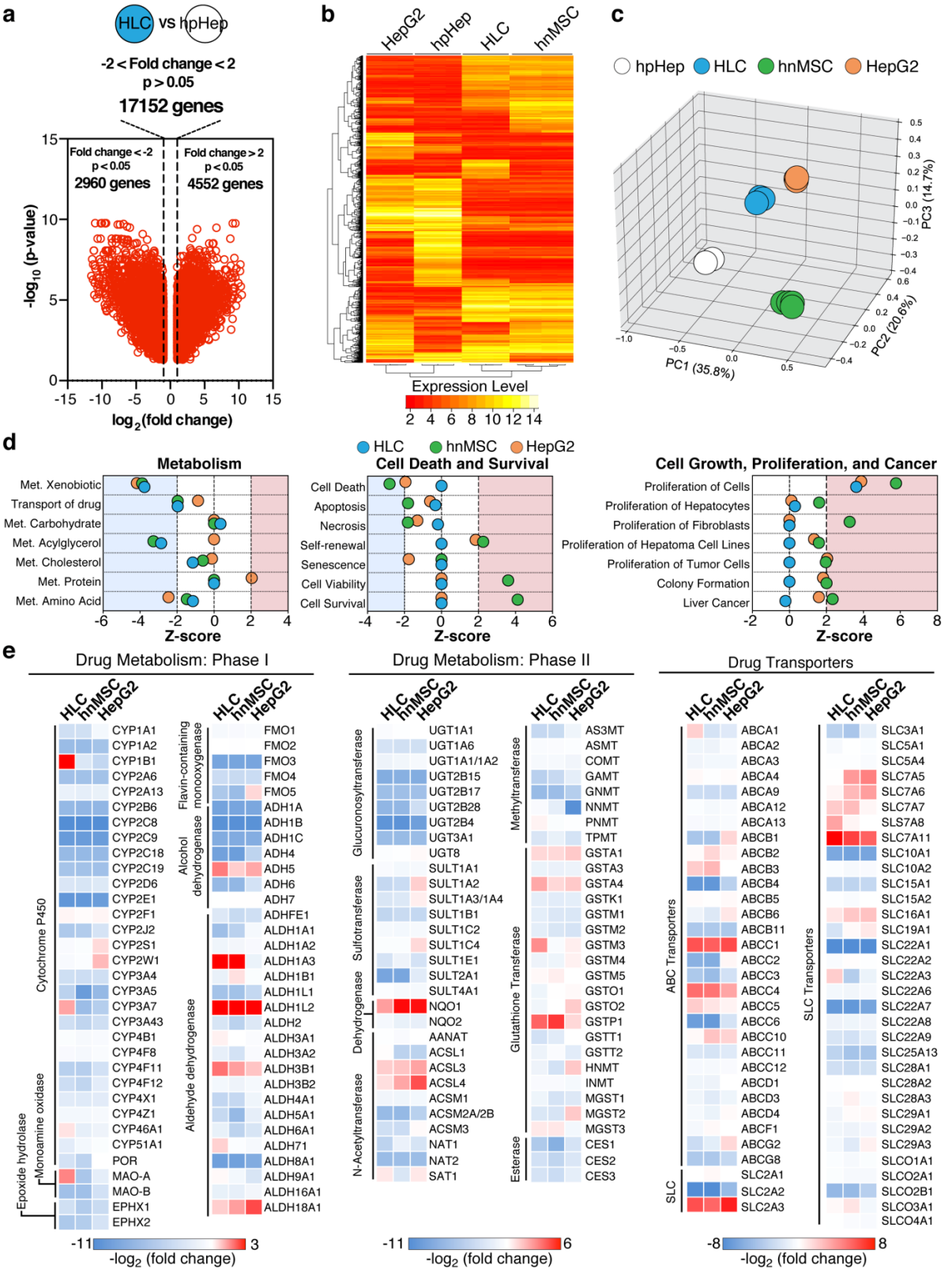

Figure 3.7 Genome wide analyses of HLC-derived from hnMSCs at day 34 of differentiation. (a) Volcano plot of differently expressed genes in HLC vs hpHep (fold change > 2, $p < 0.05$); (b) Heatmap representation of the 2000 genes with highest variance across samples in hpHeps, HLCs, hnMSCs and HepG2; (c) Principal component analysis (PCA) of gene expression profiles in hpHeps, HLCs, hnMSCs and HepG2; (d) Expression profile-based prediction of biological function activation performed with IPA for HLCs, hnMSCs, and HepG2 cells compared to

hpHeps. Positive Z-scores indicate activation whereas negative z-scores indicate repression; (e) Relative expression levels of genes involved in drug metabolism comprehending phase I, II and drug transporters in HepG2, hpHeps, HLCs and hnMSCs, compared to hpHeps.

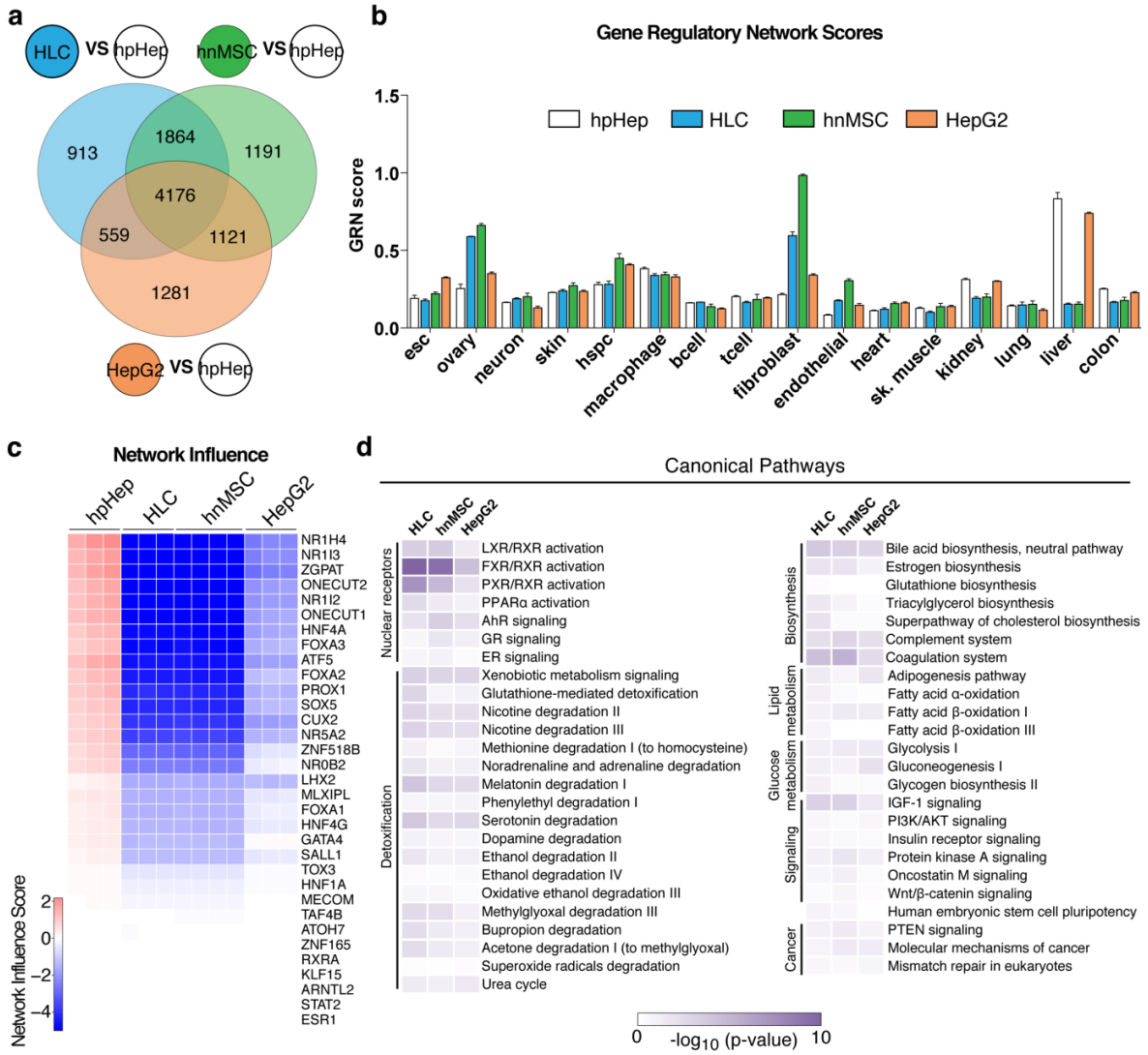

Figure 3.8 Genome wide analyses of HLC-derived from hnMSCs at day 34 of differentiation. (a) Venn diagram representing the number of differentially expressed genes in HLCs, hnMSCs and HepG2 compared to hpHeps (fold change > 2, $p < 0.05$). The diagram shows how many differentially expressed genes are common or unique to the various cell types analysed. (b-c) CellNet analysis of cell identity depicting the gene regulatory network (GRN) score (b) and network influence score for liver (c). The GNR score indicates to which level specific tissue/cell GRN are established. The network influence score indicates how the expression of each transcriptional regulator within a GRN compares to the expression levels in the target tissue/cell (in this case liver). Orange indicates higher expression and blue indicates lower expression. (d) IPA analysis of canonical pathways associated with differentially expressed genes in HLCs, hnMSCs and HepG2, compared to hpHeps.

To compare gene expression signatures between our HLCs (D34) and hpHeps, an unbiased whole genome analysis was performed. To get a better understanding on how hnMSC-derived HLCs compared to other cells we then compared our data with previously published gene

array data from undifferentiated hnMSCs and HepG2 cell line available at Gene Expression Omnibus. Interestingly, global gene expression analysis (**Figure 3.7a**), comparing differentially expressed genes in HLCs and hpHeps, estimated that ~70 % of transcripts remain the same between HLCs and hpHeps (n = 17152), using a combined criterion of $p < 0.05$ and fold change > 2. The heatmap representation and unsupervised clustering of the 2000 genes with highest variance (**Figure 3.7b**) showed that in some clusters the differentiation protocol approximates the HLC's gene expression profile to that of hpHeps, when compared to the undifferentiated hnMSCs. It also revealed similar gene expression clustering between HLCs and hpHeps, which was not observed between HepG2 and hpHeps. In HLCs, the expression of some genes involved in drug transport, amino acid metabolism and proliferation of hepatocytes was comparable to hpHeps, whereas others involved in xenobiotic metabolism remained poorly expressed (**Figure 3.7b** and **3.7d**). Accordingly, a PCA plot (**Figure 3.7c**) evidenced a partial gain of mature hepatic features of the HLCs revealing that HLCs did not reach the hpHep global gene expression profile, but are closer than the HepG2 cell line and distant from hnMSCs. In fact, a Venn diagram representing the number of differentially expressed genes in HLCs, hnMSCs and HepG2 compared to hpHeps (fold change > 2, $p < 0.05$) shows that HLCs have less differentially expressed genes than hnMSC or HepG2, when these cells are compared to hpHeps (**Figure 3.8a**). Additionally, CellNet analysis for assessing cell type identity, plotted as GRN (gene regulatory networks; **Figure 3.8b**) and network influence scores (**Figure 3.8c**), demonstrated that HLCs consist of a mixed cell type with both "fibroblast" and "ovary" features. CellNet is a platform that estimates how closely cell populations resemble their target cell/tissue type [271]. The rational is that by measuring the establishment of cell- and tissue- (C/T) specific GRNs in a cell population would serve both as a robust metric of cellular identity and a tool to identify aberrant regulatory nodes. Thus, as expected, undifferentiated hnMSCs and liver cells (hpHeps and HepG2) had a maximum GRN status score for "fibroblast" and "liver", respectively. Moreover, from the total of 16 cell/tissue types listed, no significant changes in GRN scores were observed between HLCs and hpHeps for "esc", "neuron", "skin", "hspc", "macrophage", "bcell", "tcell", "heart", "sk. muscle" and "lung". Regarding the "fibroblast" GRN status, the HLCs showed a decrease relative to the hnMSCs revealing some degree of differentiation, but still some features of MSCs from where they were derived. The network influence profile, on the other hand, was similar in HLCs and hnMSCs, whereas hpHeps presented high influence on transcription factors such as *NR1H4* (FXR), *NR1/3* (CAR), *NR1/2* (PXR), *HNF4A* (**Figure 3.8c**). The GRN score is based on the expression levels of a limited number of transcriptional regulators (**Figure 3.8c**). Therefore, to get a better assessment of the activation status of biological

pathways and functions in HLCs, we performed a bioinformatics pathway analysis herein plotted within three categories: metabolism, cell death and survival, and cell growth, proliferation and cancer in all groups relative to hpHeps (**Figure 3.7d**). All groups (HLC, HepG2 and hnMSC) presented a negative z-score indicating repression of the expression profile for drug transport, xenobiotic metabolism, and amino acid metabolism though HLCs presented a higher activation than hnMSCs and HepG2 cell line for the later two subcategories. In contrast to HepG2 or hnMSCs, cell death and survival and cell growth, proliferation and cancer categories presented the same activation in HLCs as in hpHeps (**Figure 3.7d**), suggesting that HLCs are closer to hpHeps regarding these particular bio-functions. Most importantly, **Figure 3.7d** further indicates that, unlike HepG2, HLCs display a less “cancer cell”-like profile as shown by normalized gene expression signatures associated with cell death, apoptosis, proliferation of hepatoma cell lines, proliferation of tumor cells, colony formation and liver cancer. Finally, canonical pathways representation from the IPA analysis showed an approximation of HLCs to hpHeps in glucose and lipid metabolism and in signalling pathways such as PI3K/AKT, PKA, oncostatin M and Wnt/β-catenin (**Figure 3.8d**); and major differences in the PXR/RXR and FXR/RXR activation pathways followed by xenobiotic metabolism signalling and glutathione-mediated detoxification.

In order to have a deeper insight on gene expression profile, genes were also grouped considering genes coding for key enzymes in phase I, II and II of drug metabolism (**Figure 3.7e**). High expression of the phase I enzymes *CYP1B1*, *CYP3A7* and *MAO* was observed in HLCs but not in the other groups relative to hpHeps. Moreover, there was a higher expression of *CYP3A5* and *CYP3A7* relative to HepG2 and hnMSCs; whereas the expression of relevant CYPs such as *CYP2D6*, *CYP2C9* and *CYP3A4* was similar in HLCs, HepG2 and hnMSCs, being considerably lower than hpHeps. Remarkably, some aldehyde dehydrogenase isoforms, namely from *ALDH1*, *ALDH3*, *ALDH7*, *ALDH9*, *ALDH18* subfamilies, were induced in HLCs to levels comparable to hpHeps. Phase II metabolism analysis showed a high expression of GST family genes and a low expression of UGT transcripts. In the “drug transporters” group, similar expression of some transcripts was observed in both ABC and SLC transporters, namely *ABCA*, *ABCC*, *SLC5*, *SLC7, SLC28*, *SLC29* and *SLCO* subfamilies.

To support global transcriptomic characterization, further gene and protein expression of selected mature hepatocyte markers was evaluated by qRT-PCR and immunofluorescence. Confirming qRT-PCR gene expression data (**Figure 3.9**), and despite low expression relative to hpHeps (**Figure 3.7e**), the hepatic transporters OATP-C and MRP-2 and the biotransformation enzymes CYP1A2 and CYP3A4 were detected by immunofluorescence, along with the presence of CK-18, ALB and HNF-4α and the absence of CK-19 (**Figure 3.10**).

In fact, the transcription factors *HNF4A* and *CEBPA*, the biotransformation enzymes *CYP1A1* and *CYP3A4,* the genes encoding for *ALB*, *AFP* and the enzyme involved on amino acid metabolism *TAT*, all presented increased expression from day 24 up to day 34, being *TAT*, *CK18* and *CYP3A4* higher than HepG2 (**Figure 3.9**), suggesting some level of maturation. The observed *CK18* expression level is comparable with hpHeps and higher than HepG2 cell line. *CK19* was under expressed as expected.

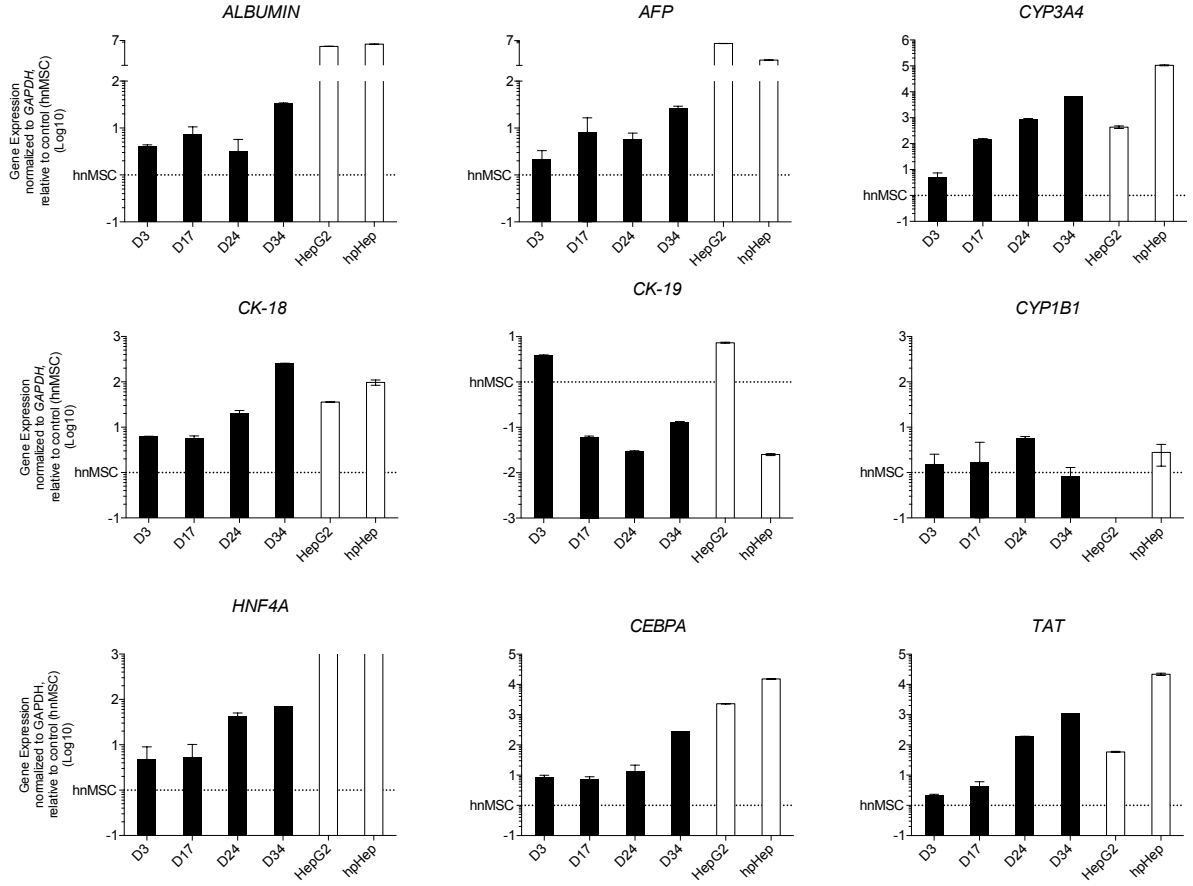

Figure 3.9 Gene expression analyses during hnMSC differentiation into HLCs upon sequential exposure to liver-specific factors and DMSO supplementation from day 10 onwards. qRT-PCR shows increased gene expression over time of the hepatic markers *ALB, AFP, CK18, HNF4A, CYP3A4, TAT* and *CEBPA* and decreased expression of the biliary marker *CK19* in HLCs (black bars). Positive controls (white bars) are HepG2 cell line and cryopreserved hpHeps. Data is normalized to the reference gene *GAPDH* and expressed in Log10 relative to hnMSCs (n = 3).

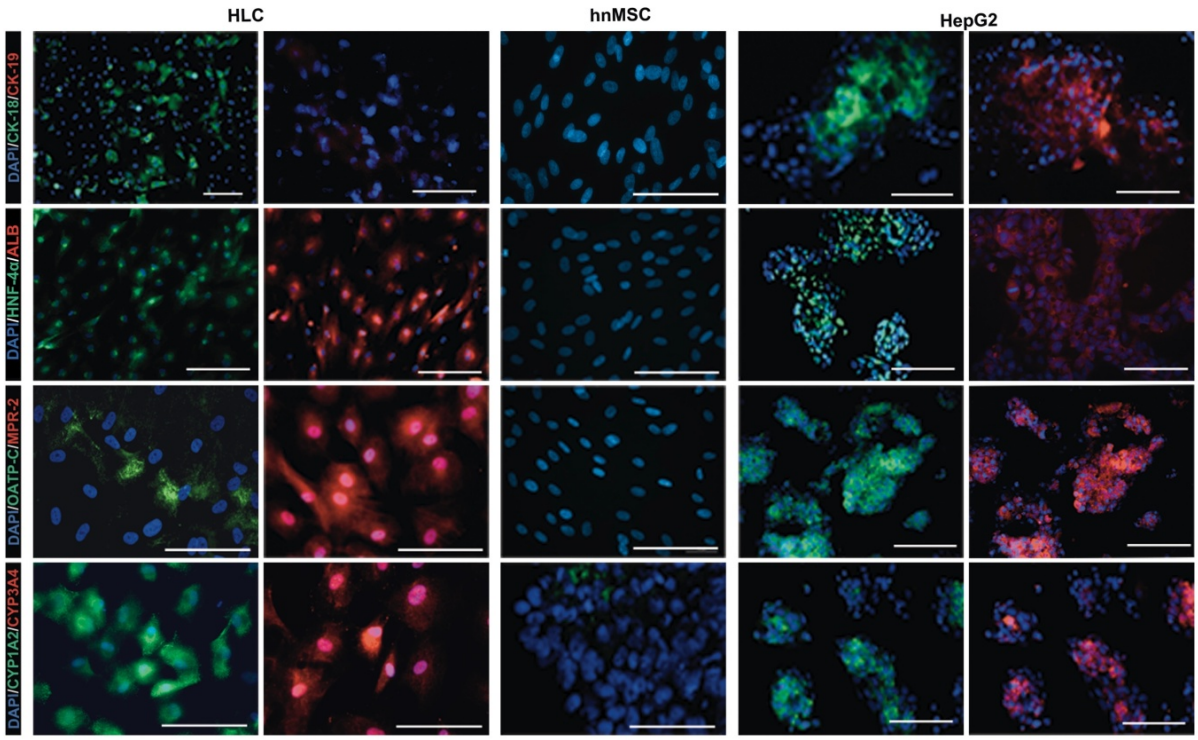

Figure 3.10 Immunocytochemical analysis of HLC-derived from hnMSCs upon sequential exposure to liver-specific factors and DMSO supplementation from day 10 onwards (D27). Representative images show the presence of the hepatic markers ALB, CK-18, HNF-4α, MRP-2, OATP-C, CYP1A2, CYP3A4 and the absence of the biliary marker CK-19. hnMSCs and HepG2 cell line were used as negative and positive controls, respectively. Cell nuclei are stained with DAPI. Scale bar = 50 µm.

The functional characterization of HLCs further supported the gain of hepatic features, namely by examining the effect of culture time on CYP and UGTs activities (**Figure 3.11**). ECOD and CYP1A1 activities were maintained with time in culture. Conversely, EROD, CYP2C9 and CYP3A4 activities and induction abilities were greatly improved by day 34, reaching levels higher than HepG2 for CYP3A4 and CYP2C9. At day 34, CYP3A4, CYP1A1 and EROD activities are also enhanced when compared to rpHeps. A 2.5-fold and ~3-fold activity increase was even observed for CYP3A4 when compared to hpHep basal and induced activities, respectively. Accordingly, UGTs activity was maintained during 13 days counting from the last day of the differentiation protocol, revealing a 2.2-fold and 2.7-fold increase in UGTs activity by day 27, when compared to HepG2 ($p < 0.01$) and rpHeps ($p < 0.001$), respectively.

In summary, the differentiation process herein developed evidenced a partial hepatic differentiation of the HLCs with relevant improvements regarding the HepG2 cell line.

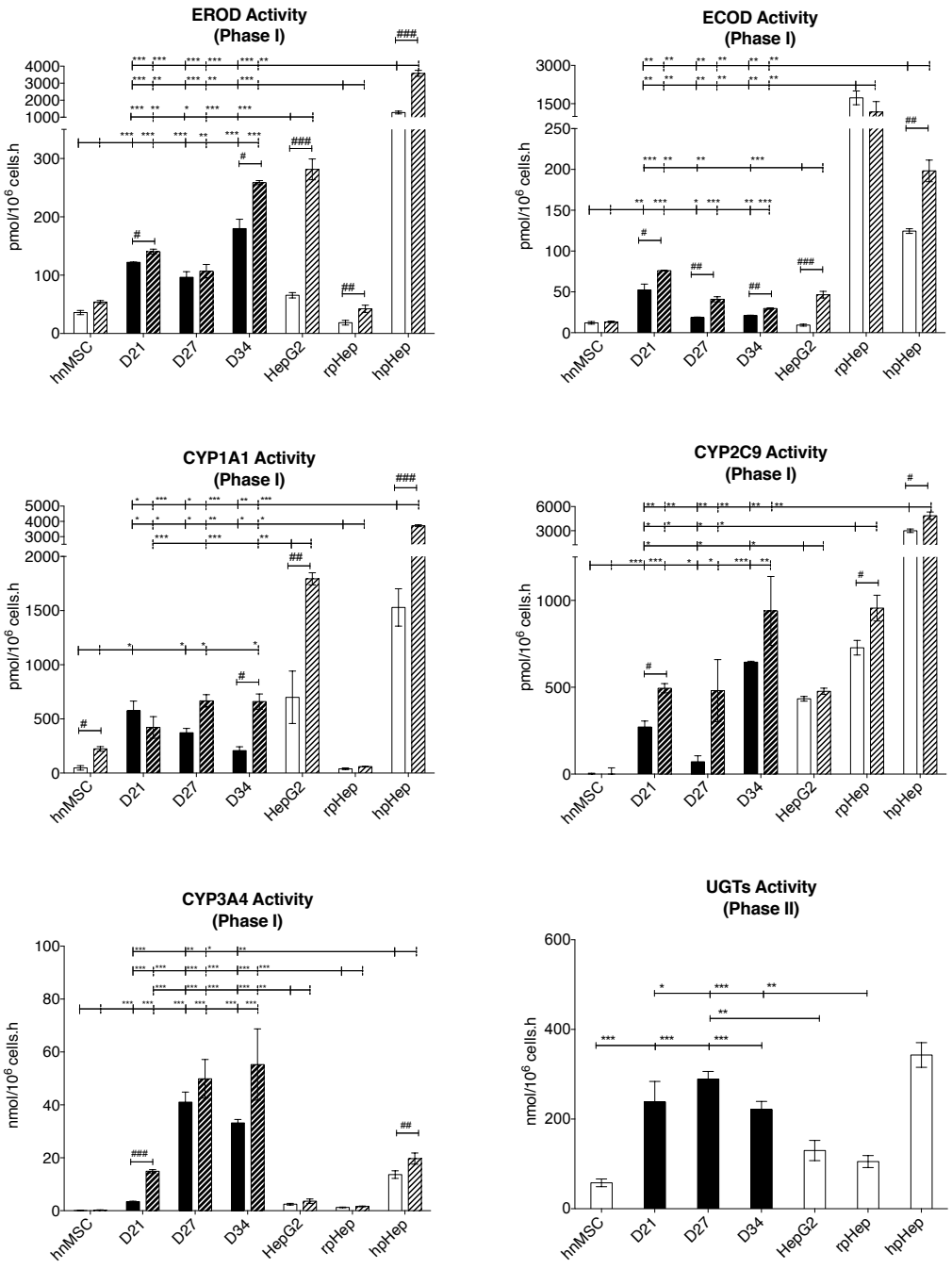

Figure 3.11 Effect of culture time on phase I and phase II activities in HLC-derived from hnMSCs up to day 34 in culture upon sequential exposure to liver-specific factors and DMSO supplementation from day 10 onwards. Phase I and phase II activity was assessed by measuring EROD, ECOD, CYP1A1, CYP2C9 and CYP3A4 and UGTs activities, respectively, at days 21, 27 and 34 (black bars). Induction assays (stripped bars) were performed with 48 hour incubation with 2.5 μM of 3-MC (CYP1A1 activity), 100 μM of omeprazole (ECOD and EROD activities) and 25 μM of rifampicin (CYP3A4 and CYP2C9 activities). Controls (white bars) are hnMSCs (negative control) and HepG2 cell line, hpHeps and rpHeps (positive controls). rpHeps and hpHeps were cultured for 72 hours and 24 hours for phase I and phase II assays, respectively. Data is represented as mean ± SEM (n = 3). *, **, *** Significantly differs among the controls with $p < 0.05$, $p < 0.01$ and $p < 0.001$, respectively. $^{\#}$, $^{\#\#}$, $^{\#\#\#}$ Significantly induced activity with $p < 0.05$, $p < 0.01$ and $p < 0.001$, respectively.

3.5 Discussion

Hepatotoxicity studies are usually limited in duration, and results may not provide a complete understanding of drug's cumulative and long-term *in vivo* effects. The inability to culture, characterize and challenge cells over longer periods of time is a relevant drawback of primary hepatocyte cell culture. Maintaining metabolic competence for longer periods of time is thus of foremost importance to investigate enzyme induction and inhibition, drug metabolism and drug chronic toxicity and it is the main reason why alternative in vitro models have not yet been fully achieved [17]. The differentiation of stem cells, MSCs in particular, into HLCs has been attempted to provide qualified model systems to study hepatic drug metabolism in vitro [168, 171, 172, 174, 179]. Many reports have shown distinct hepatic differentiation abilities among different MSCs. Although the differentiation efficiency has been greatly improved by modifying the culture conditions, the obtained HLCs are still insufficient for either toxicological or clinical applications [168]. In this work, we have demonstrated that a specific population of human neonatal MSCs isolated from the umbilical cord tissue, UCX®, [154, 258] is actually a promising cell source for deriving functional HLCs. The use of epigenetic modifiers on hepatic differentiation, especially DMSO, enabled the achievement of highly efficient hnMSC-derived HLCs, and most importantly, metabolic competence could be enhanced up to day 34 in culture. Whole genome analysis further confirmed the gain of hepatic features of HLCs and improvement regarding HepG2 cell line.

We firstly investigated the in vitro endoderm commitment potential of hnMSCs. Different MSCs have been reported to present important differences in their transcriptomes depending on their tissue source. De Kock *et al*. [160] suggested that WJ-MSCs presented a more favourable transcriptome regarding hepatocyte differentiation when compared to other types of stem cells, namely AD-MSCs, BM-MSCs and human skin-derived precursor cells. In fact, hnMSC-UCM have been described as expressing early liver specific markers, endoderm genes such as *GATA4* [151], *GATA5*, *GATA6*, *SOX9* and *SOX17* and liver progenitor markers as *DKK1*, *DPP4*, *DSG2*, *CX43* and *CK19* [150, 160]. *GATA4* has been reported to be a transactivator of *HHEX* expression [272] required for definitive endoderm tissues for normal liver development. Conversely, *GATA6* gene deletion impairs *HHEX* up-regulation needed for liver bud formation and a normal hepatic developmental program, showing that *GATA6* is essential for the earliest stages of hepatic development [273]. In liver development, the FGF family of cytokines is secreted by cardiogenic mesoderm and is required for the hepatic commitment of endoderm. Kang *et al*. [274], using mouse embryos, showed that FGF-4 is important for cell distribution in primitive endoderm but not for its formation, being later required for lineage restriction. On

the other hand, FGF-2 is a powerful inducer of foregut-derived cell lineages [275]. FGF-2 concentration determines cell differentiation fate as Ameri *et al.* [190] observed in studies of embryo development, showing that low concentrations of FGF-2 (4 ng/mL) triggers hepatic fate, whereas higher concentrations promote pancreatic and pulmonary differentiation. Thus, the effect of FGF-2 at 4 ng/mL and 10 ng/mL, alone or in combination with FGF-4, on endoderm commitment/foregut induction was evaluated by means of *HHEX* gene expression. Our data showed a basal *HHEX* expression in undifferentiated hnMSCs that was further induced by FGF-2 in a concentration-specific manner, reinforcing the differentiation potential of these cells into endoderm-derived lineages. The observed up-regulation of *HHEX* gene expression by FGF-2 at 4 ng/mL on differentiating cells is in accordance with Zhang *et al.* [275] that showed that 5 ng/mL of FGF-2 increased *HHEX* expression. Ameri *et al.* [190] also showed that higher concentrations of FGF-2 would reduce *HHEX* expression and inhibit further *ALB* expression, determining 4 ng/mL as the optimal concentration to direct hepatic cell fate. On the other hand, FGF-4 was reported to down regulate *HHEX* expression [276], which is also in agreement with our findings. The importance of *HHEX* for hepatic lineage commitment was also shown in vitro by differentiating human ESCs [270].

In this work, the differentiation strategy adopted consisted in a three-step sequential induction of hnMSC differentiation rather than through cell exposure to a cocktail. As previously reported, a sequential differentiation procedure better mimics the *in vivo* liver development [269]. In spite of the advantages of hnMSCs, few studies on hepatic differentiation are available on this cell type [172, 174, 179]. As aforementioned, one example is the report by Campard *et al.* [172], where the potential of hnMSC-UCM to derive HLCs was evaluated although not reaching a mature phenotype. Later, Zhang *et al.* [174] and Zhou *et al.* [177] published the differentiation of hnMSC-UCM into HLCs, using two-step protocols but the achieved phenotype is less mature than that reported by Campard *et al.* [172]. Therefore, the later procedure was applied to hnMSCs as our starting point (protocol 1) for the differentiation protocols developed herein.

The effect of the epigenetic modifiers TSA, 5-AZA or DMSO, with different exposure times, was tested in hepatic differentiation or maturation. DMSO is routinely used for HepaRG cell line maturation [54] and more recently for progenitor cells [217] and SC differentiation [183, 221-223]. HepaRG cell line is an important reference in cell-based assays due to its relevant phase I, phase II and phase III activities that are not usually observed on other cell lines such as HepG2 [277]. Herein, DMSO was used at 1 % as reported in literature for the maturation of foetal hepatocytes [217] and was tested alone, from days 10 and 13 onwards, and in combination with TSA or 5-AZA. TSA is an HDAC-I that presented promising differentiation-

inducing properties in human and rodent primary cultures of adult hepatocytes, hepatoma cell lines and that was also tested for hepatocyte differentiation of BM-MSCs [168]. In contrast, to our knowledge, 5-AZA effect on hepatocyte differentiation protocols in vitro has only been attempted on AD-MSCs by Seeliger *et al.* [213], and on umbilical blood-derived MSCs by Yoshida *et al.* [214], being applied 24 hours prior to the differentiation induction since proliferation is needed for the incorporation 5-AZA on cellular DNA.

Our findings indicate that a sequential differentiation protocol gradually induced cellular modifications from spindle fibroblast-like to hexagonal epithelial-like shaped binucleated cells with glycogen storage ability. These morphological changes were particularly evident upon DMSO treatment without TSA co-treatment. Accordingly, by the end of Step 3, HLCs exposed to DMSO from day 10 onwards also had increased expression of the liver-specific markers *CK18*, *ALB*, *CEBPA*, *TAT*, *HHEX*, *AFP*, *HNF4A*, *CYP1A1* and *CYP3A4.* The mechanisms through which DMSO induces hepatic differentiation are still poorly understood. However, studies by Cheety *et al.* [225] showed an activation of the retinoblastoma protein in DMSO-induced cells. Furthermore, a high proportion of cells in early G1 phase was also observed. G1 is of high importance for cell differentiation and a prolonged G1 phase has been reported as an indication of a differentiated status by reflecting loss of pluripotency and gain of lineage specific markers [226]. Thus, DMSO treatment increases the responsiveness of SC differentiation signals, enhancing differentiation across all germ layers, and improving terminal differentiation into functional derivatives [225]. DMSO has also been associated to hypo- and hipper-phosphorylation of several cellular proteins [227, 228] and on phosphatidylinositol signalling [229]. Finally, DMSO at 2 % (v/v) on rpHeps resulted on more relevant CYP enzyme activity by restoring HNF-4α and CEBPA levels that rapidly decreased in culture without DMSO [232] corroborating the observed gene expression data that showed increased expression of these factors up to day 34 in culture.

Nevertheless, the presence and expression of hepatic markers by SC-derived hepatocytes does not make them mature hepatocytes [278]. Moreover, besides obtaining a mature HLC population, a major aim of this study was to obtain functional HLCs that do not dedifferentiate with time in culture. Therefore, we further tested the functional capacity of the HLCs cultured up to day 34. During this period, the HLCs kept on exhibiting a hepatocyte phenotype by possessing liver-specific markers at the mRNA and protein levels. Additionally, functional aspects such as albumin secretion, ammonia detoxification, glycogen storage, inducible CYP activity and phase II activity were also validated against undifferentiated hnMSCs. The increase in *CK18*, *CEBPA, HNF4A, TAT, AFP* and *ALB* expression indicate that cells developed into more mature hepatocytes with time in culture.

Biotransformation capacity was also of particular interest in these extended cultures being the use of hepatocyte cultures hampered mostly by the rapid loss of CYP enzyme expression and activity in vitro. Therefore, regarding phase I metabolism, CYP3A4, CYP2C9 and CYP1A1 were evaluated due to their relevance in drug metabolism [50]. EROD and ECOD activities were also investigated covering CYP1A1/2 and CYP2B6/1A2/2E1, respectively. HLCs showed CYP activity, which was either maintained or increased with time, and responded to rifampicin and omeprazole/3-MC induction in CYP3A4/CYP2C9 and ECOD/EROD/CYP1A1, respectively. Not only *CYP3A4* and *CYP1A1* were overexpressed in HLCs (qRT-PCR analysis), but also they could convert substrates more efficiently than rpHeps, as shown by the P450-Glo™ and EROD activity assays. In addition, the P450-Glo™ substrate (PPXE) for CYP3A4 activity may also detect some activity of other CYP3A enzymes such as CYP3A5 and CYP3A7, being the later overexpressed in our transcriptomic analysis. CYP3A7 is present in liver, though it is more expressed in fetal liver, which may indicate that HLCs are following the liver fate despite presenting a less mature phenotype. Moreover, evidence supporting the shift between CYP3A7 and CYP3A4 immediately after birth has been reported [279]. This shift is apparently triggered by HNF-4α [279], herein detected by qRT-PCR at the mRNA expression and protein levels, although at a much lower extent than in hpHeps and showing a network influence negative score. Most importantly, although transcriptomic analysis points out to CYP3A4 and CYP2C9 underexpression on HLCs, their enzimatic activities reached higher levels than positive controls (D34), hence with positive implications for the use of these HLCs as an in vitro model for drug development. To note that primary hepatocytes, used as controls in functional assays, were obtained under their optimal culture conditions, *i.e.*, up to day 3 of culture, otherwise cell dedifferentiation would have been observed; and consisted of a pool of 10 donors to avoid inter-individual differences. Moreover, since cultivation of primary hepatocytes is known to induce cells dedifferentiation the whole genome analyses of hpHeps was performed in non-cultivated cells, which may justify part of the transcriptome profile distance observed between HLCs and hpHeps. In fact, previous results described that overall gene expression profiles of hpHeps approached SC-derived HLCs after an extended cultivation period [256].

Phase II enzymes and the hepatic transporters are also important determinants of pharmacological and toxicological activity of xenobiotics [255]. Glucuronidation is a major metabolic pathway by which the parent compound is converted in water-soluble derivatives and therefore more readily excreted [50, 246, 255]. Despite the low expression of UGTs observed in the hpHep transcriptome profile, the HLC's UGTs activity was observed up to day

34 in culture, being 1.7-fold and 2.1-fold higher than HepG2 or rpHeps, respectively, and similar to hpHeps, further suggesting a relevant HLC maturation level.

The hepatic transporters are essential for xenobiotic metabolism and elimination through blood or bile. SLC transporters are involved in pathways as transport of glucose and other sugars, bile salts and organic acids, metal ions and amine compounds as well as transport of vitamins nucleosides, and related molecules [176]. In particular, *SLCO1A* and *SLCO3A*, which have drug and organic anion transporter activity, presented an expression level similar to hpHeps in transcriptomic analysis. Moreover, transporters involved in amino acid transport such as SLC7 subfamily were also detected. OATP-C (*SLC21A6*) is a liver specific influx transporter, located in the sinusoidal membrane of hepatocytes and MRP-2 (*ABCC2*) is an efflux transporter, also highly expressed in liver, and located on the basolateral membrane [7]. The presence of both transporters at the protein level was detected suggesting phase III cell phenotype. Gene expression and protein presence of OATP-C have been reported on human ESC-derived HLCs [260]. MRP-2 activity has been previously published by Li *et al.* [171] on human AD-derived HLCs and gene expression of sinusoidal and basolateral drug transporters, but none of those two were reported on HLCs derived from hnMSCs. To our knowledge, the presence of MRP-2 and of OATP-C was herein shown for the first time on hnMSC-derived HLCs. Moreover, an overexpression of the ABCA1 hepatic transporter was detected in the microarray analysis, relative to hpHeps, hnMSCs and HepG2 cell line despite the low activation, the nuclear receptor canonical pathways LXR/RXR FXR/RXR and PXR/RXR. LXR is activated by cholesterol and its metabolites and consequently activates *ABCA1* expression. Bile acids activate FXR and PXR responds to fatty acids by increasing its uptake in hepatocytes [280]. This may suggest that the focus of HLC differentiation on phase I and II metabolism may be neglecting other essential features of the hepatocyte functions such as bile acids and lipid metabolism. Thus, this observation suggests that a further optimization of differentiation medium composition, namely by increasing its lipid content, should be taken into consideration in future studies, together with a broader characterization of HLCs at lipid and glucose metabolism levels. In fact, the bile salts supplementation, not commonly used in primary hepatocyte cultures, was recently reported to induce mature liver functions namely BSEP, MRP-2 and CYP7A1 [281]. In the present report, the results of a total of 8 conditions that differed in the combination and time of supplementation of three EMs are presented. Our data show that hnMSCs are capable of differentiating into HLCs upon mimicking the *in vivo* development micro-environment of hepatocytes by the addition of the epigenetic modifier DMSO from day 10 onwards. Furthermore, a genome-wide analysis increased the perception of the level of HLC maturation, indicating a partial hepatic phenotype.

Remarkably, some features were enhanced along the differentiation protocol, namely in terms of drug transporter and phase I and phase II metabolism expression and function, taking the HLCs in the direction of a mature phenotype. The acquisition of such a stable and active biotransformation capacity will be determinant for the potential applicability of liver-like in vitro models for longer-term toxicity testing.

Chapter 4. Three-dimensional spheroid cultures of human neonatal mesenchymal stem cells

This chapter includes Madalena Cipriano's work that is part of the scientific content of the following publication:

Santos JM, Camões SP, Filipe E, **Cipriano M**, Barcia R, Filipe M, Teixeira M, Mosqueira D, Nascimento DS, Simões S, Gaspar M, Pinto-do-Ó P, Cruz P, Cruz H, Castro M, Miranda JP. 2015. 3D spheroid cell culture of umbilical cord tissue-derived MSCs (UCX®) leads to enhanced paracrine induction of wound healing. Stem Cell Res Ther. 6(1): 90-109; DOI: 10.1186/s13287-015-0082-5

4.1 Abstract

3D cell culture models continue proving to be better models than the traditional 2D monolayer culture due to improved cell-to-cell interactions, cell-to-matrix interactions, and the formation of structures that better resemble the in vivo tissue architecture. Thus, 3D culture systems hold great promise for clinical applications by priming to a more physiologically relevant cell phenotype. Herein, a 3D culture model of human neonatal mesenchymal stem cells (hnMSC) was developed and characterized with respect to spheroid formation, cell phenotype and viability. We aimed at testing the hypothesis that the natural self-aggregation of hnMSC isolated from the umbilical cord stroma, is an effective system for establishing a robust 3D cell culture spheroid-based system to be further applied to the hepatic differentiation. To obtain hnMSC spheroids, two approaches were adopted: (i) dynamic cultures using spinner flask suspension cultures (SFSC); and (ii) static cultures using ultra-low attachment (ULA) plates. Both systems enabled hnMSC spheroid formation, resulting in a viable long-term culture up to 11 days, with a homogeneous spheroid size and without the presence of necrotic centres observed by H&E staining. Immunofluorescence detection of Ki-67 revealed < 5 % of proliferating cells showing a limited capacity of cell expansion under SFSC conditions, which was further confirmed by total protein quantification in both cell culture systems. In dynamic cultures, hnMSC spheroids successfully mimicked the native cell microenvironment, with sustained production of extracellular matrix (ECM) components like collagen I and fibronectin, as well as, of the basement membrane proteins laminin and collagen IV. The ULA system showed to be a robust tool for the implementation and validation of hepatic differentiation strategies whereas the scalability of SFSC system further represents a new approach for the maintenance of high cell numbers meeting the needs for clinical, pharmacological and toxicological applications.

Keywords:

Human neonatal mesenchymal stromal cells; 3D culture; Spheroids; Spinner flask suspension cultures; Ultra-low attachment plates; Extracellular matrix

4.2 Introduction

Mesenchymal stromal cells are a subset of stem cells that may be isolated from a number of adult and neonatal tissues, such as adult bone marrow [155] and adipose tissue [282], fetal blood [146], amniotic fluid, placenta [147, 148], umbilical cord blood [149] and umbilical cord stroma (Wharton's jelly – WJ-MSC) [283]. MSC present several unique characteristics that make these cells an ever-increasing subject not only for clinical research but also for in vitro toxicology applications. MSC have also been shown to display immune-modulatory properties, capacity to home to sites of inflammation and have demonstrated a quite high differentiation capacity, yielding not only osteoblasts [284], chondrocytes [285] and adipocytes [286] but also other cells of mesodermal, endodermal and ectodermal origin, such as myoblasts [287], cardiomyocytes [288], hepatocytes [172] insulin-producing cells [289] and neurons [290], amongst others.

Most of data on MSC properties has been obtained with bone marrow-derived MSC (BM-MSC) or adipose tissue-derived MSC (AT-MSC) [291, 292], while increasing evidence show that MSC from other sources could have distinct characteristics with regards to differentiation, expansion potential with concomitant genomic stability, and tissue regeneration capabilities [150, 160, 258, 292, 293]. Cells derived from extra-embryonic tissues such as placenta and umbilical cord tissue or blood became a more interesting cell source due to the non-invasive access and its more primitive origin. Indeed, neonatal MSC sources show less of the donor variability seen with other sources of MSC due to donor age, health conditions, clinical history or lifestyle [150, 160]. These cells are also obtained in more reproducible conditions, making them ideal for medium/high throughput screening, and maintain high chromosomal stability in vitro allowing for a stable expansion, which is of special interest for clinical applications [254].

A subset of human MSCs derived from the umbilical cord tissue, UCX®, have shown promising results in several non-clinical trials [257, 294]. These cells are isolated, expanded and cryopreserved according to a patented method (INPI PAT20081000083882; PCT/IB2008/054067; WO2009044379) [154]. The UCX® isolation method was particularly designed to produce a highly homogeneous population of cells, compliant with the MSC standards as defined by the International Society for Cellular Therapy (ISCT) [145]. In addition, UCX® are obtained in high numbers and have been characterized with respect to safety and potency and their isolation method has been fully adapted to the requirements to produce an advanced therapy medicinal product (ATMP), as defined by EMA guidelines [254, 258]. Recently, the UCX® tissue regeneration capacity has been functionally demonstrated in several animal models for myocardial infarction and rheumatoid arthritis [258, 294, 295], and

are already under pre-clinical trials for several auto-immune disorders [257, 258, 296]. Furthermore, in vitro and in vivo studies, performed with conditioned medium produced by UCX®, have demonstrated the potential for promoting cutaneous wound healing [257, 259].

The expansion and maintenance of MSCs is currently performed using traditional monolayer (2D) cultures where cells migrate and proliferate while adhering to the plastic surface of static culture flasks. In fact, these cell culture conditions are far from the in vivo physiological environment, as they lack the cell-to-cell and cell-to-ECM interactions. To overcome the lack of a physiologically relevant cell culture conditions, three-dimensional (3D) cell cultures have been developed, providing a more matrix-like environment. Thus, the use of MSC 3D culture systems has gained increasing attention [61, 70, 71, 297-299], being applied to enhance chondrogenic differentiation [300] or to improve the cells' therapeutic potential [298, 299]. In fact, the 3D environment showed the capacity of priming WJ-MSC to a more therapy-driven phenotype regarding wound-healing by resorting to decellularized amniotic membrane scaffolds as support for cell culture [301]. Alternatively, a less complex 3D model is the cells' self-assembling into spheroid-like structures, that enables greater cell-to-cell and cell-to-matrix interactions [61, 70, 71, 299, 302-304]. Several techniques allow for the spheroid formation, such as spinner flask suspension cultures (SFSC) and the use of non-adhesive surfaces, among others. The SFSC are amenable for both cell expansion and differentiation [305], as well as for up-scaling processes avoiding some regulatory constraints related to adhering supports and scaffolds.

The ultra-low attachment (ULA) plates consist on a non-adhesive surface enabling simple and low cost spheroid formation. ULA are advantageous for the optimization of culture medium supplementation and to test a diversity of toxic compounds using lower amounts of cells, since this system is available in 384, 96, 24 or 6-well formats. ULA plates have also been commonly used as smaller-scale cell culture systems to evaluate mesenchymal stem cell proliferation and differentiation potential [88, 89], as well as to improve the liver-like properties of the hepatic cell line HepG2 in repeated dose, high-throughput, toxicity studies [66, 90].

In this work, we aimed at testing the hypothesis that the natural self-aggregation of UCX® is an effective system for priming these cells towards a more physiological environment and, consequently, differentiation ability. For this purpose, a reproducible and scalable 3D culture system for extended maintenance of multipotent UCX® spheroids was developed, devoid of supporting matrices or the use of complex scaffolds. Two distinct 3D spheroid systems, (i) ULA plates and (ii) SFSC, were developed. In both systems, spheroids were maintained in culture for up to 11 days, showing low proliferative capacity and absence of necrotic centres.

In the SFSC, the environment within hnMSCs spheroids successfully mimicked the native cell microenvironment as seen by the sustained production of ECM components like collagen I and fibronectin, as well as of basement membrane proteins like laminin and collagen IV.

4.3 Material and Methods

4.3.1 Ethics and regulations

This study was approved by the Ethics Committee of the *Hospital Dr. José de Almeida* (Cascais, Portugal), in the scope of a research protocol between ECBio – Research & Development in Biotechnology, S.A. and *HPP Saúde – Parcerias Cascais, S.A.*. Umbilical cord donations, with written informed consents; as well as umbilical cord procurement, were made per Directive 2004/23/EC of the European Parliament and of the Council of 31 March 2004 on setting standards of quality and safety for the donation, procurements, testing, processing, preservation, storage and distribution of human tissues and cells. All animal experiments were carried out with the permission of the local animal ethical committee in accordance with the EU Directive (2010/63/UE), Portuguese law (DR 129/92, Portaria 1005/92) and all relevant legislations. The experimental protocol was approved by Direcção Geral de Alimentação e Veterinária (DGAV).

4.3.2 Cell culture reagents

Cell culture media and supplements used in this work were all purchased from Sigma-Aldrich®, unless stated otherwise. Foetal bovine serum (FBS) and Trypsin/EDTA were obtained from Gibco®.

4.3.3 hnMSC isolation and culture

4.3.3.1 hnMSC characterization

In this work, UCX® were the used hnMSC and were isolated at ECBio, S.A. according to the procedure described in the patent (INPI PAT20081000083882; PCT/IB2008/054067; WO2009044379) [154]. hnMSC cryopreserved up to P12 were thawed and used for cell culture as described below. In 2D cultures (static monolayer cultures) cells were seeded at a density of 7.0×10^3 cells/cm^2 in hnMSC medium (α-MEM with 2 mM glutamine, 1 g/L D-(+)-Glucose and 2.2 g/L sodium bicarbonate) supplemented with 10 % FBS (v/v) and incubated

at 37°C in a humidified atmosphere with 5 % CO_2. Cell passage was performed every 72h or when cells reached 70-80 % confluence.

3D spheroid cultures were performed in SFSC and ULA plates. In SFSC, 125 mL spinner vessels with ball impeller containing hnMSC medium supplemented with 10 % FBS were inoculated with single-cell suspensions obtained from 2D cultures at a concentration of 1 x 10^6 cells/mL. To promote cell aggregation, the spinner vessels were agitated at 80 rpm and kept at 37 ºC in a humidified atmosphere of 5 % CO_2. After 24 h, 50 % of cell culture supernatant was changed with fresh hnMSC medium supplemented with 10 % FBS (v/v). The stirring rate was adjusted to keep spheroid size below 350 μm. FBS was reduced to 5 % (v/v) at day 2 of culture and completely removed at day 5.

In ULA plates 3D cultures, 1.2 x 10^5, 2.4 x 10^5 and 3.6 x 10^5 cells/mL were inoculated on 24-well plates with 0.5 mL of UCX® medium per well, containing 10 % or 20 % of FBS (v/v). FBS was reduced to 5 % at day 1 of culture and completely removed at day 4.

In 3D cultures medium was changed every 3-4 days to guarantee nutrient availability and to decrease the accumulation of toxic by-products.

For plating back spheroids into to 2D cultures, a 5 mL cell suspension from 3D cultures was collected at day 7. Spheroids were digested with 0.25 % Trypsin/EDTA resulting in smaller spheroids that were inoculated in a 6-well plate. Cells adhered and proliferated for 1 passage, being afterwards collected for flow cytometry analysis of cell surface marker expression, and assessment of tri-lineage differentiation potential as described below.

4.3.3.2 Flow cytometry

Cell surface marker expression was analyzed by flow cytometry. For the characterization of hnMSC in both 2D and 3D cultures, cell detachment from culture flasks and dissociation from spheroids were achieved by using 0.25 % Trypsin/EDTA and the resulting single-cell suspension washed with 2 % BSA in PBS. Detection of cell surface markers was performed with the following antibodies and their respective isotypes after incubation for 1h at 4 ºC (all from BioLegend® unless stated otherwise): PE anti-human CD105 (eBioScience®); APC anti-human CD73; PE anti-human CD90; APC anti-human CD44; PerCP/Cy5.5 anti-human CD45; FITC anti-human CD34; FITC anti-human CD31; PerCP/Cy5.5 anti-human CD14; Pacific Blue anti-human CD19 and pacific-blue anti-human HLA-DR. All samples were acquired on a Gallios (Beckman Coulter) and the results analyzed with Kaluza software (Beckman Coulter). A minimum of 1.0 x 10^4 events was acquired per surface marker.

4.3.3.3 Tri-lineage differentiation

Tri-lineage differentiation was performed in hnMSC 2D and 3D cultures. Spheroids were dissociated into a single-cell suspension with 0.25 % Trypsin/EDTA and transferred to the appropriate culture plates for cell proliferation and expansion. Adipogenic and osteogenic differentiation was initiated when cultures reached 80-100 % confluence. For the chondrogenic differentiation, non-dissociated spheroids were also used for differentiation. To induce adipogenic differentiation, cultured cells were incubated in adipogenic differentiation medium, for 3 days, consisting of α-MEM supplemented with 20 % FBS, 2 mM L-glutamine, 10 µg/mL insulin, 200 µM indomethacin, 0.5 mM isobutylmetylxantine, and 1 µM dexamethasone; and subsequently 1 day in adipogenic maintenance medium, consisting of α-MEM supplemented with 20 % FBS, 2 mM L-glutamine and 10 µg/mL insulin. Medium replacement cycles were repeated during 21 days after which histochemical staining was performed. To induce osteogenic differentiation, cells were incubated in osteogenic differentiation medium consisting of α-MEM, 10 % FBS, 1 g/L glucose, 2 mM glutamine, 10 mM β-glycerol phosphate, 50µg/mL ascorbate-2-phosphate and 100 nM dexamethasone. The medium was changed every 3 days during 21 days. Finally, for chondrogenic differentiation, cells (both dissociated cells and spheroids) were maintained in suspension as pellets, incubated in differentiation medium consisting on DMEM-LG, 1 % FBS, 2 mM L-glutamine, 6.25µg/mL insulin, 10 ng/mL TGF-β1 (Tebubio) and 50µM ascorbate-2-phosphate. The medium was replaced every 3 days during 21 days and histochemical staining was performed. For cytochemical staining cells were fixed with paraformaldehyde 4 % for 20 minutes. In adipogenic and osteogenic differentiation protocols, cells were stained with Oil Red O and alkaline phosphatase, respectively. For chondrogenic differentiation, spheroids were cut into sections and stained with alcian blue. The presence of stained cells was confirmed by inverted microscopy with phase contrast (Leica, DMIL HC).

4.3.4 hnMSC viability evaluation

4.3.4.1 Cell membrane integrity assay

The qualitative assessment of the cell plasma membrane integrity during culture was performed using the enzyme substrate fluorescein diacetate (FDA) and the DNA-dye propidium iodide (PI). Briefly, cell aggregates were incubated with 20 μg/mL FDA and 1 μg/mL PI in PBS for 2–5 minutes and then observed using an inverted fluorescence microscope (Nikon Eclipse Ti-U).

4.3.4.2 hnMSC spheroid visualization and measurement

hnMSC spheroids were observed by bright field microscopy (Olympus CK30), and their average diameter determined by measuring at least 30 spheroids per condition. Spheroid diameters were measured using Motic Images Version 2.0 software.

4.3.4.3 Haematoxylin and eosin staining

hnMSC spheroids were resuspended in Tissue Tek® O.C.T.™ (Sakura®) for preparing cryosections of 10 µm. Slides were first stained with Harris's haematoxylin (Sigma-Aldrich®) for 10 min, followed by an incubation step with HCl 1 % (v/v) in 70 % EtOH, and by Eosin Y (Sigma-Aldrich®) staining for 2 min. Slides were then submitted to increasing concentrations of ethanol and finally incubated in xylene (EMD Chemicals). Samples were mounted with Entellan® (Merck). Images were acquired on an Olympus CK30 inverted microscope and processed using Motic Images Version 2.0 software.

4.3.5 Immunofluorescence microscopy

Cryosections from hnMSC spheroids were prepared as described above. Tissue sections were fixed with cold acetone for 10 minutes and blocked for 1 h with 4 % FBS (v/v) and 1 % bovine serum albumin (BSA) (v/v) in PBS. Incubation with primary antibody was performed in a humidified chamber for 2 h at RT or overnight at 4 ºC. The primary antibodies used were: Ki-67 (Rabbit IgG, AB16667, Abcam®) diluted 1:100; Collagen IV (Goat, AB769, Millipore) diluted 1:10; Fibronectin (Rabbit, F-3648, Sigma-Aldrich®) diluted 1:400; Laminin (Rabbit IgG, L9393, Sigma-Aldrich®) diluted 1:50; collagen I (Rabbit IgG, AB21285, Abcam®) diluted 1:200. All primary antibodies were diluted in 1 % BSA (v/v) in PBS. The incubation with secondary antibodies was carried out for 1 h at RT. The secondary antibodies used were as follows: goat anti-rabbit 594 (1:500) for Ki-67 staining; rabbit anti-goat-biotin (1:400) followed by streptavidin 555 (1:500) for Collagen IV staining; donkey anti-rabbit IgG 568 (1:1000) for Laminin staining; donkey anti-rabbit IgG 647 (1:1000) for Collagen I staining and goat anti-rabbit 488 (1:1000) for Fibronectin staining. All secondary antibodies were purchased from Invitrogen™. Sections were mounted using ProLong gold antifade with DAPI (Invitrogen™), and observed on an inverted fluorescence microscope (Axiovert 200M, Carl Zeiss) coupled with a monochrome camera (AxioCam MNC, Carl Zeiss).

4.3.6 Protein quantification

Protein concentration was determined as described in **Chapter 3**.

4.3.7 Statistical analysis

Data analysis and graphs were plotted using GraphPad Prism® software (GraphPad Software, San Diego, CA, USA). Values presented in the text and figures are as average ± standard deviations of at least three independent experiments, except otherwise specified.

4.4 Results

4.4.1 Isolation and characterization of hnMSC cells

The hnMSC have been isolated as described in Santos, J. M. *et al*. [154] (2009) "Optimized and defined method for isolation and preservation of precursor cells from human umbilical cord" (INPI PAT20081000083882; PCT/IB2008/054067; WO2009044379) [154]. From the time the patent has been submitted, the method has been further optimized at ECBio, S.A., to be GMP compliant. The optimization process, which was not in the scope of this thesis, resulted in further robustness and essentially can produce a homogeneous population of > 95 % MSCs (according to the International Society of Cell Therapy - ISCT) without the need to use cell sorting. Thus, with the ECBio, S.A., methodology, which is reproducible, the cells obtained are consistently 1) adherent to plastic, 2) > 95 % positive for CD105, CD90 and CD73 and < 2 % positive for CD14, CD19, CD34, CD45 and HLA-DR, and 3) capable of differentiating into osteoblasts, chondrocytes and adipocytes when adequately stimulated with the correct differentiation factors in vitro. In addition, ECBio, S.A. showed that these 3 ISCT criteria for defining MSC are preserved along cell expansion enabling at least 55 cumulative population doublings (P22) before reaching the first signs of senescence (data not shown). Cells isolated as to the abovementioned protocol, were cultured in monolayer (2D) and expanded for further use in this Chapter and in the **Chapters 3**, **5** and **6**.

4.4.2 hnMSC form viable spheroids in spinner flask suspension cultures (SFSC) and ultra-low attachment (ULA) plates

For the development of static spheroid cultures, using 6-well ULA plates, cell density (1.2 x 10^5, 2.4 x 10^5 and 3.6 x 10^5 cells/mL) and FBS initial concentration (10 and 20 %, v/v) were evaluated. Within ULA plates, compact hnMSC spheroids could be observed during the first

24 h after cell inoculation in all conditions, reaching an average spheroid size above 300 µm (**Figure 4.1b**) at day 3. The lower inoculum presented less than 2.5 % of aggregates bigger than 300 µm whereas this value was of 10 % to 2.4 x 10^5 cells/mL and of 25 % to 0.36 x 10^5 cells/mL inocula. In contrast, the FBS concentrations tested showed no differences on aggregate formation and consequently, 10 % FBS (v/v) was preferred to 20 % (v/v) for allowing a quicker reduction of FBS concentration to 0 %. Thus, the optimized conditions for hnMSC spheroid formation under static culture conditions consisted in an inoculum of 1.2 x 10^5 cells/mL, with 10 % FBS (v/v). FBS concentration was afterwards reduced to 5 % (v/v), at day 1, and removed at day 4 without causing changes on achievable aggregate sizes (spheroid diameters of 105 ± 6 µm (Average + SEM) (**Figure 4.1b**) or on spheroid compact morphology.

In parallel, a SFSC system was developed and optimized to obtain hnMSC 3D spheroids (**Figure 4.1**). For this purpose, different culture parameters such as inoculum concentration, impeller type and agitation rate were evaluated. Two impeller types (ball and paddle) were tested and two cell densities (1.0 x 10^6 cells/mL and 0.5 x 10^6 cells/mL) were chosen as starting points according to previous observations [306]. hnMSC were cultured in 125 mL spinner flasks for 11 days in a perfusion mode consisting of 50 % culture medium replacement at days 2, 6 and 9.

Compact multicellular spheroids of hnMSC could be obtained when using the ball impeller, but not with the paddle impeller, due to lower cell viability and lower size and shape homogeneity (data not shown). Consequently, only the ball impeller cultures were further maintained and monitored. Herein, the agitation rate was set to 80 rpm for the first 2 days of culture and increased to 100-120 rpm once the aggregates were formed to control the aggregate size. Phase contrast microscopy shows that hnMSC first form small low-density cell aggregates of approximately 50-100 μm diameter (Days 1-2, **Figure 4.1b**). Compact spheroids could only be obtained when a higher cell density was used as inoculum (1x10^6 cells/mL) that, once assembled, did not increase in size. Measurements of spheroids were based on phase-contrast images throughout the whole culture period (days 2, 4, 6, 9 and 11 of culture) yielding a size-distribution plot (**Figure 4.1b**). On average, spheroid diameters were 143 μm $\pm$ 9.78 μm (Average + SEM) after 2 days and 308 μm $\pm$ 9 μm (Average + SEM) from day 4 to day 11 of culture (**Figure 4.1b**). The formation of necrotic centers on spheroids was circumvented by maintaining the average spheroid size under 350 μm, which was achieved by optimizing the inoculum (**Figure 4.1** and **4.2**), FBS concentration and by controlling the stirring rate. Thus, FBS reduction was also attempted since several potential applications of 3D MSC cultures, either in vitro pharmacology or in regenerative medicine, require serum free conditions. Cells were inoculated with 10 % of FBS (v/v) that was then reduced to 5 % (v/v) at

day 2 of culture and completely removed at day 5. The complete FBS removal was achieved without compromising spheroids structure or/and cell viability (data not shown).

The results showed that our optimized culture conditions, namely an inoculum of 1 x 10^6 cells/mL inoculum and ball impeller, enabled the formation and maintenance of hnMSC spheroids for at least 11 days.

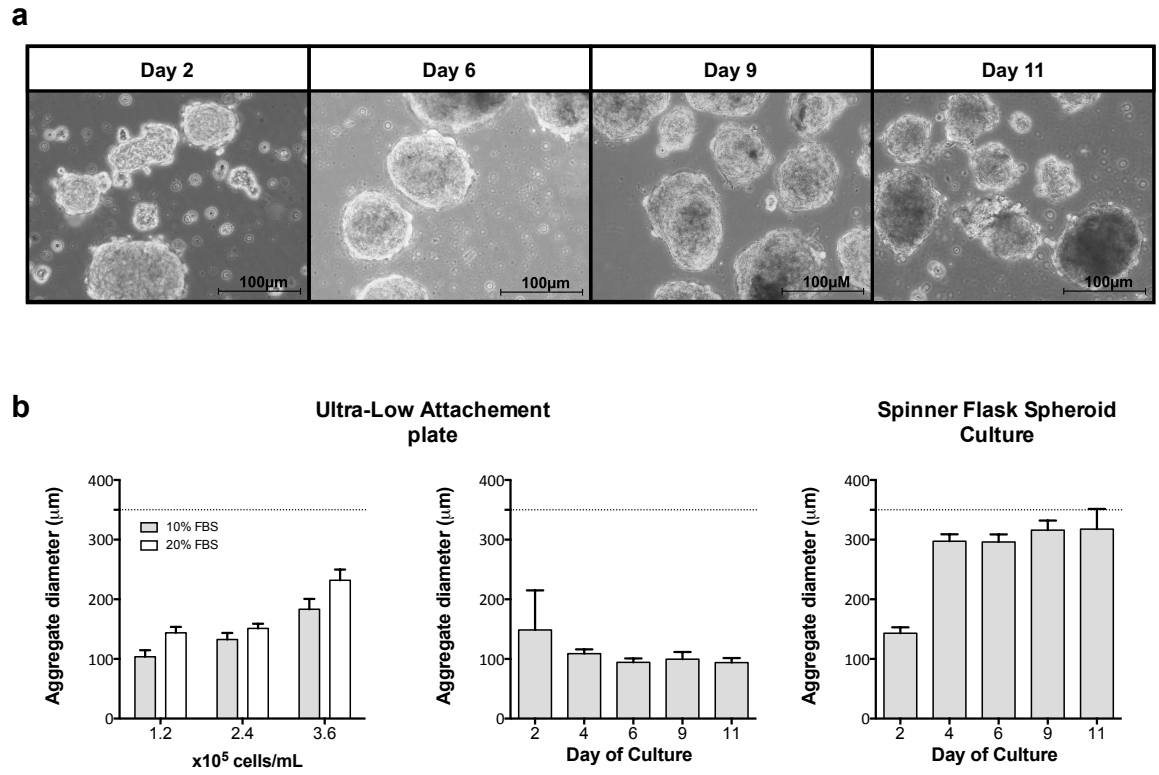

Figure 4.1 hnMSC form spheroid structures. a) Phase contrast microscopy representative of the time course of the aggregation of hnMSC into spheroids cultured in ULA plates with an inoculum of 1.2 x 10^5 cells/mL. Scale bar 100 µm. b) Sizes of hnMSC spheroids generated in ULA plates at day 3, when optimizing inocula and serum concentration, and in both systems evaluated at days 2, 4, 6, 9 and 11, when seeded at 1.2 x 10^5 cells/mL and 10 % FBS (v/v) (ULA) or at 1 x 10^6 cells/mL (SFSC). Aggregates diameters were measured from captured images of spheroids (n=3). Data is shown in Average ± SEM.

Cells within spheroids may have less access to nutrients, thus the evaluation of cellular viability under the optimized 3D culture conditions is critical. To assess cell proliferation and viability within hnMSC spheroids, samples were collected for H&E, FDA/PI and Ki-67 staining and biomass quantification at various time points (**Figure 4.2**) To follow spheroid morphology, histological analysis of spheroid sections was performed at days 3, 9 and 11 (**Figure 4.2a**). H&E staining of sections revealed that spheroids were solid with evenly distributed cells, embedded in extracellular matrix, presenting no evidence of necrotic cores (**Figure 4.2a**). The surface of the spheroid had a layer of epithelium-like cells that were flatter and more elongated

in appearance. Ki-67 staining of spheroid cryo-sections showed the presence of only < 5 % of cells were actively proliferating at day 3 and less at day 11 (**Figure 4.2b**). These results are in accordance with biomass quantification values that did not significantly change during culture time; whereas the decrease in biomass values are associated to cultures reefed (**Figure 4.2c**). Moreover, no significant cell lysis occurred as assessed by quantification of LDH (data not shown) and the live/dead (FDA/PI) assay showed high cell viability (> 70 %) in the spheroids (**Figure 4.2a**). It demonstrates that spheroids size range was not critical regarding cell viability and the formation of necrotic centres. The results showed that both 3D culture conditions enabled the formation and maintenance of UCX® spheroids comprising viable cells for at least 11 days.

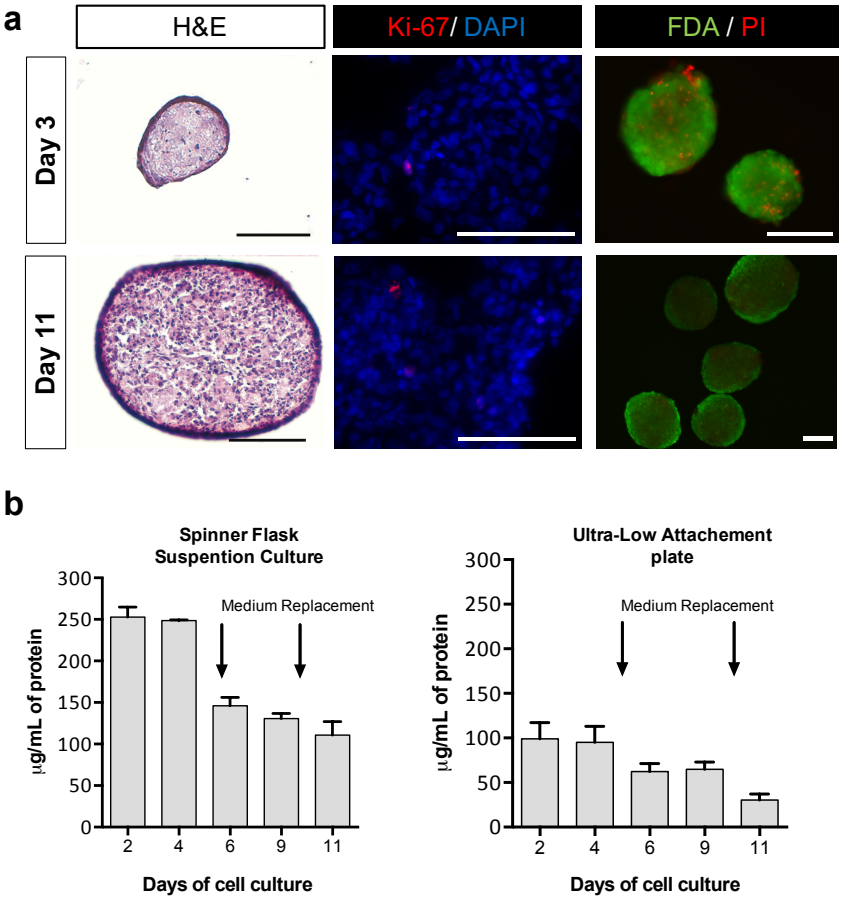

Figure 4.2 3D spheroid cultures allow the extended maintenance of viable hnMSC without necrotic cores. a) Phase contrast and fluorescence images representatives of spheroids at days 3, and 11. From left to right: H&E staining of hnMSC spheroid sections; Immunofluorescence images representatives of hnMSC spheroid cryossections labelled with Ki-67 (red) and DAPI (blue); and, Viability of hnMSC spheroids in culture as assessed by staining with FDA (live cells, green) and PI (dead cells, red). b) Biomass quantification at days 2, 4, 6, 9 and 11 on hnMSC spheroids cultured on SFSC (Left) and ULA plates (Right). Data is shown in Average ± SEM (n=3). Scale bar 100 μ m.

4.4.3 hnMSC grown in 3D culture conditions maintain MSC antigen expression phenotype

hnMSC cell-surface marker expression was analyzed by flow cytometry (data not shown). The surface epitopes of hnMSC dissociated from spheroids were like the surface epitopes of hnMSC obtained from adherent monolayers (2D) dissociated under the same conditions. From day 4 onwards, the population of 3D-spheroid-dissociated cells showed a decrease in CD105 and CD90 expression levels, most likely due to the smaller cell size while in spheroids than in 2D which, by resulting in a lower yield of fluorescence emission, shifted the signal to the negative region of the histograms. In fact, flow cytometry side scatter results indicate that cells grown in 3D spheroids were approximately 30 % smaller in size when compared to cells grown in 2D monolayer cultures (data not shown). The expression of CD105 and CD90 surface epitopes increased again to high levels once hnMSC grown in 3D spheroids were plated back (culture day 7) in 2D monolayer conditions (replated cells, data not shown), supporting the hypothesis that the observed lowered expression was due to smaller cell size when cells grow in aggregates.

To assess if 3D culture conditions altered hallmark properties of hnMSC, namely their differentiation potential, cells in 3D culture were dissociated from spheroids at days 3, 6 and 9, plated onto culture flasks and grown as monolayers. Plated cells retained the ability to adhere and proliferate on a plastic surface. Cell multipotency was then assessed and confirmed by the ability of hnMSCto differentiate in vitro into adipocyte-, osteoblast- and chondrocyte-like cells (data not shown). Adipogenic and osteogenic biochemical differentiation, evidenced by lipid vacuole formation and matrix mineralization, respectively, could be confirmed at all time points. In turn, chondrogenic differentiation was attempted using both, 3D-spheroid dissociated cells and intact 3D-spheroids directly. Chondrocyte differentiation was obtained with dissociated cells, but was greatly enhanced by cells in aggregates already embedded in their own chondrogenic-type extracellular matrix. Overall, cells obtained from 3D cultures and plated back under 2D conditions show a similar differentiation capacity as cells grown in conventional 2D cultures at similar passages.

4.4.4 hnMSC spheroid structures mimic the native environment ex vivo

A crucial component of the stem/progenitor cell niche is the extracellular matrix, by modulating cell-fate, making available a large array of biochemical and biophysical cues. To evaluate whether the hnMSC spheroids replicate the native tissue environment *ex vivo* by producing the Wharton's jelly ECM, the expression of major ECM proteins was analyzed (**Figure 4.3**).

Immunohistochemical evaluation of cells in spheroids showed sustained expression of the ECM components collagen I, fibronectin, as well as of the basement membrane proteins laminin and collagen IV, between days 3 and 11 in vitro (**Figure 4.3**), suggesting that an environment resembling that of the native tissue was formed within the aggregates. Moreover, no differences in terms of ECM distribution/composition between the aggregate inner core and outer layer in any of the different-sized aggregates were observed. A uniform distribution of laminin, collagen IV and fibronectin expression, with interspersed regions of collagen I deposition generically characterized the hnMSC spheroids.

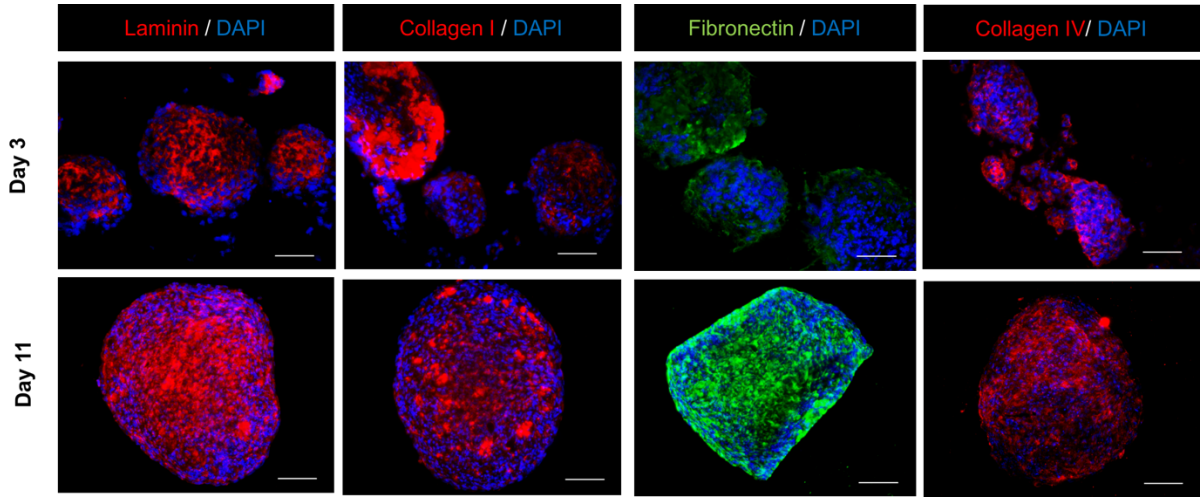

Figure 4.3 Expression of extracellular matrix proteins by hnMSC spheroids. Immunostaining of representative cryosections of hnMSC grown in 3D culture demonstrate the expression of relevant ECM molecules. Within the spheroid, laminin and collagen IV define the basal lamina surrounding hnMSC which is in close association with the ECM proteins fibronectin and collagen I. A similar ECM composition was observed irrespectively of the culture duration when considering the analyzed time-points of day 3 and 11. Scale bar, 100 μm.

4.5 Discussion

MSCs are commonly cultured and expanded under conventional adherent monolayer (2D) culture conditions. However, cells replicative ability, colony-forming efficiency and differentiation capacity might decrease over time in culture [307]. In fact, cells change their shape and influence tissue mechanic properties during development and tissue healing in response to morphogens, cell-to-cell contact, adhesion to extracellular matrix, among other factors [308]. 2D systems fail to mimic the in vivo physiological environment of MSCs, which might limit their potential applications. In an attempt to recreate the complex microenvironment of living systems, the use of MSCs three-dimensional (3D) culture models has gained increasing attention [61, 70, 71, 85, 297-299], namely as a procedure for enhancing the differentiation of the cells [300, 309] or for increasing their therapeutic potential [298, 299, 310]. Self-assembled spheroids are a 3D strategy that enables a greater cell-to–cell and cell--to-matrix interactions [61, 70, 71, 85, 297-299] and is amenable for both cell expansion and differentiation [305]. Thus, the work presented here was designed to obtain a 3D culture of hnMSC, using spheroids as strategy, and discuss how the cells phenotype under this 3D culture might be advantageous for its potential applications. The spheroid formation and culturing techniques, SFSC and ULA, were selected due to the possibility of up-scaling processes (SFSC), and by being devoid of supporting matrices or complex scaffolds that might result in some regulatory constraints when applying the cells for therapeutic proposes. Furthermore ULA plates allow for high throughput screening, important for the optimization of cell differentiation strategies and further use for in vitro toxicology studies.

The development of a viable homogenous long-term 3D culture of hnMSC spheroids required the optimization of several factors, namely the initial inoculum, the FBS concentration and, in SFSC the use of an appropriate impeller and the optimization of the agitation rate. Mechanically stirred culture conditions, as in SFSC, creates a hydro-dynamic shear stress that must be optimized in order to balanced cellular stress and death with cell performance [72]. Mechanical forces may ultimately compromise cell viability, morphology, gene expression and differentiation potential [311]. Therefore, the obtained 3D hnMSC structures were fully characterized and monitored throughout the whole culture period, not only in terms of cell viability, proliferation and morphology, but also regarding cell surface protein expression and cell plasticity. Firstly, both a ball and paddle impeller were tested for our 3D spheroid culture in the SFSC. Compact multicellular spheroids of hnMSC could be obtained when using the ball impeller, but not with the paddle impeller (data not shown), which is in accordance with Yirme *et al*. [312] that observed higher viability, cell growth, size and shape homogeneity on

hESC cultured on SFSC with ball impeller rather than using paddle impeller [312]. The ULA plates, under a static cell culture condition, also resulted in compact viable multicellular spheroids of hnMSC observed by H&E analysis, with a low aggregate size distribution. A homogeneous cell culture regarding spheroid size is of major importance to achieve a homogeneous population of differentiated cells for in vitro toxicology studies, namely to achieve reproducible induction of a specific lineage commitment. The awareness of necrotic centers formation is also an important feature on the 3D spheroid culture implementation. Necrotic centers may be formed in aggregates larger than 350 μm [313]. Moreover, higher spheroid size might contain cells in various stages, usually including proliferating, quiescent, apoptotic, hypoxic, and necrotic cells, since in large size spheroids, the core cells receive less oxygen, growth factors, and nutrients from the medium, and tend to be in a quiescent or hypoxic state [314]. This may be particularly relevant in tumor cell cultures, but our study aimed at creating a viable 3D culture of hnMSC that might enhance its differentiation and tissue regeneration properties. Thus, the average spheroid size, in both static and stirred 3D hnMSC cultures, was maintained under 350 μm. In fact, necrotic centers were not present in our 3D cultures as observed in the H&E analysis and LDH assay.

Serum-free conditions were also successfully applied to our cell culture systems without compromising the cell culture viability or spheroid morphology. This was also reported on bovine umbilical cord derived-MSC 2D and 3D cultures [306] as well as on human BM-MSC [88]. Alimperti *et al.* [88] used static cultures (ULA plates) to screen the media mixtures and the components based on cell proliferation potential to obtain a prototype serum-free medium that was characterized in both static (ULA plates) and dynamic culture (SFSC) by examining the proliferation and differentiation potential of BM-MSC spheroids produced [88]. In fact, serum free culturing is of high interest for MSC clinical and in vitro applications. Serum composition has a high variability, being a mixture rich of growth factors, proteins, vitamins, trace elements and hormones, among others [315], which has profound effects on cells proliferation and differentiation and causes phenotypical differences, resulting in reduced reproducibility of experimental results [316]. Although FBS composition favours cell growth, it is well recognized that use of FBS is not desirable for clinical applications due to the lack of a well-defined composition, the high batch-to-batch variability [315] and the risk of contamination agents that might induce immunogenic reactions when transfused into patients [88]. For this reason, UCX® isolation and culture was adapted towards the production of an advanced therapy medicinal products (ATMP) by Martins *et al.* [254]. ATMP adaptation included the use of human serum, tested for virus and endotoxin presence, and assured the maintenance of UCX®'s immunomodulatory properties [254]. Nevertheless, serum-free conditions are also

required to evaluate the cells' conditioned medium composition and how cells secretome may exert a biological effect devoid of serum contribution. The UCX® secretome, produced in low serum (2 %, v/v) [257] and serum-free conditions, demonstrated a relevant biologic effect in vitro [257, 259] and in vivo on wound healing [259]. The paracrine effect of UCX® secretome, was further improved by 3D culturing that resulted in an increased production of MMP-2, MMP-9, VEGF, G-CSF, HGF, FGF-2, TGF-ß1 and IL-6, and revealed its direct involvement in all phases of wound healing, *i.e.* homeostasis, inflammation, proliferation and remodelling [259]. In fact, *Santos et al.* [259] showed that the cells conditioned medium is an important alternative to the use of cells in the final formulation of ATMP by providing a proof-of-concept that a reproducible system to produce UCX®-conditioned medium, the 3D UCX® spheroids cultured on SFSC, can be used to prime a secretome for eventual clinical applications [259]. In fact, several studies showed that MSC cultured in serum-free formulations resulted in enhanced anti-inflammatory, angiogenic and immunomodulatory properties [88, 259, 306, 317, 318]. The adaptation of MSC spheroids to serum free conditions is also of major importance for in vitro applications such as the induction of cell differentiation into a specific lineage. The lack of a well-defined composition may also interfere with the effect of the cytokines and growth factors used to induce cell differentiation. Moreover, it may also mask the toxicity of several chemicals. For this reason, the use of serum-free is recommended in the guidelines for good cell culture practice as well as by the ECVAM Advisory Committee that strongly recommends the use of serum-free substitutes for both current and future in vitro methods [319].

In our study, 3D culturing showed an effect on cell morphology, proliferation, differentiation and ECM production capacity. MSC morphology is spherical when cultured in spheroids and becomes more elongated in 2D conditions. The size of MSC in spheroids is also drastically smaller than cells in 2D monolayer as seen by microscopy and evaluated by flow-cytometry. This has also been reported in literature, with 3D culturing resulting in 75 % reduction in individual cell volume [31, 57-59]. Proliferation and differentiation in culture are mainly regulated by cell density via increased juxtracrine (contact-dependent) and paracrine signaling [308]. In fact, contact-dependent signaling is one of the major differences between 2D and 3D culture conditions, differentially regulating cell signaling and fate. The proliferation rates of cells in spheroids is generally lower than in 2D and are cell line and matrix dependent [233, 320-322]. Under our optimized conditions, spheroid cell viability could be maintained up to 11 days, whereas cell proliferation greatly decreased (< 5 %) when compared to monolayer cultures. However, as reported by other authors [297-299], when spheroids are cultured back to monolayer conditions, similar proliferation rates and multilineage differentiation were observed as in cells maintained in 2D, reinforcing the effect of contact-dependent signaling.

The contact-dependent signaling has also been correlated to cell differentiation, since hMSC differentiation depends not only on cytokines and growth factors but also on mechanical gradients [307, 308, 323]. Ruiz *et al*. [323] observed that changing the shape of the multicellular sheet surface from convex to concave surfaces modulates the differentiation of BM-MSC into osteogenic or adipogenic, respectively [323]. The degree of cell spreading also showed to be able to switch BM-MSC commitment between lineage fates, in which well spread cells undergo osteogenesis while less spread cells undergo adipogenesis [324]. In fact, our 3D cell culture conditions enhanced chondrogenic differentiation, resulting in increased alcian blue stained chondrospheres, which is in accordance to previous observations that suggested that 3D cultures of MSC yield more homogeneous differentiated populations [300, 325].

ECM is also a crucial component of the stem cell niche which, by making available a large array of biochemical and biophysical cues, modulates cell fate. In fact, Wharton's jelly is a connective tissue layer very rich in ECM fibrous proteins, interstitial proteins and signaling molecules, whereas the WJ-ECM is mainly composed of collagens such as collagen type I, II, III, IV and VI, laminin and fibronectin [326, 327]. Immunostaining of the hnMSC spheroids showed that cells were embedded in a rich ECM composed of collagen I, fibronectin, laminin and collagen IV, suggesting that an environment resembling that of the native tissue was formed within the aggregates. Besides, it has been demonstrated that the preservation of an endogenous ECM in human MSC aggregates improves multilineage potential, while cells preserve its MSCs properties [327]. Previous studies using mRNA/cDNA microarrays demonstrated marked differences between transcriptome profiles of MSCs maintained in spheroids versus MSCs cultured in monolayers, including those confirming widespread changes to the cellular architecture and ECM [299, 328, 329]. The fact that the cell proliferation/metabolism is rather different between the two systems may also have an important effect upon the overall cellular activity. Thus, the production of ECM within the aggregate may have also increased the overall cell homeostasis, preserving cells from entering *anoikis*, the apoptotic process induced by the loss of interaction between the cell and the ECM [330].

In conclusion, by resorting to scalable commercially available systems, the 3D culture of hnMSC spheroids was successfully developed. Both 3D cell culture systems enabled the long-term maintenance of viable, multipotent hnMSC within self-assembled spheroids. The ULA system showed to be a robust tool for the implementation and validation of cell differentiation strategies whereas the scalability of SFSC system further represents a new approach for cell culturing and differentiation with potential for both, clinical and pharmacology/toxicology applications.

Chapter 5. Self-assembled 3D spheroids and hollow-fiber bioreactors improve MSC-derived hepatocyte-like cell maturation in vitro

The scientific content of the present chapter has been included in the following publication:

Cipriano M, Freyer N, Knöspel F, Oliveira NG, Barcia R, Cruz P, Cruz H, Santos JM, Zeilinger K, Miranda JP. 2016. *Self-Assembled 3D Spheroids and Hollow-fibre Bioreactors improve MSC-Derived Hepatocyte-Like Cell Maturation In Vitro*. Arch Toxicol. 2017;91:1815-32. DOI 10.1007/s00204-016-1838-0

5.1 Abstract

3D cultures of human stem cell-derived hepatocyte-like cells (HLCs) have emerged as promising models for maintaining hepatocyte phenotype in short and long-term in vitro cultures by better resembling the *in vivo* environment of the liver and consequently increase the translational value of the resulting data.

In this study, the first stage of hepatic differentiation of human neonatal mesenchymal stem cells (hnMSCs) was performed in 2D monolayer cultures for 17 days. The second stage was performed by either maintaining cells in 2D cultures for an extra 10 days as control, or alternatively cultured in 3D as self-assembled spheroids or in multi-compartment membrane bioreactor system. All systems enabled hnMSC differentiation into HLCs as shown by positive immune-staining of hepatic markers CK-18, HNF-4α, albumin, the hepatic transporters OATP-C and MRP-2 as well as drug metabolizing enzymes as CYP1A2 and CYP3A4. Similarly, all models also displayed relevant glucose, phase I and phase II metabolism, the ability to produce albumin and to convert ammonia into urea. However, EROD activity and urea production were increased in both 3D systems. Moreover, the spheroids revealed higher bupropion conversion whereas bioreactor showed increased albumin production and capacity to biotransform diclofenac. Additionally, diclofenac resulted in an IC_{50} value of 1.51 ± 0.05 and 0.98 ± 0.03 in 2D and spheroid cultures, respectively. This data suggests that the 3D models tested improved HLC maturation showing a relevant biotransformation capacity and thus provide more appropriate reliable models for mechanistic studies and more predictive systems for in vitro toxicology applications

Keywords:

Spheroids; Hollow-fiber bioreactor; Hepatocyte-like cells; Human neonatal mesenchymal stem cells; In vitro toxicology

5.2 Introduction

Drug development suffers from a lack of predictive toxicity identification at early stages, leading to an unacceptable high number of new compounds failing into progress toward clinical use. Clearly, current non-clinical models and approaches in drug discovery poorly predict toxic events: cellular models often lack the complexity to cover key mechanisms driving adverse events, animal models lack translational confidence to humans and genetic variability of susceptible human subpopulations is not adequately addressed. Stem cell (SC)-derived hepatocyte-like cells (HLCs) can present relevant clinical and toxicology testing applications as soon as a satisfactory hepatocyte-like functional phenotype can be achieved. In toxicology, HLCs can be used as a platform for in vitro liver disease modeling [199], toxicological screening or for mechanistic hepatotoxicity studies [331] whereas within the clinical field, HLCs can contribute to the recovery of injured liver tissues, not only by cell replacement but also by delivering trophic factors that support endogenous liver regeneration [332].

In vitro hepatotoxicity studies are still mostly performed using liver slices, genetically engineered cells, two-dimensional (2D) monolayer cultures, or suspension cultures of either human hepatoma cell lines or primary hepatocytes. These culture models present major challenges like cell availability and/or maintenance of a functional phenotype in vitro [7, 50], which sustains the need for alternative cellular models.

SC-derived HLCs have been reported as a relevant alternative due to their ability to maintain a mature HLC phenotype such as the expression of liver-specific markers as well as a satisfactory activity of drug metabolizing and detoxifying enzymes, including phase I, phase II and hepatic transporters [252]. However, SC-derived HLCs show in some aspects a reduced hepatic functionality when compared to human hepatocytes. Several factors contribute to this immature phenotype, namely the SC nature/source, SC isolation technology and the culture system applied. We have recently demonstrated that a specific subset of human neonatal MSCs (hnMSCs) derived from the umbilical cord tissue, termed UCX®, have a strong ability to differentiate into highly functional and durable HLCs [333].

Three-dimensional (3D) culture systems have been implemented in order to overcome the immature phenotype observed in long-term primary hepatocyte cultures. Primary hepatocytes grown in 3D cultures showed increased functionality in vitro, such as the role of many transporter proteins [62] and the activities of some drug metabolizing enzymes [61, 85] when compared to cells grown and maintained in traditional 2D monolayer cultures. 3D cell cultures allow high cell-to-cell and cell-to-extracellular matrix (ECM) contacts that are essential for the acquisition of cell polarity during development [7, 259]. In fact, hepatoblasts are essentially

non-polarized cells that present little cell-to-cell contacts whereas hepatocytes present a highly polar epithelial morphology that depends on the ECM composition and stiffness to maintain their functions [7]. Some authors have attempted to mimic the ontogenic environment of liver by using 3D cell cultures in order to promote hepatogenic differentiation. As an example, 3D culturing proved to be successful in improving the hepatocyte-like phenotype in terms of biotransformation activity, as shown by spheroid-based cultures of either hESCs-derived or iPSC-derived HLCs [236, 237, 334, 335]. In particular, the differentiation of hESCs in a hollow-fiber bioreactor resulted in an upregulation of pathways related to steroid hormone biosynthesis, ABC transporters and cytochrome P-450 (CYP)-dependent metabolism of xenobiotics in comparison to 2D cultures, also revealing maturation of the HLCs in this environment [243]. Apart from hESCs and iPSCs, MSCs have also been effectively used to derive HLCs in 3D culture conditions [239]. By resorting to nano-scaffold structures, human bone marrow-MSC-derived HLCs showed increased ability to produce urea and transferrin [245]. However, although evidence suggests that 3D culture systems offer advantages over 2D culture systems in terms of HLC derivation, it is still not clear which system provides the best differentiation and maintenance conditions.

3D cultures can be achieved using either dynamic or static systems, comprehending spheroid formation [85], cell adherence to a scaffold or more complex cellular systems such as hollow-fiber bioreactors [63]. The multicellular spheroid technique, a 3D system that uses the capacity of cells to self-assemble, has been shown to improve primary hepatocyte phenotype over extended periods in culture when compared to 2D cultures [61, 70, 85]. Non-adherent surfaces are especially advantageous for spheroid formation and culturing due to the ease of culture set up and scale-up, and likely adaptable to high-throughput screening. More complex systems, such as hollow-fiber cartridge bioreactors, originally developed to function as extracorporeal liver support systems, have also been designed to accommodate dynamic 3D high-density culture of human liver cells [63, 64, 94, 95].

Herein an HLC differentiation protocol from a specific subset of human neonatal MSCs (UCX®) was developed and applied two different 3D cell culture systems: a spheroid-based 3D static culture system and in a bioreactor consisting on three independent interwoven capillary systems for arterio-venous medium perfusion, oxygen supply, and carbon dioxide removal [63]. The results were compared to HLC differentiation in a traditional 2D monolayer culture system in order to identify specific relevant differences and define the best cell culture conditions for HLC maturation and maintenance. We present evidence that deriving HLCs using 3D approaches result in a cell population with considerably higher liver functional features, namely phase I and phase II metabolizing capacity, but also higher urea and albumin

production. Moreover, we have defined a differentiation protocol for obtaining mature and homogeneous hepatocyte-like cell populations of human origin that can be used in the future as an alternative for biotransformation studies in vitro.

5.3 Material and Methods

5.3.1 Reagents

Trypsin-EDTA, fetal bovine serum (FBS) and insulin-transferrin-selenium solution (ITS) were purchased from Gibco®/Life Technologies (Madrid, Spain). Penicillin-Streptomycin-Amphotericin B (P/S/A), non-essential amino acids supplement (NEAA) and sodium pyruvate (NaP) were purchased from Lonza (Basel, Switzerland). 7-ethoxyresorufin was purchased from Alfa Aesar (Karlsruhe, Germany). Hepatocyte growth factor (HGF), fibroblast growth factors (FGF-2 and FGF-4) and oncostatin-M (OSM) were purchased from Peprotech (Rocky Hill, NJ, USA). Iscove's modified Dulbecco's medium (IMDM), alpha modified Eagle's minimum essential medium (α-MEM), epidermal growth factor (EGF), dexamethasone, dimethyl sulfoxide (DMSO), nicotinamide, 5-azacytidine (5-AZA), periodic acid, Schiff's reagent Mayer's hematoxylin, Harris's haematoxylin, Eosin Y Eosin, α-amylase, β-glucuronidase/arylsulfatase, resorufin, 3-methylcholanthrene (3-MC), omeprazole and rifampicin were acquired from Sigma-Aldrich (Madrid, Spain).

5.3.2 Cell cultures

Rat primary hepatocytes (rpHep) were isolated and cultured as described in **Chapter 3**. HepG2 cells and cryopreserved human primary hepatocytes were cultured as described in **Chapter 3.**

5.3.3 Human neonatal MSC cultivation and differentiation into HLCs

This study was approved by the Ethics Committee of the Hospital Dr. José de Almeida (Cascais, Portugal), in scope of a research protocol between ECBio (Research & Development in Biotechnology, S.A.) and HPP Saúde (Parcerias Cascais, S.A.). Umbilical cord donations, with written informed consents, as well as umbilical cord procurement, were made according to Directive 2004/23/EC of the European Parliament and of the Council of 31 March 2004 on setting standards of quality and safety for the donation, procurements, testing, processing, preservation, storage and distribution of human tissues and cells. hnMSCs (UCX®) were isolated and fully characterized as described previously [257, 259] and expanded

as undifferentiated cells in α-MEM supplemented with 10 % of FBS (v/v). A three-step differentiation protocol was used for generating HLCs. Briefly, hnMSCs were seeded at a density of 1.5 x 10^5 cells/cm^2 in a rat-tail collagen coated surface, as described in **Chapter 3**. In the first step, cells were maintained in IMDM with 1 % P/S/A supplemented with 2 % FBS, 10 ng/mL of EGF and 4 ng/mL of FGF-2, for 48 hours. In the second step, cells were maintained for 10 days with BM supplemented with 20 ng/mL of HGF, 4 ng/mL of FGF-2, 10 ng/mL of FGF-4, 0.61 g/L of nicotinamide, 1 % ITS and 1 % DMSO. From day 13 onwards (third step), cells were supplemented with BM containing 8 ng/mL of OSM, 1 μM of dexamethasone, 1 % ITS and 1 % DMSO. Culture medium was changed every 3 days. At day 17, cells were trypsinized and reinoculated in medium containing 20 μM of 5-azacytidine (5-AZA) and 5 % of FBS into (i) 2D culture plates pre-coated with collagen (2 x 10^4 cells/cm^2); (ii) ultra-low attachment plates (2.5 x 10^4 cells/mL) in order to obtain a 3D spheroid culture; and (iii) 3D miniaturized hollow-fiber bioreactors with a cell compartment volume of 0.5 mL pre-coated with collagen (40 x 10^6 cells/bioreactor). Medium was changed 24 h after inoculation to remove 5-AZA and FBS. Cells were maintained in third step differentiation medium, with medium replacement every 3 days.

5.3.3.1 Bioreactor technology

The hollow-fiber multi-compartment bioreactor system consists of an electronically controlled perfusion device with pumps for medium recirculation and feed, temperature control and a valve-regulated gas mixing unit. The miniaturized bioreactor is made of capillary layers that serve for counter-current medium perfusion through two independent capillary systems and direct membrane oxygenation of the cells located between the capillaries as represented in **Figure 5.1** [62-64]. Medium was recirculated at a rate of 3.0 mL/h through the bioreactor and fresh medium was added with 0.2 mL/h, at a constant total volume of the recirculation circuit of 12 mL. In the recirculating medium, oxygen, glucose and lactate concentrations and pH values were measured daily with a blood gas analyser (ABL 700, Radiometer, Copenhagen, Denmark); the release of lactate dehydrogenase (LDH), that can be correlated with cell viability, was measured with an automated clinical chemistry analyzer (Modular P800, Roche Diagnostics, Heidelberg, Germany).

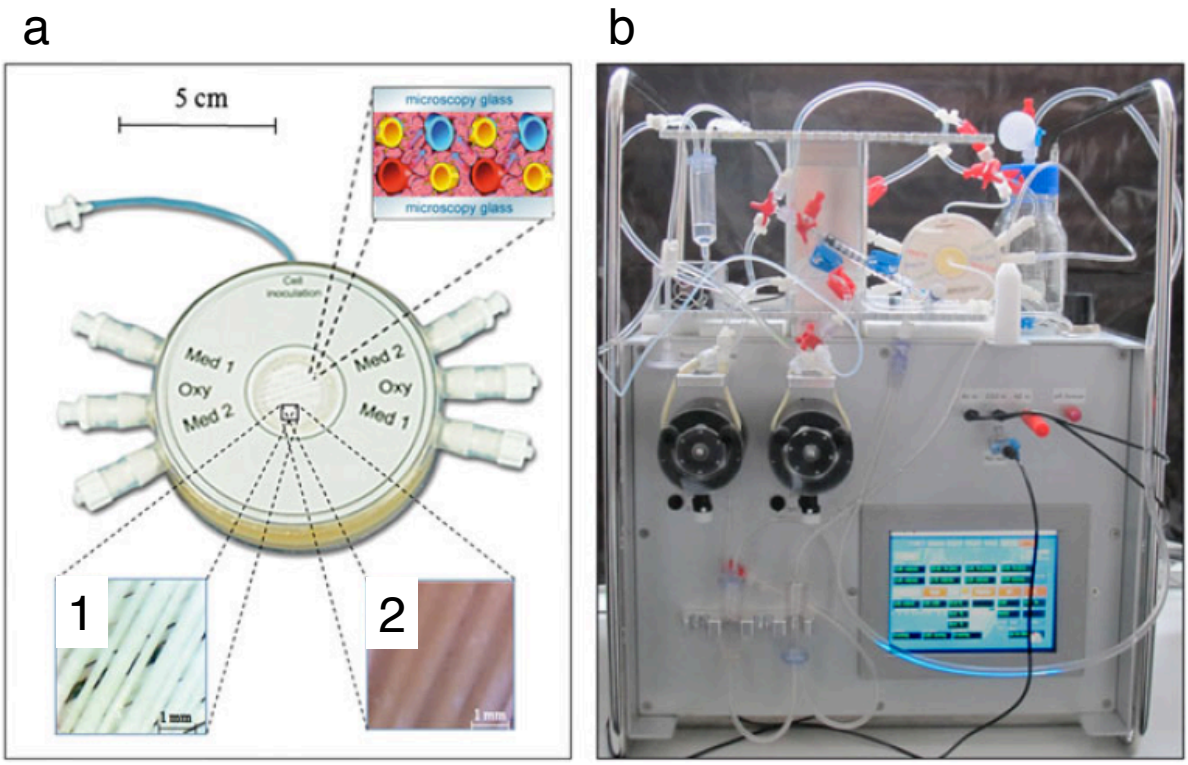

Figure 5.1 Miniaturized 3D multi-compartment bioreactor for high-density liver cell perfusion (a). The bioreactor has two capillary layers (see upper right insert) that serve for counter-current medium perfusion through two independent capillary systems (red and blue) and direct membrane oxygenation (yellow) of the cells located between the capillaries. The lower inserts show microscopic pictures (30-fold magnification) of (1) the capillary bed before inoculation and (2) immediately after cell inoculation, revealing a homogenous distribution of the inoculated cell suspension between the capillaries. Bioreactor operation in an electronically controlled perfusion device (b) equipped with pumps for medium recirculation and medium feed, temperature control and with a valve-regulated gas mixing unit. Perfusion parameters are automatically monitored and can be regulated via an integrated touch screen. Adapted from [64]

5.3.4 Cell viability assays

Diclofenac cytotoxicity was evaluated in both 2D monolayer and 3D spheroid cultures using the MTS reduction assay and by the determination of LDH activity. Briefly, cells were seeded in 100 µl of culture medium at a density of 6,400 and 16,000 cells per well in 96-well collagen coated and ultra-low attachment (ULA) plates, in 2D and 3D cultures, respectively. Cultures were then incubated and exposed to concentrations of diclofenac of 4.0, 3.0, 2.0, 1.6, 1.0, 0.8, 0.2, 0.1, 0.05 or 0.0 mM. After 24 h incubation, the cell culture supernatants were collected for LDH activity measurement using TOX-7 kit (Sigma-Aldrich, St. Louis, MO) as a measure of cell lysis and cells were incubated with MTS (Promega, Madison, WI, USA) in IMDM to measure mitochondrial activity. Both methods were applied according to the manufacturer's

instructions. IC_{50} was calculated using a non-linear regression fit for the Log10 transformation of the concentration values using GraphPad Prism version 6.0 (GraphPad Software, La Jolla, CA, USA). Five independent experiments were performed.

5.3.5 Determination of albumin secretion and urea synthesis

Albumin and urea secretion were quantified in the cell culture supernatants as described in **Chapter 3**.

5.3.6 Biotransformation activity

Cytochrome P-450 (CYP) activity was measured by means of 7-ethoxyresorufin-O-deethylase (EROD) activity and luminescent CYP-Glo™ assays (Promega, Madison, WI, USA) for CYP3A4, CYP2C9 and CYP1A1. Uridine 5'-diphosphate glucuronosyltransferases (UGTs) activity was measured by means of 4-methylumbelliferone (4-MU) conjugation by several UGTs. CYP450 and UGTs activities were measure as described in **Chapter 3.**

5.3.6.1 Substrate Conversion

The HLCs competence to convert the substrates bupropion (100 µM) and diclofenac (9 µM) was evaluated. The functional enzyme activity test for drug specific CYP activity comprised CYP2B6 and CYP2C9 and was based on probe reactions, by quantification of the substrates 1-OH-bupropion and 4-OH-diclofenac, respectively. Methanol as the initial solvent of CYP substrates was removed by evaporation (40 min) and substrates were dissolved in culture medium before application. Samples from cell culture medium were taken at 0, 0.5, 1, 3, 5 and 6 h after substrate injection. For the bioreactor, the system was kept in recirculation mode without feeding during the CYP activity assays. Samples were snap-frozen and stored at -80 ºC until analysis. Quantification of metabolites was performed in medium by a LC–MS/MS method as described previously [62, 64, 94].

5.3.7 Gene (transcript) expression

RNA isolation and extraction, cDNA synthesis and quantitative real-time PCR (qPCR) was performed as described in **Chapter 3.**

5.3.8 Histology

5.3.8.1 Sample preparation

Histological analyses were performed in 3D spheroid or bioreactor sections or in 2D monolayer cultures. After culture termination, bioreactors were disassembled and the capillaries were perfused with a 4% formalin solution for 1 h, followed by dehydration and paraffin embedding using standard procedures. Sections (2.5-3.5 μm thick) were deparaffinized in Paraclear® and rehydrated in solutions with decreasing ethanol concentrations. 3D spheroids were resuspended in Tissue Tek® O.C.T.™ (Sakura®) for preparing cryosections of 5-7 μm and fixed with cooled acetone for 10 min. In monolayer cultures, cells were cultured on collagen coated glass slides (Nunc™, Lab-Tek™ II Chamber Slide™) and fixed with a 4% formalin solution for 10 min.

5.3.8.2 Immunocytochemistry

Samples from the bioreactor were pre-treated with 0.1 M citrate buffer in a pressure cooker at 120 ºC for 15 min in order to unmask antigens. Blocking was performed with 3% bovine serum albumin and 2% FBS (both from Sigma-Aldrich, Munich, Germany) for 1 h. Primary and secondary antibodies were diluted in blocking buffer for the staining procedure. Incubation with primary antibodies was performed overnight at 4 ºC, using the following dilutions: mouse anti-human CK-18 (Chemicon, International, Temecula, CA) at 1:200; rabbit anti-human CK-19 at 1:50, rabbit anti-human albumin at 1:500; rabbit anti-human MRP-2 at 1:50; mouse anti-human OATP-C at 1:50; mouse anti-human CYP1A2 at 1:100 (all Santa Cruz Biotechnology®, Heidelberg, Germany); mouse anti-human HNF-4α (R&D Systems, Minneapolis, MI, USA) at 1:500; and rabbit anti-human CYP3A4 (Nosan Corporation, Yokohama, Japan) at 1:500. Incubations with secondary antibodies were performed for 1 h at RT, using goat anti-mouse Alexa Fluor 488 (green staining) and goat anti-rabbit Alexa Fluor 594 (red staining) (Invitrogen, Carlsbad, CA). Staining of nuclei was performed using 4',6-diamidino-2-phenylindole (DAPI; Molecular Probes, Eugene, USA). Slides were mounted with Aqua-Poly/Mount cover slipping medium (Polyscience Europe, Eppenheim, Germany).

Microphotographs were taken using a Zeiss Axiovert 200M microscope (Carl Zeiss, Göttingen, Germany) with a Retiga 2000R digital camera (QImaging, Surrey BC, Canada) and Image Pro Plus software (Media Cybernetics, Silver Spring, MD, USA).

HepG2 were used as positive controls while undifferentiated hnMSCs cultured as spheroids were used as negative control.

5.3.8.3 Periodic acid Schiff's (PAS) staining

PAS staining was performed to detect glycogen stored in HLCs after differentiation. Cultures were incubated with 1 % periodic acid in PBS for 10 minutes, Schiff's reagent for 15 minutes and Mayer's hematoxylin counterstaining for 30 seconds. The preparations were washed with H_2O between each step. For negative control differentiated HLCs and human liver histological sections were treated with 1 g/L of amylase in 30 mM $CaCl_2$ for 15 minutes at 37 °C before staining, in order to digest the existent glycogen. Anonymized liver tissue samples were obtained from tissue remained from partial liver resection with informed consent of the patients and approval by the Ethical Committee of the Charité - Universitätsklinikum Berlin.

5.3.8.4 Haematoxylin and Eosin (H&E) staining

Slides were stained with Harris's haematoxylin for 10 min, followed by an incubation step with HCl 1% (v/v) in 70% EtOH, and by Eosin Y staining for 2 min. Slides were then submitted to increasing concentrations of ethanol and finally incubated in Paraclear® (EMD Chemicals). Samples were mounted with Entellan® (Merck).

5.3.9 Statistical analysis

The results are given as the mean ± SEM. Statistical data analysis was performed using GraphPad Prism version 6.0 (GraphPad Software, La Jolla, CA, USA). To estimate the significance of the differences of the obtained data a two-way ANOVA with Holm-Sidak method was used with $p < 0.05$ considered as statistically significant.

5.4 Results

5.4.1 5-AZA triggers HLCs maturation

In an attempt to promote hepatic differentiation and maturation of hnMSC the effect of 5-AZA was tested under 2D culture conditions. 5-AZA was added to the culture medium at day 17, after cell detachment and re-inoculation, and compared with non-5-AZA-supplemented cells. A cell passage was introduced at this point since cell proliferation is required for 5-AZA activity as a DNA methylation inhibitor. Also at day 17 a change in cell morphology from fibroblastic to epithelial appearance was observed and the hepatoblast/early hepatocyte markers, such as *CK18, ALB* and *AFP* (**Figure 5.2a**), were overexpressed. Therefore, we classified the pre-differentiated cells at day 17 as hepatoblast-like cells (HbLCs).

At day 27, cells exhibited an epithelial polygonal hepatocyte-like morphology with some bi-nucleated cells and stained positive for PAS (data not shown). Overexpression of hepatocyte-specific genes such as *ALB*, *HNF4A*, *CEBPA*, *HHEX*, *TAT* and the CYP genes (*CYP1A1*, *CYP3A4*, *CYP1B1),* as confirmed by qPCR analysis, was also observed (**Figure 5.2a**). In fact, no significant differences were detected in albumin production with both protocols (**Figure 5.2b**). However, in the presence of 5-AZA, a significant increase in urea production (2-fold) and in EROD activity (1.2-fold) was observed at day 27 when compared to non-treated cells (**Figure 5.2c** and **5.2d**). In addition, UGTs activity remained at a high level both in the presence and in the absence of 5-AZA (days 21 and 27) (**Figure 5.2e**). These data suggest that 5-AZA supplementation promoted HLC maturation obtaining phenotypically and functionally competent HLCs at day 27.

5.4.2 3D cultures allow the formation of viable tissue-like structures of HLCs

To test whether 3D culturing improves HLC metabolic functions, cells were cultured in 3D miniaturized multi-compartment hollow-fiber membrane bioreactors, or as self-assembled spheroid-based suspension cultures in ULA plates after the re-inoculation step (day 17). In parallel, cells were maintained under 2D monolayer (2D) static conditions as control. The viability of trypsinized cells was always above 95% (data not shown). In ULA plates, cells formed clusters after 24 h that progressively compacted in smooth spheroids with relatively small diameters of 109.5 ± 27.6 μm (Mean ± SD) (**Figure 5.3e**), thus avoiding the formation of necrotic centers (**Figure 5.3a**). In the bioreactor, after cell inoculation, the cells remained viable as daily assessed by LDH determination (**Figure 5.3f**). No evidence of cell proliferation was observed in either 2D or 3D confluent cultures. Moreover, both 3D cell culture systems allowed for the formation of tissue-like structures (**Figure 5.3a** and **5.3b**), while a homogeneous population of polygonal shaped cells presenting some binucleated cells was observed in 2D cultures (**Figure 5.3c**).

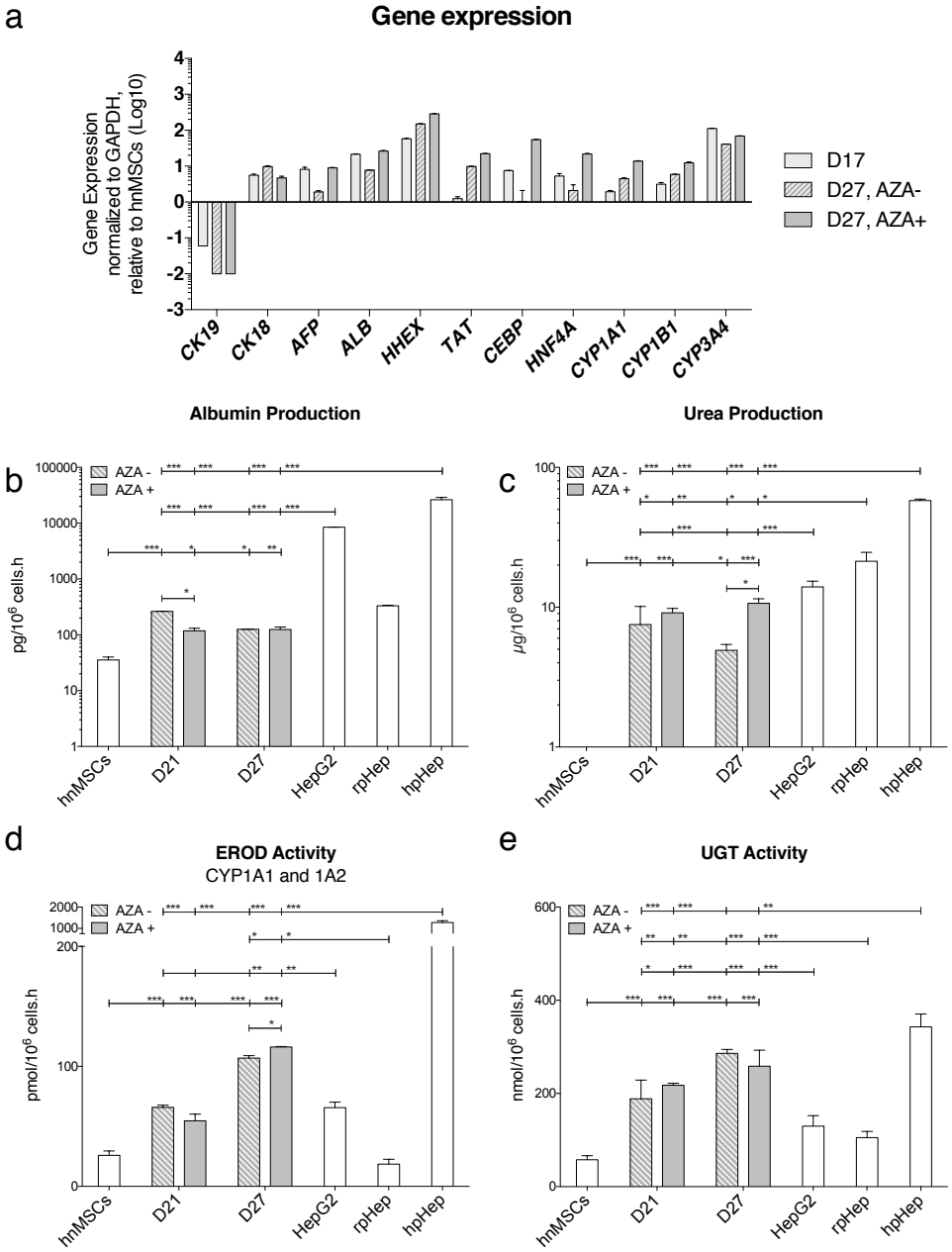

Figure 5.2 5-AZA triggers HLCs maturation. Gene expression analyses (a) of the hepatic markers on hepatoblast-like cells (day 17, light grey bars) and on HLCs (day 27) cultured in 2D culture, with and without 5-AZA treatment (grey and black bars, respectively). qPCR shows over expression of the hepatic markers *ALB, AFP, CK18, HNF4A, CEBPA, CYP1A1, CYP1B1, CYP3A4, TAT* and *HHEX* and under expression of the biliary marker *CK19* (black and grey bars) for both conditions. 5-AZA supplemented HLCs present higher expression of all genes except for CK18 and CK19. Data is normalized to the reference gene *GAPDH* and expressed in Log10 relative to hnMSCs (n= 3). Metabolic capacity of HLCs in 2D cultures until day 27, with and without 5-AZA treatment differentiation (grey and black bars, respectively) and on the controls: undifferentiated cells (hnMSCs) HepG2 cell line, and primary hepatocytes, human (hpHep) and rat (rpHep) (white bars), is shown by albumin production (b), urea secretion (c), EROD activity (phase I) (c) and UGTs activity (phase II) (e), (n=3 Mean ± SEM).

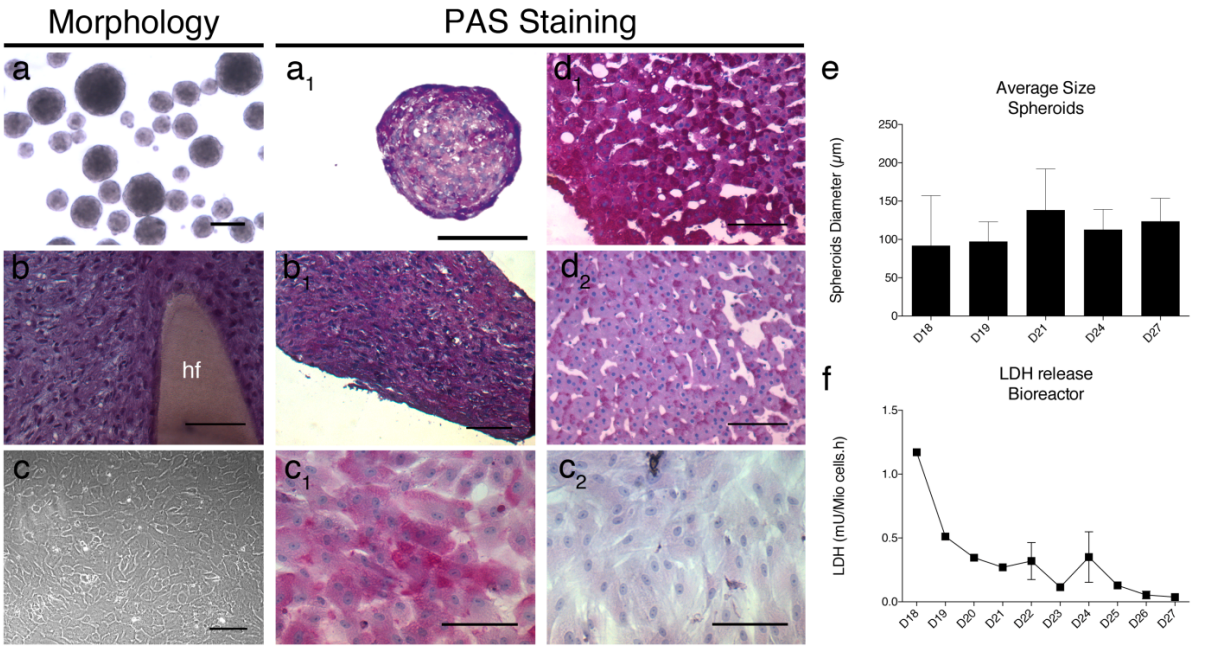

Figure 5.3 HLCs cell culture characterization in spheroids, bioreactors and in 2D cultures. Cell morphology and glycogen storage capacity demonstrated on (a) HLCs in 3D spheroids; (b) HLCs in the hollow-fiber (hf) bioreactor; (c) HLCs in 2D cultures and compared with (d) human liver sections; (a) and (c) are representative images of living cells and (b) is H&E stained, showing cells tightly adhered to the hollow-fiber membrane (hf). (a_1), (b_1) (c_1) and (d_1) are representative images of PAS stained cells whereas c_2 and d_2 were treated with 5 g/L of amylase before PAS staining as glycogen specificity control. Representative images were acquired at day 27 with phase-contrast microscopy. Scale bar = 50 μm. (e) Represents the homogeneity of spheroids size from day 19 to day 27 and (f) shows LDH release to the recirculation medium in the BR indicating some cell lyses after inoculation (day18) and remains constantly low from day 20 onwards, reflecting the viability of culture.

5.4.3 Hepatic-specific markers are upregulated in HLC 3D cultures

Along with the HLC morphology the presence of hepatocyte-specific markers further sustaining a hepatocyte-like phenotype was obtained in all culture systems at day 27. The cytoskeleton protein CK-18, present in hepatocytes, was highly detected in HLCs both at transcript (**Figure 5.4**) and protein levels (**Figure 5.5**), whereas CK-19, present in biliary cells, bi-potent progenitor cells (oval cells) or hepatocarcinoma cells, was under-expressed in HLCs. In fact, *CK19* expression (**Figure 5.4**) was ~3-fold, 2.5-fold and 4.5-fold lower in HLCs (day 27) in spheroids, bioreactor and 2D cultures, respectively, when compared to hepatoblast-like cells (day 17) (**Figure 5.2a**). Moreover, the same profile of *CK19*/*CK18* gene expression was observed in HLCs and in primary hepatocytes in contrast to HepG2 cells (**Figure 5.4**). The expression levels of *AFP* and *CYP3A4* in HLCs were higher in cells grown and maintained in 3D systems, when compared to 2D cultures (**Figure 5.4**); whereas the transcript levels of *HNF4A*, a liver enriched transcription factor, *CYP1A1* and *CEBPA* was similar between

bioreactor and 2D and *ALB* mRNA levels were higher in the bioreactor than in spheroids and 2D culture. Nevertheless, at day 27 the mature hepatocyte marker genes (*ALB, CEBPA, HNF4A, CYP1A1, CYP1B1*) were unregulated relative to undifferentiated cells and to cells at day 17 of differentiation (**Figure 5.2a**).

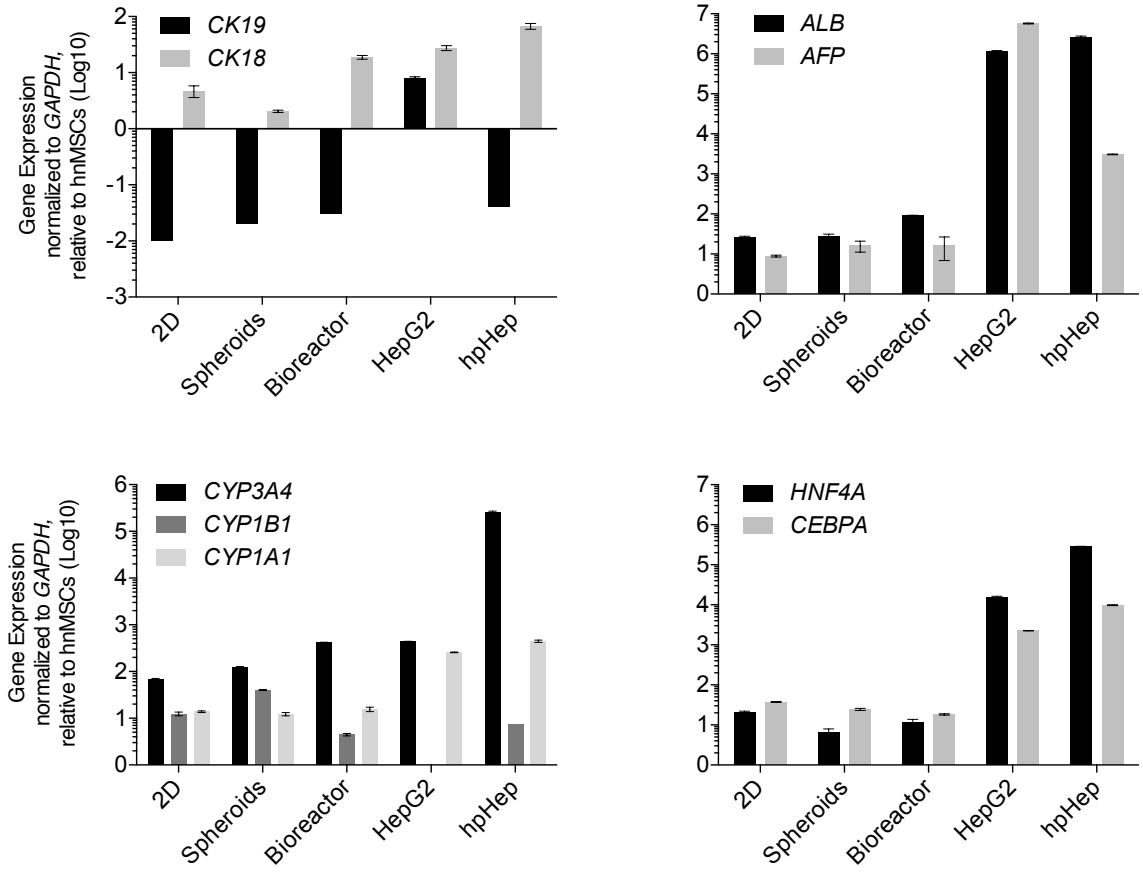

Figure 5.4 Gene expression analyses of the hepatic markers on HLCs (day 27) cultured in 2D culture, in spheroids and in bioreactors. qPCR shows over expression of the hepatic markers *ALB, AFP, CK18, HNF4A, CEBPA, CYP1A1, CYP1B1* and *CYP3A4* and under expression of the biliary marker *CK19* for all samples, except for HepG2 cell line that presented overexpression of *CK19.* Positive controls are HepG2 cell line and cryopreserved hpHep. Data is normalized to the reference gene *GAPDH* and expressed in Log10 relative to hnMSCs (n= 3).

The relative expression of *ALB*, *HNF4A* and *CYP3A4* was confirmed by immunofluorescence with HNF-4α showing a clear nuclear localization (**Figure 5.5**). In turn, the uptake transporter protein OATP-C and the efflux hepatic transporter MRP-2 revealed a different localization in the 3D culture systems when compared to 2D (**Figure 5.5**), showing a certain degree of cellular polarization, an important characteristic of differentiated hepatocytes. The presence of phase I enzyme CYP1A2 was also observed (**Figure 5.5**), further demonstrating the presence and upregulation of hepatic-specific markers in HLC 3D cultures.

5.4.4 3D culturing improves cell metabolic activity

The glucose metabolism, ammonia conversion and albumin production were evaluated in the hnMSC-derived HLCs maintained as spheroids or in bioreactors and compared to the cells maintained as 2D monolayer. The metabolic activity of HLCs was examined in cell culture supernatants and in the bioreactor-circulating medium during the differentiation period.

The lactate production levels and profiles in 2D, spheroids and bioreactor culture were similar (**Figure 5.6b**). All systems presented glucose metabolism as shown by glycogen storage data (**Figure 5.3**) and glucose release to the medium, shown as negative glucose consumption (**Figure 5.6a**). The latter could be observed in 2D cultures from day 24, consistently showing higher levels than 3D cultures ($p < 0.01$). Conversely, the 3D cell culture systems presented an improved metabolic profile regarding urea production, a specific metabolic function of hepatocytes. In fact, at the end of cultivation (day 27) ammonia conversion into urea was 5.8- and 8.3-fold higher in the bioreactor and in the spheroid-based culture, respectively, when compared to 2D cultures ($p < 0.05$) (**Figure 5.6c**). The urea production levels observed in the bioreactor and in the spheroid-based culture were also respectively similar and higher to levels observed in HepG2 and primary hepatocyte spheroids (Supplementary Material, **Table 5.1**). In turn, albumin production was improved in HLCs cultured in the bioreactor, which resulted in a 2.9-fold induction relative to 2D ($p < 0.001$). Spheroid culture albumin production was similar to 2D (**Figure 5.6d**). Overall, 3D culturing improved cells' metabolic activity, particularly for urea production in the spheroids and for albumin production in the bioreactor.

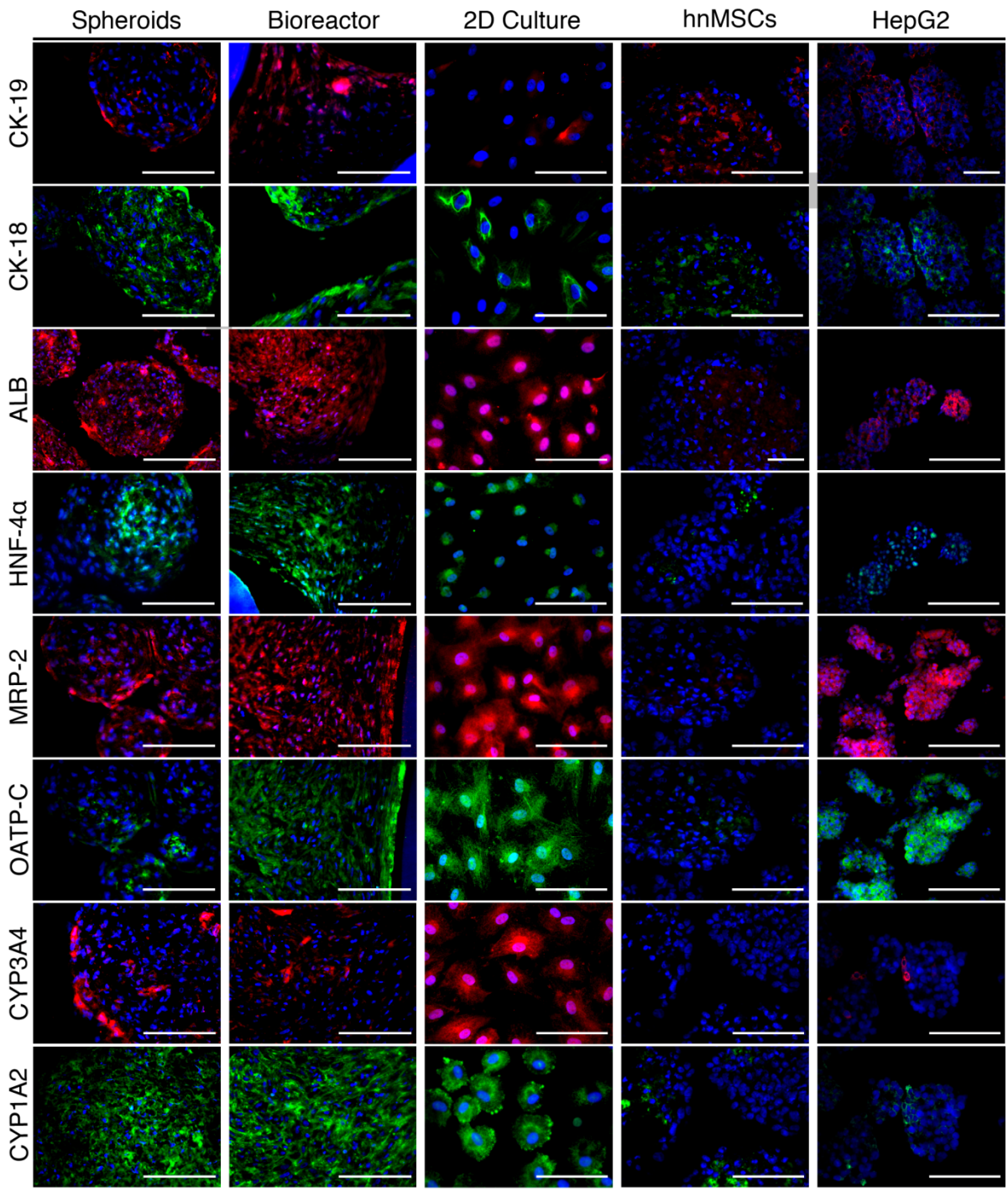

Figure 5.5 Immunohistochemical analysis of HLC-derived hnMSCs cultured in spheroids, in bioreactors and in 2D cultures (day 27). Representative images show the presence of the hepatic markers CK-18, the plasma protein ALB, the transcription factor HNF-4α, the efflux transporter MRP-2, the uptake transporter protein OATP-C, the biotransformation enzymes CYP1A2 and CYP3A4 and slight presence of the biliary marker CK-19. hnMSCs and HepG2 cell line cultured in 3D spheroids were used as negative and positive controls, respectively. Cell nuclei are stained with DAPI. Scale bar: 50 μm.

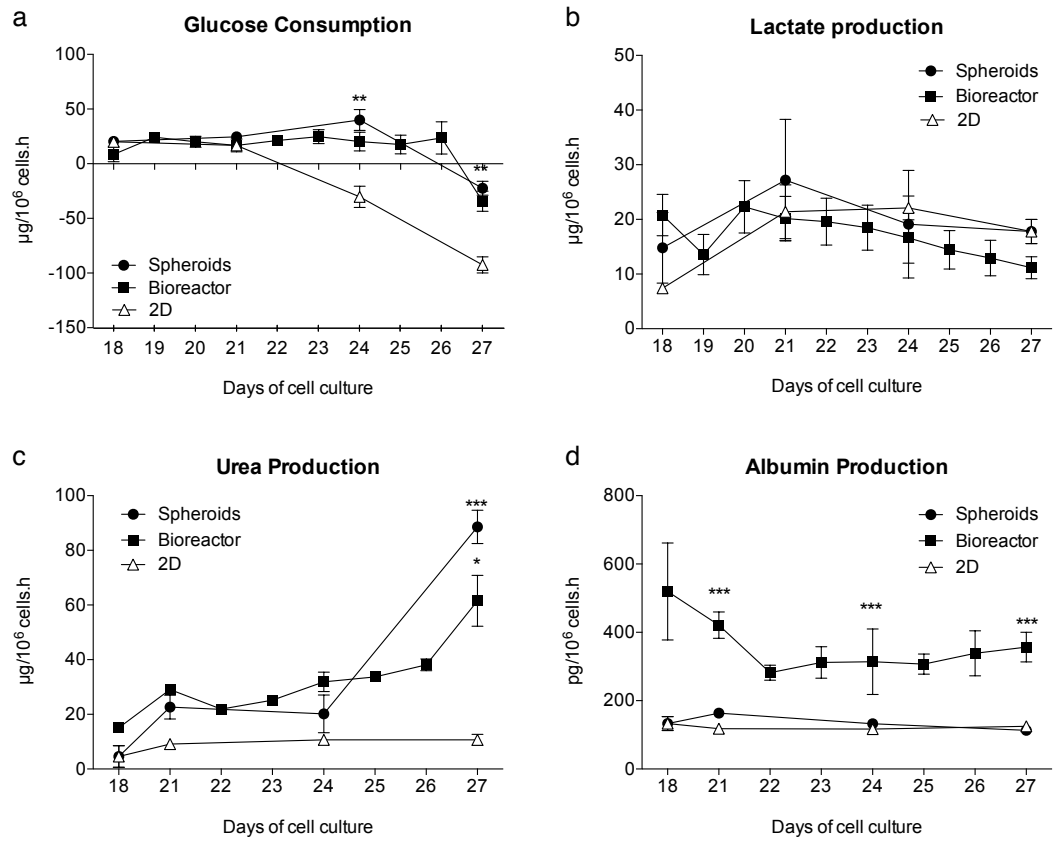

Figure 5.6 Metabolic capacity of HLCs cultured in 3D cultures, bioreactor and spheroids, and in 2D cultures as a control from day 18 until day 27 is shown by (a) Glucose consumption as well as (b) Lactate (c) Albumin and (d) Urea production. * $p < 0.05$, ** $p < 0.01$ and *** $p < 0.001$ relative to 2D (n=3 Mean ± SEM).

5.4.5 HLC Phase I and II enzyme activity is improved in 3D culture conditions

HLC potential applications in drug metabolism studies imply their biotransformation competence. HLC metabolic capacity was monitored regarding phase I and II enzymes at different time points. The activity levels of CYP enzymes were measured by EROD, CYP1A1/2, CYP2C9 and CYP3A4 activity (**Figure 5.7a**, **5.7b**, **5.7c** and **5.8**). Phase II metabolism was evaluated by UGTs activity (**Figure 5.7d**). EROD (CYP1A1/2) was performed in all culture systems on day 27 (**Figure 5.8**). However, enzymatic activities could be monitored in spheroid-based and 2D-culture distinct time points (days 21 and 27). These two cell culture systems are more amenable to screen a higher number of features, including induction studies, and therefore CYP1A1, CYP3A4, CYP2C9 activities and their ability to be induced by 3-MC (CYP1A1) or rifampicin (CYP3A4 and CYP2C9) were also evaluated (**Figure 5.7**).

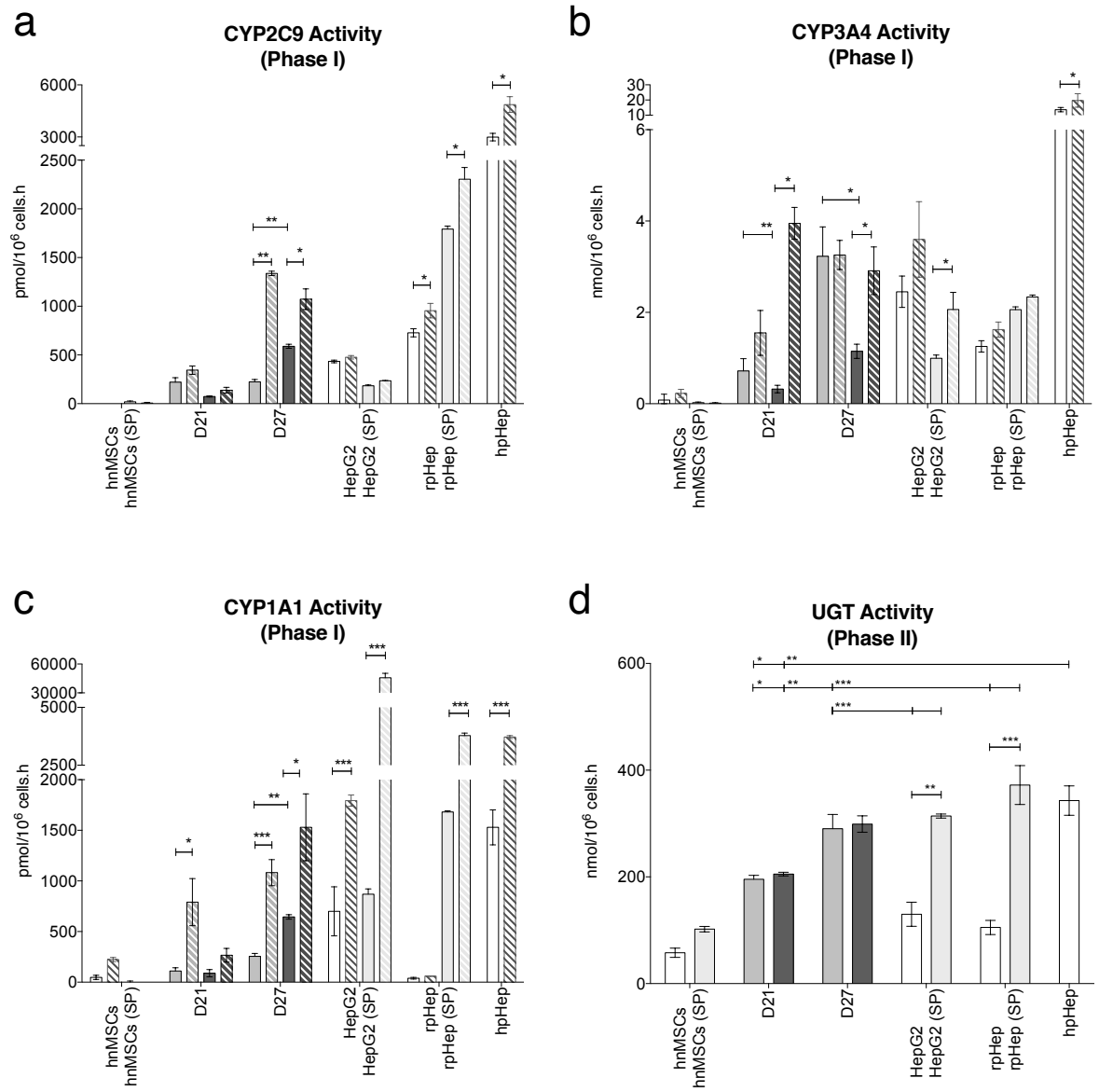

Figure 5.7 Phase I and Phase II metabolism on HLCs. CYP2C9 (a), CYP3A4 (b), CYP1A1 (c) and UGTs (d) activity is shown in 2D cultures (grey bars) and spheroids (dark grey bars) as well as the ability to be induced (striped bars) by rifampicin (CYP3A4 and CYP2C9) or by 3-MC (CYP1A1) at days 21 and 27 of cell culture. Undifferentiated cells (hnMSCs), HepG2 cell line, and primary hepatocytes, human (hpHep) and rat (rpHep) were used as controls. All controls were performed in 2D (white bars) and in spheroids culture (SP, light grey bars) except for hpHep. All HLCs activities were superior to hnMSCs (*). * $p < 0.05$, ** $p < 0.01$, *** $p < 0.001$ (n=3 Mean ± SEM).

Phase I and II enzyme activity increased along the differentiation protocol, in both spheroid and 2D conditions. HLCs cultured in both 3D systems presented EROD activity higher than that of HepG2 cell line and rpHep ($p < 0.01$) (**Figure 5.8**). In fact, a 4.8- and 3.8- fold increase was observed in the bioreactor and spheroid-based cultures, respectively, when compared to 2D monolayer cultures.

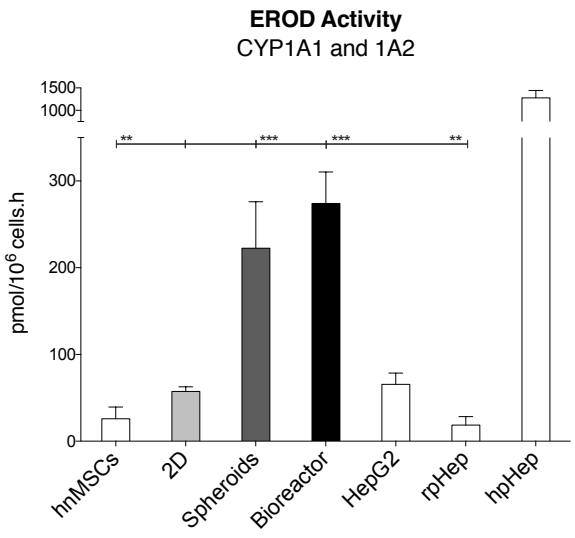

Figure 5.8 EROD activity on HLCs cultured in bioreactors, spheroids and 2D cultures at day 27 of the differentiation (black and grey bars) and on the controls undifferentiated cells (hnMSCS), HepG2 cell line, and primary hepatocytes, human (hpHep) and rat (rpHep) (white bars). ** $p < 0.01$ and *** $p < 0.01$ relative to 2D (n=3 Mean ± SEM).

3D spheroids showed a significant increase in CYP3A4, CYP2C9 and CYP1A1 enzymes activity from day 21 to day 27 ($p < 0.05$). CYP1A1 and CYP3A4 activity in HLCs culture in 3D and 2D conditions were similar to those observed in HepG2 cell line. Moreover, HLCs in 3D and 2D culture surpassed the activity level of CYP2C9 in HepG2 cells in both monolayer and spheroid cultures. In addition, CYP1A1, CYP2C9 and CYP3A4 were consistently induced in spheroid HLCs, in contrast to 2D cultures where no induction of CYP3A4 was observed. Most importantly, CYP3A4 activity was induced by ~2.5-fold in spheroid HLCs whereas the hpHep were only induced by 1.5-fold (**Figure 5.7b**) at day 27. The same trend was observed for CYP1A1 (1.7-fold induction) and CYP2C9 (6-fold induction) activities in HLC spheroids and in hpHep. Moreover, CYP2C9 induction was detected in HLC spheroids and hpHep cultures but not in HepG2 cell line in both monolayer or spheroids culture.

Phase II metabolism (**Figure 5.7d**), observed by the ability to convert 4-MU by several UGTs, increased in both cultures throughout time, being similar to primary hepatocytes (cultured for 24h) and statistically higher than in HepG2 spheroid cultures ($p < 0.01$).

HLCs obtained and maintained in the three culture systems showed to be metabolic competent as quantified by both phase I and phase II enzyme activities. CYP activity levels of HLCs were higher than those obtained with the HepG2 cell line for CYP2C9, CYP3A4, EROD and UGT activity. Moreover, CYP activity and induction capacity was either maintained or increased over time in spheroid-based cultures, further sustaining that the 3D cultures improved HLC maturation.

5.4.6 hnMSC-derived HLCs metabolize diclofenac and bupropion

Considering the maintenance of enzyme activity of the HLCs between day 21 and 27, and the better performance in albumin and urea production, glucose metabolism and CYP activity on day 27, the ability to convert drugs, namely diclofenac and bupropion, to their specific metabolites was evaluated in all systems at this time point. HLCs showed the capacity to biotransform diclofenac and bupropion whereas undifferentiated hnMSCs revealed the presence of residual metabolites in significantly lower amounts (**Figure 5.9**). The spheroids showed a higher capacity to metabolize bupropion (CYP2B6), followed by the bioreactor and the 2D cultures (**Figure 5.9b**). On the other hand, the bioreactor presented the higher metabolic conversion rate for diclofenac (**Figure 5.9a**) into 4-OH-diclofenac.

5.4.7 HLCs show higher toxicity to diclofenac in spheroid suspension cultures

To examine the applicability of hnMSC-derived HLCs to be used for predicting drug induced cytotoxicity, treatment with a drug that causes hepatotoxicity was performed. Diclofenac at concentrations ranging from 0.05 to 4 mM was used for testing HLC suitability for drug screening. In addition, cell viability was evaluated by MTS reduction assay and by the determination of LDH activity in both the spheroid and the 2D models in order to identify the most relevant culture system. Our results show that both assays have a dose-response profile after a 24 h-period of incubation with cells maintained in spheroid-based cultures being significantly more sensitive to diclofenac exposure than HLCs in 2D cultures ($p < 0.001$) (**Figure 5.10**). The calculated IC_{50} values for 3D spheroid and 2D monolayer cultures exposed to diclofenac were 0.98 ± 0.03 mM and 1.51 ± 0.05 mM, respectively, for the MTS assay (**Figure 5.10**). For the LDH release assay a significant increase was only observed for concentrations above 2mM in both culture systems (data not shown). Therefore, the results herein observed may suggest that a higher bioconversion of diclofenac and its metabolites may be occurring in the spheroid-based system.

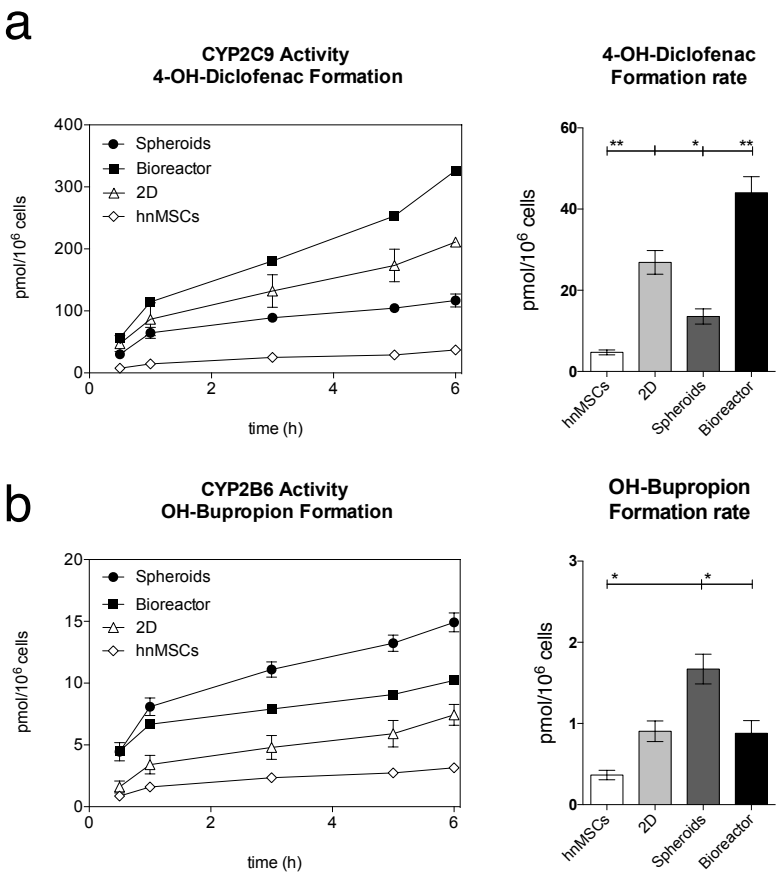

Figure 5.9 Metabolic competence of HLCs evaluated by exposure to (a) diclofenac and (b) bupropion. Time course of product formation over 6 h and formation rates (calculated over 3 h) of CYP specific metabolites (OH-diclofenac for CYP2C9 and OH-bupropion for CYP2B6) in undifferentiated cells (hnMSCs) and HLCs in spheroid and bioreactor cultures (3D, black marks) and HLCs in 2D cultures (white marks) at day 27 of cell culture. * $p < 0.05$ and ** $p < 0.01$ relative to 2D (n=3 Mean ± SEM).

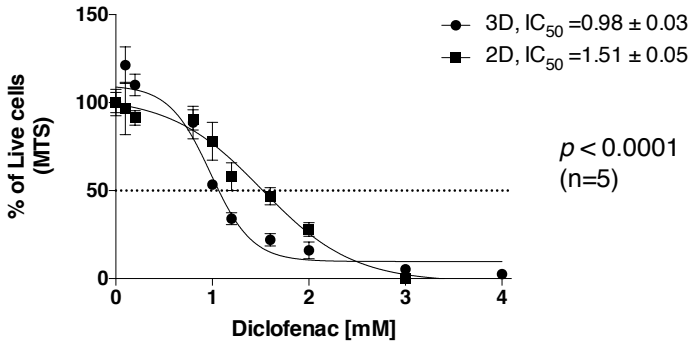

Figure 5.10 Comparison of diclofenac cytotoxicity in 3D spheroids and 2D monolayer cultures evaluated by MTS mitochondrial activity assay. The HLCs were incubated with 4.0, 3.0, 2.0, 1.6, 1.0, 0.8, 0.2, 0.1, 0.05 and 0.0 mM of diclofenac. The relative amount of live cells is calculated to non-treated HLCs (Mean ± SEM).

5.5 Discussion

The liver function is partially ensured by the hepatocytes. A function that is dependent on the establishment of relevant cell-to-cell and cell-to-matrix interactions as well as on maintenance of gradients of oxygen, nutrients, endobiotics and xenobiotics and their metabolites. 3D cultures provide environmental characteristics that mimic the liver physiology *in vivo* better than traditional monolayer cultures [7]. Thus, by applying 3D cell culture systems to HbLC maturation, we hypothesized that the HLC phenotype and functionality could be improved. Our hypothesis rests on our previously reported efficient differentiation protocol for deriving HLCs from a specific population of umbilical cord tissue derived-hnMSCs. This protocol was developed in monolayer culture conditions that resulted in HLCs with drug metabolizing capacity lower than primary hepatocytes (**Chapter 3**). Herein, such protocol was improved and successfully adapted to highly reproducible 3D cell culture systems that improved HLC maturation. Most importantly, the HLCs derived from our hnMSC population showed significant drug metabolizing capacity comparable to primary hepatocytes, which is crucial for in vitro toxicology applications.

For a more efficient HLC differentiation, some further improvements were introduced to our previously developed protocol [333]. Hepatoblasts are characterized by their bi-potency and represent a highly proliferative stage of hepatogenesis [336]. Thus, a cell passage step was applied to HbLC at differentiation day 17, in order to allow for cell proliferation which is otherwise not occurring in a confluent monolayer cell culture. A proliferative stage is also necessary for 5-AZA incorporation into the DNA, since it is a cytidine analogue that inhibits DNA methylation [209]. To our knowledge, 5-AZA effects on hepatocyte differentiation protocols in vitro has only been attempted on human adipose-derived stem cells by Seeliger *et al.* [213], and on umbilical cord blood derived MSCs by Yoshida *et al.* [214] being applied 24 h prior to the differentiation induction. Seeliger *et al.* tested the DNA methylation effect of 5-AZA (5 to 20 µM). The best result was observed with 5-AZA at 20 µM [213] with improved glucose secretion, and CYP1A1/2 and CYP2B6 activity. Urea production was similar to both freshly isolated hepatocytes and cells not exposed to 5-AZA [213]. On the other hand, Yoshida *et al.* achieved a significantly higher proportion of ALB, c/EBP-α, CYP1A1/2 and PAS positive cells, as well as higher urea production and *ALB* gene expression after 21 days of differentiation than on non-5-AZA-treated cells [214]. However, a less mature phenotype than that observed by Seeliger *et al.* [213]. 5-AZA was previously tested on HLC differentiation at day 0, using our hnMSC source [333] but no significant HLC functionality improvement was observed. Therefore, 5-AZA was herein tested on day 17 after a cell passage step. This should

inhibit DNA methylation by 5-AZA as well as increase the expression of genes in a presence of a chemical cocktail that is inducing the hepatic differentiation and maturation. In fact, this approach resulted in increased urea production, EROD activity and the expression of hepatic-specific marker genes, namely *ALB, CEBP, HNF4A, CYP1A1, CYP1B1* (day 27) when compared to non-differentiated cells.

Several reports on the generation of functional HLCs from human SC have been described. The majority of these studies use direct developmental signaling of embryonic and induced SC for deriving HLCs in monolayer cultures. However, fully functional hepatocytes have not been obtained so far. Some reports describe the differentiation of hnMSCs into HLCs [172, 174, 179], but only two of them resort to 3D cell culturing, one using a collagen scaffold [337] and another culturing HLCs as spheroids [338]. 3D culture conditions promote a structural organization which is important for the maintenance of liver cell characteristics [7], as shown by the higher albumin secretion, ammonia detoxification, amino acid metabolism, glycogenolysis, bile secretion, enzymatic activity related to biotransformation and the polar distribution of transporters observed in primary hepatocyte cultures performed in several different 3D culture settings [61, 64, 70, 71, 85]. 3D culturing also proved successful in improving the hepatocyte-like phenotype in terms of biotransformation activity, as shown by spheroid-based cultures of either hESCs-derived or iPSC-derived HLCs [236, 237, 334, 335]. In particular, the differentiation of hESCs in a hollow-fiber bioreactor resulted in an upregulation of pathways related to steroid hormone biosynthesis, ABC transporters and CYP-dependent metabolism of xenobiotics in comparison to 2D cultures, also revealing maturation of the HLCs in this environment [243]. Apart from hESCs and iPSCs, MSCs have also been effectively used to derive HLCs in 3D culture conditions [239]. By resorting to nano-scaffold structures, human bone marrow-MSC-derived HLCs showed increased ability to produce urea and transferrin [245]. Although evidence is clear about the advantages of 3D culture systems over 2D culture systems in terms of HLCs derivation, it is still not clear which system provides better differentiation and maintenance conditions. In this work, a static spheroid cell culture model and a perfused bioreactor system were applied and compared to traditional monolayer cultures in terms of promotion of HLCs phenotype and function.

In this study, cells were adapted to 3D cell culture systems at the trypsinization step (day 17) and their hepatocyte specific features were evaluated up to differentiation day 27. It has been described that cells cultured in three-dimensional systems are able to form ECM, thus providing high cell-to-cell and cell-to-matrix interactions. This effect was previously observed in primary hepatocytes either cultured in spheroids [61, 71] or in a perfused bioreactor [94]. In fact, a compact cell organization with distinct localization of hepatic transports among cell

membrane could be observed in HLC 3D cultures, which resulted in higher phase I metabolic activity. However, when developing an HLC-based in vitro system other hepatocyte specific features such as urea or albumin production, herein improved, should not be disregarded.

The 3D configuration creates a gradient with higher oxygen, glucose and nutrients presence in the outer layer of the spheroid and in cells closer to the capillaries in the bioreactor, which may mimic the liver periportal environment characterized by higher xenobiotic metabolism and glycogen synthesis from glucose as well as lower urea production [7, 50]. Therefore, a more heterogeneous cell population is expected in 3D cultures than in monolayer cultures. Indeed, CYP1A2 and CYP3A4 are detected in the tissue-structure, whereas the hepatic transporters OATP-C and MRP-2 are predominantly located near the hollow-fiber capillary suggesting some phenotype zonation in the bioreactor. The same could be observed in the spheroids, although at a lesser extent. Conversely, a homogeneous distribution of phase I enzymes and the hepatic transporters is observed in monolayer cultures.

In the present study, cells maintained in both 2D or 3D culture systems revealed a gene expression profile closer to hpHep, particularly in terms of CK19 and AFP gene expression when compared to HepG2 cell line. In turn, *CK19* gene and protein expression were lowered in 3D culture conditions reflecting a higher maturity of the HLCs in those environments. In fact, *CK19* is present in progenitor cells of the developing liver, hepatoblasts and later in the development in ductal plates. In normal mature liver, CK19 is exclusively expressed in biliary duct cells and in oval cells, a type of bi-potent cells involved in hepatocyte and cholangiocyte differentiation [339, 340]. Thus, the isolated CK19 positive cells observed in 2D cultures reflect the presence of less differentiated cells whereas the presence of CK19 clusters, more evident in the spheroid-based cultures, can reveal some differentiation into biliary-like cells.

Furthermore, by providing a perfused cell culture system with a bioreactor, characterized by higher cell-to-cell contacts, we achieved improved albumin production by HLCs, as observed by increased ALB gene expression, intracellular presence and secretion. This has not been observed in spheroid-based cultures. However, cells kept in the spheroid-based culture were able to show higher albumin secretion than cells kept in the 2D system, from day 27 to day 34 (**Figure 5.11**), suggesting that long-term cultivation may indeed allow cell maturation.

On the other hand, HLC spheroids showed CYP induction capacity and UGT activity. UGT activity is associated with later hepatocyte maturity [341] and it is scarcely reported on stem cell-derived HLCs. Herein, we can observe a higher glucuronidation capacity in the spheroids, showing a 2-fold increase from day 21 to day 27, to levels comparable to cryopreserved hpHep cultured for 24h. In agreement with previous studies by Hamilton *et al.* [342] showing that the

induction of CYP enzymes is dependent on cell density and cell-to-cell contacts in hpHep cultures, the induction of CYP activity was consistently observed in the spheroid-based cultures but not in the monolayer system. Finally, the expression of CYP3A4 was higher in HLCs from 3D cultures, which is reflected by CYP activity on day 27 when compared to cells in 2D cultures.

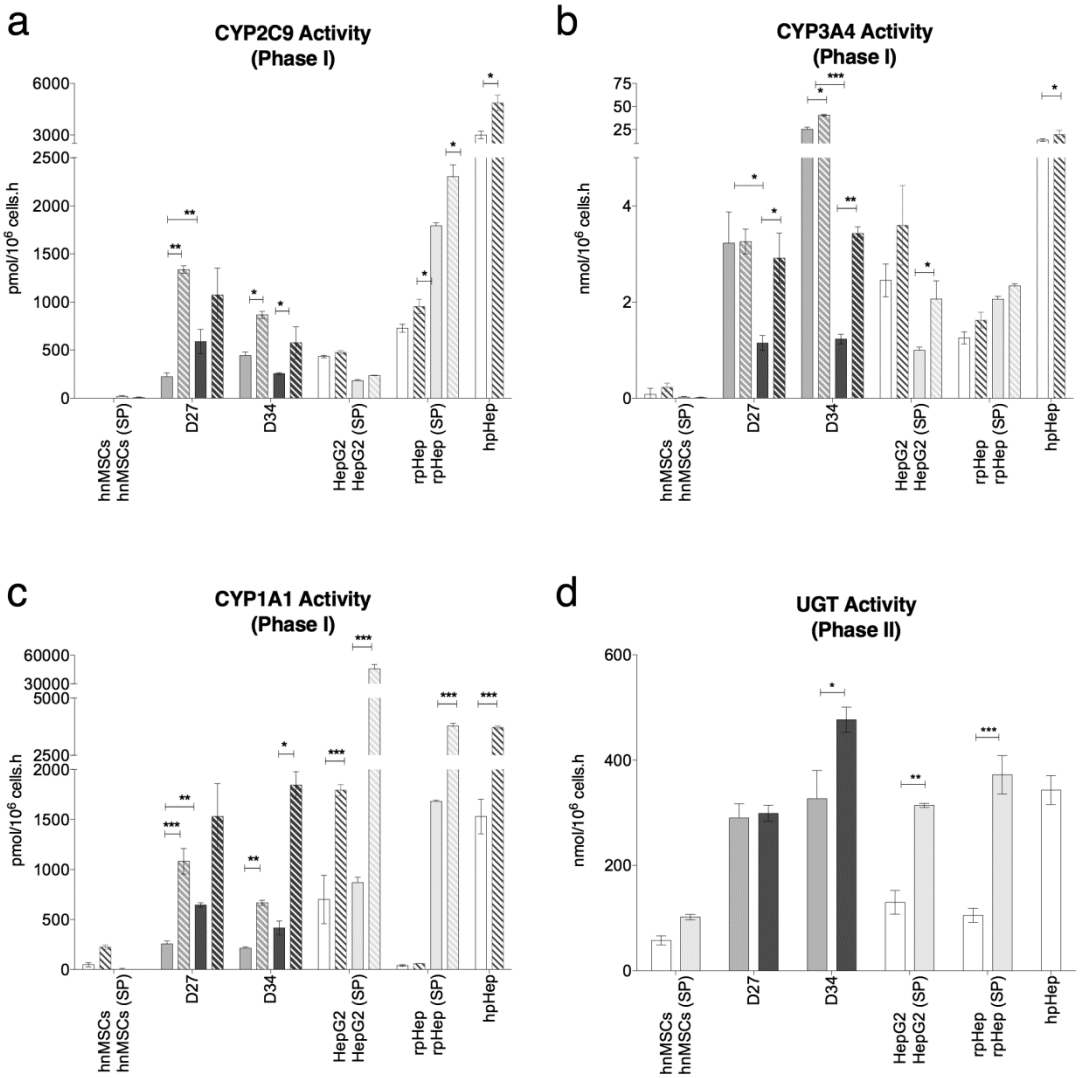

Figure 5.11 Phase I and II metabolism on HLCs up to day 34. CYP2C9 (a), CYP3A4 (b), CYP1A1 (c) and UGTs (d) activity is shown in 2D cultures (grey bars) and spheroids (dark grey bars) as well as the ability to be induced (striped bars) by rifampicin (CYP3A4 and CYP2C9) or by 3-MC (CYP1A1) at days 27 and 34 of cell culture. Undifferentiated cells (hnMSCs), HepG2 cell line, and primary hepatocytes, human (hpHep) and rat (rpHep) were used as controls. All controls were performed in 2D (white bars) and in spheroids culture (SP, light grey bars) except for hpHep. All HLCs activities were superior to hnMSCs (*). * $p < 0.05$, ** $p < 0.01$, *** $p < 0.001$ (n=3 Mean ± SEM).

The presence of hepatic transporters and CYP metabolism is particularly relevant for in vitro toxicology applications. Gieseck *et al.* [244] compared iPSC-derived HLCs in 2D conditions with iPSC-derived HLCs in 3D conditions and observed that the expression of the MRP-2, an efflux transporter protein, occurred only in the HLCs obtained from 3D cultures consisting of cells clustered onto a collagen matrix. Additionally, a stable CYP3A4 activity and albumin production was maintained, while AFP production decreased [244]. Subramanian *et al.* [236] also showed a phenotype improvement of HLCs derived from hESCs when cultured on spheroid static cultures, namely the decrease of AFP expression and an increase of albumin production and expression. Finally, Okura *et al.* [239] observed hepatocyte-like characteristics on HLCs clusters derived from adipose tissue hMSCs as indicated by ALB and antithrombin presence, urea production and glycogen storage capacity, but the comparison with 2D cell cultures is scarce. In the present study, we could observe not only MRP-2 presence, but also an influx transporter with great impact in pharmacokinetics, OATP-C.

Notably, HLCs cultured in any of the three systems presented a relevant biotransformation capacity by converting bupropion and diclofenac into their corresponding metabolites, 1-OH-bupropion and 4-OH-diclofenac. Moreover, CYP3A4 is present in all cell cultures systems at protein level and its activity was confirmed in spheroids and 2D culture by the luminescent assay and in bioreactor by midazolam conversion into 1-OH-midazolam (data not shown). Diclofenac is mainly metabolized by CYP2C9 into 4-OH-diclofenac and also, in a lower extent, converted into 5-OH-diclofenac by CYP3A4. Diclofenac and OH-diclofenac are glucuronidized by UGT2B7 and excreted across the canalicular plasma membrane into the bile via MRP-2 [102]. Therefore, diclofenac metabolism comprises phase I, II and III enzyme activities and its toxic effects can be associated to its reactive metabolites 4-OH-diclofenac, diclofenac-acyl-glucuronide and 4-OH-diclofenac-acyl-glucuronide [102]. In addition, diclofenac is one of the most prescribed nonsteroidal anti-inflammatory drug (NSAID) worldwide [102]. There are several lines of evidence demonstrating drug induced liver injury (DILI) by diclofenac including in vitro, in vivo and epidemiological data. Diclofenac causes rare albeit significant cases of serious hepatotoxicity. Due to the large number of patients treated the absolute number of reported cases of hepatotoxic adverse drug reaction by diclofenac is still impressive with fatality rate of 10 % [102]. As such, diclofenac was herein selected as a hepatotoxicant dependent of bioactivation. Herein, the cells kept in spheroids showed lower IC_{50} values for diclofenac than cells cultured in monolayer conditions, which can be a result of a higher CYP2C9 activity in spheroids. The IC_{50} values for diclofenac among the literature are highly variable. For conditions of 24 h of diclofenac exposure to hpHep monolayer cultures IC_{50} values of 0.76 mM [104] and 1.41 mM [106] have been reported. The value calculated for our

spheroid culture of 0.98 ± 0.03 mM falls within this range. The 2D culture, in turn, showed a higher IC_{50} value (1.51 ± 0.05 mM) similar to what has previously been reported for iPSC-derived HLCs (IC_{50} of 1.85 mM and 1.92 mM) [343]. Diclofenac toxicity studies are scarce in comparing monolayer and 3D cell cultures. To our knowledge, the study of Xu *et al.* [103] is the only one reporting the effects of diclofenac in rat primary hepatocyte and HepG2 spheroids [103]. In a recent study diclofenac metabolism and toxicity was investigated in perfused 3D bioreactors using primary human hepatocytes [95]. However, no data for its comparison with monolayer cell culture is reported. Although no IC_{50} value was calculated, these authors observed toxicity for concentrations higher than 0.5 μM. Moreover, it was observed that diclofenac significantly decreased LDH release in liver spheroids but not in HepG2 spheroids [103], pointing out the importance of using metabolic competent cells to assess the toxicity of this drug. Herein, higher levels of 4-OH diclofenac are observed in monolayer, but an increased phase I (CYP2C9 and CYP3A4) and II (UGTs) activities is shown for spheroid cultures. Therefore, the results herein observed may suggest that a higher bioconversion of diclofenac and its metabolites in spheroids may be occurring, resulting in its more toxic sub-products and consequently in higher cytotoxicity.

An important achievement of this study is a thorough characterization of HLCs derived from MSCs in distinct culture conditions. The findings herein described support the potential of hnMSC-derived HLCs as an alternative cell type for human biotransformation studies, thus reinforcing the importance of the cell culture environment as a key factor for the maintenance of the hepatocyte-like phenotype [61, 70, 71, 85]. Overall, the 3D culture systems tested clearly improved a liver specific phenotype, with biotransformation capacity of the resulting HLCs, with no major differences between the spheroid-based culture system and the hollow-fiber bioreactor. However, the subtle differences between phenotypic impacts promoted by each of the 3D models adopted are enough to entail that optimal culture systems should be selected depending on the scientific applications. Furthermore, our study supports the viability of the abundant and ethically safe hnMSCs (UCX®) to serve as precursors to achieve a mature HLC phenotype. Differentiated UCX® presented high and persistent levels of biotransformation activity in vitro that meet the pharmaceutical industry needs in terms of high-throughput drug screening.

5.6 Supplementary Material

Table 5.1 Albumin Production on the controls: undifferentiated cells (hnMSCS), HepG2 cell line, and primary hepatocytes, human (hpHep) and rat (rpHep) in 2D and in spheroids culture

Albumin Production (pg/10^6cells.h) Mean ± SD		
	2D	**3D (Spheroids)**
hnMSCs	35.47 ± 7.75	44.17 ± 9.63
HepG2	8472.47 ± 33.97	14807.09 ± 1125.66
rpHep	331.69 ± 13.32	469.56 ± 59.77
hpHep	26318.39 ± 4478.80	-

Table 5.2 Urea Production on the controls: undifferentiated cells (hnMSCS), HepG2 cell line, and primary hepatocytes, human (hpHep) and rat (rpHep) in 2D and in spheroids culture

Urea Production (μg/10^6cells.h) Mean ± SD		
	2D	**3D (Spheroids)**
hnMSCs	0.31 ± 0.11	1.20 ± 0.22
HepG2	13.97 ± 3.37	35.47 ± 2.83
rpHep	21.32 ± 10.06	71.47 ± 7.24
hpHep	57.96 ± 1,89	-

Chapter 6. The integrated assessment of nevirapine biotransformation unveils the biocompetence of a 3D in vitro model of human hepatocyte-like cells for liver function studies

The scientific content of the present chapter has been included in the following publication:

Cipriano M, Pinheiro PFP, Sequeira C, Santos JM, Oliveira NG, Marques MM, Castro M, Pereira AS, Miranda JP. The integrated assessment of nevirapine biotransformation unveils the biocompetence of a 3D in vitro model of human hepatocyte-like cells for liver function studies (submitted for publication)

6.1 Abstract

Three-dimensional (3D) cultures have been demonstrated to better mimic the in vivo hepatic tissues and maintain metabolic functions in primary hepatocyte and hepatocyte-like cell (HLC) cultures. Herein, we used NVP as a model drug for to assess the adequacy of human neonatal mesenchymal stem cell (hnMSC)-derived HLCs as a hepatic model for drug biotransformation studies. Nevirapine (NVP) is an antiretroviral drug with associated hepatotoxicity, partially related to its extensive hepatic metabolism and its auto-induction capacity. Studies on NVP bioactivation/toxicity are still needed and challenging, due to unclear reactivity of its metabolites and impaired detection of reliable biomarkers of toxicity. Since the toxic effects of NVP appear to be strongly associated with the generation of reactive metabolites that form covalent adducts with biomacromolecules, determining the cells' *thiolomic* profile could represent a relevant strategy for the early detection of electrophilic/oxidative stress. HLCs cultured as 3D self-assembled spheroids or as a monolayer were exposed to 300 μM of NVP for 3 and 10 days. Both 3D and 2D HLC cultures yielded all known phase I NVP metabolites, *i.e.*, 2-OH-NVP>12-OH-NVP>3-OH-NVP>8-OH-NVP. Induced ECOD and SULT1A1 activities and increased gene expression of *CYP3A4* and *CYP2D6* were also observed upon NVP exposure. In addition, 3D cultures presented upregulated *CYP2B6* (phase I), *UGT1A1*, *SULT1A1* and *GSTA1-A2* (phase II) and *MRP7* (phase III), which resulted in higher amounts of NVP phase I and II metabolites. Regarding the *thiolomic* profile analyses, in contrast to the 2D system, the HLC 3D model responded to NVP exposure at all evaluated levels, namely by showing an increased total free GSH amount in the supernatant and maintenance of the intercellular levels of its precursors, CYS and GLU-CYS. Moreover, regarding the glutathione oxidation status, only 3D-HLC presented an increased intracellular GSSG/GSH ratio. Our results demonstrate the adequacy of hnMSC-derived HLC 3D model as a metabolic competent system comprising phase I, II and III regulation at gene expression and enzymatic activity levels, namely presenting auto-induction of its own metabolism. These data highlight the relevance of human hepatocyte-like cells derived from stem cell as alternative in vitro models to study drug metabolism and unveil toxicity alerts associated with drug metabolism and bioactivation.

Keywords:

In vitro alternative models; Nevirapine biotransformation; Human mesenchymal stem cells; Hepatocyte-like cells; 3D culture

6.2 Introduction

Alternative in vitro hepatotoxicity studies have been explored due to the well-known drawbacks of primary hepatocytes and hepatic cell lines, such as availability and long-term metabolic stability, and metabolic competence, respectively [7]. Stem cells constitute a source of human cells which differentiation into hepatocytes has already been attempted. The differentiation of human induced pluripotent stem cells (hiPSC), human embryonic stem cells (hESC) and human mesenchymal stem cells (MSC) into hepatocyte-like cells (HLC) have been extensively reported [75], but none has been yet validated for routine hepatotoxicity testing.

3D cultures of primary hepatocytes have shown to display an enhanced phenotype than traditional monolayer cultures concerning cell biotransformation and functional ability over time in culture [61, 63, 64, 70, 71, 85, 91, 95, 98]. It allows higher cell-to-cell and cell-to-matrix contact, the presence of gradients of nutrients and oxygen and cell polarization. This is essential for hepatocyte functional specialization, which can be of enormous impact when studying drugs susceptibility in vitro [7]. Therefore, promising for an early assessment of molecules as therapeutic targets or detecting its potential toxic effects, with higher accuracy and decreased number of sacrificed animals. 3D cell cultures comprise cells adherent to a scaffold [76, 77], multicellular spheroids [61, 70, 71, 85], or more complex cellular systems such as hollow-fiber bioreactors [64, 173]. The last two conditions have been previously explored by our group for deriving HLC from human neonatal MSC [173]. In such work, the phenotype of hnMSC-derived HLC was improved by resorting to more physiologically relevant cell culture systems, namely, self-assembled spheroids formed in non-adhesive surfaces (ULA static system) and perfused hollow-fiber bioreactors (perfused system) [173]. Ultra-low attachment multi-well plate presents itself as a simpler non-adhesive surface format for multicellular spheroids formation. It is particularly advantageous for the optimization culture media supplementation or to test compounds' toxicological effects and has been used in smaller-scale cell culture systems, applied either to stem cell [88, 89] or hepatic cell lines [90].

Nevirapine (NVP) is a non-nucleoside reverse transcriptase inhibitor (NNRTI) approved by the US Food and Drug Administration and by the European Medicines Agency for the treatment of HIV type-1 infection, being the most prescribed NNRTI in the world, and the most prescribed antiretroviral in countries with limited economic resources [91]. NVP is mostly used in mother-to-child transmission HIV infection prophylaxis. It is also the most tolerated NNRTI though it presents skin and hepatic toxicity [344, 345], which conferred NVP a *black box warning* for hepatotoxicity that occurs in 6 % of patients within the first six weeks of treatment and can be

life threatening if resulting in fulminant liver failure [345]. NVP is extensively metabolized, being only 2.7 % of NVP excreted in urine in human as parent compound [346]. Its half-life is reduced from 45 h after first dose to 30 h after two weeks of dosing [347], corresponding to the NVP auto-induction period. NVP is biotransformed by phase I and II enzymes, whereas both NVP and its metabolites can regulate their own metabolism. Indeed, NVP induces CYP2B6 and CYP3A4 [348], whereas 2-OH-NVP induces SULT1A1 [91]. NVP phase I metabolites 2-OH-NVP, 12-OH-NVP, 3-OH-NVP and 8-OH-NVP present increasing plasma concentrations during the first 4 weeks of treatment [349], but may also suffer secondary oxidation, such as the conversion of 12-OH-NVP into 4-COOH-NVP that is only detected in plasma after 1 month of treatment [349]. On the other hand, 12-OH-NVP may suffer glucuronidation or sulfonation. 12-sulfoxy-NVP is a more reactive product able to form adducts with proteins and DNA with consequent toxic effects [350, 351] that may be detoxified trough glutathione conjugation, namely by GSTA1-1, GSTM1-1 and GSTA3-1 [352]. Due to its bioactivation, detoxification and toxicity mechanisms, NVP in vitro studies require a functional cellular model, namely regarding phase I, II and III enzymes activity. Therefore, NVP has shown to be a relevant tool for the evaluation of in vitro cellular models of biotransformation particularly when resorting to physiologically relevant cell culture systems as the 3D spheroids [91, 348]. As such, the aim of this study was to evaluate hnMSC-derived HLCs cultured in 2D and 3D as a human based-alternative in vitro tool for toxicology studies. The formation of NVP metabolites over long-term culture was analysed together with its effect on gene expression and activity of phase I, II and hepatic transporters, NVP metabolite quantification and on cell *thiolomic* profile.

6.3 Material and Methods

6.3.1 Reagents

Trypsin-EDTA, fetal bovine serum (FBS) and insulin-transferrin-selenium solution (ITS) were purchased from Gibco®/Life Technologies (Madrid, Spain). Penicillin-Streptomycin-Amphotericin B (P/S/A), non-essential amino acids supplement (NEAA) and sodium pyruvate (NaP) were obtained from Lonza (Basel, Switzerland) and 7-ethoxycoumarin from Alfa Aesar (Karlsruhe, Germany). Hepatocyte growth factor (HGF), fibroblast growth factors (FGF-2 and FGF-4) and oncostatin-M (OSM) were purchased from Peprotech (Rocky Hill, NJ, USA). Iscove's modified Dulbecco's medium (IMDM), alpha modified Eagle's minimum essential medium (α-MEM), epidermal growth factor (EGF), dexamethasone, dimethyl sulfoxide (DMSO), nicotinamide, 5-azacytidine (5-AZA), trypan blue, Hank’s balanced salt solution

(HBSS), 4-methylumbelliferone (4-MU), β-glucuronidase/arylsulfatase and reagents used for SULT1A1 activity and *thiolomic* profile determination were acquired from Sigma-Aldrich (Madrid, Spain). Nevirapine (NVP) was a gift from Dr. F. A. Beland (National Center for Toxicological Research, Jefferson, AR, USA). NVP stock solution was prepared in tissue culture grade DMSO at a concentration of 150 mM. Finally, high-performance liquid chromatography (HPLC)-grade solvents that were used in the extraction and mobile phases of the chromatography experiments were purchased from VWR (Leuven, Belgium).

6.3.2 Cell culture

hnMSC (UCX®) were isolated and fully characterized as described previously [257, 259] and expanded as undifferentiated cells in α-MEM supplemented with 10 % of FBS. HepG2 cell line was cultured as described in **Chapter 3**. A three-step differentiation protocol was used for generating HLCs as described in **Chapter 5**. Briefly, hnMSC were seeded at a density of 1.5 x 10^5 cells/cm^2 in a rat-tail collagen coated surface, used at a concentration of 0.2 mg/mL. At day 17 of differentiation, cells were trypsinized and reinoculated in differentiation medium (IMDM containing 8 ng/mL of OSM, 1 μM of dexamethasone, 1 % of DMSO and 1 % ITS) containing 20 μM of 5-azacytidine (5-AZA) and 5 % of FBS into (i) ultra-low attachment plates (2.5x10^4 cells/mL) to obtain a 3D spheroid culture or (ii) 2D culture plates pre-coated with collagen (2 x 10^4 cells/cm^2) as control. Cells were maintained for 24h and then the medium was replaced by third step differentiation medium. Medium replacement occurred every 3 days.

At day 24 of the differentiation cells were incubated with 300 μM of Nevirapine [91, 98] and exposed for 3 and 10 days. HepG2 and hnMSC were treated for 72h. DMSO concentration was 1 % DMSO (v/v) in both NVP-treated cells and non-treated cells since this is the DMSO concentration used in the differentiation media.

Cell culture was monitored microscopically using phase contrast microscopy (Olympus CK30 inverted microscope). Images were acquired using Moticam 5.0 (Motic) and recorded with Motic Images Plus 2.0 software. The spheroid diameter was evaluated every 3 days according to **Chapter 4.**

6.3.3 Biotransformation activity

CYP enzyme activity was measured by means of 7-ethoxycoumarin-*O*-deethylase (ECOD) activity and P450-GloTM assays (Promega, Madison, WI, USA) and UGTs activity by means of 4-MU conjugation as described in **Chapter 3.**

The thermostable SULT1A1 activity was assessed in cell homogenates from both 2D and 3D cultures. Cell homogenates were obtained by sonication of cell pellets, containing ~0.07 x 10^6 cells, suspended in 200 μL of sonication buffer (10 mM triethanolamine at pH 7.4 with 0.25 M sucrose and 5 mM β-mercaptoethanol). Sonication procedures were performed on ice. SULT1A1 activity was assessed using the 2-naphthol sulfonation assay in cell homogenates as previously described [91]. A reaction mixture containing 50 mM phosphate buffer (pH 7.5), 5 mM $MgCl_2$, 0.5 mM EDTA, 20 μM of adenosine 3′-phosphate 5′-phosphosulfate (PAPS), 5 mM of potassium *p*-nitrophenol sulfate (KNPS) and 100 μM of 2-Nafthol (2-NAF) 5 mM 4-nitrophenyl sulfate. An effective PAPS-regenerating system results from the the addition of *p*-nitrophenyl sulfate. SULT1A1 catalyzes the synthesis of 2-naphthylsulfate from 2-NAF and PAPS, producing *p*-nitrophenol. The measurement of *p*-nitrophenol absorbance at 405 nm is therefore an indirect measure of sulfotransferase activity. A calibration curve was built with *p*-nitrophenol and absorbance registered at 405 nm (SPECTROstar Omega, BMG Labtech) after 5 hours incubation at 37 ºC in a humidified atmosphere.

The ECOD, CYP3A4/5, UGTs and SULT1A1 activities were normalized to incubation time and cell number as described in **Chapter 3**. Data is expressed as fold induction of NVP treated cultures relative to non-treated cultures.

6.3.4 Gene expression

RNA isolation was performed using Trizol® (Life Technologies, Madrid, Spain). RNA was quantified prior to cDNA synthesis as previously described [173, 353]. cDNA synthesis was performed from 0.5 μg of RNA using a commercially available kit (NZYTech, Lisbon, Portugal) and quantitative real-time PCR (qPCR) performed using PowerUp™ SYBR® Green Master Mix (Applied Biosystems, Thermo Fisher Scientific, USA), according to the manufacturer's instructions. A final reaction volume of 15 μL, with 1 μL of template cDNA and 0.1 μM of forward and reverse primers (**Table 6.1**) was used and the reaction was performed in the Real-time PCR system (ABI7300; Applied Biosystems®/ Life Technologies, Madrid, Spain). The amplification of cDNA consisted on a denaturation step at 95 °C for 10 minutes, 40 cycles of denaturation at 95 °C for 15 seconds, annealing at 60 °C for 1 minute and extension at 72 °C for 30 seconds. As a quality and specificity measure, a dissociation stage was added to determine the melting temperature in all runs. The comparative Ct method ($2^{-\Delta\Delta CT}$) was used to quantify the amount of target genes, normalized to a reference gene *BACTIN* and relative to NVP non-treated cells unless otherwise stated. The efficiency of each PCR reaction was

estimated from a serially diluted cDNA from HepG2 non-treated cells in order to construct a standard curve (1, 10^{-1}, 10^{-2}) for each gene, considering efficiencies between 1.8-2.2.

Table 6.1 Primers used for qRT-PCR characterization of differentiated HLCs, undifferentiated hnMSCs and HepG2 cell line

	Primers	Melting temperature (Tm)	Reference
***BACTN*_F**	CATGTACGTTGCTATCCAGGC	87,6	PrimerBank ID 4501885a1[354]
***BACTN*_R**	CTCCTTAATGTCACGCACGAT		
***CYP3A4*_F**	ATTCAGCAAGAAGAACAAGGACA	81.84	[267]
***CYP3A4*_R**	TGGTGTTCTCAGGCACAGAT		
***CYP2B6*_F**	TTCCTACTGCTTCCGTCTATCAAA	79.7	[355]
***CYP2B6*_R**	GTGCAGAATCCCACAGCTCA		
***CYP2D6*_F**	TGGCAAGGTCCTACGCTTC	86.3	[355]
***CYP2D6*_R**	GCCACCACTATGCACAGGTT		
***SULT1A1*_F**	CGGCACTACCTGGGTAAGC	81.9	PrimerBank ID: 29540539a1[354]
***SULT1A1*_R**	CACCCGCATGAAGATGGGAG		
***UGT1A1*_F**	TGACGCCTCGTTGTACATCAG	78.8	[355]
***UGT1A1*_R**	CCTCCCTTTGGAATGGCAC		
***GSTA1-A2*_F**	TGCAACAATTAAGTGCTTTACCTAAGTG	74	[355]
***GSTA1-A2*_R**	TTAACTAAGTGGGTGAATAGGAGTTGTATT		
***MRP7*_F**	TGGCACATTCCCCTCATGG	82.2	[355]
***MRP7*_R**	CCACAACACGGTCAGCACTA		

6.3.5 Quantification of nevirapine metabolites

Supernatants from 3D and 2D cell cultures were collected (triplicates) on days 27 and 34 of the differentiation, and treated separately. For the quantification of phase I and phase II NVP metabolites, 15 mL of cell culture supernatants were incubated for 24 hours at 37 °C in the absence (free metabolites) or presence of sulfatase (type H-1 from *Helix pomatia*, E.C. 3.1.6.1, 100 U/mL) and saccharic acid 1,4-lactone (4 mg/mL) for the detection of free metabolites plus sulfate conjugates [356] or β-glucuronidase (type VII-A from *E.coli*, E.C. 3.2.1.31, 100 U/mL) for the detection of free metabolites plus glucuronic acid conjugates [357]. The pH of all samples was readjusted to 7.0 before the double extraction with dichloromethane (2 x 15 mL). The residues obtained from the organic extracts, upon evaporation, were

dissolved in 150 μL of H_2O/MeOH (1/1) and analyzed on an Agilent 1100 Series HPLC-UV system (Agilent Technologies Inc.) as detailed in Marinho *et al.* [358]. The metabolite levels were normalized with the cell numbers and expressed as ng/10^6 cells.

6.3.6 Determination of the *thiolomic* profile

For the determination of the thiolomic profile of the cultures, both cells (intracellular fraction) and cell supernatants (extracellular fraction) were collected from 3D and 2D cultures in the absence or presence of NVP.

The extracellular thiolomic profile studied herein included glutathione and its catabolism product cysteinylglycine (CYS-GLY) in their total non-protein-bound (free) forms, designated as low molecular weight thiols (LMWT). The intracellular thiolomic profile study included glutathione and its precursors cysteine (CYS) and glutamylcysteine (GLU-CYS). These three moieties were analyzed in their S-thiolated protein (RSSP) forms [S-glutathionylated (GSSP), S-cysteinylated (CysSSP), and S- glutamylcysteinylated (GluCysSSP) proteins, respectively] and in their LMWT forms. The latter were composed by the reduced (RSH) fractions, including the reduced glutathione (GSH), CysSH and GlyCysSH, and the respective oxidized disulfides (RSSR).

Cell culture supernatants (extracellular fraction) and cell lysates (intracellular fraction) were collected at days 27 and 34 of the differentiation and treated as described below. The thiolomic profile was measured as detailed previously [359]. Briefly, the cells were collected and immediately sonicated in 200 μL of ice-cold phosphate-buffered saline with 1 % Triton. The amount of total thiols (RSSP+RSH+RSSR) was obtained by reducing the sulphydryl groups with tris(2-carboxyethyl)phosphine hydrochloride (TCEP) (100 g/L). After a 30 min incubation at room temperature, the samples were treated with trichloroacetic acid (TCA; 100 g/L) containing EDTA (1 mM), for protein precipitation. After centrifugation (13000 x g, 10 min, 4°C), the supernatant was collected for derivatization of the free sulphydryl groups. Derivatization was performed with 7-fluorobenzo-2-oxa-1,3-diazole-4-sulfonic acid ammonium salt (SBD-F) at 1 g/L in buffer, 125 mM sodium tetraborate, 4 mM EDTA and 1.55 M NaOH) at 60 ºC for 1 h, protected from light. Finally, a volume of 30 μL was analyzed by HLPC.

The quantification of the free forms was performed in cells and in cell culture supernatants. The latter were collected on ice and centrifuged for 5 min at 10000 x g at 4º C for cell debris removal, whereas cell samples were prepared as mentioned above. Samples were then submitted to protein precipitation with TCA, with subsequent centrifugation (13000 x g, 10 min, at 4ºC) [360] and reduced with TCEP for R LMWT quantification or incubated with reverse

osmosis water to obtain the naturally reduced RSH fraction. After 30 min incubation at room temperature, the previously described derivatization protocol was followed. HPLC analysis was performed on a Shimadzu LC-10AD VP system (Shimadzu Scientific Instruments Inc) using a reversed-phase C18 LiChroCART 250-4 column (LiChrospher 100 RP-18, 5 μm, VWR, USA), at 29 ºC with a fluorescence detector (λEx: 385 nm/ λEm: 515 nm). The mobile phase consisted of 100 mM ammonium acetate buffer (pH 4.5) and methanol [98:2 (v/v)]. The analytes were separated in isocratic elution mode for 22 min, at a flow rate of 0.6 mL/min.

The data, expressed as average ± SD, was normalized with cell number and was represented as nmol/106 cells for non-treated cells and as fold induction in NVP-treated cultures relative to non-treated cultures.

6.3.7 Statistical analysis

Statistical data analysis was performed using GraphPad Prism version 6.0 (GraphPad Software, La Jolla, CA, USA). The data were compared by the two-way ANOVA with Holm-Sidak method, with differences considered statistically significant for $p < 0.05$.

6.4 Results

6.4.1 NVP modulates key biotransformation enzymes in 2D and 3D cultures

NVP metabolism comprises phase I, II and III enzyme players. It is primarily metabolized into its phase I metabolites 2-OH-NVP, by CYP3A4/5, 12-OH-NVP by CYP3A4/5, CYP2D6 and CYP2C9, 3-OH-NVP by CYP2B6 and 8-OH-NVP by CYP3A4/5, CYP2B6 and CYP2D6 [91, 348]. These may undergo further phase II biotransformation through glucuronic acid conjugation or sulfate conjugations [91], the later involved in NVP bioactivation. Within NVP bioactivation the quinone methide from NVP, 12-OH-NVP and 12-sulfoxy-NVP are particularly reactive being associated to NVP-induced hepatotoxicity. Thus, to evaluate the biotransformation competence of this in vitro model the gene expression levels of *CYP3A4*, *CYP2B6*, *CYP2D6*, *UGT1A1*, *SULT1A1*, *GSTA1-A2* and *MRP7* (**Figure 6.1**) were assessed. The same genes were evaluated in undifferentiated cells (hnMSC) and in HepG2 cell line cultured as monolayer exposed to NVP for 3 days. ECOD, CYP3A4/5, UGTs and SULT1A1 activities as well as the formation of NVP phase I (2-OH-NVP, 3-OH-NVP, 8-OH-NVP and 12-OH-NVP) and II (respective sulfate and glucuronic acid conjugates) metabolites were also studied upon NVP treatment for 3 (D27) and 10 (D34) days in both 3D (3D-HLC) and

monolayer HLC (2D-HLC) cultures (**Figure 6.2**). NVP non-treated cells and hnMSCs were used as controls. Results are summarized in **Table 6.2**.

Upon NVP treatment the total cell number remained similar to non-treated cultures during the whole culture time, indicating no cell loss due to possible cytotoxic effect of NVP or its metabolites in HLC, HepG2 and hnMSC cultures (data not shown).

Gene expression analysis showed that all evaluated genes were more upregulated by NVP in 3D HLC than in 2D HLCs or HepG2 (**Figure 6.1a, 6.1b** and **6.1c**). Remarkably, when exposed to NVP all the studied genes were also upregulated in 3D-HLC relative to 2D-HLCs (**Figure 6.1d**). This difference was further increased from day 27 to day 34, except for *CYP3A4*, *CYP2D6* and *GSTA1-A2* (**Figure 6.1d**).

Accordingly, CYP3A4/5 activity was induced 5-fold and 1.5-fold, at D27, in 3D- and 2D-HLC cultures, respectively (**Figure 6.2**); whereas after 10 days of NVP exposure (D34) both 3D- and 2D-HLC cultures showed ~1.5-fold induction of CYP3A4/5 activity relative to non-treated cultures (**Figure 6.2**). CYP3A4 participates in 2-OH-NVP, 12-OH-NVP and 8-OH-NVP formation. However, it is particularly relevant for 2-OH-NVP production, given that CYP3A4/5 is the only CYP450 enzyme known to be involved on its formation. The conversion of NVP into 2-OH-NVP (total fraction) was decreased in both 2D and 3D cultures from day 27 to day 34. In contrast, in both systems 12-OH-NVP was enhanced or maintained from D27 to D34. 12-OH-NVP is associated to CYP3A4/5 but also CYP2D6, whose expression at the gene level was slightly increased upon NVP treatment.

Finally, 8-OH-NVP metabolite was barely detected within our model. 8-OH-NVP is also produced via CYP2B6 and its detection increased only in 3D-HLCs from day 27 to day 34. Herein, ECOD, which reflects CYP2B6, 1A1 and 1A2 activities, was induced 1.3-fold and 3.7-fold on 3D-HLC after 3 and 10 days of treatment with NVP in comparison with non-treated cultures, respectively; whereas in monolayer its induction was only observed after 3 days treatment (2.5-fold) (**Figure 6.2**). CYP2B6 is also involved in 3-OH-NVP metabolism and, in fact, in 3D cultures, a ~2-fold induction from D27 (~35 ng/10^6 cells) to D34 (~76 ng/10^6 cells) was observed. In 2D cultures, the amount of 3-OH-NVP (~10 ng/10^6 cells) was unaltered throughout culture time (**Figure 6.3**). Some NVP biotransformation activity was also displayed by hnMSC (**Figure 6.3a**). However, in accordance to phase I and II activities measurements (**Figure 6.2**) the level of NVP metabolites is also low (**Figure 6.3a**).

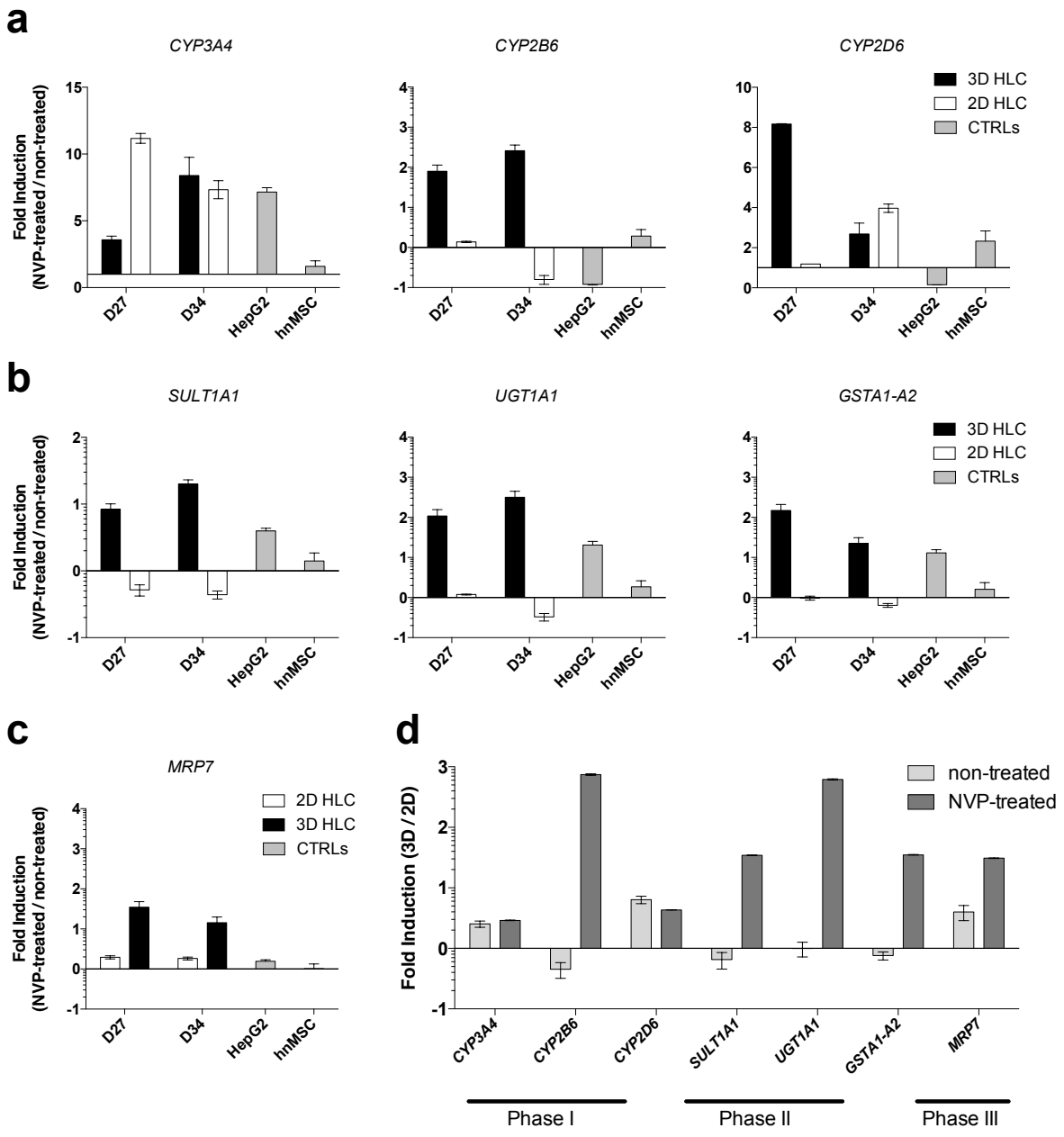

Figure 6.1 Gene expression analyses of 3D- and 2D-HLCs after 3 (day 27) and 10 days (day 34) of NVP treatment. (a) Gene expression of phase I enzymes comprising *CYP3A4*, *CYP2B6* and *CYP2D6* in NVP-treated cells relative to non-treated cells. (b) Gene expression of phase II enzymes comprising *SULT1A1*, *UGT1A1* and *GSTA1-A2* in NVP-treated cells relative to non-treated cells. (c) Gene expression of the MRP7 transporter in NVP-treated cells relative to non-treated cells. (d) Combined phase I, II and III gene expression in 3D-HLCs relative to 2D-HLCs in NVP-treated and non-treated cells at day 34. Data for HepG2 cells and hnMSC exposed to NVP for 3 days and used as positive and negative controls, respectively, are also shown (a, b and c). The data (AVG ± SD, n=3) is normalized to the reference gene *BACTIN* and expressed as the Log_{10} of the ratios, except for *CYP3A4* and *CYP2D6.*

Phase II biotransformation enzyme activity and transcript levels within 3D and 2D-HLC incubated with NVP were also monitored. Upon exposure to NVP, and in comparison to non-treated cultures, *UGT1A1*, *SULT1A1* and *GSTA1-A2* overexpression was only observed in 3D-HLC (**Figure 6.1**), being *UGT1A1* and *SULT1A1* expression higher at D34. Accordingly, at D34 both UGT ($p < 0.05$) and SULT1A1 activities were increased in 3D-HLC, whereas in 2D-HLC only SULT1A1 was enhanced (**Figure 6.2**). In non-treated HLCs, UGT [173] and SULT1A1 (data not shown) activities are maintained in 2D-HLC and increase in 3D-HLC from D27 to D34 ($p < 0.01$).

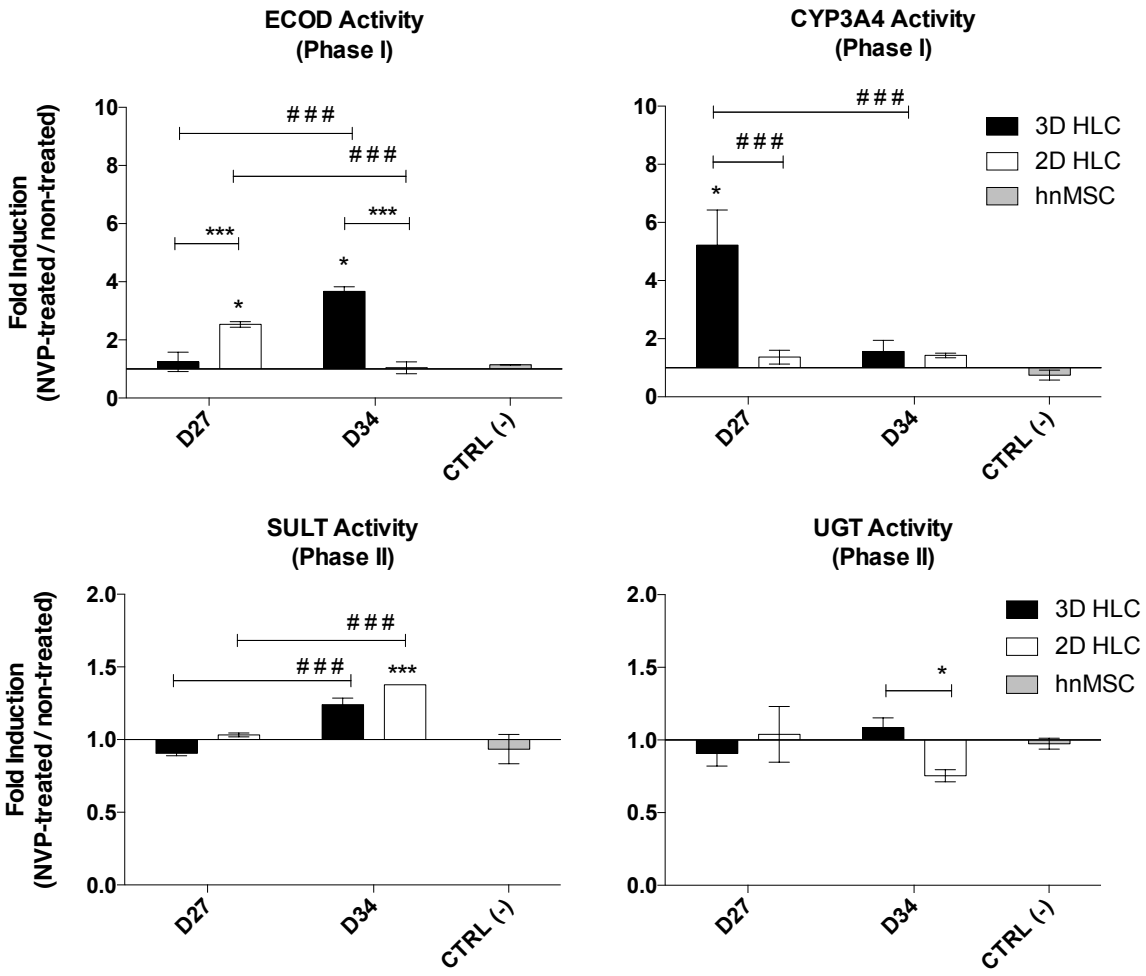

Figure 6.2. Enzymatic induction in 3D- and 2D-HLCs after 3 (day 27) and 10 days (day 34) of NVP treatment. The data for hnMSC, cultured in monolayer and exposed to NVP for 3 days, are presented as negative control. * $p < 0.05$, ** $p < 0.01$ and *** $p < 0.001$ relative to 2D-HLCs or relative to non-treated cells according to the scheme, # $p < 0.05$ and ### $p < 0.001$ relative to day 27 of culture. The data (AVG ± SD, n=3) is represented as fold induction in NVP-treated cells relative to control cells.

When measuring phase II metabolites it was observed that 2-OH-NVP and 12-OH-NVP sulfonation decreased over the time in both cultures, being absent in 2D-HLCs at D34. In

contrast, the amount of 3-OH-NVP sulfate conjugates was increased at day 34 in both cultures and ~8-fold higher in 3D relative to 2D cultures. 3-OH-NVP was the metabolite showing higher sulfate conjugation, representing 95 % and 60 % of the total 3-OH-NVP detected in 3D- and 2D-HLCs, respectively.

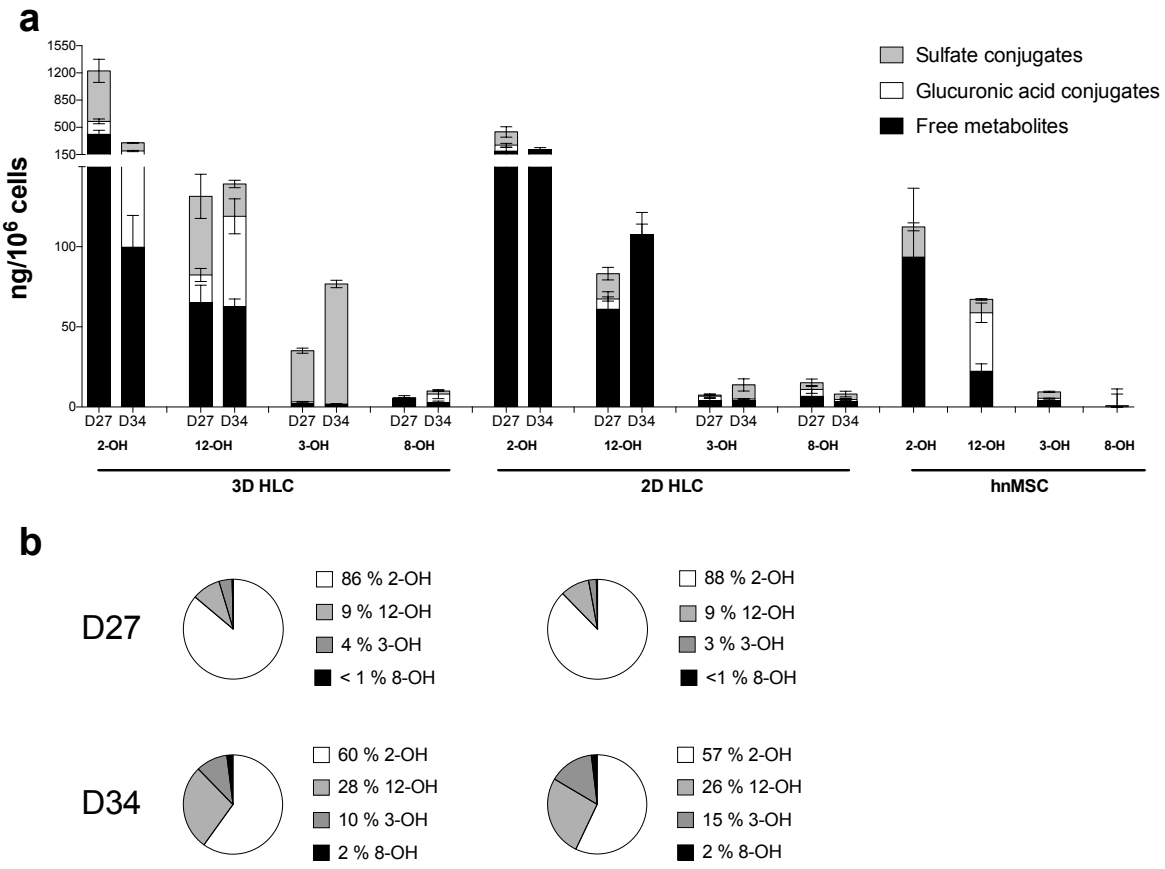

Figure 6.3 Levels of NVP phase I and II metabolites in 3D- and 2D-HLCs after 3 (day 27) and 10 days (day 34) of NVP treatment. (a) Quantification of phase I and II NVP metabolites in HLCs and in hnMSC, cultured in monolayer and exposed to NVP for 3 days and (b) relative proportions of total NVP metabolites (free metabolites + sulfate conjugates + glucuronic acid conjugates) at days 27 and 34. The data (AVG ± SD, n=3) is normalized to total cell number.

Glucuronic acid conjugates were mainly detected in 3D cultures as well. Most glucuronic acid conjugated metabolites are 2-OH-NVP and 12-OH-NVP, but also 8-OH-NVP, and all increased from day 27 to day 34 in 3D-HLC. In fact, in 3D cultures the amount of 12-OH-NVP and 2-OH-NVP conjugates increased from ~13 % (D27) to ~40 % (D34) and to ~32 % (D34), respectively. Conversely, in 2D-HLCs the level of 12-OH-NVP and 2-OH-NVP conjugates decreased from ~8 % and ~17 % to undetected, respectively, which is in accordance with both UGT1A1 expression and UGTs activity. Overall, NVP induced gene expression and the activity of the enzymes responsible for its own metabolism, particularly in 3D culture conditions

(**Table 6.2**). Most importantly, such increase was further observed when increasing NVP treatment time, covering the induction period of NVP.

6.4.2 3D cultures *thiolomic* profile is altered upon NVP exposure

To test how NVP altered the *thiolomic* profile of HLCs, thiols quantification was primarily performed in NVP non-treated 3D and 2D-HLC cultures (**Figure 6.4**), followed by its quantification in treated cells (**Figure 6.5** and **Figure 6.6**).

Firstly, the total CYS, GLU-CYS and GSH intracellular content was compared in NVP non-treated cultures. CYS is the first substrate for GSH formation and GLU-CYS, an intermediate element of GSH formation. CYS was detected in higher amounts in 3D-HLCs than 2D-HLCs at day 27 ($p < 0.01$) and similar in both cultures at day 34. GLU-CYS amounts were higher in 3D-HLC relative to 2D-HLC, being both higher than in hnMSC (data not shown). In addition, GSH was increased from day 27 to day 34, although only significantly in 3D-HLCs ($p < 0.05$) (**Figure 6.4a, Table 6.2**).

The same approach was performed in extracellular fractions. Herein, CYS-GLY and GSH were evaluated on its free form. CYS-GLY is a product of GSH degradation by the action of γGT membrane enzyme. CYS-GLY and GSH amount were statistically higher in HLCs relative to hnMSC at days 27 and 34 ($p < 0.01$, data not shown). Moreover, at day 27 both CYS-GLY and GSH levels were higher in 2D-HLC than in 3D-HLC ($p < 0.05$), which was inverted at day 34 (**Figure 6.4a**). The free low molecular (R LMWT) and protein bond (RSSP) fractions of the evaluated thiols was similar in both cultures at day 27. However, the fraction of GSSP is significantly higher in 3D-HLC than in 2D HLC ($p < 0.01$) (**Figure 6.4b**).

The *thiolomic* profile was then accessed upon NVP treatment. The intracellular *thiolomic* profile remained unchanged in 2D-HLCs, whilst a significant decrease on GLU-CYS and GSH was observed in 3D-HLC ($p < 0.01$) after 10 days of NVP treatment (**Figure 6.5a** and **Table 6.2**). On the other hand, extracellular thiol levels increased similarly from D27 to D34 in both 3D and 2D-HLCs (**Figure 6.5a**) ($p < 0.05$). As for the free low molecular and protein bond fractions differences between 2D and 3D-HLCs were only observed at 34. Herein, we observed an increase of intracellular protein-S-cysteinylation in 3D-HLC and an increase of intracellular free CYS and GLU-CYS in 2D-HLC ($p < 0.001$) (**Figure 6.5b**). Moreover, S-glutathionylation of proteins and the amounts of free GSH were particularly decreased in 3D-HLCs ($p < 0.001$) (**Figure 6.5b**) indicating that its oxidized fraction (GSSG) is increased. In fact, a higher GSSG/GSH ratio ($p < 0.05$) (**Figure 6.6 and Table 6.2**) was observed in 3D-HLCs suggesting increased oxidative/electrophilic stress in 3D-HLC upon NVP exposure.

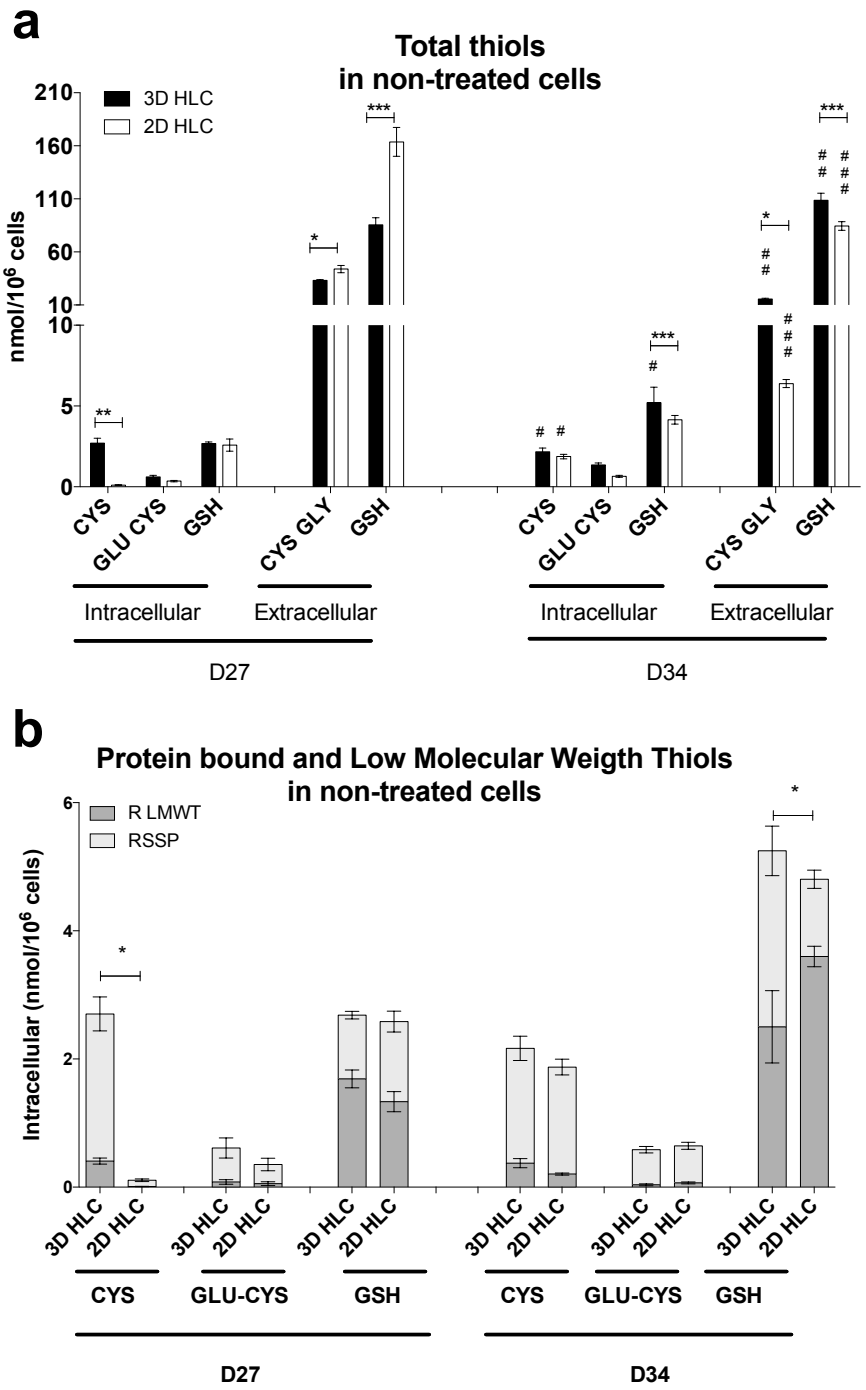

Figure 6.4. Intracellular and extracellular *thiolomic* profile in non-NVP-treated 3D- and 2D-HLCs at day 27 and day 34. (a) Intracellular levels of total CYS, GLU-CYS and GSH and extracellular levels of total CYS-GLY and GSH. (b) Intracellular levels of protein-bound (RSSP) and free low molecular weight (R LMWT) CYS, GLU-CYS and GSH. * $p < 0.05$, ** $p < 0.01$ and *** $p < 0.001$ relative to 2D-HLCs; # $p < 0.05$, ## $p < 0.01$ and ### $p < 0.001$ relative to day 27 of culture. The data is represented as AVG ± SD, n=3

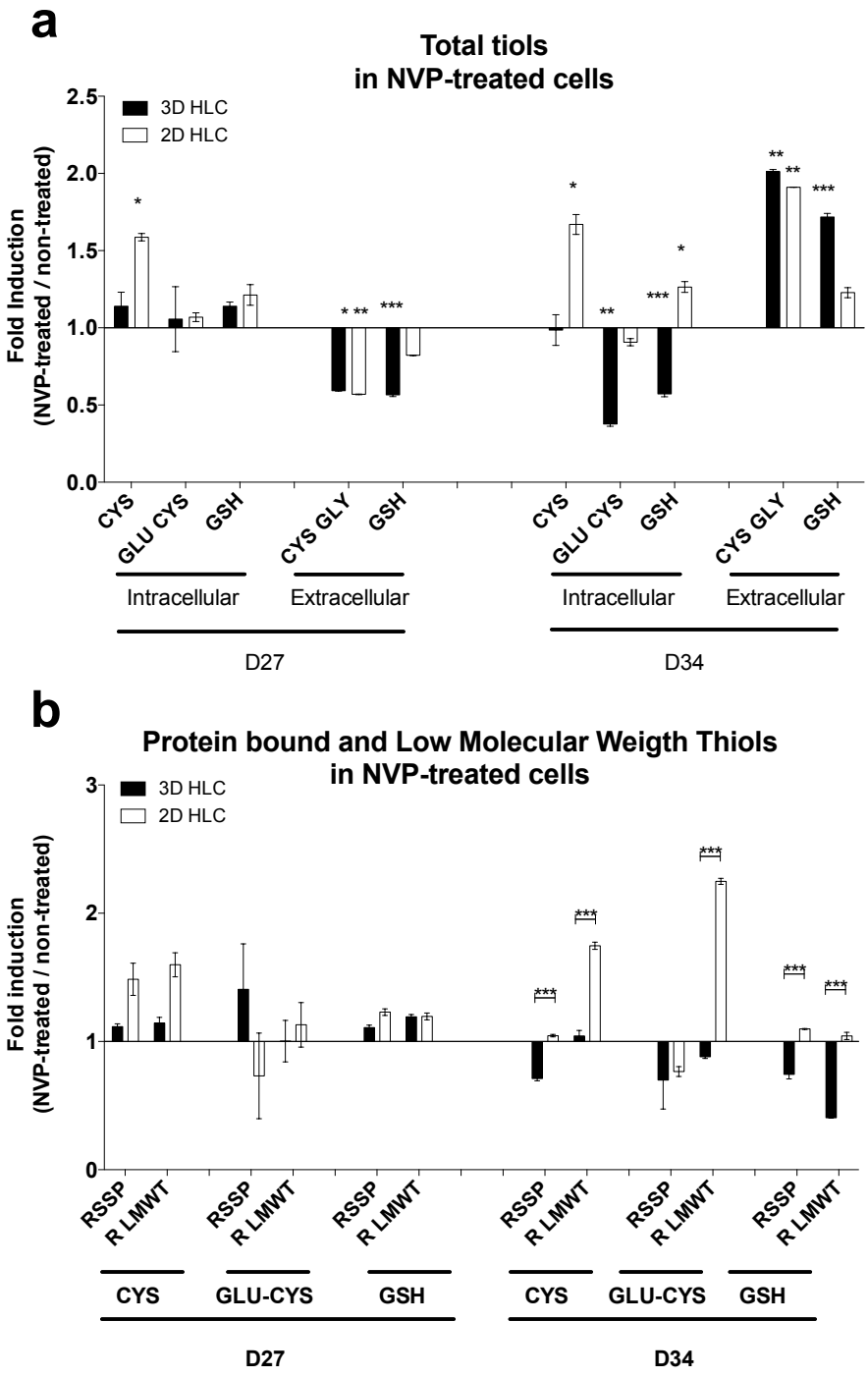

Figure 6.5. Intracellular and extracellular *thiolomic* profile in 3D- and 2D-HLCs after 3 (day 27) and 10 (day 34) days of NVP treatment. (a) NVP effect on intracellular levels of total CYS, GLU-CYS and GSH and on extracellular levels of total CYS-GLY and GSH. (b) NVP effect on intracellular levels of protein-bound (RSSP) and free low molecular weight (R LMWT) CYS, GLU-CYS and GSH measured at days 27 and 34 of the differentiation (3 and 10 days of exposure, respectively). * $p < 0.05$, ** $p < 0.01$ and *** $p < 0.001$ relative to non-treated cells (a) and to 2D-HLCs (b). The data is represented as AVG ± SD, n=3.

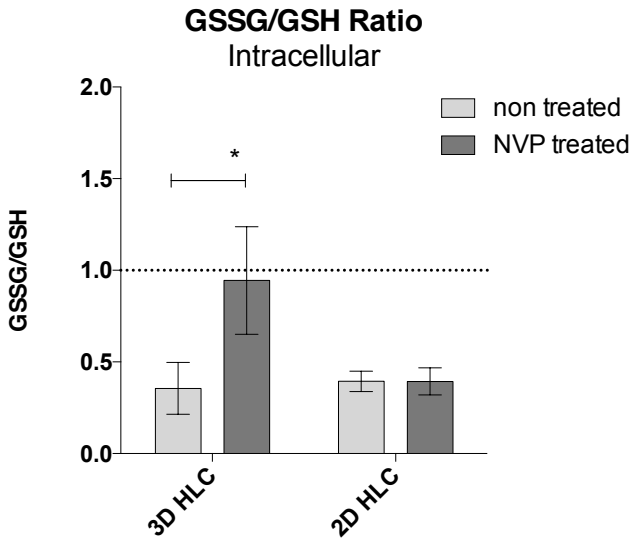

Figure 6.6 NVP effect on glutathione oxidation (intracellular GSSG/GSH ratio) in 3D- and 2D-HLCs after 10 days of NVP treatment (day 34). * $p < 0.05$ relative to non-treated cells. The data is represented as AVG ± SD, n=3.

Table 6.2 Comparative summary of 3D- and 2D-HLC metabolic capacity upon 10 days of NVP treatment (day 34)

	Endpoint[a]		3D-HLC (NVP treated / non-treated)	2D-HLC (NVP treated / non-treated)	3D-HLC / 2-HLC (NVP treated)
Gene expression	Phase I	***CYP3A4***	+	+	+
		CYP2B6	+++	unchanged	+++
		CYP2D6	+	+	+
	Phase II	***SULT1A1***	+	unchanged	++
		UGT1A1	+	unchanged	+++
		GSTA1-A2	+	unchanged	++
	Phase III	***MRP7***	+	unchanged	++
Enzymatic activity	Phase I	**ECOD (CYP2B6)**	++	unchanged	+
		CYP3A4	unchanged	unchanged	unchanged
	Phase II	**UGTs**	unchanged	unchanged	+
		SULT1A1	unchanged	unchanged	unchanged
NVP metabolites	Phase I	**2-OH-NVP** *(CYP3A4)*	detected	detected	+
		12-OH-NVP (*CYP3A4/2D6/2C9)*	detected	detected	+
		3-OH-NVP *(CYP2B6)*	detected	detected	++
		8-OH-NVP ***(****CYP3A4/2D6/2C9)*	detected	detected	unchanged
	Phase II	**Sulfate conjugates**	detected	detected	++
		Glucuronic acid conjugates	detected	not detected	+++
Glutathione content		**extracellular GSH**	+	unchanged	-
		intracellular GSH	-	+	+
		GSSG	+	unchanged	+

[a]Gene expression: (+) 1-20 fold increase, (++) 20-250 fold increase, (+++) >250-fold increase;

Enzymatic activity, NVP metabolites and glutathione content: (-) <1-fold decrease; (+) 1-4-fold increase; (++) 4-10fold increase; (+++) >10-fold increase.

[b] detected/not detected: production of nevirapine metabolites in nevirapine-treated cultures

6.5 Discussion

The effect of NVP on CYP450 activity was previously shown in microsomal preparations [348] and on an ex vivo placenta pharmacokinetic model [361]. However, a complete study of biotransformation mechanisms of NVP and its metabolites, including induction of enzymatic activity of phase I and II metabolites has only been achieved recently, when resorting to an in vitro 3D hepatocyte culture [91, 98]. Pinheiro *et al.* study [91] integrated information about NVP phase I and II biotransformation, regulation of biotransformation enzymes by the parent drug and its metabolites and detoxification and bioactivation/toxicity pathways of reactive metabolites was provided, further enabling a thorough in vitro study of xenobiotics bioactivation and the identification of NVP specific biomarkers [91, 98]. The modulation of SULT1A1 activity by NVP and 2-OH-NVP was also observed, in first hand, pointing out to a synergistic effect of the parent drug and its main phenolic metabolite as a key factor in the formation of the toxic NVP metabolite [91, 98]. In the present study, due to its complex metabolic profile, NVP was selected as a model drug to substantiate the applicability of our HLC-based 3D culture system as an in vitro toxicology model. Herein, the NVP effects on gene expression and enzymatic activity resulted in its bioactivation by our system along with the production of all the known NVP metabolites (phase I and II). In addition, an effect on HLCs' *thiolomic* profile was also shown.

The information available on the literature on the steady state relative proportions of nevirapine metabolites differ greatly. It further depends on the type of study, *i.e.*, in vivo animal studies, in vitro studies or clinical trials (**Table 6.3**).

As shown in **Table 6.3** clinical studies report that 2-OH-NVP and 12-OH-NVP are the major NVP metabolites whereas 3-OH-NVP relative amounts vary in the literature. The decrease of 2-OH-NVP and increase of 12-NVP-OH from single dose to steady state is also reported in clinical studies [362], indicating that our data might refer to the NVP induction period, that lasts about two weeks in vivo [349]. Our data showed that even though there were an increase of 12-OH-NVP of 3-fold from day 27 to day 34, 2-OH-NVP was always the major metabolite, in both cell culture systems (60 % and 57 % for 3D- and 2D-HLCs at day 34, respectively), followed by 12-OH-NVP (28 % and 26 % for 3D- and 2D-HLCs, respectively). Erickson et al. [348] also showed that the formation rate of 2-OH-NVP is ~2-fold higher than of 12-OH-NVP by human CYP3A4/5 microsomal preparations [348].

3-OH-NVP turned to be the third most abundant metabolite at day 34 (10 % and 15 % for 3D- and 2D-HLCs, respectively), followed by 8-OH-NVP with a proportion of less than 2 % for all conditions. 8-OH is consensually a minor metabolite only detected in samples derived from

human systems such as human plasma [349, 363], human urine [346], human microsomal preparations [348] and is not detected after single dose [362]. Herein, it increased from day 27 to day 34 only in 3D-HLC reflecting the high CYP2B6 activity and its induction in HLCs, and the clinical studies observations, as a result of NVP auto-induction of CYP2B6 activity.

Table 6.3 Comparison of relative levels (expressed as percentage) of NVP metabolites in clinical, pre-clinical and *in* vitro studies.

Study type	Sample	2-OH-NVP *	12-OH-NVP *	3-OH-NVP *	8-OH-NVP *	Refs
Clinical, 2 weeks of NVP treatment	plasma	13	43	39	2.0	[349]
Clinical, 4 weeks of NVP treatment	plasma	15	43	42	2.0	[349]
Clinical, Steady state NVP treatment	urine	23	33	33	1.0	[346]
Clinical, Steady state NVP treatment	plasma	13	80	6.0	0.0	[358]
Clinical, Steady state NVP treatment	plasma	16	75	7.0	2.0	[363]
Clinical, Single Dose NVP treatment	plasma	32	52	16	0.0	[362]
Clinical, Steady state NVP treatment	plasma	5	51	9	35	[362]
Non-clinical (chimpanzee)	urine	68	19	13	0.0	[364]
In vitro, spheroids of freshly isolated rat primary hepatocytes, exposed to NVP for 11 days	Cell culture supernatant	25	57	18	0.0	[91]
In vitro, human cryopreserved microssomal preparations	Microssomes reaction buffer	39	27	27	7.0	[348]
In vitro, HLC spheroids exposed to NVP for 10 days	Cell culture supernatant	60	28	10	2.0	

* the relative amounts of NVP metabolites were collected from the literature considering total amounts of metabolites, including phase II metabolites that were also incorporated in its phase I form

Glutathione conjugation might result from either spontaneously or enzymatic reactions catalyzed by GST. GSTs (GSH-S-transferase) are of major importance in liver as a cellular defence mechanism. GSTA1 and GSTA2 account for 3 % of total hepatocyte cytoplasmic proteins and is a particularly important GST family in the liver. In cultured human hepatocytes, *GSTA* gene expression drops quickly to 10 % of freshly isolated cells [20]. GSTA1 and GSTA2 present common expression, regulation mechanisms and substrates [365] and catalyze the glutathione conjugation with a wide range of electrophiles, possess glutathione-dependent

steroid isomerase activity, and glutathione-dependent (selenium-independent) peroxidase (GPx) activity [366]. Herein, *GSTA1-A2* gene expression was induced upon NVP exposure in 3D- but not in 2D-HLCs. The induction of GSTA1-A2 is an adaptive response that protects against oxidative stress, resulting from the activation of the transcription factors regulated by a different signaling pathway for chemoprotective agents and electrophilic toxicants response [367]. Cytoprotective agents induce GSTA2 and concomitantly activate the PI3K-Akt/ERK-RSK1-mTOR pathways that activate the transcription factors favoring cell viability [367]. NVP metabolites 3-OH-NVP and 12-sulfoxy-NVP were the only metabolites that have been shown to form glutathione conjugates [352]. 3-OH-NVP glutathione derivatives are reported to be non-enzymatic or mediated by GSTP1-1, whereas 12-sulfoxy-NVP glutathione derivatives are mediated by GSTA1-1, GSTM1-1 and GSTA3-1 [352]. Thus, we evaluated *GSTA1-A2* expression levels upon NVP treatment as well as quantified GSH, its precursors and its degradation productions in intracellular and extracellular fractions. To clarify the effect of NVP biotransformation on HLCs redox homeostasis and glutathione biosynthesis regulation HLCs' thiolomic profile was also evaluated.

GSH may undergo extracellular γ-glutamyltranspeptidase (γGT)-mediated cleavage of the γ-glutamyl moiety, leaving a cysteinyl-glycine (CYS-GLY) conjugate that is further cleaved by dipeptidase, resulting in a cysteinyl conjugate [368]. Physiologically, γGT provides CYS from GSH to the cells to be used in *de novo* biosynthesis of GSH [369]. In our HLC cultures, CYS-GLY was significantly increased in NVP treated cells, at day 34, in both 3D- and 2D-HLCs, revealing the above mentioned response to the presence of NVP and of its metabolites. In fact, GSH degradation to CYS-GLY is only performed extracellularly by cells with γGT, such as the hepatocyte [368].

The rate of GSH synthesis is determined by cysteine availability and glutamate cysteine ligase (GCL) activity. In our cell culture context, cysteine was highly available in cell culture medium. Thus, the higher GSH in 3D cultures at day 34 in cells ($p < 0.01$) and in cell culture supernatants ($p < 0.01$) probably reflected a higher GCL activity in the 3D-HLC. Interestingly, it is reported that the gene expression of GCL catalytic subunit (GCLC) is upregulated where increased cellular defence is necessary [368], namely as a mechanism of defence against oxidative stress mediated by the transcription factors Nrf2 and HNF1β [370]. GLU-CYS is formed by the action of GCL and is the limiting substrate for GSH synthesis by glutathione synthethase (GS). Total GLU-CYS amounts were similar in 3D- and 2D-HLCs and slightly increased over the time in culture. However, intracellular CYS levels were significantly increased in the 3D-HLCs at day 27 resulting in higher GSH levels in non-treated cultures at days 27 and 34. This might indicate that GSH synthesis is occurring at a higher rate in the 3D

cultures, which is corroborated by the unchanged levels of glutathione synthesis precursors in 3D and not in 2D cultures upon NVP exposure.

An increased S-glutathionylation of proteins was proposed by MaGarry *et al.* [371] as an adaptive response determinant to paracetamol toxicity [371]. Our data showed that S-glutathionylation of proteins is slightly increased at day 27 in both NVP-treated cultures. On the other hand, at day 34, besides total GSH is increased in 3D-HLCs up on NVP treatment, its free and protein bond forms are decreased suggesting a higher exposure to oxidative harm. This was observed by the higher GSSG/GSH ratio, the induction of GSTA1-A2 expression and increased gluthathione biosynthesis, which is possibly reflecting an adaptation to the oxidative harm caused by reactive species such as 12-sulfoxy-NVP.

3D spheroids of rat primary hepatocytes previously showed to be superior on mimicking the in vivo metabolism of NVP, providing integrated information on its biotransformation regulation as well as on detoxification and bioactivation/toxicity pathways [91]. HLCs, in both 2D and 3D cultures, showed a response to NVP exposure, but intracellular GSSG was only significantly increased in 3D HLC.

In conclusion, the biotransformation competence of our 3D-HLC model was herein reinforced by the correct profiling of NVP biotransformation, as well as by mimicking the NVP auto-induction processes as observed in man. Moreover, the *thiolomic* analysis reflected the higher glutathione production in 3D cultures, which together with a more effective glucuronic acid conjugation also suggests a higher protection in the 3D HLCs. In sum, 3D-HLC showed to be advantageous relative to the traditional monolayer cell culture by displaying a more complete phenotype comprising phase I, II and III of drug metabolism that was maintained or increased over the time in culture, being suitable to be applied in mechanistic models for hepatotoxicity testing.

In a near future, the introduction of such human stem cell derived physiologically relevant hepatic 3D models might take part in in vitro pharmacokinetic studies and may indeed significantly contribute to the reduction of compound attritions' rate by the selection of safer lead molecules, and have an important role in drug discovery and development.

Chapter 7. Concluding remarks and future perspectives

The enormous development of cell and tissue engineering approaches over the last decade resulted in a growing interest on improving in vitro testing and on using new in vitro technologies to generate more robust data on the potential risks to humans brought by environmental agents and pharmaceuticals. Major interest scopes expanding capabilities to test target molecules more efficiently, reducing animal testing, increasing drug development efficiency and improving prediction of adverse drug reactions [48, 121-128]. Alternative approaches are already scientifically validated, accepted by competent regulatory bodies and in use for regulatory toxicology purposes in several areas, namely in dermatology and immunology [129]. However, no toxicokinetic or hepatic metabolism studies have been validated and accepted yet by the regulatory authorities as alternative methods [130]. Those are essentially performed in animal models despite the evidence for relevant interspecies differences [118].

The liver is one of the main targets for toxicity caused by pharmaceuticals, reason why the evaluation of potential hepatotoxicity represents a critical step in the development of new drugs. Given that the liver is the main organ responsible for xenobiotic metabolism, it is also the first tissue contacting with the majority of toxicants and their metabolic products. Although biotransformation reactions generally parallel detoxification processes, the formation of reactive metabolites is relatively frequent. Indeed, drug induced hepatotoxicity accounts for more than 50 % of the cases of acute liver failure [372].

Currently, in vitro hepatotoxicity testing is performed using monolayer (2D) cell cultures or suspensions of human hepatoma cell lines or primary hepatocytes, having both major drawbacks [48, 50]. Primary cultures of hepatocytes originate the more representative phenotypic and functional profile. However, this phenotype is lost within the first days in culture, there are important interspecies differences when cells are isolated from rats or have limited availability when isolated from human donors. Hepatoma cell lines have poor metabolizing capacity [51]. Therefore, the short-term functional culture of primary hepatocytes and the low biotransformation capacity of hepatoma cell lines make it difficult for the detection of the toxicity that compounds exert through metabolism and restricts repeat dosing studies. 3D controlled culture conditions have allowed the maintenance and further improvement of some hepatocyte functional features for longer periods in culture [61, 62, 64, 71, 95]. On the other hand, to overcame the low availability of human functional cells as well as to improve the reliability and accuracy of drug screening, an efficient production of differentiated hepatocytes from stem cells has also been sought by researchers, upon request from regulatory bodies and the pharmaceutical industry [163]. Merging 3D culture techniques and

stem cells as cell source might offer an important potential alternative for the development of an alternative in vitro hepatic model for toxicology applications, including long-term studies.

Derivation of hepatocyte-like cell populations have been attempted from hESCs [48, 51, 122, 134, 140, 164-167, 180, 183], MSCs [150, 161, 168, 170, 172, 174, 176-179, 200, 202-204, 239, 240, 242, 265], bipotent liver progenitor cells [180] and iPSCs [138, 184, 235, 244, 246, 373] although no study has reported a fully satisfactory HLC functional phenotype. Several strategies have been followed to derive HLC from SC by in vitro mimicking the in vivo liver development. This has been performed by the addition of soluble factors, including growth factors, cytokines and hormones to the cell culture media, reproducing the in vivo cell-to-matrix and cell-to-cell interactions using alternative cell culture strategies, and determining cell fate via genetic modification or epigenetic modulation [180]. The original work presented in this thesis focused on deriving hepatocyte-like cells from human neonatal mesenchymal stromal cells for potential drug screening applications. The developed strategy enclosed the importance of the chemical cocktail and of the tissue architecture needed to mimic the tissue development in vivo. The major challenges of the application of SC-derived hepatocytes in toxicology were considered, namely the immature phenotype of the HLC reported in literature at the time [166, 252, 253], the lack of defined and validated endpoints for hepatic differentiation and maturation, the lack of standardization and use of relevant positive controls for differentiation, and the need of generating significant numbers of HLC [253]. In this Chapter, we integrate our new findings on human neonatal MSC differentiation potential with the current state of the art and conclude on how close we might be from presenting a real in vitro alternative for biotransformation and hepatotoxicity studies.

Firstly, UCX® were selected as the stem cell source because of their genotypic and phenotypic characteristics. UCX® is a highly homogeneous, extensively characterized and therapy-driven population of human neonatal MSCs, registered as a trademark and resulting from a patented method [154]. These hnMSCs are obtained in high numbers and present high genomic stability upon expansion, enabling at least 55 cumulative population doublings (up to passage 22) before reaching senescence, preserving the ISCT criteria for defining MSC along cell expansion, including differentiation capacity into osteoblasts, chondrocytes and adipocytes [154]. Hence, UCX® are a great candidate to use as an alternative cell source for the hepatic differentiation to obtain models for in vitro toxicology. Neonatal MSC sources are advantageous over other MSCs sources given their neonatal nature which makes them independent of health condition, clinical history or lifestyle. Furthermore, neonatal MSCs

maintain high chromosomal stability upon in vitro expansion as opposed to ESCs [151] and iPSCs [144, 149, 156-158]. Neonatal MSC have also demonstrated high differentiation capacity namely into cells of mesodermal origin such as myoblasts and cardiomyocytes [159], ectodermal as neurons, and endodermal origin. The relevance of a human neonatal source of stem cells for hepatic differentiation has also been shown by several studies [198] that compared different sources of MSCs, where neonatal stem cells presented better hepatocyte differentiation phenotype, reinforcing the importance of a primordial MSC source and most importantly, revealing that each MSC type have different differentiation capabilities and potential applications [160, 161]. Despite the advantages of hnMSC, few studies are available on these cells [172, 174, 176, 179, 199].

The first main objective of this work was to establish an optimized hepatic differentiated protocol for obtaining fully competent hepatic cells. The hepatic differentiation is usually implemented by mimicking the in vivo ontogenic development of the liver. The translation of these stages to the in vitro differentiation of stem cells is particularly challenging on defining the timing and composition of the differentiation cocktails. Indeed, a sequential exposure to cytokines and growth factors has been shown of utmost importance to achieve a more homogeneous population of HLC [269, 374], which is further corroborated by the finding that there is a strict control of growth factor secretion during development [375, 376]. Moreover, the best combination of timing and differentiation cocktail composition for deriving stem cells into hepatocytes is far from being consensual and may vary according to the type of stem cell [168, 180, 201, 269, 374, 377, 378]. In this work, we first optimized a protocol under traditional monolayer cell culture conditions using sequential exposure of cytokines and growth factors in a three-step protocol. The hepatic differentiation protocol aimed, at first, at promoting the endoderm commitment, the first step in liver development. Endoderm commitment is controlled by a time and concentration-dependent secretion of growth factors, namely FGFs [185-187]. In fact, FGF-2 concentrations are a key factor on tissue development signalling, as previously reported [190], being also a powerful inducer of foregut-derived cell lineages [275]. This was observed in our cells in **Chapter 3** by a FGF-2 concentration dependent effect on *HHEX* gene expression. The second step of the hepatic differentiation is hepatic commitment (D3-D13), which is mimicked by HGF supplementation. To further mimic the liver development in vivo, a third step for hepatoblast maturation and differentiation into hepatocytes was introduced by dexamethasone and oncostatin M from day 13 onwards.

Epigenetic modifiers have been described as having a role on hepatic differentiation [201]. Therefore, with the aim of optimizing the best differentiation strategy; an extensive/exhaustive comparison of several differentiation protocols was performed by further adding epigenetic modifiers [201] to the core differentiation protocol. To our knowledge, this is the first work that compares three distinct epigenetic modifiers TSA, 5-AZA and DMSO, separately or in combination, and at different time-points (**Chapter 3**). We first, attempted to reproduce the most promising protocols in the literature applied to MSCs [168, 172]. Snykers *et al.* [377] tested 100-1000 nM of TSA on hepatic differentiation of bone marrow MSCs showing that the concentration of 1000 nM improved HLC phenotype when added at day 6 of the differentiation protocol [168, 377]. We also tested the effect of 100, 500 and 1000 nM of TSA on UCX® differentiation (data not shown). On deriving UCX® under these conditions [377], we observed that an epithelial morphology could only be achieved with 500 nM TSA, whereas CK-18 presence and glycogen storage ability was only observed when using 100 and 500 nM of TSA. The concentration of 500 nM of TSA resulted on the higher EROD and UGT activities, of 17.5 ± 2.6 (Average ± SEM) and 173.7 ± 12.5 (Average ± SEM) (unpublished data), respectively. For this reason, 500 nM of TSA was tested at days 6, 10 and 13 of the differentiation using a protocol adapted from Campard *et al.* [172]. By the time this thesis was initiated (**Chapter 3**) the work by Campard *et al.* [172] was the only one using WJ-MSC, the same hnMSC source as UCX®, where the derived HLCs displayed relevant biotransformation activity [172]. More recently, other studies have been published on hnMSC-derived HLCs [161, 174, 177, 200, 202-204]. However, the study from Campard *et al.* [172] is still the only one showing biotransformation activity and the incapacity of CYP3A4 induction by phenobarbital [172]. Interestingly, in our battery of protocols the use of DMSO alone resulted in a better HLC phenotype (**Chapter 3**) and for this reason, the use of TSA was not further explored. DMSO has been described for the differentiation of HepaRG cells [54] and as improving the hepatic differentiation [183, 217, 220-224]. To our knowledge, DMSO has only been used on the differentiation of MSCs from the adipose tissue and at the concentration of 0.1 % [220, 221, 239]. Banas *et al.* [221] and Okura *et al.* [239] included DMSO at 0.1 % in their sequential protocols hindering the possibility of specifically evaluating its effect; whereas Alizadeh *et al.* [220] tested HGF and HGF+DMSO using a cocktail-based protocol. In the work by Alizadeh *et al.* [220], cells morphology was fibroblast-like, but DMSO resulted in an upregulation of *AFP*, *CK18*, *ALB* and *HNF4A* relative to non-treated cells [220]. On the other hand, the differentiation protocol described by Banas *et al.* [221] resulted in epithelial-like morphology, positive PAS staining and LDL uptake as well as ALB presence. The weakness of both studies is the absence of positive controls, such as primary hepatocytes or hepatic cell lines [220,

221]. DMSO was also evaluated in other stem cells than MSCs. Pal *et al*. [222] tested 0.01, 0.1 and 1 % of DMSO on embryoid bodies of hESC after spontaneous differentiation [222]. Hay *et al.* [183, 379] used 1 % of DMSO on hESC, before differentiation [379] and after endoderm partening induction [183], and the last conditions increased the proportion of hepatocytes in the end population to approximately 70 % [183]. The DMSO effect on endoderm commitment in the first days of the in vitro differentiation is still controversial and was only reported for hESC [183, 223, 225]. MSC are from the mesenchymal origin whereas hepatocytes derive from the endodermal layer. Thus, the process of differentiation of MSC into HLC must involve a successful *transdifferentiation.* This is a still poorly understood process [180], and distinguishes the hepatic differentiation of pluripotent stem cells (ESC and ipSC) from MSC. In this study, one of the most remarkable achievements (**Chapter 3**) was the introduction of DMSO at day 10 of the protocol, which resulted in a significant improvement of the HLC phenotype and its maintenance during an extended period, *i.e*. for 13 days. The transcriptomic analyses of the obtained HLCs was also a remarkable achievement that better clarified how close we were from the in vitro hepatic golden standards, the human hepatocytes, normally used for drug metabolism and hepatotoxicity studies [256, 281]. This analysis revealed a partial hepatic differentiation degree, by the shared expression of gene groups between HLC and human primary hepatocytes that were not observed between HepG2 and hpHep. In addition, bioinformatic analysis of gene expression data placed our HLC between the HepG2 cell line and hpHep and distant from hnMSC. This fact, together with the noteworthy activity of CYP3A4 and the presence of hepatic transporters were the most important features of our achieved HLC at this point of this thesis (**Chapter 3**).

The major difficulty in comparing stem cell-derived HLC studies is the lack of proper controls and the inclusion of enzymatic activity evaluation. The absence of appropriate controls enables the comparison of the achieved HLC with other protocols [122, 236, 238, 242, 243]. Most importantly it also impairs the evaluation of how close or how far might the achieved phenotype be from the hepatocyte. It is surprising the number of studies claiming a successful differentiation of stem cells into HLC that do not perform or do not show results on a gold-standard subject to the same experimental conditions, *e.g.* a primary hepatocyte or, at least, a hepatoma cell line. Particularly with hnMSC-derived HLC and to our best knowledge, only the work presented in this thesis, Zhang *et al.* [174] and Raut *et al.* [204] presented data on human cryopreserved primary hepatocytes, human primary hepatocytes or adult liver, respectively, as positive controls. The later, however, only presented the control for gene expression studies but not for albumin and urea secretion. Nevertheless, the evaluation of

those characteristics is of utmost importance for the validation of a differentiated and functional cell type.

The control of proliferation is also of utmost importance during liver development. There are two main stages of higher cell proliferation within the liver development, a first stage, such as the outgrowing bud of proliferating endodermal cells present in the ventral floor of the foregut, and afterwards, a second proliferation stage is triggered by the septum transversum mesenchyme, which is required for expansion and complete differentiation of the hepatocytes [380]. For designing a hepatic differentiation protocol, we intended to create an initial step where endoderm commitment was favoured and where proliferation signals were slowly silenced, triggering differentiation signalling pathways in a synchronous way in all cells to produce a homogenous population of HLC. In fact, the homogeneity of the differentiated HLCs have been reported as a problem for pluripotent stem cells, hESC and hiPSC, differentiation with 60 to 80 % of albumin positive cells [381]. However, the second-high proliferation stage of hepatic commitment had not been yet considered in our differentiation protocol obtained in **Chapter 3**. As such, the second-high proliferation stage of hepatic development was recreated by introducing a cell passage step at day 17, when cells were considered to be hepatoblast-like at the gene expression level (**Chapter 5**). The cell passage step (day 17) was tested with and without the presence of 5-AZA. To our knowledge, 5-AZA effect on hepatocyte MSC-differentiation protocols in vitro had only been attempted by Seeliger *et al.* [213] and Yoshida *et al.* [214]. In these works, 5-AZA was applied 24h prior the differentiation induction since proliferation is needed for the incorporation 5-AZA on cellular DNA. Herein, the cell passage step brought up the opportunity to test the effect of 5-AZA later in the differentiation protocol, and this approach was the innovative feature that resulted in the best tested protocol.

The significant results achieved with this optimized hepatic procedure led us to step up into the 3D cultures as a strategy to improve hepatic differentiation by rebuilding the in vivo cell-to-matrix and cell-to-cell interaction, going into the direction of the second main objective of this work. In this context, undifferentiated hnMSC cultures under three-dimensional conditions were firstly established in parallel, using a self-assembled spheroid approach (**Chapter 4**). This approach aimed at evaluating if our hnMSC 3D cultures would maintain an undifferentiated phenotype and differentiation capacity. Indeed, hnMSC spheroids fully retained a mesenchymal phenotype as defined by ISCT up to day 3 of culture, which represented a safer window for initiating differentiation. As expected, 3D spheroid structures

also primed cells to produce a rich ECM (**Chapter 4**) as well as a distinct cytokine and growth factor profile [259]. A reduction of the cells proliferation rate was another observation of our work, presenting itself as an advantage given that low cell proliferation is required for triggering cell differentiation.

The hepatic differentiation in 3D cultures, both as spheroids or in a hollow-fiber bioreactor, was attempted starting at day 0 of the differentiation (unpublished data). In 3D spheroids histological analysis showed absence of necrotic cores and positive cells for glycogen, CK18, HNF-4α and ALB. Urea production was also observed. However, there was high loss in cell number over the time in culture and ECOD and CYP3A4 activities were not detected, possibly indicating that a mature phenotype was not achieved (unpublished data). In the hollow-fiber bioreactor, the long-term culturing also lead to cell loss, as observed by LDH release and by low lactate production. Histological analysis showed a non-compact tissue structure, and although the cells were positive for glycogen ALB, CK-18, CK-19, HNF-4α, MRP-2, OATPC, CYP1A2 and CYP3A4, and able to secrete urea, no EROD activity was observed (unpublished data). Elevated cell loss in long-term HLC spheroid differentiation was also reported by Okura *et al.* [239] that observed up to 50 % of cell loss, evaluated by DNA quantification [239]. Still, it is interestingly to note that most 3D HLC cultures are inoculated into the 3D system at day 0 of the differentiation [122, 184, 238-242, 245], but few report on using a differentiation step in 2D prior to 3D culturing [236, 243, 244]. The last present longer cell culture times, up to day 32 [236] and 45 of the differentiation [244], and higher hepatocyte-like phenotype, namely regarding maintenance of albumin production and CYP3A4 activity [173, 244]. This raised the question of whether long differentiation time under 3D conditions, *i.e.* from day 0, do enable MSC derivation and maintenance of the achieved hepatocyte-like phenotype. In fact, the cell passage step at the hepatoblast-like stage, represented an opportunity to perform the first 17 days of differentiation in monolayer, followed by a final maturation step in 3D (**Chapters 5**). In Chapter 5, this integrated culturing/differentiation strategy was approached and cells hepatic-specific features evaluated up to differentiation day 27, in the bioreactor, and up to day 34, in spheroids. HLC cultured in both three-dimensional systems formed ECM (**Chapter 5**), which provided high cell-to-cell and cell-to-matrix interactions, as previously observed in primary hepatocytes either cultured in spheroids [61, 71] or in a perfused bioreactor [94]. In fact, the ECM composition in the developing liver is dynamic and distinct from the adult [7]. Fibronectin and type IV collagen increase during development whereas types I and III collagen and laminin decrease [382, 383]. In the adult liver parenchyma, ECM is constituted by fibronectin and type I and III collagen [7]. Moreover, the hepatoblast expansion and growth of primitive liver bud is a step in the liver development that requires ECM remodelling [384] highlighting the

importance of studying the ECM composition of our 3D-HLC to evaluate if this would better mimic the developing liver microenvironment or the adult liver ECM.

Importantly, our integrated system showed that overall 3D HLC present a better behaviour regarding key features of drug metabolism, comprising phase I and phase II enzymatic activities and drug transporters (**Chapter 5**). The formation of definitive endoderm in the developing embryo occurs in a monolayer of cells [385]. Sivertsson *et al.* [243] tested the inoculation of differentiating hESC in a hollow-fiber bioreactor at the definitive endoderm stage and at the hepatic progenitor stage; and evaluated the transcriptional patterns and mechanistic pathways that were affected by the 3D culturing system relative to 2D and by the time of inoculation in 3D. High transcriptional differences were observed between the 2D and 3D cultured cells [243]. Another feature that may have positively contributed to the success of our integrated approach is the fact that OSM (included from days 13 onwards) has a proliferative effect on the hepatoblasts [193, 194]; and despite the fact that the cell culture remains completely confluent, during the 2D culture period, some cell loss was observed which might have been compensated by cell proliferation further leading to cell selection.

The 3D configuration also creates a gradient that led us to discuss the possible hepatic zonation that these cell culture systems might generate. Hepatic zonation is defined as the distinct functions exerted by the hepatocytes according to its localization in the hepatic lobule and occurs, physiologically, as a response to the gradient that results from the different composition of periportal and perivenous blood. It is expected to have higher oxygen, glucose and nutrients in the outer side of the spheroid or in cells near to the medium in capillaries in the bioreactor, which may better mimic the liver periportal environment rather than the perivenous. The perivenous hepatocytes are characterized by a higher xenobiotic metabolism, important regarding our objective, by glycogen synthesis from glucose and have less access to oxygen, and thus closer to physiologic conditions of the inner cells [7, 50].

The differentiation medium established in this work contains high amounts of insulin (1.72 μM) and glucose (25 mM), being insulin a signalling molecule present in higher concentrations in the periportal hepatocytes [386, 387]. A more periportal-like phenotype was observed in the 2D cultures, regarding urea secretion capacity and glucose metabolism behaviour. In the 2D culture we observed lower glycogen stain, and higher glucose release into the cell culture medium than in both 3D cultures (**Chapter 5**). Nevertheless, preliminary work of our group demonstrated that HLCs exposed to low concentrations of glucose (5mM), no insulin and no dexamethasone overexpressed genes involved in glycolysis and lipogenesis (*PDK4* and *GLUT1*), gluconeogenesis (*PEPCK* and *G6P*), bile acid metabolism (*FXR*) and mitochondrial

function and biogenesis (*PGC1A*) [388]. This was in accordance with our ingenuity pathway analysis of HLC canonical pathways showing that HLCs are closer to hpHep than HepG2 cell line regarding Gluconeogenesis (**Chapter 4**). Bell and co-workers [87] showed that the long-term maintenance of regulated metabolic pathways such as glycolysis, gluconeogenesis and the γ-glutamyl cycle, a key pathway in maintaining redox homeostasis [389], was only observed in human cryopreserved hepatocyte spheroids, resembling intact liver tissues, whereas 2D monolayer cultures originating from the same livers presented relevant deregulation of these pathways [87]. This fact reinforces the importance of the relevant expression of such pathways on our hnMSC-derived HLCs.

Interestingly, the spheroids presented a higher glycogen stain in the outer cells of the spheroid whereas the bioreactor presented a homogeneous glycogen stain (**Chapter 5**). This may suggest that the HLCs in the bioreactor are using both glucose and lactate to synthetize glycogen, depending on the cell's localization within the 3D structure. Therefore, the bioreactor might present a more balanced presence of periportal-like and perivenous-like cells whereas perivenous-like phenotype might be scarcer in the spheroid culture, sustaining also the higher urea production observed on the 3D cultures, and particularly in the spheroids culture. In turn, albumin production, which is more associated with the perivenous phenotype [6] and is also stimulated by blood flow-mediated shear stress [390], was improved in HLC cultured in the bioreactor. The effect of medium flow on inducing albumin secretion was demonstrated by Prodanov *et al.* [390] using a human primary hepatocyte 3D microfluidic system [390]. Additionally, McCarty *et al.* [387] demonstrated the creation of spatially-controlled zonation across multiple hepatocyte metabolism levels through the application of precise concentration gradients of exogenous hormone (insulin and glucagon) and chemical (3-methylcholanthrene) induction agents in a microfluidic device, using a monolayer rat primary hepatocytes [387]. In the same study, a high concentration of insulin was directly correlated with a gradient in glycogen storage via periodic acid-Schiff staining and urea production via carbamoyl phosphatase synthetase I staining [387]. This is in accordance with our observations for HLC glycogen storage and urea production in relation to high insulin concentrations, mimicking the in vivo hepatic zonation. The effect of the gradient and blood flow-mediated shear stress have also been reported on the expression and activity of biotransformation proteins [72-74, 387, 390]. McCarty *et al.* [387] observed a gradient on cell viability upon the exposure to allyl alcohol and paracetamol reflecting the in vitro creation of hepatocyte carbohydrate, nitrogen, alcohol degradation, and drug conjugation metabolic zonation staining [387].

Our immunofluorescence data (**Chapter 5**) may also suggest some phenotype zonation in the bioreactor since CYP1A2 and CYP3A4 are present within the tissue and not near the

capillaries whereas the hepatic transporters OATP-C and MRP-2 are predominantly located. This was also observed with the spheroids to a lower extent. Herein, MRP-2 is predominant in the spheroid outer layer, whereas OATP-C is widespread within the spheroid. Therefore, a more organized cell culture system as within both 3D models, may present an overall higher level of both periportal-like and perivenous-like cells than the 2D culture.

Overall, the findings described in **Chapter 5** reinforce the importance of the cell culture environment as a key factor for the maintenance of the hepatocyte-like phenotype as initially hypothesised. It further supported that the subtle differences between phenotypic impacts promoted by each of the 3D models adopted are enough to entail that optimal culture systems should be selected depending on the scientific applications.

This work intended to build a physiologically relevant alternative method using human cells for studying xenobiotic biotransformation as well as its mechanisms of action. This has been demonstrated in **Chapter 6** where HLCs displayed relevant biotransformation and detoxification responses regarding the model drug nevirapine. Both 2D and 3D models presented the 4 main metabolites of NVP as well as its phase II metabolites. The later were detected in much higher amounts in 3D HLC than in 2D HLC as a consequence of the auto-induction of NVP and its metabolites. Moreover, only 3D HLCs presented an overexpression of *GSTA1-A2*, which is induced by oxidative stress, and of the *MRP7* transporter. A complete response to NVP and its metabolites on the *thilomic* profile was also only observed in 3D HLC, by showing GSH synthesis (**Chapter 6**). Additionally, only 3D-HLC showed increased intracellular GSSG levels, probably as a result of a higher synthesis of the toxic metabolite 12-sulphoxy-NVP. Thus, the work described in **Chapter 6** supports that our 3D HLCs are a competent system amenable to be applied to the study of hepatotoxicity of xenobiotics.

A better understanding of the mechanisms contributing to de-differentiation or loss of phenotype of primary hepatocytes would also be interesting to develop better strategies to improve stem cell derived HLC phenotype in culture. As reported by Godoy *et al.* [281], cultured human primary hepatocytes gene regulatory network alterations resemble those of inflammatory liver diseases [281]. The same group, in a previous gene networks study identified, by cluster analysis, highly correlated groups of genes associated with mature liver functions [256]. Interestingly, one of the 3 clusters that fail to reach the expression levels of hepatocytes is controlled by the transcription factors HNF1, CAR, FXR and PXR. This cluster strongly overlaps with genes repressed in cultivated hepatocytes compared to freshly isolated

hepatocytes, suggesting that current in vitro conditions lack stimuli required to maintain hepatocyte-like gene expression. This explains the resulting deficient HLC-like phenotype [256]. Indeed, the 3D cell culture systems had proven a lot in the field of improving cell function and would be interesting to further compare freshly isolated hepatocytes with cultured hepatocytes and stem cell-derived hepatocytes also under 3D culture systems. Considering the cellular complexity of the liver and the functional sophistication of the hepatocyte, together with the fact that it exhibits more individual functions (>500) than any of the other ~200 terminally differentiated cell types in the human body [4], it is not surprising that the maintenance of a fully functional hepatocyte in culture is difficult to achieve. Therefore, this makes hepatocytes amongst the most challenging cell types to mature artificially.

Final Remarks

This thesis was that 3D culture conditions in the presence of cytokines and growth factors involved in liver embryogenesis would result in a hMSC-based in vitro model more representative of the liver physiological conditions. Moreover, we intended to develop a system that could be standardized and therefore routinely used for toxicology screening, with possible applications in cell therapy. Altogether, the results here presented support the viability of abundant and ethically safe hnMSC to serve as precursors to achieve a mature HLC phenotype. Indeed, a more mature HLC phenotype was achieved by resorting to 3D spheroids, particularly regarding biotransformation capacity. We also demonstrate that HLC and particularly 3D HLC as a long-term tool to access drug induced alterations on biotransformation, considering phase I, II and hepatic transport, as well as on the regulation of detoxification pathways, such as glutathione synthesis. It is agreed that there are still many challenges on improving stem cell derived HLC. The international community strongly supports new in vitro alternatives to animal testing as long as methods were correctly validated. SC based technologies, integrating testing systems, can be a valuable tool to reduce, and possibly replace, the current ethical-problematic animal experimentation in drug discovery, safety pharmacology and toxicology. We may still be away from the day that stem cell-derived HLC are used for regulatory proposes in the drug development process, but we believe that the work here presented is a step forward on the establishment of a human in vitro hepatic model, suitable for in vitro toxicology applications.

Future Perspectives

Although the present work showed noteworthy achievements, it also raised several questions, namely on how to optimize the cell culture conditions for providing the best environment for HLCs' function. In general, the hepatocyte culture medium composition studies were performed with the focus of maintaining hepatocyte biotransformation capacity and this might explain the high concentrations of dexamethasone usually applied. Dexamethasone is a glucocorticoid that induces hepatocyte maturation, namely phase I metabolic activity [196, 391]. The transcriptome analysis of the canonical pathways activation showed a similar activation in HLC and hpHep (**Chapter 4**) for *glucocorticoid receptor signalling*. Glucocorticoids may also cause insulin resistance and therefore, interfere with cell energy metabolism [392]. Thus, medium composition could be optimized to increase cell sensitivity to such insults. Specifically, a medium that would better mimic the composition of blood in the human body would be extremely relevant, containing additional biomolecules such as bile acids and cholesterol, thus allowing the possibility of using HLC to develop relevant hepatotoxicity mechanisms rather than hepatic cytotoxicity [281]. In fact, our transcriptome analysis data identified that the canonical pathways of *Bile acids biosynthesis, Triacylglrlicerol biosynthesis* and the *Superpathway of cholesterol biosysntesis* were downregulated relative to HepG2 and hpHep (**Chapter 4**). One relevant mechanism of DILI is the development of a cholestasis phenotype upon drug exposure that represents 20-50 % of the DILI cases and is associated with drugs with hepatic elimination [40]. Cholestatic liver injury results from dysfunction of the mechanisms of bile formation [40]. In vitro mimicking of cholestatic-like phenotype depends on the presence of functional bile canaliculi. This structure formation has been reported on primary hepatocyte cultures, only under 3D conditions [87, 281, 393] and its function implies also the maintenance of efflux transporters over the time in culture. Sandwich culture of primary hepatocyte showed that long-term culturing led to leaking and damaged bile canaliculi [393]. It has been suggested that the in vitro formation of such structures depends not only on the 3D culture conditions but also on the chemical composition of the surrounding medium [394]. Bile secretion can only occur when bile formation is observed. Bile is formed by water, bile salts, lipids namely phosphatidylcholine and cholesterol, proteins, vitamins and several organic and inorganic solutes of considerable complexity and its formation is regulated by a multitude of post transcriptional regulatory pathways and cytokine and hormone signals [394]. In fact, HLC culture medium is commonly serum-free and not supplemented with lipids or bile salts, whereas human primary hepatocyte cultures carry at least intracellularly some components needed for bile formation. The hypothesis of improving primary hepatocyte cultures by bile acid supplementation was also suggested by Godoy *et al.* [281] that observed

that cultured hepatocytes presented a cluster of downregulated genes involved in bile salt metabolism, when compared with non-cultured hepatocytes [281]. In addition, bile salts have been reported to induce mature liver functions in pluripotent and foetal liver cells [395] and in hepatocyte-like cells derived from MSC [396], although those are not routinely used in hepatocyte culture media [281].

The work developed here focused mainly on HLC capacity to metabolize drugs and for this reason much effort was made on characterizing CYP enzymes, phase II enzymes and hepatic transporters. Nevertheless, it would be also interesting to further improve medium composition considering the HLC lipid metabolism and bioenergetic profile, also resorting to 3D cultures.

Finally, in the toxicology field, a HLC spheroid culture in the SFSC system equipped with a perfused set-up would allow to perform pharmacokinetic studies and allow further validation HLC biotransformation capacities.

Bibliography

1. European Commission Staff Working Document. Pharmaceutical Industry: A Strategic Sector for the European Economy. [Internet] Brussels (BE) 26 p. SWD 216 final/2, Aug 2014. Available from: http://ec.europa.eu/DocsRoom/documents/7649/attachments/1/translations/en/renditions/native.

2. Kola, I., Landis, J. Can the pharmaceutical industry reduce attrition rates? Nat Rev Drug Discov. 2004;3(8):711-5.

3. Wilke, R. A., Lin, D. W., Roden, D. M., Watkins, P. B., Flockhart, D., Zineh, I.*, et al.* Identifying genetic risk factors for serious adverse drug reactions: current progress and challenges. Nat Rev Drug Discov. 2007;6(11):904-16.

4. Goldring, C., Antoine, D. J., Bonner, F., Crozier, J., Denning, C., Fontana, R. J.*, et al.* Stem cell-derived models to improve mechanistic understanding and prediction of human drug-induced liver injury. Hepatology. 2017;65(2):710-721.

5. Bhatia, S. N., Underhill, G. H., Zaret, K. S., Fox, I. J. Cell and tissue engineering for liver disease. Sci Transl Med. 2014;6(245):245sr2.

6. Jungermann, K., Kietzmann, T. Zonation of parenchymal and nonparenchymal metabolism in liver. Annu Rev Nutr. 1996;16:179-203.

7. Godoy, P., Hewitt, N. J., Albrecht, U., Andersen, M. E., Ansari, N., Bhattacharya, S.*, et al.* Recent advances in 2D and 3D in vitro systems using primary hepatocytes, alternative hepatocyte sources and non-parenchymal liver cells and their use in investigating mechanisms of hepatotoxicity, cell signaling and ADME. Arch Toxicol. 2013;87(8):1315-530.

8. Ramadori, G., Moriconi, F., Malik, I., Dudas, J. Physiology and pathophysiology of liver inflammation, damage and repair. J Physiol Pharmacol. 2008;59 Suppl 1:107-17.

9. Gregus Z., Parkinson A., Ogilivie B.W., Buckley D.B., Kazmi F., Czerwinski M., Parkinson O., Jaeschke H., 2013. Chapters: Mechanisms of toxicity, Biotransformation of xenobiotics and Toxic responses of the liver. In: Casarett & Doull's Toxicology: The basic science of poisons. Eighth Edition ed. San Francisco: McGraw-Hill, Medical Publishing Division. 49-122 p., 185-366 p. and 669-664 p.

10. Wienkers, L. C., Heath, T. G. Predicting in vivo drug interactions from in vitro drug discovery data. Nat Rev Drug Discov. 2005;4(10):825-33.

11. Hilal-Dandan R, Brunton L.L., Goodman and Gilman's Manual of Pharmacology and Therapeutics [Internet], Second Edition ed. New York, NY: McGraw-Hill, Chapter 6, Drug Metabolism. Available from: http://accesspharmacy.mhmedical.com/content.aspx?bookid=1810&Sectionid=124489935. Nov, 2016.

12. Pascussi, J. M., Gerbal-Chaloin, S., Drocourt, L., Maurel, P., Vilarem, M. J. The expression of CYP2B6, CYP2C9 and CYP3A4 genes: a tangle of networks of nuclear and steroid receptors. Biochim Biophys Acta. 2003;1619(3):243-53.

13. Watkins, P. B. Basic mechanisms of normal and abnormal gastrointestinal function: Drug metabolism and transport in the liver and intestine (Part 1: Section 26). In: Yamada, T., editor. Textbook of Gastroenterology. 1. Fifth Edition ed. West Sussex, PO19 8SQ, UK: Blackwell Publishing/John Wiley & Sons; 2009. p. 1744.

14. Strassburg, C. P., Oldhafer, K., Manns, M. P., Tukey, R. H. Differential expression of the UGT1A locus in human liver, biliary, and gastric tissue: identification of UGT1A7 and UGT1A10 transcripts in extrahepatic tissue. Mol Pharmacol. 1997;52(2):212-20.

15. Kiang, T. K., Ensom, M. H., Chang, T. K. UDP-glucuronosyltransferases and clinical drug-drug interactions. Pharmacol Ther. 2005;106(1):97-132.

16. Gamage, N., Barnett, A., Hempel, N., Duggleby, R. G., Windmill, K. F., Martin, J. L.*, et al.* Human sulfotransferases and their role in chemical metabolism. Toxicol Sci. 2006;90(1):5-22.

17. Hewitt, N. J., Lechon, M. J., Houston, J. B., Hallifax, D., Brown, H. S., Maurel, P.*, et al.* Primary hepatocytes: current understanding of the regulation of metabolic enzymes and transporter proteins, and pharmaceutical practice for the use of hepatocytes in metabolism, enzyme induction, transporter, clearance, and hepatotoxicity studies. Drug Metab Rev. 2007;39(1):159-234.

18. Zanger U.M. and Schwab M., Cytochrome P450 enzymes in drug metabolism: regulation of gene expression, enzyme activities, and impact of genetic variation. Pharmacol Ther. 2013. 138(1):103-41

19. Jancova, P., Anzenbacher, P., Anzenbacherova, E. Phase II drug metabolizing enzymes. Biomed Pap Med Fac Univ Palacky Olomouc Czech Repub. 2010;154(2):103-16.

20. Morel, F., Fardel, O., Meyer, D. J., Langouet, S., Gilmore, K. S., Meunier, B.*, et al.* Preferential increase of glutathione S-transferase class alpha transcripts in cultured human hepatocytes by phenobarbital, 3-methylcholanthrene, and dithiolethiones. Cancer Res. 1993;53(2):231-4.

21. Mulder, T. P., Court, D. A., Peters, W. H. Variability of glutathione S-transferase alpha in human liver and plasma. Clin Chem. 1999;45(3):355-9.

22. Kalliokoski, A., Niemi, M. Impact of OATP transporters on pharmacokinetics. Br J Pharmacol. 2009;158(3):693-705.

23. Kullak-Ublick, G. A., Becker, M. B. Regulation of drug and bile salt transporters in liver and intestine. Drug Metab Rev. 2003;35(4):305-17.

24. Omiecinski, C. J., Vanden Heuvel, J. P., Perdew, G. H., Peters, J. M. Xenobiotic metabolism, disposition, and regulation by receptors: from biochemical phenomenon to predictors of major toxicities. Toxicol Sci. 2011;120 Suppl 1:S49-75.

25. Pascussi, J. M., Gerbal-Chaloin, S., Duret, C., Daujat-Chavanieu, M., Vilarem, M. J., Maurel, P. The tangle of nuclear

receptors that controls xenobiotic metabolism and transport: crosstalk and consequences. Annu Rev Pharmacol Toxicol. 2008;48:1-32.

26. Handschin, C., Meyer, U. A. Induction of drug metabolism: the role of nuclear receptors. Pharmacol Rev. 2003;55(4):649-73.

27. Faber, K. N., Muller, M., Jansen, P. L. Drug transport proteins in the liver. Adv Drug Deliv Rev. 2003;55(1):107-24.

28. Tolson, A. H., Wang, H. Regulation of drug-metabolizing enzymes by xenobiotic receptors: PXR and CAR. Adv Drug Deliv Rev. 2010;62(13):1238-49.

29. Duanmu, Z., Locke, D., Smigelski, J., Wu, W., Dahn, M. S., Falany, C. N.*, et al.* Effects of dexamethasone on aryl (SULT1A1)- and hydroxysteroid (SULT2A1)-sulfotransferase gene expression in primary cultured human hepatocytes. Drug Metab Dispos. 2002;30(9):997-1004.

30. Bell, L. N., Chalasani, N. Epidemiology of idiosyncratic drug-induced liver injury. Semin Liver Dis. 2009;29(4):337-47.

31. Ju, C. Immunological mechanisms of drug-induced liver injury. Curr Opin Drug Discov Devel. 2005;8(1):38-43.

32. European Medicies Agency, Viramune -EMEA/H/C/000183 -IB/0123. 12/02/2016. Available from: http://www.ema.europa.eu/docs/en_GB/document_library/EPAR_-_Product_Information/human/000183/WC500051481 .pdf

33. Larson, A. M. Diagnosis and management of acute liver failure. Curr Opin Gastroenterol. 2010;26(3):214-21.

34. Russmann, S., Kullak-Ublick, G. A., Grattagliano, I. Current concepts of mechanisms in drug-induced hepatotoxicity. Curr Med Chem. 2009;16(23):3041-53.

35. Roth, R. A., Ganey, P. E. Intrinsic versus idiosyncratic drug-induced hepatotoxicity--two villains or one? J Pharmacol Exp Ther. 2010;332(3):692-7.

36. Grattagliano, I., Bonfrate, L., Diogo, C. V., Wang, H. H., Wang, D. Q., Portincasa, P. Biochemical mechanisms in drug-induced liver injury: certainties and doubts. World J Gastroenterol. 2009;15(39):4865-76.

37. Singh, B. K., Tripathi, M., Chaudhari, B. P., Pandey, P. K., Kakkar, P. Natural terpenes prevent mitochondrial dysfunction, oxidative stress and release of apoptotic proteins during nimesulide-hepatotoxicity in rats. PLoS One. 2012;7(4):e34200.

38. Timbrell, J. Introduction to toxicology. 3th ed. London: Taylor and Francis; 2002. 215 p.

39. Boelsterli, U. A. Mechanistic Toxicology. First Edition ed: Francis and Taylor; 2005. 314 p.

40. Padda, M. S., Sanchez, M., Akhtar, A. J., Boyer, J. L. Drug-induced cholestasis. Hepatology. 2011;53(4):1377-87.

41. Liu, J., Waalkes, M. P. Liver is a target of arsenic carcinogenesis. Toxicol Sci. 2008;105(1):24-32.

42. Dumas, E. O., Pollack, G. M. Opioid tolerance development: a pharmacokinetic/pharmacodynamic perspective. AAPS J. 2008;10(4):537-51.

43. Zanger, U. M., Klein, K., Saussele, T., Blievernicht, J., Hofmann, M. H., Schwab, M. Polymorphic CYP2B6: molecular mechanisms and emerging clinical significance. Pharmacogenomics. 2007;8(7):743-59.

44. Brockmoller, J., Tzvetkov, M. V. Pharmacogenetics: data, concepts and tools to improve drug discovery and drug treatment. Eur J Clin Pharmacol. 2008;64(2):133-57.

45. Tonder, J. J. V., Steenkamp, V., Gulumian, M. Pre-Clinical Assessment of the Potential Intrinsic Hepatotoxicity of Candidate Drugs [Inernet] In: Gowder, Sivakumar ed, New Insights into Toxicity and Drug Testing, Chapter 1. Jan 2013. Available from: https://www.intechopen.com/books/new-insights-into-toxicity-and-drug-testing/pre-clinical-assessment-of-the-potential-intrinsic-hepatotoxicity-of-candidate-drugs

46. Gebhardt, R., Hengstler, J. G., Muller, D., Glockner, R., Buenning, P., Laube, B.*, et al.* New hepatocyte in vitro systems for drug metabolism: metabolic capacity and recommendations for application in basic research and drug development, standard operation procedures. Drug Metab Rev. 2003;35(2-3):145-213.

47. Chapin, R. E., Stedman, D. B. Endless possibilities: stem cells and the vision for toxicology testing in the 21st century. Toxicol Sci. 2009;112(1):17-22.

48. Mandenius, C. F., Andersson, T. B., Alves, P. M., Batzl-Hartmann, C., Bjorquist, P., Carrondo, M. J.*, et al.* Toward preclinical predictive drug testing for metabolism and hepatotoxicity by using in vitro models derived from human embryonic stem cells and human cell lines - a report on the Vitrocellomics EU-project. Altern Lab Anim. 2011;39(2):147-71.

49. Society of Toxicology (SOT) Express Statement on Alternative toxicity test methods: Reducing, Refining, and Replacing, Animal Use for Safety Testing; Available from: http://www.toxicology.org/pubs/docs/pr/ToxTopics/TT3_InVitro_SOT.pdf Apr 2015

50. Gerets, H. H., Tilmant, K., Gerin, B., Chanteux, H., Depelchin, B. O., Dhalluin, S.*, et al.* Characterization of primary human hepatocytes, HepG2 cells, and HepaRG cells at the mRNA level and CYP activity in response to inducers and their predictivity for the detection of human hepatotoxins. Cell Biol Toxicol. 2012;28(2):69-87.

51. Sartipy, P., Bjorquist, P., Strehl, R., Hyllner, J. The application of human embryonic stem cell technologies to drug discovery. Drug Discov Today. 2007;12(17-18):688-99.

52. Westerink, W. M., Schoonen, W. G. Cytochrome P450 enzyme levels in HepG2 cells and cryopreserved primary human

hepatocytes and their induction in HepG2 cells. Toxicol In Vitro. 2007;21(8):1581-91.

53. Westerink, W. M., Schoonen, W. G. Phase II enzyme levels in HepG2 cells and cryopreserved primary human hepatocytes and their induction in HepG2 cells. Toxicol In Vitro. 2007;21(8):1592-602.

54. Guillouzo, A., Corlu, A., Aninat, C., Glaise, D., Morel, F., Guguen-Guillouzo, C. The human hepatoma HepaRG cells: a highly differentiated model for studies of liver metabolism and toxicity of xenobiotics. Chem Biol Interact. 2007;168(1):66-73.

55. Bort, R., Signore, M., Tremblay, K., Martinez Barbera, J., Zaret, K. Hex homeobox gene controls the transition of the endoderm to a pseudostratified, cell emergent epithelium for liver bud development. Dev Biol. 2006;290(1):44-56.

56. Lubberstedt, M., Muller-Vieira, U., Mayer, M., Biemel, K. M., Knospel, F., Knobeloch, D.*, et al.* HepaRG human hepatic cell line utility as a surrogate for primary human hepatocytes in drug metabolism assessment in vitro. J Pharmacol Toxicol Methods. 2011;63(1):59-68.

57. Aninat, C., Piton, A., Glaise, D., Le Charpentier, T., Langouet, S., Morel, F.*, et al.* Expression of cytochromes P450, conjugating enzymes and nuclear receptors in human hepatoma HepaRG cells. Drug Metab Dispos. 2006;34(1):75-83.

58. Ulvestad, M., Darnell, M., Molden, E., Ellis, E., Asberg, A., Andersson, T. B. Evaluation of organic anion-transporting polypeptide 1B1 and CYP3A4 activities in primary human hepatocytes and HepaRG cells cultured in a dynamic three-dimensional bioreactor system. J Pharmacol Exp Ther. 2012;343(1):145-56.

59. Bachour-El Azzi, P., Sharanek, A., Burban, A., Li, R., Guevel, R. L., Abdel-Razzak, Z.*, et al.* Comparative Localization and Functional Activity of the Main Hepatobiliary Transporters in HepaRG Cells and Primary Human Hepatocytes. Toxicol Sci. 2015;145(1):157-68.

60. Tibbitt, M., Anseth, K. Hydrogels as extracellular matrix mimics for 3D cell culture. Biotechnol Bioeng. 2009;103(4):655-63.

61. Miranda, J. P., Rodrigues, A., Tostoes, R. M., Leite, S., Zimmerman, H., Carrondo, M. J.*, et al.* Extending hepatocyte functionality for drug-testing applications using high-viscosity alginate-encapsulated three-dimensional cultures in bioreactors. Tissue Eng Part C Methods. 2010;16(6):1223-32.

62. Müller, D., Tascher, G., Muller-Vieira, U., Knobeloch, D., Nuessler, A. K., Zeilinger, K.*, et al.* In-depth physiological characterization of primary human hepatocytes in a 3D hollow-fiber bioreactor. J Tissue Engineering Regen Med. 2011;5(8):e207-18.

63. Zeilinger, K., Schreiter, T., Darnell, M., Soderdahl, T., Lubberstedt, M., Dillner, B.*, et al.* Scaling down of a clinical three-dimensional perfusion multicompartment hollow fiber liver bioreactor developed for extracorporeal liver support to an analytical scale device useful for hepatic pharmacological in vitro studies. Tissue Eng Part C Methods. 2011;17(5):549-56.

64. Lubberstedt, M., Muller-Vieira, U., Biemel, K. M., Darnell, M., Hoffmann, S. A., Knospel, F.*, et al.* Serum-free culture of primary human hepatocytes in a miniaturized hollow-fibre membrane bioreactor for pharmacological in vitro studies. J Tissue Engineering Regen Med. 2012.

65. Schyschka, L., Sanchez, J. J., Wang, Z., Burkhardt, B., Muller-Vieira, U., Zeilinger, K.*, et al.* Hepatic 3D cultures but not 2D cultures preserve specific transporter activity for acetaminophen-induced hepatotoxicity. Arch Toxicol. 2013;87(8):1581-93.

66. Fey, S. J., Wrzesinski, K. Determination of drug toxicity using 3D spheroids constructed from an immortal human hepatocyte cell line. Toxicol Sci. 2012;127(2):403-11.

67. Molina-Jimenez, F., Benedicto, I., Dao Thi, V. L., Gondar, V., Lavillette, D., Marin, J. J.*, et al.* Matrigel-embedded 3D culture of Huh-7 cells as a hepatocyte-like polarized system to study hepatitis C virus cycle. Virology. 2012;425(1):31-9.

68. Wrzesinski, K., Rogowska-Wrzesinska, A., Kanlaya, R., Borkowski, K., Schwammle, V., Dai, J.*, et al.* The Cultural Divide: Exponential Growth in Classical 2D and Metabolic Equilibrium in 3D Environments. PLoS One. 2014;9(9):e106973.

69. Lu, H. F., Lim, S. X., Leong, M. F., Narayanan, K., Toh, R. P., Gao, S.*, et al.* Efficient neuronal differentiation and maturation of human pluripotent stem cells encapsulated in 3D microfibrous scaffolds. Biomaterials. 2012;33(36):9179-87.

70. Tostoes, R. M., Leite, S. B., Miranda, J. P., Sousa, M., Wang, D. I., Carrondo, M. J.*, et al.* Perfusion of 3D encapsulated hepatocytes--a synergistic effect enhancing long-term functionality in bioreactors. Biotechnol Bioeng. 2011;108(1):41-9.

71. Miranda, J. P., Leite, S. B., Muller-Vieira, U., Rodrigues, A., Carrondo, M. J., Alves, P. M. Towards an extended functional hepatocyte in vitro culture. Tissue Eng Part C Methods. 2009;15(2):157-67.

72. Conway, D. E., Sakurai, Y., Weiss, D., Vega, J. D., Taylor, W. R., Jo, H.*, et al.* Expression of CYP1A1 and CYP1B1 in human endothelial cells: regulation by fluid shear stress. Cardiovasc Res. 2009;81(4):669-77.

73. Shvartsman, I., Dvir, T., Harel-Adar, T., Cohen, S. Perfusion cell seeding and cultivation induce the assembly of thick and functional hepatocellular tissue-like construct. Tissue Eng Part A. 2009;15(4):751-60.

74. Vinci, B., Duret, C., Klieber, S., Gerbal-Chaloin, S., Sa-Cunha, A., Laporte, S.*, et al.* Modular bioreactor for primary human hepatocyte culture: medium flow stimulates expression and activity of detoxification genes. Biotechnol J. 2011;6(5):554-64.

75. Lauschke, V. M., Hendriks, D. F., Bell, C. C., Andersson, T. B., Ingelman-Sundberg, M. Novel 3D Culture Systems for

Studies of Human Liver Function and Assessments of the Hepatotoxicity of Drugs and Drug Candidates. Chem Res Toxicol. 2016.

76. Haycock, J. 3D cell culture: a review of current approaches and techniques. Methods Mol Biol. 2011;695:1-15.

77. Lin, R. Z., Chang, H. Y. Recent advances in three-dimensional multicellular spheroid culture for biomedical research. Biotechnol J. 2008;3(9-10):1172-84.

78. Novik, E., Maguire, T. J., Chao, P., Cheng, K. C., Yarmush, M. L. A microfluidic hepatic coculture platform for cell-based drug metabolism studies. Biochem Pharmacol. 2010;79(7):1036-44.

79. Domansky, K., Inman, W., Serdy, J., Dash, A., Lim, M. H., Griffith, L. G. Perfused multiwell plate for 3D liver tissue engineering. Lab Chip. 2010;10(1):51-8.

80. Chan, C., Berthiaume, F., Nath, B. D., Tilles, A. W., Toner, M., Yarmush, M. L. Hepatic tissue engineering for adjunct and temporary liver support: critical technologies. Liver Transpl. 2004;10(11):1331-42.

81. Bavli, D., Prill, S., Ezra, E., Levy, G., Cohen, M., Vinken, M.*, et al.* Real-time monitoring of metabolic function in liver-on-chip microdevices tracks the dynamics of mitochondrial dysfunction. Proc Natl Acad Sci U S A. 2016;113(16):E2231-40.

82. Tsamandouras, N., Kostrzewski, T., Stokes, C. L., Griffith, L. G., Hughes, D. J., Cirit, M. Quantitative Assessment of Population Variability in Hepatic Drug Metabolism Using a Perfused Three-Dimensional Human Liver Microphysiological System. J Pharmacol Exp Ther. 2017;360(1):95-105.

83. Guillouzo, A. Liver cell models in in vitro toxicology. Environ Health Perspect. 1998;106 Suppl 2:511-32.

84. Zeilinger, K., Freyer, N., Damm, G., Seehofer, D., Knospel, F. Cell sources for in vitro human liver cell culture models. Exp Biol Med (Maywood). 2016;241(15):1684-98.

85. Leite, S. B., Teixeira, A. P., Miranda, J. P., Tostoes, R. M., Clemente, J. J., Sousa, M. F.*, et al.* Merging bioreactor technology with 3D hepatocyte-fibroblast culturing approaches: Improved in vitro models for toxicological applications. Toxicol In Vitro. 2011;25(4):825-32.

86. Leite, S. B., Wilk-Zasadna, I., Zaldivar, J. M., Airola, E., Reis-Fernandes, M. A., Mennecozzi, M.*, et al.* Three-dimensional HepaRG model as an attractive tool for toxicity testing. Toxicol Sci. 2012;130(1):106-16.

87. Bell, C. C., Hendriks, D. F., Moro, S. M., Ellis, E., Walsh, J., Renblom, A.*, et al.* Characterization of primary human hepatocyte spheroids as a model system for drug-induced liver injury, liver function and disease. Sci Rep. 2016;6:25187.

88. Alimperti, S., Lei, P., Wen, Y., Tian, J., Campbell, A. M., Andreadis, S. T. Serum-free spheroid suspension culture maintains mesenchymal stem cell proliferation and differentiation potential. Biotechnol Prog. 2014;30(4):974-83.

89. Wang, Y. H., Wu, J. Y., Chou, P. J., Chen, C. H., Wang, C. Z., Ho, M. L.*, et al.* Characterization and evaluation of the differentiation ability of human adipose-derived stem cells growing in scaffold-free suspension culture. Cytotherapy. 2014;16(4):485-95.

90. Ramaiahgari, S. C., Den Braver, M. W., Herpers, B., Terpstra, V., Commandeur, J. N., Van De Water, B.*, et al.* A 3D in vitro model of differentiated HepG2 cell spheroids with improved liver-like properties for repeated dose high-throughput toxicity studies. Arch Toxicol. 2014;88(5):1083-95.

91. Pinheiro, P. F., Pereira, S. A., Harjivan, S. G., Martins, I. L., Marinho, A. T., Cipriano, M.*, et al.* Hepatocyte spheroids as a competent in vitro system for drug biotransformation studies: nevirapine as a bioactivation case study. Arch Toxicol. 2017;91(3):1199-211.

92. Darnell, M., Schreiter, T., Zeilinger, K., Urbaniak, T., Soderdahl, T., Rossberg, I.*, et al.* Cytochrome P450-dependent metabolism in HepaRG cells cultured in a dynamic three-dimensional bioreactor. Drug Metab Dispos. 2011;39(7):1131-8.

93. Darnell, M., Ulvestad, M., Ellis, E., Weidolf, L., Andersson, T. B. In vitro evaluation of major in vivo drug metabolic pathways using primary human hepatocytes and HepaRG cells in suspension and a dynamic three-dimensional bioreactor system. J Pharmacol Exp Ther. 2012;343(1):134-44.

94. Hoffmann, S. A., Muller-Vieira, U., Biemel, K., Knobeloch, D., Heydel, S., Lubberstedt, M.*, et al.* Analysis of drug metabolism activities in a miniaturized liver cell bioreactor for use in pharmacological studies. Biotechnol Bioeng. 2012;109(12):3172-81.

95. Knöspel, F., Jacobs, F., Freyer, N., Damm, G., De Bondt, A., Van Den Wyngaert, I.*, et al.* In Vitro Model for Hepatotoxicity Studies Based on Primary Human Hepatocyte Cultivation in a Perfused 3D Bioreactor System. Int Mol Sci. 2016;17(4).

96. Gerlach, J. C., Mutig, K., Sauer, I. M., Schrade, P., Efimova, E., Mieder, T.*, et al.* Use of primary human liver cells originating from discarded grafts in a bioreactor for liver support therapy and the prospects of culturing adult liver stem cells in bioreactors: a morphologic study. Transplantation. 2003;76(5):781-6.

97. Soldatow, V. Y., Lecluyse, E. L., Griffith, L. G., Rusyn, I. In vitro models for liver toxicity testing. Toxicol Res. 2013;2(1):23-39.

98. Marinho, A. T., Dias, C. G., Pinheiro, P. F., Lemos, A. R., Antunes, A. M., Marques, M. M.*, et al.* Nevirapine modulation of paraoxonase-1 in the liver: An in vitro three-model approach. Eur J Pharm Sci. 2016;82:147-53.

99. Kostadinova, R., Boess, F., Applegate, D., Suter, L., Weiser, T., Singer, T.*, et al.* A long-term three dimensional liver co-culture system for improved prediction of clinically relevant drug-induced hepatotoxicity. Toxicol Appl Pharmacol.

2013;268(1):1-16.

100. Tostões, R. M., Leite, S. B., Serra, M., Jensen, J., Bjorquist, P., Carrondo, M. J.*, et al.* Human liver cell spheroids in extended perfusion bioreactor culture for repeated-dose drug testing. Hepatology. 2012;55(4):1227-36.

101. Gunness, P., Mueller, D., Shevchenko, V., Heinzle, E., Ingelman-Sundberg, M., Noor, F. 3D organotypic cultures of human HepaRG cells: a tool for in vitro toxicity studies. Toxicol Sci. 2013;133(1):67-78.

102. Boelsterli, U. A. Diclofenac-induced liver injury: a paradigm of idiosyncratic drug toxicity. Toxicol Appl Pharmacol. 2003;192(3):307-22.

103. Xu, J., Ma, M., Purcell, W. M. Characterisation of some cytotoxic endpoints using rat liver and HepG2 spheroids as in vitro models and their application in hepatotoxicity studies. II. Spheroid cell spreading inhibition as a new cytotoxic marker. Toxicol Appl Pharmacol. 2003;189(2):112-9.

104. Bort, R., Ponsoda, X., Jover, R., Gomez-Lechon, M. J., Castell, J. V. Diclofenac toxicity to hepatocytes: a role for drug metabolism in cell toxicity. J Pharmacol Exp Ther. 1999;288(1):65-72.

105. Lauer, B., Tuschl, G., Kling, M., Mueller, S. O. Species-specific toxicity of diclofenac and troglitazone in primary human and rat hepatocytes. Chem Biol Interact. 2009;179(1):17-24.

106. Lin, J., Schyschka, L., Muhl-Benninghaus, R., Neumann, J., Hao, L., Nussler, N.*, et al.* Comparative analysis of phase I and II enzyme activities in 5 hepatic cell lines identifies Huh-7 and HCC-T cells with the highest potential to study drug metabolism. Arch Toxicol. 2012;86(1):87-95.

107. Ponsoda, X., Bort, R., Jover, R., Gomez-Lechon, M. J., Castell, J. V. Molecular mechanism of diclofenac hepatotoxicity: Association of cell injury with oxidative metabolism and decrease in ATP levels. Toxicol In Vitro. 1995;9(4):439-44.

108. Wang, K., Shindoh, H., Inoue, T., Horii, I. Advantages of in vitro cytotoxicity testing by using primary rat hepatocytes in comparison with established cell lines. J Toxicol Sci. 2002;27(3):229-37.

109. Goda, K., Takahashi, T., Kobayashi, A., Shoda, T., Kuno, H., Sugai, S. Usefulness of in vitro combination assays of mitochondrial dysfunction and apoptosis for the estimation of potential risk of idiosyncratic drug induced liver injury. J Toxicol Sci. 2016;41(5):605-15.

110. Chojkier, M. Troglitazone and liver injury: in search of answers. Hepatology. 2005;41(2):237-46.

111. Sahi, J., Hamilton, G., Sinz, M., Barros, S., Huang, S. M., Lesko, L. J.*, et al.* Effect of troglitazone on cytochrome P450 enzymes in primary cultures of human and rat hepatocytes. Xenobiotica. 2000;30(3):273-84.

112. Kassahun, K., Pearson, P. G., Tang, W., Mcintosh, I., Leung, K., Elmore, C.*, et al.* Studies on the metabolism of troglitazone to reactive intermediates in vitro and in vivo. Evidence for novel biotransformation pathways involving quinone methide formation and thiazolidinedione ring scission. Chem Res Toxicol. 2001;14(1):62-70.

113. Smith, M. T. Mechanisms of troglitazone hepatotoxicity. Chem Res Toxicol. 2003;16(6):679-87.

114. Shen, M. Nodal signaling: developmental roles and regulation. Development. 2007;134(6):1023-34.

115. Izumi, T., Enomoto, S., Hosiyama, K., Sasahara, K., Shibukawa, A., Nakagawa, T.*, et al.* Prediction of the human pharmacokinetics of troglitazone, a new and extensively metabolized antidiabetic agent, after oral administration, with an animal scale-up approach. J Pharmacol Exp Ther. 1996;277(3):1630-41.

116. Hendriks, D. F., Fredriksson Puigvert, L., Messner, S., Mortiz, W., Ingelman-Sundberg, M. Hepatic 3D spheroid models for the detection and study of compounds with cholestatic liability. Sci Rep. 2016;6:35434.

117. Oecd. OECD Test No 417: Toxicokinetics. Guideline for the testing of chemicals. Paris: OECD; 2010.

118. Coecke, S., Pelkonen, O., Leite, S. B., Bernauer, U., Bessems, J. G., Bois, F. Y.*, et al.* Toxicokinetics as a key to the integrated toxicity risk assessment based primarily on non-animal approaches. Toxicol In Vitro. 2013;27(5):1570-7.

119. Toxicity Testing in the 21st Century: A Vision and a Strategy. Committee on Toxicity Testing and Assessment of Environmental Agents; Board on Environmental Studies and Toxicology; Institute for Laboratory Animal Research; Division on Earth and Life Studies. Washington DC: The National Academies Press; 2007.

120. Daneshian, M., Kamp, H., Hengstler, J., Leist, M., Van De Water, B. Highlight report: Launch of a large integrated European in vitro toxicology project: EU-ToxRisk. Arch Toxicol. 2016;90(5):1021-4.

121. Andersen, M. E., Krewski, D. Toxicity testing in the 21st century: bringing the vision to life. Toxicol Sci. 2009;107(2):324-30.

122. Baharvand, H., Hashemi, S. M., Kazemi Ashtiani, S., Farrokhi, A. Differentiation of human embryonic stem cells into hepatocytes in 2D and 3D culture systems in vitro. Int J Dev Biol. 2006;50(7):645-52.

123. Davila, J. C., Cezar, G. G., Thiede, M., Strom, S., Miki, T., Trosko, J. Use and application of stem cells in toxicology. Toxicol Sci. 2004;79(2):214-23.

124. Giri, S., Nieber, K., Bader, A. Hepatotoxicity and hepatic metabolism of available drugs: current problems and possible solutions in preclinical stages. Expert Opin Drug Metab Toxicol. 2010;6(8):895-917.

125. Krewski, D., Andersen, M. E., Mantus, E., Zeise, L. Toxicity testing in the 21st century: implications for human health risk assessment. Risk Anal. 2009;29(4):474-9.

126. Shukla, S. J., Huang, R., Austin, C. P., Xia, M. The future of toxicity testing: a focus on in vitro methods using a quantitative

high-throughput screening platform. Drug Discov Today. 2010;15(23-24):997-1007.

127. Trosko, J. E. Commentary on "Toxicity testing in the 21st century: a vision and a strategy": stem cells and cell-cell communication as fundamental targets in assessing the potential toxicity of chemicals. Hum Exp Toxicol. 2010;29(1):21-9.

128. Balls, M. Modern alternative approaches to the problem of drug-induced liver injury. Altern Lab Anim. 2011;39(2):103-7.

129. Kandarova, H., Letasiova, S. Alternative methods in toxicology: pre-validated and validated methods. Interdiscip Toxicol. 2011;4(3):107-13.

130. Zuang V. D., Barroso J., Belz S., Bopp S.; Bostroem A.C., Boufid M., *et al.*. EURL ECVAM Status Report on the Development, Validation and Regulatory Acceptance of Alternative Methods and Approaches (2016) [Internet]. Health, Consumers and Reference Materials, JRC103522; Out 2016, Available from: http://publications.jrc.ec.europa.eu/repository/handle/JRC103522

131. Suter-Dick, L., Alves, P. M., Blaauboer, B. J., Bremm, K. D., Brito, C., Coecke, S.*, et al.* Stem cell-derived systems in toxicology assessment. Stem Cells Dev. 2015;24(11):1284-96.

132. Thomson, J. A., Itskovitz-Eldor, J., Shapiro, S. S., Waknitz, M. A., Swiergiel, J. J., Marshall, V. S.*, et al.* Embryonic stem cell lines derived from human blastocysts. Science. 1998;282(5391):1145-7.

133. Zuba-Surma, E. K., Jozkowicz, A., Dulak, J. Stem cells in pharmaceutical biotechnology. Curr Pharm Biotechnol. 2011;12(11):1760-73.

134. Stummann, T. C., Bremer, S. Embryonic stem cells in safety pharmacology and toxicology. Adv Exp Med Biol. 2012;745:14-25.

135. European Commission Press Release, European Commission proposes strict ethical guidelines on EU funding of human embryonic stem cell research [Internet]. IP/03/969, Brussels, July 2003, Available from: http://europa.eu/rapid/press-release_IP-03-969_en.htm?locale=en

136. Greely, H. T. Moving human embryonic stem cells from legislature to lab: remaining legal and ethical questions. PLoS Med. 2006;3(5):e143.

137. Vojnits, K., Bremer, S. Challenges of using pluripotent stem cells for safety assessments of substances. Toxicology. 2010;270(1):10-7.

138. Behbahan, I. S., Duan, Y., Lam, A., Khoobyari, S., Ma, X., Ahuja, T. P.*, et al.* New approaches in the differentiation of human embryonic stem cells and induced pluripotent stem cells toward hepatocytes. Stem Cell Rev. 2011;7(3):748-59.

139. Takebe, T., Sekine, K., Enomura, M., Koike, H., Kimura, M., Ogaeri, T.*, et al.* Vascularized and functional human liver from an iPSC-derived organ bud transplant. Nature. 2013;499(7459):481-4.

140. Toivonen, S., Ojala, M., Hyysalo, A., Ilmarinen, T., Rajala, K., Pekkanen-Mattila, M.*, et al.* Comparative analysis of targeted differentiation of human induced pluripotent stem cells (hiPSCs) and human embryonic stem cells reveals variability associated with incomplete transgene silencing in retrovirally derived hiPSC lines. Stem Cells Transl Med. 2013;2(2):83-93.

141. Herberts, C. A., Kwa, M. S., Hermsen, H. P. Risk factors in the development of stem cell therapy. J Transl Med. 2011;9:29.

142. Peterson, S. E., Loring, J. F. Genomic instability in pluripotent stem cells: implications for clinical applications. J Biol Chem. 2014;289(8):4578-84.

143. Cai, J., Weiss, M. L., Rao, M. S. In search of "stemness". Exp Hematol. 2004;32(7):585-98.

144. Filipe, E. C. Optimization of low serum umbilical cord matrix mesenchymal stem cell (ucmMSC) culture for conditioned media preparation: in vitro ans in vivo wound healing applications. Lisboa: Universidade de Lisboa; 2011.Available from: http://repositorio.ul.pt/bitstream/10451/6309/1/ulfc092793_tm_elysse_filipe.pdf

145. Dominici, M., Le Blanc, K., Mueller, I., Slaper-Cortenbach, I., Marini, F., Krause, D.*, et al.* Minimal criteria for defining multipotent mesenchymal stromal cells. The International Society for Cellular Therapy position statement. Cytotherapy. 2006;8(4):315-7.

146. Campagnoli, C., Roberts, I. A., Kumar, S., Bennett, P. R., Bellantuono, I., Fisk, N. M. Identification of mesenchymal stem/progenitor cells in human first-trimester fetal blood, liver, and bone marrow. Blood. 2001;98(8):2396-402.

147. In 'T Anker, P. S., Scherjon, S. A., Kleijburg-Van Der Keur, C., De Groot-Swings, G. M., Claas, F. H., Fibbe, W. E.*, et al.* Isolation of mesenchymal stem cells of fetal or maternal origin from human placenta. Stem Cells. 2004;22(7):1338-45.

148. In 'T Anker, P. S., Scherjon, S. A., Kleijburg-Van Der Keur, C., Noort, W. A., Claas, F. H., Willemze, R.*, et al.* Amniotic fluid as a novel source of mesenchymal stem cells for therapeutic transplantation. Blood. 2003;102(4):1548-9.

149. Erices, A., Conget, P., Minguell, J. J. Mesenchymal progenitor cells in human umbilical cord blood. Br J Haematol. 2000;109(1):235-42.

150. Buyl, K., De Kock, J., Najar, M., Lagneaux, L., Branson, S., Rogiers, V.*, et al.* Characterization of hepatic markers in human Wharton's Jelly-derived mesenchymal stem cells. Toxicol In Vitro. 2014;28(1):113-9.

151. La Rocca, G., Anzalone, R., Corrao, S., Magno, F., Loria, T., Lo Iacono, M.*, et al.* Isolation and characterization of Oct-4+/HLA-G+ mesenchymal stem cells from human umbilical cord matrix: differentiation potential and detection of new markers. Histochemistry and cell biology. 2009;131(2):267-82.

152. La Rocca, G., Lo Iacono, M., Corsello, T., Corrao, S., Farina, F., Anzalone, R. Human Wharton's jelly mesenchymal stem cells maintain the expression of key immunomodulatory molecules when subjected to osteogenic, adipogenic and chondrogenic differentiation in vitro: new perspectives for cellular therapy. Curr Stem Cell Res Ther. 2013;8(1):100-13.

153. Secunda, R., Vennila, R., Mohanashankar, A. M., Rajasundari, M., Jeswanth, S., Surendran, R. Isolation, expansion and characterisation of mesenchymal stem cells from human bone marrow, adipose tissue, umbilical cord blood and matrix: a comparative study. Cytotechnology. 2014.

154. Santos JMS, Soares R, Martins JP, Basto V, Coelho M, Cruz P, *et al.* Optimised and defined method for isolation and preservation of precursor cells from human umbilical cord. INPI PAT20081000083882;PCT/IB2008/054067; WO2009044379. Medinfar, ECBio. 2008. Avaible from: https://patentscope.wipo.int/search/en/detail.jsf?docId=WO2009044379.

155. Da Silva Meirelles, L., Chagastelles, P. C., Nardi, N. B. Mesenchymal stem cells reside in virtually all post-natal organs and tissues. J Cell Sci. 2006;119(Pt 11):2204-13.

156. Muller, I., Kordowich, S., Holzwarth, C., Spano, C., Isensee, G., Staiber, A.*, et al.* Animal serum-free culture conditions for isolation and expansion of multipotent mesenchymal stromal cells from human BM. Cytotherapy. 2006;8(5):437-44.

157. Barry, F. P., Murphy, J. M. Mesenchymal stem cells: clinical applications and biological characterization. Int J Biochem Cell Biol. 2004;36(4):568-84.

158. Zeddou, M., Briquet, A., Relic, B., Josse, C., Malaise, M. G., Gothot, A.*, et al.* The umbilical cord matrix is a better source of mesenchymal stem cells (MSC) than the umbilical cord blood. Cell Biol Int. 2010;34(7):693-701.

159. Fukuda, K. Molecular characterization of regenerated cardiomyocytes derived from adult mesenchymal stem cells. Congenit Anom (Kyoto). 2002;42(1):1-9.

160. De Kock, J., Najar, M., Bolleyn, J., Al Battah, F., Rodrigues, R. M., Buyl, K.*, et al.* Mesoderm-derived stem cells: the link between the transcriptome and their differentiation potential. Stem Cells Dev. 2012;21(18):3309-23.

161. Anzalone, R., Lo Iacono, M., Corrao, S., Magno, F., Loria, T., Cappello, F.*, et al.* New emerging potentials for human Wharton's jelly mesenchymal stem cells: immunological features and hepatocyte-like differentiative capacity. Stem Cells Dev. 2010;19(4):423-38.

162. Rodrigues, R. M., Branson, S., De Boe, V., Sachinidis, A., Rogiers, V., De Kock, J.*, et al.* In vitro assessment of drug-induced liver steatosis based on human dermal stem cell-derived hepatic cells. Arch Toxicol. 2016;90(3):677-89.

163. Guillouzo, A., Guguen-Guillouzo, C. Evolving concepts in liver tissue modeling and implications for in vitro toxicology. Expert Opin Drug Metab Toxicol. 2008;4(10):1279-94.

164. Duan, Y., Ma, X., Zou, W., Wang, C., Bahbahan, I. S., Ahuja, T. P.*, et al.* Differentiation and characterization of metabolically functioning hepatocytes from human embryonic stem cells. Stem Cells. 2010;28(4):674-86.

165. Safinia, N., Minger, S. L. Generation of hepatocytes from human embryonic stem cells. Methods Mol Biol. 2009;481:169-80.

166. Takayama, K., Inamura, M., Kawabata, K., Katayama, K., Higuchi, M., Tashiro, K.*, et al.* Efficient generation of functional hepatocytes from human embryonic stem cells and induced pluripotent stem cells by HNF4alpha transduction. Mol Ther. 2012;20(1):127-37.

167. Touboul, T., Hannan, N. R., Corbineau, S., Martinez, A., Martinet, C., Branchereau, S.*, et al.* Generation of functional hepatocytes from human embryonic stem cells under chemically defined conditions that recapitulate liver development. Hepatology. 2010;51(5):1754-65.

168. Snykers, S., Vanhaecke, T., De Becker, A., Papeleu, P., Vinken, M., Van Riet, I.*, et al.* Chromatin remodeling agent trichostatin A: a key-factor in the hepatic differentiation of human mesenchymal stem cells derived of adult bone marrow. BMC Dev Biol. 2007;2;7:24.

169. Dong, X., Pan, R., Zhang, H., Yang, C., Shao, J., Xiang, L. Modification of histone acetylation facilitates hepatic differentiation of human bone marrow mesenchymal stem cells. PLoS One. 2013;8(5):e63405.

170. Banas, A. Purification of adipose tissue mesenchymal stem cells and differentiation toward hepatic-like cells. Methods Mol Biol. 2012;826:61-72.

171. Li, X., Yuan, J., Li, W., Liu, S., Hua, M., Lu, X.*, et al.* Direct differentiation of homogeneous human adipose stem cells into functional hepatocytes by mimicking liver embryogenesis. J Cell Physiol. 2014;229(6):801-12.

172. Campard, D., Lysy, P. A., Najimi, M., Sokal, E. M. Native umbilical cord matrix stem cells express hepatic markers and differentiate into hepatocyte-like cells. Gastroenterology. 2008;134(3):833-48.

173. Cipriano, M., Freyer, N., Knospel, F., Oliveira, N. G., Barcia, R., Cruz, P. E.*, et al.* Self-assembled 3D spheroids and hollow-fibre bioreactors improve MSC-derived hepatocyte-like cell maturation in vitro. Arch Toxicol. 2016.

174. Zhang, Y. N., Lie, P. C., Wei, X. Differentiation of mesenchymal stromal cells derived from umbilical cord Wharton's jelly into hepatocyte-like cells. Cytotherapy. 2009;11(5):548-58.

175. Zhang, S., Chen, L., Liu, T., Zhang, B., Xiang, D., Wang, Z.*, et al.* Human umbilical cord matrix stem cells efficiently rescue acute liver failure through paracrine effects rather than hepatic differentiation. Tissue Eng Part A. 2012;18(13-14):1352-64.

176. Zhao, Q., Ren, H., Li, X., Chen, Z., Zhang, X., Gong, W.*, et al.* Differentiation of human umbilical cord mesenchymal stromal cells into low immunogenic hepatocyte-like cells. Cytotherapy. 2009;11(4):414-26.

177. Zhou, R., Li, Z., He, C., Li, R., Xia, H., Li, C.*, et al.* Human umbilical cord mesenchymal stem cells and derived hepatocyte-like cells exhibit similar therapeutic effects on an acute liver failure mouse model. PLoS One. 2014;9(8):e104392.

178. Liang, X. J., Chen, X. J., Yang, D. H., Huang, S. M., Sun, G. D., Chen, Y. P. Differentiation of human umbilical cord mesenchymal stem cells into hepatocyte-like cells by hTERT gene transfection in vitro. Cell Biol Int. 2012;36(2):215-21.

179. Yoon, H. H., Jung, B. Y., Seo, Y. K., Song, K. Y., Park, J. K. In vitro hepatic differentiation of umbilical cord-derived mesenchymal stem cell. Process Biochem. 2010;45(12):1857-64.

180. Snykers, S., De Kock, J., Rogiers, V., Vanhaecke, T. In vitro differentiation of embryonic and adult stem cells into hepatocytes: state of the art. Stem Cells. 2009;27(3):577-605.

181. Zorn, A. M. Liver Development. StemBook [Internet]. Cambridge (MA): Harvard Stem Cell Institute Oct 2008 Available from: http://www.stembook.org/node/512.html

182. D'amour, K. A., Agulnick, A. D., Eliazer, S., Kelly, O. G., Kroon, E., Baetge, E. E. Efficient differentiation of human embryonic stem cells to definitive endoderm. Nat Biotechnol. 2005;23(12):1534-41.

183. Hay, D. C., Zhao, D., Fletcher, J., Hewitt, Z. A., Mclean, D., Urruticoechea-Uriguen, A.*, et al.* Efficient differentiation of hepatocytes from human embryonic stem cells exhibiting markers recapitulating liver development in vivo. Stem Cells. 2008;26(4):894-902.

184. Freyer, N., Knospel, F., Strahl, N., Amini, L., Schrade, P., Bachmann, S.*, et al.* Hepatic Differentiation of Human Induced Pluripotent Stem Cells in a Perfused Three-Dimensional Multicompartment Bioreactor. Biores Open Access. 2016;5(1):235-48.

185. Calmont, A., Wandzioch, E., Tremblay, K., Minowada, G., Kaestner, K., Martin, G.*, et al.* An FGF response pathway that mediates hepatic gene induction in embryonic endoderm cells. Dev Cell. 2006;11(3):339-48.

186. Mclin, V., Rankin, S., Zorn, A. Repression of Wnt/beta-catenin signaling in the anterior endoderm is essential for liver and pancreas development. Development. 2007;134(12):2207-17.

187. Chen, Y., Pan, F., Brandes, N., Afelik, S., Sölter, M., Pieler, T. Retinoic acid signaling is essential for pancreas development and promotes endocrine at the expense of exocrine cell differentiation in Xenopus. Dev Biol. 2004;271(1):144-60.

188. Zaret, K. Liver specification and early morphogenesis. Mech Develop. 2000;92:83-8.

189. Ben Z. Stanger, D. K. P. Basic mechanisms of normal and abnormal gastrointestinal function: Development of the gastrointestinal system (Part 1: Section 23). In: Yamada, T., editor. Textbook of Gastroenterology. 1. Fifth Edition ed. West Sussex, PO19 8SQ, UK: Blackwell Publishing/John Wiley & Sons; 2009. p. 1744.

190. Ameri, J., Stahlberg, A., Pedersen, J., Johansson, J., Johannesson, M., Artner, I.*, et al.* FGF2 specifies hESC-derived definitive endoderm into foregut/midgut cell lineages in a concentration-dependent manner. Stem Cells. 2010;28(1):45-56.

191. Rossi, J., Dunn, N., Hogan, B., Zaret, K. Distinct mesodermal signals, including BMPs from the septum transversum mesenchyme, are required in combination for hepatogenesis from the endoderm. Gene Dev. 2001;15(15):1998-2009.

192. Wang, Z., Dollé, P., Cardoso, W., Niederreither, K. Retinoic acid regulates morphogenesis and patterning of posterior foregut derivatives. Dev Biol. 2006;297(2):433-45.

193. Kamiya, A. K., T.; Miyajima, A. . Oncostatin M and Hepatocyte Growth Factor Induce Hepatic Maturation Via Distinct Signaling Pathways. FEBS Lett. 2001(492):90-4.

194. Kamiya, A., Kinoshita, T., Ito, Y., Matsui, T., Y., M., Senba, E.*, et al.* Fetal Liver Development requires a paracrine action of Oncostatin M Through the gp130 Signal Transducer. EMBO J. 1999;18(8):2127-36.

195. Odom, D., Zizlsperger, N., Gordon, D., Bell, G. W., Rinaldi, N., Murray, H.*, et al.* Control of pancreas and liver gene expression by HNF transcription factors. Science. 2004;303(5662):1378-81.

196. Michalopoulos, G. K., Bowen, W. C., Mule, K., Luo, J. HGF-, EGF-, and dexamethasone-induced gene expression patterns during formation of tissue in hepatic organoid cultures. Gene Expr. 2003;11(2):55-75.

197. Tasnim, F., Toh, Y. C., Qu, Y., Li, H., Phan, D., Narmada, B. C.*, et al.* Functionally Enhanced Human Stem Cell Derived Hepatocytes in Galactosylated Cellulosic Sponges for Hepatotoxicity Testing. Mol Pharm. 2016;13(6):1947-57.

198. Lee, H. J., Jung, J., Cho, K. J., Lee, C. K., Hwang, S. G., Kim, G. J. Comparison of in vitro hepatogenic differentiation potential between various placenta-derived stem cells and other adult stem cells as an alternative source of functional hepatocytes. Differentiation. 2012;84(3):223-31.

199. Paganelli, M., Dallmeier, K., Nyabi, O., Scheers, I., Kabamba, B., Neyts, J.*, et al.* Differentiated umbilical cord matrix stem cells as a new in vitro model to study early events during hepatitis B virus infection. Hepatology. 2013;57(1):59-69.

200. Lee, H. J., Cha, K. E., Hwang, S. G., Kim, J. K., Kim, G. J. In vitro screening system for hepatotoxicity: comparison of bone-marrow-derived mesenchymal stem cells and Placenta-derived stem cells. J Cell Biochem. 2011;112(1):49-58.

201. Snykers, S., Henkens, T., De Rop, E., Vinken, M., Fraczek, J., De Kock, J.*, et al.* Role of epigenetics in liver-specific gene transcription, hepatocyte differentiation and stem cell reprogrammation. J Hepatol. 2009;51(1):187-211.

202. An, S. Y., Han, J., Lim, H. J., Park, S. Y., Kim, J. H., Do, B. R.*, et al.* Valproic acid promotes differentiation of hepatocyte-like cells from whole human umbilical cord-derived mesenchymal stem cells. Tissue Cell. 2014;46(2):127-35.

203. Mortezaee, K., Minaii, B., Sabbaghziarani, F., Ragerdi Kashani, I., Hassanzadeh, G., Pasbakhsh, P.*, et al.* Retinoic Acid as the Stimulating Factor for Differentiation of Wharton's Jelly-Mesenchymal Stem Cells into Hepatocyte-like Cells. Avicenna J Med Biotechnol. 2015;7(3):106-12.

204. Raut, A., Khanna, A. Enhanced expression of hepatocyte-specific microRNAs in valproic acid mediated hepatic trans-differentiation of human umbilical cord derived mesenchymal stem cells. Exp Cell Res. 2016;343(2):237-47.

205. El-Serafi, A. T., Oreffo, R. O., Roach, H. I. Epigenetic modifiers influence lineage commitment of human bone marrow stromal cells: Differential effects of 5-aza-deoxycytidine and trichostatin A. Differentiation. 2011;81(1):35-41.

206. Mahmud, N., Petro, B., Baluchamy, S., Li, X., Taioli, S., Lavelle, D.*, et al.* Differential effects of epigenetic modifiers on the expansion and maintenance of human cord blood stem/progenitor cells. Biol Blood Marrow Transplant. 2014;20(4):480-9.

207. Zych, J., Stimamiglio, M. A., Senegaglia, A. C., Brofman, P. R., Dallagiovanna, B., Goldenberg, S.*, et al.* The epigenetic modifiers 5-aza-2'-deoxycytidine and trichostatin A influence adipocyte differentiation in human mesenchymal stem cells. Braz J Med Biol Res. 2013;46(5):405-16.

208. Santi, D. V., Norment, A., Garrett, C. E. Covalent bond formation between a DNA-cytosine methyltransferase and DNA containing 5-azacytosine. Proc Natl Acad Sci U S A. 1984;81(22):6993-7.

209. Komashko, V. M., Farnham, P. J. 5-azacytidine treatment reorganizes genomic histone modification patterns. Epigenetics. 2010;5(3).

210. Bhuvanagiri, M., Lewis, J., Putzker, K., Becker, J. P., Leicht, S., Krijgsveld, J.*, et al.* 5-azacytidine inhibits nonsense-mediated decay in a MYC-dependent fashion. EMBO Mol Med. 2014.

211. Bhuvanagiri, M., Schlitter, A. M., Hentze, M. W., Kulozik, A. E. NMD: RNA biology meets human genetic medicine. Biochem J. 2010;430(3):365-77.

212. Rothrock, R., Lee, K. L., Isham, K. R., Kenney, F. T. Changes in hepatic differentiation following treatment of rat fetuses with 5-azacytidine. Arch Biochem Biophys. 1988;263(2):237-44.

213. Seeliger, C., Culmes, M., Schyschka, L., Yan, X., Damm, G., Wang, Z.*, et al.* Decrease of global methylation improves significantly hepatic differentiation of Ad-MSCs: possible future application for urea detoxification. Cell Transplant. 2013;22(1):119-31.

214. Yoshida, Y., Shimomura, T., Sakabe, T., Ishii, K., Gonda, K., Matsuoka, S.*, et al.* A role of Wnt/beta-catenin signals in hepatic fate specification of human umbilical cord blood-derived mesenchymal stem cells. Am J Physiol Gastrointest Liver Physiol. 2007;293(5):G1089-98.

215. Van Roozendaal, K. E., Darling, D., Farzaneh, F. DMSO and retinoic acid induce HL-60 differentiation by different but converging pathways. Exp Cell Res. 1990;190(1):137-40.

216. Kamiya, A., Kojima, N., Kinoshita, T., Sakai, Y., Miyaijma, A. Maturation of fetal hepatocytes in vitro by extracellular matrices and oncostatin M: induction of tryptophan oxygenase. Hepatology. 2002;35(6):1351-9.

217. Liu, W. H., Liu, Z. C., You, N., Zhang, N., Wang, T., Gong, Z. B.*, et al.* Several important in vitro improvements in the amplification, differentiation and tracing of fetal liver stem/progenitor cells. PLoS One. 2012;7(10):e47346.

218. Koyama, T., Ehashi, T., Ohshima, N., Miyoshi, H. Efficient proliferation and maturation of fetal liver cells in three-dimensional culture by stimulation of oncostatin M, epidermal growth factor, and dimethyl sulfoxide. Tissue Eng Part A. 2009;15(5):1099-107.

219. Sakai, Y., Jiang, J., Kojima, N., Kinoshita, T., Miyajima, A. Enhanced in vitro maturation of fetal mouse liver cells with oncostatin M, nicotinamide, and dimethyl sulfoxide. Cell Transplant. 2002;11(5):435-41.

220. Alizadeh, E., Zarghami, N., Eslaminejad, M. B., Akbarzadeh, A., Barzegar, A., Mohammadi, S. A. The effect of dimethyl sulfoxide on hepatic differentiation of mesenchymal stem cells. Artif Cells Nanomed Biotechnol. 2016;44(1):157-64.

221. Banas, A., Teratani, T., Yamamoto, Y., Tokuhara, M., Takeshita, F., Osaki, M.*, et al.* Rapid hepatic fate specification of adipose-derived stem cells and their therapeutic potential for liver failure. J Gastroenterol Hepatol. 2009;24(1):70-7.

222. Pal, R., Mamidi, M. K., Das, A. K., Bhonde, R. Diverse effects of dimethyl sulfoxide (DMSO) on the differentiation potential of human embryonic stem cells. Arch Toxicol. 2012;86(4):651-61.

223. Czysz, K., Minger, S., Thomas, N. DMSO efficiently down regulates pluripotency genes in human embryonic stem cells during definitive endoderm derivation and increases the proficiency of hepatic differentiation. PLoS One. 2015;10(2):e0117689.

224. Medine, C. N., Lucendo-Villarin, B., Zhou, W., West, C. C., Hay, D. C. Robust generation of hepatocyte-like cells from human embryonic stem cell populations. StemBook [Internet]. Cambridge (MA): Harvard Stem Cell Institute Jun 2010. Available from: http://www.stembook.org/node/736.html

225. Chetty, R., Slavin, J. L. Epithelioid sarcoma with extensive chondroid differentiation. Histopathology. 1994;24(4):400-1.

226. Calder, A., Roth-Albin, I., Bhatia, S., Pilquil, C., Lee, J. H., Bhatia, M.*, et al.* Lengthened G1 Phase Indicates Differentiation Status in Human Embryonic Stem Cells. Stem Cells Dev. 2013;22(2):279-95.

227. Earp, H. S., Rubin, R. A., Austin, K. S., Dy, R. C. DMSO increases tyrosine residue phosphorylation in membranes from murine erythroleukemia cells. Biochem Biophys Res Commun. 1983;112(2):413-8.

228. Yen, A., Varvayanis, S. DMSO, sodium butyrate, and TPA induce hypophosphorylation of RB with HL-60 cell differentiation. In Vitro Cell Dev Biol Anim. 1995;31(3):164-7.

229. Rubbini, S., Cocco, L., Manzoli, L., Lutterman, J., Billi, A. M., Matteucci, A.*, et al.* Phosphoinositide signalling in nuclei of Friend cells: DMSO-induced differentiation reduces the association of phosphatidylinositol-transfer protein with the nucleus. Biochem Biophys Res Commun. 1997;230(2):302-5.

230. Notman, R., Noro, M., O'malley, B., Anwar, J. Molecular basis for dimethylsulfoxide (DMSO) action on lipid membranes. J Am Chem Soc. 2006;128(43):13982-3.

231. He, F., Liu, W., Zheng, S., Zhou, L., Ye, B., Qi, Z. Ion transport through dimethyl sulfoxide (DMSO) induced transient water pores in cell membranes. Mol Membr Biol. 2012;29(3-4):107-13.

232. Su, T., Waxman, D. J. Impact of dimethyl sulfoxide on expression of nuclear receptors and drug-inducible cytochromes P450 in primary rat hepatocytes. Arch Biochem Biophys. 2004;424(2):226-34.

233. Li, Y., Guo, G., Li, L., Chen, F., Bao, J., Shi, Y. J.*, et al.* Three-dimensional spheroid culture of human umbilical cord mesenchymal stem cells promotes cell yield and stemness maintenance. Cell Tissue Res. 2015.

234. Zhang, S., Liu, P., Chen, L., Wang, Y., Wang, Z., Zhang, B. The effects of spheroid formation of adipose-derived stem cells in a microgravity bioreactor on stemness properties and therapeutic potential. Biomaterials. 2015;41:15-25.

235. Zhang, R. R., Takebe, T., Miyazaki, L., Takayama, M., Koike, H., Kimura, M.*, et al.* Efficient hepatic differentiation of human induced pluripotent stem cells in a three-dimensional microscale culture. Methods Mol Biol. 2014;1210:131-41.

236. Subramanian, K., Owens, D. J., Raju, R., Firpo, M., O'brien, T. D., Verfaillie, C. M.*, et al.* Spheroid culture for enhanced differentiation of human embryonic stem cells to hepatocyte-like cells. Stem Cells Dev. 2014;23(2):124-31.

237. Takayama, K., Kawabata, K., Nagamoto, Y., Kishimoto, K., Tashiro, K., Sakurai, F.*, et al.* 3D spheroid culture of hESC/hiPSC-derived hepatocyte-like cells for drug toxicity testing. Biomaterials. 2013;34(7):1781-9.

238. Kim, S. J., Park, M. H., Moon, H. J., Park, J. H., Ko Du, Y., Jeong, B. Polypeptide thermogels as a three dimensional culture scaffold for hepatogenic differentiation of human tonsil-derived mesenchymal stem cells. ACS Appl Mater Interfaces. 2014;6(19):17034-43.

239. Okura, H., Komoda, H., Saga, A., Kakuta-Yamamoto, A., Hamada, Y., Fumimoto, Y.*, et al.* Properties of hepatocyte-like cell clusters from human adipose tissue-derived mesenchymal stem cells. Tissue Eng Part C Methods. 2010;16(4):761-70.

240. Lin, N., Lin, J., Bo, L., Weidong, P., Chen, S., Xu, R. Differentiation of bone marrow-derived mesenchymal stem cells into hepatocyte-like cells in an alginate scaffold. Cell Prolif. 2010;43(5):427-34.

241. Li, J., Tao, R., Wu, W., Cao, H., Xin, J., Li, J.*, et al.* 3D PLGA scaffolds improve differentiation and function of bone marrow mesenchymal stem cell-derived hepatocytes. Stem Cells Dev. 2010;19(9):1427-36.

242. Kazemnejad, S., Allameh, A., Seoleimani, M., Gharehbaghian, A., Mohammadi, Y., Amirizadeh, N.*, et al.* Functional hepatocyte-like cells derived from human bone marrow mesenchymal stem cells on a novel 3-dimensional biocompatible nanofibrous scaffold. International J Artif Organs. 2008;31(6):500-7.

243. Sivertsson, L., Synnergren, J., Jensen, J., Bjorquist, P., Ingelman-Sundberg, M. Hepatic differentiation and maturation of human embryonic stem cells cultured in a perfused three-dimensional bioreactor. Stem Cells Dev. 2013;22(4):581-94.

244. Gieseck, R. L., 3rd, Hannan, N. R., Bort, R., Hanley, N. A., Drake, R. A., Cameron, G. W.*, et al.* Maturation of induced pluripotent stem cell derived hepatocytes by 3D-culture. PLoS One. 2014;9(1):e86372.

245. Kazemnejad, S., Allameh, A., Soleimani, M., Gharehbaghian, A., Mohammadi, Y., Amirizadeh, N.*, et al.* Biochemical and molecular characterization of hepatocyte-like cells derived from human bone marrow mesenchymal stem cells on a novel three-dimensional biocompatible nanofibrous scaffold. J Gastroenterol Hepatol. 2009;24(2):278-87.

246. Sjogren, A. K., Liljevald, M., Glinghammar, B., Sagemark, J., Li, X. Q., Jonebring, A.*, et al.* Critical differences in toxicity mechanisms in induced pluripotent stem cell-derived hepatocytes, hepatic cell lines and primary hepatocytes. Arch Toxicol. 2014;88(7):1427-37.

247. Holmgren, G., Sjogren, A. K., Barragan, I., Sabirsh, A., Sartipy, P., Synnergren, J.*, et al.* Long-term chronic toxicity testing using human pluripotent stem cell-derived hepatocytes. Drug Metab Dispos. 2014;42(9):1401-6.

248. Medine, C. N., Lucendo-Villarin, B., Storck, C., Wang, F., Szkolnicka, D., Khan, F.*, et al.* Developing high-fidelity hepatotoxicity models from pluripotent stem cells. Stem Cells Transl Med. 2013;2(7):505-9.

249. Kang, S. J., Lee, H. M., Park, Y. I., Yi, H., Lee, H., So, B.*, et al.* Chemically induced hepatotoxicity in human stem cell-induced hepatocytes compared with primary hepatocytes and HepG2. Cell Biol Toxicol. 2016;32(5):403-17.

250. Kajiwara, M., Aoi, T., Okita, K., Takahashi, R., Inoue, H., Takayama, N.*, et al.* Donor-dependent variations in hepatic differentiation from human-induced pluripotent stem cells. Proc Natl Acad Sci U S A. 2012;109(31):12538-43.

251. Rodrigues, R. M., De Kock, J., Branson, S., Vinken, M., Meganathan, K., Chaudhari, U.*, et al.* Human skin-derived stem cells as a novel cell source for in vitro hepatotoxicity screening of pharmaceuticals. Stem Cells Dev. 2014;23(1):44-55.

252. Guguen-Guillouzo, C., Corlu, A., Guillouzo, A. Stem cell-derived hepatocytes and their use in toxicology. Toxicology.

2010;270(1):3-9.

253. Wobus, A. M., Loser, P. Present state and future perspectives of using pluripotent stem cells in toxicology research. Arch Toxicol. 2011;85(2):79-117.

254. Martins, J. P., Santos, J. M., De Almeida, J. M., Filipe, M. A., De Almeida, M. V., Almeida, S. C*., et al.* Towards an advanced therapy medicinal product based on mesenchymal stromal cells isolated from the umbilical cord tissue: quality and safety data. Stem Cell Res Ther. 2014;5(1):9.

255. Gomez-Lechon, M. J., Tolosa, L., Conde, I., Donato, M. T. Competency of different cell models to predict human hepatotoxic drugs. Expert Opin Drug Metab Toxicol. 2014;10(11):1553-68.

256. Godoy, P., Schmidt-Heck, W., Natarajan, K., Lucendo-Villarin, B., Szkolnicka, D., Asplund, A*., et al.* Gene networks and transcription factor motifs defining the differentiation of stem cells into hepatocyte-like cells. J Hepatol. 2015;63(4):934-42.

257. Miranda, J. P., Filipe, E., Fernandes, A. S., Almeida, J. M., Martins, J. P., De La Fuente, A*., et al.* The Human Umbilical Cord Tissue-Derived MSC Population UCX® Promotes Early Motogenic Effects on Keratinocytes and Fibroblasts and G-CSF-Mediated Mobilization of BM-MSCs When Transplanted In Vivo. Cell Transplant. 2015;24(5):865-77.

258. Santos, J. M., Barcia, R. N., Simoes, S. I., Gaspar, M. M., Calado, S., Agua-Doce, A*., et al.* The role of human umbilical cord tissue-derived mesenchymal stromal cells (UCX®)) in the treatment of inflammatory arthritis. J Transl Med. 2013;11:18.

259. Santos, J. M., Camoes, S. P., Filipe, E., Cipriano, M., Barcia, R. N., Filipe, M*., et al.* Three-dimensional spheroid cell culture of umbilical cord tissue-derived mesenchymal stromal cells leads to enhanced paracrine induction of wound healing. Stem Cell Res Ther. 2015;6:90.

260. Brolen, G., Sivertsson, L., Bjorquist, P., Eriksson, G., Ek, M., Semb, H*., et al.* Hepatocyte-like cells derived from human embryonic stem cells specifically via definitive endoderm and a progenitor stage. J Biotechnol. 2010;145(3):284-94.

261. Ulvestad, M., Nordell, P., Asplund, A., Rehnstrom, M., Jacobsson, S., Holmgren, G*., et al.* Drug metabolizing enzyme and transporter protein profiles of hepatocytes derived from human embryonic and induced pluripotent stem cells. Biochem Pharmacol. 2013;86(5):691-702.

262. Rajan, N., Habermehl, J., Cote, M. F., Doillon, C. J., Mantovani, D. Preparation of ready-to-use, storable and reconstituted type I collagen from rat tail tendon for tissue engineering applications. Nat Protocol. 2006;1(6):2753-8.

263. Warnes, G. R., Bolker, B., Bonebakker, L., Gentleman, R., Huber, W., Liaw, A., Lumley, T., Maechler, M., Magnusson, A., Moeller, S. And Schwartz, M. gplots: Various R programming tools for plotting data. . R package version, 2(4). 2009.

264. Oliveros, J. C. VENNY. An interactive tool for comparing lists with Venn Diagrams. http://bioinfogp.cnb.csic.es/tools/venny/index.html. 2007.

265. Schwartz, R. E., Reyes, M., Koodie, L., Jiang, Y., Blackstad, M., Lund, T*., et al.* Multipotent adult progenitor cells from bone marrow differentiate into functional hepatocyte-like cells. J Clin Invest. 2002;109(10):1291-302.

266. Chen, M. L., Lee, K. D., Huang, H. C., Tsai, Y. L., Wu, Y. C., Kuo, T. M*., et al.* HNF-4alpha determines hepatic differentiation of human mesenchymal stem cells from bone marrow. World J Gastroenterol. 2010;16(40):5092-103.

267. Wilkening, S., Bader, A. Influence of culture time on the expression of drug-metabolizing enzymes in primary human hepatocytes and hepatoma cell line HepG2. J Biochem Mol Toxicol. 2003;17(4):207-13.

268. Wilkening, S., Stahl, F., Bader, A. Comparison of primary human hepatocytes and hepatoma cell line Hepg2 with regard to their biotransformation properties. Drug Metab Dispos. 2003;31(8):1035-42.

269. Snykers, S., Vanhaecke, T., Papeleu, P., Luttun, A., Jiang, Y., Vander Heyden, Y*., et al.* Sequential exposure to cytokines reflecting embryogenesis: the key for in vitro differentiation of adult bone marrow stem cells into functional hepatocyte-like cells. Toxicol Sci. 2006;94(2):330-41.

270. Kubo, A., Kim, Y. H., Irion, S., Kasuda, S., Takeuchi, M., Ohashi, K*., et al.* The homeobox gene Hex regulates hepatocyte differentiation from embryonic stem cell-derived endoderm. Hepatology. 2010;51(2):633-41.

271. Cahan, P., Li, H., Morris, S. A., Lummertz Da Rocha, E., Daley, G. Q., Collins, J. J. CellNet: network biology applied to stem cell engineering. Cell. 2014;158(4):903-15.

272. Denson, L. A., Mcclure, M. H., Bogue, C. W., Karpen, S. J., Jacobs, H. C. HNF3beta and GATA-4 transactivate the liver-enriched homeobox gene, Hex. Gene. 2000;246(1-2):311-20.

273. Zhao, R., Watt, A. J., Li, J., Luebke-Wheeler, J., Morrisey, E. E., Duncan, S. A. GATA6 is essential for embryonic development of the liver but dispensable for early heart formation. Mol Cell Biol. 2005;25(7):2622-31.

274. Kang, M., Piliszek, A., Artus, J., Hadjantonakis, A. K. FGF4 is required for lineage restriction and salt-and-pepper distribution of primitive endoderm factors but not their initial expression in the mouse. Development. 2013;140(2):267-79.

275. Zhang, W., Yatskievych, T. A., Baker, R. K., Antin, P. B. Regulation of Hex gene expression and initial stages of avian hepatogenesis by Bmp and Fgf signaling. Dev Biol. 2004;268(2):312-26.

276. Dessimoz, J., Opoka, R., Kordich, J. J., Grapin-Botton, A., Wells, J. M. FGF signaling is necessary for establishing gut tube domains along the anterior-posterior axis in vivo. Mech Dev. 2006;123(1):42-55.

277. Andersson, T. B. The application of HepRG cells in evaluation of cytochrome P450 induction properties of drug compounds. Methods Mol Biol. 2010;640:375-87.

278. Hengstler, J. G., Brulport, M., Schormann, W., Bauer, A., Hermes, M., Nussler, A. K.*, et al.* Generation of human hepatocytes by stem cell technology: definition of the hepatocyte. Expert Opin Drug Metab Toxicol. 2005;1(1):61-74.

279. Vyhlidal, C. A., Gaedigk, R., Leeder, J. S. Nuclear receptor expression in fetal and pediatric liver: correlation with CYP3A expression. Drug Metab Dispos. 2006;34(1):131-7.

280. Rui, L. Energy metabolism in the liver. Compr Physiol. 2014;4(1):177-97.

281. Godoy, P., Widera, A., Schmidt-Heck, W., Campos, G., Meyer, C., Cadenas, C.*, et al.* Gene network activity in cultivated primary hepatocytes is highly similar to diseased mammalian liver tissue. Arch Toxicol. 2016;90(10):2513-29.

282. Zuk, P. A., Zhu, M., Ashjian, P., De Ugarte, D. A., Huang, J. I., Mizuno, H.*, et al.* Human adipose tissue is a source of multipotent stem cells. Mol Biol Cell. 2002;13(12):4279-95.

283. Wang, H. S., Hung, S. C., Peng, S. T., Huang, C. C., Wei, H. M., Guo, Y. J.*, et al.* Mesenchymal stem cells in the Wharton's jelly of the human umbilical cord. Stem Cells. 2004;22(7):1330-7.

284. Jaiswal, N., Haynesworth, S. E., Caplan, A. I., Bruder, S. P. Osteogenic differentiation of purified, culture-expanded human mesenchymal stem cells in vitro. J Cell Biochem. 1997;64(2):295-312.

285. Matsuda, C., Takagi, M., Hattori, T., Wakitani, S., Yoshida, T. Differentiation of Human Bone Marrow Mesenchymal Stem Cells to Chondrocytes for Construction of Three-dimensional Cartilage Tissue. Cytotechnology. 2005;47(1-3):11-7.

286. Pittenger, M. F., Mackay, A. M., Beck, S. C., Jaiswal, R. K., Douglas, R., Mosca, J. D.*, et al.* Multilineage potential of adult human mesenchymal stem cells. Science. 1999;284(5411):143-7.

287. Gang, E. J., Jeong, J. A., Hong, S. H., Hwang, S. H., Kim, S. W., Yang, I. H.*, et al.* Skeletal myogenic differentiation of mesenchymal stem cells isolated from human umbilical cord blood. Stem Cells. 2004;22(4):617-24.

288. Makino, S., Fukuda, K., Miyoshi, S., Konishi, F., Kodama, H., Pan, J.*, et al.* Cardiomyocytes can be generated from marrow stromal cells in vitro. J Clin Invest. 1999;103(5):697-705.

289. Wu, L. F., Wang, N. N., Liu, Y. S., Wei, X. Differentiation of Wharton's jelly primitive stromal cells into insulin-producing cells in comparison with bone marrow mesenchymal stem cells. Tissue Eng Part A. 2009;15(10):2865-73.

290. Ma, L., Feng, X. Y., Cui, B. L., Law, F., Jiang, X. W., Yang, L. Y.*, et al.* Human umbilical cord Wharton's Jelly-derived mesenchymal stem cells differentiation into nerve-like cells. Chin Med J. 2005;118(23):1987-93.

291. Bartaula-Brevik, S., Pedersen, T. O., Blois, A. L., Papadakou, P., Finne-Wistrand, A., Xue, Y.*, et al.* Leukocyte transmigration into tissue-engineered constructs is influenced by endothelial cells through toll-like receptor signaling. Stem Cell Res Ther. 2014;5(6):143.

292. Chen, J. S., Wong, V. W., Gurtner, G. C. Therapeutic potential of bone marrow-derived mesenchymal stem cells for cutaneous wound healing. Front Immunol. 2012;3:192.

293. Troyer, D. L., Weiss, M. L. Wharton's jelly-derived cells are a primitive stromal cell population. Stem Cells. 2008;26(3):591-9.

294. Nascimento, D. S., Mosqueira, D., Sousa, L. M., Teixeira, M., Filipe, M., Resende, T. P.*, et al.* Human umbilical cord tissue-derived mesenchymal stromal cells attenuate remodeling following myocardial infarction by pro-angiogenic, anti-apoptotic and endogenous cell activation mechanisms. Stem Cell Res Ther. 2014;5(1):5.

295. Barcia, R. N., Santos, J. M., Teixeira, M., Filipe, M., Pereira, A. R., Ministro, A.*, et al.* Umbilical cord tissue-derived mesenchymal stromal cells maintain immunomodulatory and angiogenic potencies after cryopreservation and subsequent thawing. Cytotherapy. 2016.

296. Gartner, A., Pereira, T., Armada-Da-Silva, P., Amado, S., Veloso, A., Amorim, I.*, et al.* Effects of umbilical cord tissue mesenchymal stem cells (UCX®) on rat sciatic nerve regeneration after neurotmesis injuries. J Stem Cells Regen Med. 2014;10(1):14-26.

297. Baraniak, P. R., Mcdevitt, T. C. Scaffold-free culture of mesenchymal stem cell spheroids in suspension preserves multilineage potential. Cell Tissue Res. 2012;347(3):701-11.

298. Bartosh, T. J., Ylostalo, J. H., Mohammadipoor, A., Bazhanov, N., Coble, K., Claypool, K.*, et al.* Aggregation of human mesenchymal stromal cells (MSCs) into 3D spheroids enhances their antiinflammatory properties. Proc Natl Acad Sci U S A. 2010;107(31):13724-9.

299. Frith, J. E., Thomson, B., Genever, P. G. Dynamic three-dimensional culture methods enhance mesenchymal stem cell properties and increase therapeutic potential. Tissue Eng Part C Methods. 2010;16(4):735-49.

300. Arufe, M. C., De La Fuente, A., Fuentes-Boquete, I., De Toro, F. J., Blanco, F. J. Differentiation of synovial CD-105(+) human mesenchymal stem cells into chondrocyte-like cells through spheroid formation. J Cell Biochem. 2009;108(1):145-55.

301. Sabapathy, V., Sundaram, B., V, M. S., Mankuzhy, P., Kumar, S. Human Wharton's Jelly Mesenchymal Stem Cells plasticity augments scar-free skin wound healing with hair growth. PLoS One. 2014;9(4):e93726.

302. Hsu, S. H., Hsieh, P. S. Self-assembled adult adipose-derived stem cell spheroids combined with biomaterials promote wound healing in a rat skin repair model. Wound Repair Regen. 2014.

303. Ballotta, V., Smits, A. I., Driessen-Mol, A., Bouten, C. V., Baaijens, F. P. Synergistic protein secretion by mesenchymal stromal cells seeded in 3D scaffolds and circulating leukocytes in physiological flow. Biomaterials. 2014;35(33):9100-13.

304. Rettinger, C. L., Fourcaudot, A. B., Hong, S. J., Mustoe, T. A., Hale, R. G., Leung, K. P. In vitro characterization of scaffold-free three-dimensional mesenchymal stem cell aggregates. Cell Tissue Res. 2014;358(2):395-405.

305. Serra, M., Brito, C., Sousa, M. F., Jensen, J., Tostoes, R., Clemente, J.*, et al.* Improving expansion of pluripotent human embryonic stem cells in perfused bioreactors through oxygen control. J Biotechnol. 2010;148(4):208-15.

306. Cardoso, T. C., Ferrari, H. F., Garcia, A. F., Novais, J. B., Silva-Frade, C., Ferrarezi, M. C.*, et al.* Isolation and characterization of Wharton's jelly-derived multipotent mesenchymal stromal cells obtained from bovine umbilical cord and maintained in a defined serum-free three-dimensional system. BMC Biotechnol. 2012;12:18.

307. Cesarz, Z., Tamama, K. Spheroid Culture of Mesenchymal Stem Cells. Stem Cells Int. 2016;2016:9176357.

308. Bellas, E., Chen, C. S. Forms, forces, and stem cell fate. Curr Opin Cell Biol. 2014;31:92-7.

309. Wang, W., Itaka, K., Ohba, S., Nishiyama, N., Chung, U. I., Yamasaki, Y.*, et al.* 3D spheroid culture system on micropatterned substrates for improved differentiation efficiency of multipotent mesenchymal stem cells. Biomaterials. 2009;30(14):2705-15.

310. Qihao, Z., Xigu, C., Guanghui, C., Weiwei, Z. Spheroid formation and differentiation into hepatocyte-like cells of rat mesenchymal stem cell induced by co-culture with liver cells. DNA Cell Biol. 2007;26(7):497-503.

311. Serra, M., Correia, C., Malpique, R., Brito, C., Jensen, J., Bjorquist, P.*, et al.* Microencapsulation technology: a powerful tool for integrating expansion and cryopreservation of human embryonic stem cells. PLoS One. 2011;6(8):e23212.

312. Yirme, G., Amit, M., Laevsky, I., Osenberg, S., Itskovitz-Eldor, J. Establishing a dynamic process for the formation, propagation, and differentiation of human embryoid bodies. Stem Cells Dev. 2008;17(6):1227-41.

313. Moreira, J. L., Alves, P. M., Aunins, J. G., Carrondo, M. J. Hydrodynamic effects on BHK cells grown as suspended natural aggregates. Biotechnol Bioeng. 1995;46(4):351-60.

314. Edmondson, R., Broglie, J. J., Adcock, A. F., Yang, L. Three-dimensional cell culture systems and their applications in drug discovery and cell-based biosensors. Assay Drug Dev Technol. 2014;12(4):207-18.

315. Stein, A. Decreasing variability in your cell culture. Biotechniques. 2007;43(2):228-9.

316. Mannello, F., Tonti, G. A. Concise review: no breakthroughs for human mesenchymal and embryonic stem cell culture: conditioned medium, feeder layer, or feeder-free; medium with fetal calf serum, human serum, or enriched plasma; serum-free, serum replacement nonconditioned medium, or ad hoc formula? All that glitters is not gold! Stem Cells. 2007;25(7):1603-9.

317. Wu, M., Han, Z. B., Liu, J. F., Wang, Y. W., Zhang, J. Z., Li, C. T.*, et al.* Serum-free media and the immunoregulatory properties of mesenchymal stem cells in vivo and in vitro. Cell Physiol Biochem. 2014;33(3):569-80.

318. Oskowitz, A., Mcferrin, H., Gutschow, M., Carter, M. L., Pochampally, R. Serum-deprived human multipotent mesenchymal stromal cells (MSCs) are highly angiogenic. Stem Cell Res. 2011;6(3):215-25.

319. Riebeling, C., Schlechter, K., Buesen, R., Spielmann, H., Luch, A., Seiler, A. Defined culture medium for stem cell differentiation: applicability of serum-free conditions in the mouse embryonic stem cell test. Toxicol In Vitro. 2011;25(4):914-21.

320. Lei, Y., Jeong, D., Xiao, J., Schaffer, D. V. Developing Defined and Scalable 3D Culture Systems for Culturing Human Pluripotent Stem Cells at High Densities. Cell Mol Bioeng. 2014;7(2):172-83.

321. Lei, Y., Schaffer, D. V. A fully defined and scalable 3D culture system for human pluripotent stem cell expansion and differentiation. Proc Natl Acad Sci U S A. 2013;110(52):E5039-48.

322. Zhao, G., Liu, F., Lan, S., Li, P., Wang, L., Kou, J.*, et al.* Large-scale expansion of Wharton's jelly-derived mesenchymal stem cells on gelatin microbeads, with retention of self-renewal and multipotency characteristics and the capacity for enhancing skin wound healing. Stem Cell Res Ther. 2015;6:38.

323. Ruiz, S. A., Chen, C. S. Emergence of patterned stem cell differentiation within multicellular structures. Stem Cells. 2008;26(11):2921-7.

324. Mcbeath, R., Pirone, D. M., Nelson, C. M., Bhadriraju, K., Chen, C. S. Cell shape, cytoskeletal tension, and RhoA regulate stem cell lineage commitment. Dev Cell. 2004;6(4):483-95.

325. Baraniak, P. R., Cooke, M. T., Saeed, R., Kinney, M. A., Fridley, K. M., Mcdevitt, T. C. Stiffening of human mesenchymal stem cell spheroid microenvironments induced by incorporation of gelatin microparticles. J Mech Behav Biomed Mater. 2012;11:63-71.

326. Hao, H., Chen, G., Liu, J., Ti, D., Zhao, Y., Xu, S.*, et al.* Culturing on Wharton's jelly extract delays mesenchymal stem cell senescence through p53 and p16INK4a/pRb pathways. PLoS One. 2013;8(3):e58314.

327. Nanaev, A. K., Kohnen, G., Milovanov, A. P., Domogatsky, S. P., Kaufmann, P. Stromal differentiation and architecture of the human umbilical cord. Placenta. 1997;18(1):53-64.

328. Potapova, I. A., Brink, P. R., Cohen, I. S., Doronin, S. V. Culturing of human mesenchymal stem cells as three-dimensional aggregates induces functional expression of CXCR4 that regulates adhesion to endothelial cells. J Biol Chem. 2008;283(19):13100-7.

329. Potapova, I. A., Gaudette, G. R., Brink, P. R., Robinson, R. B., Rosen, M. R., Cohen, I. S., *et al.* Mesenchymal stem cells support migration, extracellular matrix invasion, proliferation, and survival of endothelial cells in vitro. Stem Cells. 2007;25(7):1761-8.

330. Lee, J. H., Han, Y. S., Lee, S. H. Long-Duration Three-Dimensional Spheroid Culture Promotes Angiogenic Activities of Adipose-Derived Mesenchymal Stem Cells. Biomol Ther (Seoul). 2016;24(3):260-7.

331. Schwartz, R. E., Fleming, H. E., Khetani, S. R., Bhatia, S. N. Pluripotent stem cell-derived hepatocyte-like cells. Biotechnol Adv. 2014;32(2):504-13.

332. Woo, D. H., Kim, S. K., Lim, H. J., Heo, J., Park, H. S., Kang, G. Y., *et al.* Direct and indirect contribution of human embryonic stem cell-derived hepatocyte-like cells to liver repair in mice. Gastroenterology. 2012;142(3):602-11.

333. Cipriano, M., Medeiros, A., Filipe, E., Santos, J. M., Barcia, R., Cruz, H., *et al.* UCX® cells: A primordial stem cell source for in vitro differentiation into hepatocyte-like cells (HLCs). Toxicol Lett. 2014;229:S140-S.

334. Sengupta, S., Johnson, B. P., Swanson, S. A., Stewart, R., Bradfield, C. A., Thomson, J. A. Aggregate culture of human embryonic stem cell-derived hepatocytes in suspension are an improved in vitro model for drug metabolism and toxicity testing. Toxicol Sci. 2014;140(1):236-45.

335. Ramasamy, T. S., Yu, J. S., Selden, C., Hodgson, H., Cui, W. Application of three-dimensional culture conditions to human embryonic stem cell-derived definitive endoderm cells enhances hepatocyte differentiation and functionality. Tissue Eng Part A. 2013;19(3-4):360-7.

336. Tanimizu, N., Mitaka, T. Re-evaluation of liver stem/progenitor cells. Organogenesis. 2014;10(2):208-15.

337. Talaei-Khozani, T., Khodabandeh, Z., Jaberipour, M., Hosseini, A., Bahmanpour, S., Vojdani, Z. Comparison of hepatic nuclear factor-4 expression in two- and three-dimensional culture of Wharton's jelly-derived cells exposed to hepatogenic medium. Rom J Morphol Embryol. 2015;56(4):1365-70.

338. Ong, S. Y., Dai, H., Leong, K. W. Inducing hepatic differentiation of human mesenchymal stem cells in pellet culture. Biomaterials. 2006;27(22):4087-97.

339. Haruna, Y., Saito, K., Spaulding, S., Nalesnik, M. A., Gerber, M. A. Identification of bipotential progenitor cells in human liver development. Hepatology. 1996;23(3):476-81.

340. Fausto, N. Liver regeneration and repair: hepatocytes, progenitor cells, and stem cells. Hepatology. 2004;39(6):1477-87.

341. Strassburg, C. P., Strassburg, A., Kneip, S., Barut, A., Tukey, R. H., Rodeck, B., *et al.* Developmental aspects of human hepatic drug glucuronidation in young children and adults. Gut. 2002;50(2):259-65.

342. Hamilton, G. A., Jolley, S. L., Gilbert, D., Coon, D. J., Barros, S., Lecluyse, E. L. Regulation of cell morphology and cytochrome P450 expression in human hepatocytes by extracellular matrix and cell-cell interactions. Cell Tissue Res. 2001;306(1):85-99.

343. Tasnim, F., Phan, D., Toh, Y. C., Yu, H. Cost-effective differentiation of hepatocyte-like cells from human pluripotent stem cells using small molecules. Biomaterials. 2015;70:115-25.

344. Sharma, A. M., Novalen, M., Tanino, T., Uetrecht, J. P. 12-OH-nevirapine sulfate, formed in the skin, is responsible for nevirapine-induced skin rash. Chem Res Toxicol. 2013;26(5):817-27.

345. Sharma, A. M., Li, Y., Novalen, M., Hayes, M. A., Uetrecht, J. Bioactivation of nevirapine to a reactive quinone methide: implications for liver injury. Chem Res Toxicol. 2012;25(8):1708-19.

346. Riska, P., Lamson, M., Macgregor, T., Sabo, J., Hattox, S., Pav, J., *et al.* Disposition and biotransformation of the antiretroviral drug nevirapine in humans. Drug Metab Dispos. 1999;27(8):895-901.

347. Luzuriaga, K., Bryson, Y., Mcsherry, G., Robinson, J., Stechenberg, B., Scott, G., *et al.* Pharmacokinetics, safety, and activity of nevirapine in human immunodeficiency virus type 1-infected children. J Infect Dis. 1996;174(4):713-21.

348. Erickson, D. A., Mather, G., Trager, W. F., Levy, R. H., Keirns, J. J. Characterization of the in vitro biotransformation of the HIV-1 reverse transcriptase inhibitor nevirapine by human hepatic cytochromes P-450. Drug Metab Dispos. 1999;27(12):1488-95.

349. Hall, D. B., Macgregor, T. R. Case-control exploration of relationships between early rash or liver toxicity and plasma concentrations of nevirapine and primary metabolites. HIV Clin Trials. 2007;8(6):391-9.

350. Kranendonk, M., Alves, M., Antunes, P., Rueff, J. Human sulfotransferase 1A1-dependent mutagenicity of 12-hydroxy-nevirapine: the missing link? Chem Res Toxicol. 2014;27(11):1967-71.

351. Antunes, A. M., Godinho, A. L., Martins, I. L., Justino, G. C., Beland, F. A., Marques, M. M. Amino acid adduct formation by the nevirapine metabolite, 12-hydroxynevirapine--a possible factor in nevirapine toxicity. Chem Res Toxicol. 2010;23(5):888-99.

352. Dekker, S. J., Zhang, Y., Vos, J. C., Vermeulen, N. P., Commandeur, J. N. Different Reactive Metabolites of Nevirapine Require Distinct Glutathione S-Transferase Isoforms for Bioinactivation. Chem Res Toxicol. 2016;29(12):2136-44.

353. Cipriano, M., Correia, J. C., Camoes, S. P., Oliveira, N. G., Cruz, P., Cruz, H., *et al.* The role of epigenetic modifiers in extended cultures of functional hepatocyte-like cells derived from human neonatal mesenchymal stem cells. Arch Toxicol. 2016.

354. Spandidos, A., Wang, X., Wang, H., Seed, B. PrimerBank: a resource of human and mouse PCR primer pairs for gene

expression detection and quantification. Nucleic Acids Res. 2010;38(Database issue):D792-9.

355. Antherieu, S., Chesne, C., Li, R., Camus, S., Lahoz, A., Picazo, L.*, et al.* Stable expression, activity, and inducibility of cytochromes P450 in differentiated HepaRG cells. Drug Metab Dispos. 2010;38(3):516-25.

356. Justino, G. C., Santos, M. R., Canario, S., Borges, C., Florencio, M. H., Mira, L. Plasma quercetin metabolites: structure-antioxidant activity relationships. Arch Biochem Biophys. 2004;432(1):109-21.

357. Babu, S. R., Lakshmi, V. M., Huang, G. P., Zenser, T. V., Davis, B. B. Glucuronide conjugates of 4-aminobiphenyl and its N-hydroxy metabolites. pH stability and synthesis by human and dog liver. Biochem Pharmacol. 1996;51(12):1679-85.

358. Marinho, A. T., Rodrigues, P. M., Caixas, U., Antunes, A. M., Branco, T., Harjivan, S. G.*, et al.* Differences in nevirapine biotransformation as a factor for its sex-dependent dimorphic profile of adverse drug reactions. J Antimicrob Chemother. 2014;69(2):476-82.

359. Grilo, N. M. C., M.J.; Miranda, J.P.; Cipriano, M.; Serpa, J.; Marques, M.M.; Monteiro, E.C.; Antunes, A.A; Diogo, L.L.; Pereira, S.A. Unmasking efavirenz neurotoxicity: time matters to the underlying mechanisms. Eur J of Pharm Sci. 2017; 105:47-54

360. Przemyslaw, W., Piotr, K., Grazyna, C., Danuta, K. P., Malgorzata, I., Bernadeta, M.*, et al.* Total, free, and protein-bound thiols in plasma of peritoneal dialysis and predialysis patients. Int Urol Nephrol. 2011;43(4):1201-9.

361. De Sousa Mendes, M., Lui, G., Zheng, Y., Pressiat, C., Hirt, D., Valade, E.*, et al.* A Physiologically-Based Pharmacokinetic Model to Predict Human Fetal Exposure for a Drug Metabolized by Several CYP450 Pathways. Clin Pharmacokinet. 2017; 56 (5), 537-550.

362. Fan-Havard, P., Liu, Z., Chou, M., Ling, Y., Barrail-Tran, A., Haas, D. W.*, et al.* Pharmacokinetics of phase I nevirapine metabolites following a single dose and at steady state. Antimicrob Agents Chemother. 2013;57(5):2154-60.

363. Marinho, A. T., Godinho, A. L. A., Novais, D. A., Antunes, A. M. M., Marques, M. M., Ramos, T.*, et al.* Development and validation of an HPLC-UV method for quantifying nevirapine and its main phase I metabolites in human blood. Anal Methods. 2014;6(5):1575-80.

364. Riska, P. S., Joseph, D. P., Dinallo, R. M., Davidson, W. C., Keirns, J. J., Hattox, S. E. Biotransformation of nevirapine, a non-nucleoside HIV-1 reverse transcriptase inhibitor, in mice, rats, rabbits, dogs, monkeys, and chimpanzees. Drug Metab Dispos. 1999;27(12):1434-47.

365. Chang, B. X., You, S. L., Liu, H. L., Mao, P. Y., Xin, S. J. Establishment of cytochrome P450 3A4 and glutathione S-transferase A1-transfected human hepatoma cell line and functional analysis. Genet Mol Res. 2014;13(3):6949-61.

366. Coles, B. F., Kadlubar, F. F. Human alpha class glutathione S-transferases: genetic polymorphism, expression, and susceptibility to disease. Methods Enzymol. 2005;401:9-42.

367. Kim, S. G., Lee, S. J. PI3K, RSK, and mTOR signal networks for the GST gene regulation. Toxicol Sci. 2007;96(2):206-13.

368. Lu, S. C. Regulation of glutathione synthesis. Mol Aspects Med. 2009;30(1-2):42-59.

369. Forman, H. J., Zhang, H., Rinna, A. Glutathione: overview of its protective roles, measurement, and biosynthesis. Mol Aspects Med. 2009;30(1-2):1-12.

370. Lopes-Coelho, F., Gouveia-Fernandes, S., Goncalves, L. G., Nunes, C., Faustino, I., Silva, F.*, et al.* HNF1beta drives glutathione (GSH) synthesis underlying intrinsic carboplatin resistance of ovarian clear cell carcinoma (OCCC). Tumour Biol. 2016;37(4):4813-29.

371. Mcgarry, D. J., Chakravarty, P., Wolf, C. R., Henderson, C. J. Altered protein S-glutathionylation identifies a potential mechanism of resistance to acetaminophen-induced hepatotoxicity. J Pharmacol Exp Ther. 2015;355(2):137-44.

372. Stummann, T. C., Bremer, S. The possible impact of human embryonic stem cells on safety pharmacological and toxicological assessments in drug discovery and drug development. Curr Stem Cell Res Ther. 2008;3(2):118-31.

373. Hay, D. C., Fletcher, J., Payne, C., Terrace, J. D., Gallagher, R. C., Snoeys, J.*, et al.* Highly efficient differentiation of hESCs to functional hepatic endoderm requires ActivinA and Wnt3a signaling. Proc Natl Acad Sci U S A. 2008;105(34):12301-6.

374. De Kock, J., Vanhaecke, T., Biernaskie, J., Rogiers, V., Snykers, S. Characterization and hepatic differentiation of skin-derived precursors from adult foreskin by sequential exposure to hepatogenic cytokines and growth factors reflecting liver development. Toxicol In Vitro. 2009;23(8):1522-7.

375. Perrimon, N., Pitsouli, C., Shilo, B. Z. Signaling mechanisms controlling cell fate and embryonic patterning. Cold Spring Harb Perspect Biol. 2012;4(8):a005975.

376. Bohm, F., Kohler, U. A., Speicher, T., Werner, S. Regulation of liver regeneration by growth factors and cytokines. EMBO Mol Med. 2010;2(8):294-305.

377. Snykers, S., De Kock, J., Tamara, V., Rogiers, V. Hepatic differentiation of mesenchymal stem cells: in vitro strategies. Methods Mol Biol. 2011;698:305-14.

378. Snykers, S., Vinken, M., Rogiers, V., Vanhaecke, T. Differential role of epigenetic modulators in malignant and normal stem cells: a novel tool in preclinical in vitro toxicology and clinical therapy. Arch Toxicol. 2007;81(8):533-44.

379. Hay, D. C., Zhao, D., Ross, A., Mandalam, R., Lebkowski, J., Cui, W. Direct differentiation of human embryonic stem cells to hepatocyte-like cells exhibiting functional activities. Cloning Stem Cells. 2007;9(1):51-62.

380. Duncan, S. A. Mechanisms controlling early development of the liver. Mech Dev. 2003;120(1):19-33.

381. Pettinato, G., Ramanathan, R., Fisher, R. A., Mangino, M. J., Zhang, N., Wen, X. Scalable Differentiation of Human iPSCs in a Multicellular Spheroid-based 3D Culture into Hepatocyte-like Cells through Direct Wnt/beta-catenin Pathway Inhibition. Sci Rep. 2016;6:32888.

382. Reif, S., Sykes, D., Rossi, T., Weiser, M. M. Changes in transcripts of basement components during rat liver development: increase in laminin messenger RNAs in the neonatal period. Hepatology. 1992;15(2):310-5.

383. Reif, S., Terranova, V. P., El-Bendary, M., Lebenthal, E., Petell, J. K. Modulation of extracellular matrix proteins in rat liver during development. Hepatology. 1990;12(3 Pt 1):519-25.

384. Zaret, K. S. Regulatory phases of early liver development: paradigms of organogenesis. Nat Rev Genet. 2002;3(7):499-512.

385. Wells, J. M., Melton, D. A. Vertebrate endoderm development. Annu Rev Cell Dev Biol. 1999;15:393-410.

386. Torre, C., Perret, C., Colnot, S. Transcription dynamics in a physiological process: beta-catenin signaling directs liver metabolic zonation. Int J Biochem Cell Biol. 2011;43(2):271-8.

387. Mccarty, W. J., Usta, O. B., Yarmush, M. L. A Microfabricated Platform for Generating Physiologically-Relevant Hepatocyte Zonation. Sci Rep. 2016;6:26868.

388. Rodrigues, J. S. The use of MSC derived hepatocyte-like cells (HLCs) in microfluidic culture systems: an approach for studying the metabolic syndrome: Instituto Superior Técnico, Universidade de Lisboa; 2016. Available from: https://fenix.tecnico.ulisboa.pt/cursos/mebiom/dissertacao/565303595501027

389. Wu, G., Fang, Y. Z., Yang, S., Lupton, J. R., Turner, N. D. Glutathione metabolism and its implications for health. J Nutr. 2004;134(3):489-92.

390. Prodanov, L., Jindal, R., Bale, S. S., Hegde, M., Mccarty, W. J., Golberg, I.*, et al.* Long-term maintenance of a microfluidic 3D human liver sinusoid. Biotechnol Bioeng. 2016;113(1):241-6.

391. Pascussi, J. M., Drocourt, L., Gerbal-Chaloin, S., Fabre, J. M., Maurel, P., Vilarem, M. J. Dual effect of dexamethasone on CYP3A4 gene expression in human hepatocytes. Sequential role of glucocorticoid receptor and pregnane X receptor. Eur J Biochem. 2001;268(24):6346-58.

392. Ferris, H. A., Kahn, C. R. New mechanisms of glucocorticoid-induced insulin resistance: make no bones about it. J Clin Invest. 2012;122(11):3854-7.

393. Deharde, D., Schneider, C., Hiller, T., Fischer, N., Kegel, V., Lubberstedt, M.*, et al.* Bile canaliculi formation and biliary transport in 3D sandwich-cultured hepatocytes in dependence of the extracellular matrix composition. Arch Toxicol. 2016;90(10):2497-511.

394. Boyer, J. L. Bile formation and secretion. Compr Physiol. 2013;3(3):1035-78.

395. Avior, Y., Levy, G., Zimerman, M., Kitsberg, D., Schwartz, R., Sadeh, R.*, et al.* Microbial-derived lithocholic acid and vitamin K2 drive the metabolic maturation of pluripotent stem cells-derived and fetal hepatocytes. Hepatology. 2015;62(1):265-78.

396. Sawitza, I., Kordes, C., Gotze, S., Herebian, D., Haussinger, D. Bile acids induce hepatic differentiation of mesenchymal stem cells. Sci Rep. 2015;5:13320.